OPTICAL CHARACTERIZATION OF PULSED INFRARED LIGHT EVOKED CORTICAL BRAIN ACTIVITY

By

Jonathan Matthew Cayce

Dissertation

Submitted to the Faculty of the

Graduate School of Vanderbilt University

in partial fulfillment of the requirements

of the degree of

DOCTOR OF PHILOSOPHY

In

Biomedical Engineering

May, 2013

Nashville, Tennessee

Approved:

Dr. Anita Mahadevan-Jansen

Dr. E. Duco Jansen

Dr. Anna Roe

Dr. Peter Konrad

Dr. Elizabeth Hillman

ABSTRACT

Infrared neural stimulation (INS) uses pulsed infrared light to directly stimulate neural tissue with high spatiotemporal precision and is well documented for peripheral nerve applications; however, prior to this dissertation, INS had not been demonstrated for the central nervous system. This dissertation presents the first successful application of INS in the central nervous system and increases our understanding the effects of pulsed infrared light irradiation on cellular dynamics in the brain. Pulsed infrared light is shown to evoke both excitatory and inhibitory neural activity, and evokes robust optical intrinsic signals indicating multiple cellular mechanisms are activated by INS. Optical imaging of calcium signals evoked by INS identified astrocyte sensitivity to pulsed infrared light confirming that both neurons and astrocytes are stimulated. Application of INS in non-human primate visual cortex demonstrated that pulsed infrared light evokes excitatory neural activity and modulates visually evoked signals, identifying the potential of INS to encode functionally relevant signals into cortex. Overall, these results establish INS as neurostimulation modality for use in the brain, and this dissertation provides the necessary foundation to further develop INS for use in the central nervous system in both research and clinical applications.

To my wife, Elizabeth, son, Nathan, and my family

for your love, encouragement and support.

ACKNOWLEDGEMENTS

I first would like to acknowledge my advisor, Dr. Anita Mahadevan-Jansen, who allowed me to study under her tutelage and become an independent researcher. Through her mentorship, she provided encouragement, guidance, and patience that allowed me to be successful. I would like to thank Dr. Duco Jansen for his advice and mentoring towards my research. His expertise on laser tissue interactions was crucial for this project and his willingness to share his career experiences and expertise were invaluable. I want to thank Dr. Anna Roe for believing in my project and allowing me to conduct research as a member of her lab. She provided valuable resources to complete this research and her advice and expertise were crucial in shaping the research discussed in Chapter IV and VI. I want to thank Dr. Elizabeth Hillman for asking the tough questions concerning my research and for allowing me to visit her lab to learn new techniques and perform crucial experiments for Chapter V. Finally, I would like to thank Dr. Konrad for his expertise in neurosurgery as well as his enthusiasm for my research and its possible future impacts on society.

Over the course of this dissertation, I have had the privilege of working with a number of intelligent and talented individuals that made this research possible. First, I would like to acknowledge Dr. Chris Kao for teaching me the techniques required for Chapter III. Dr. Robert Friedman was the most influential individual during the course of this dissertation. He personally taught me the ins and outs of optical imaging and electrophysiology, he spent many nights in Wilson Hall with me, and he always was willing to listen and provide advice when I hit a roadblock in my research. I want to

thank Dr. Gang Chen for his willingness to help with the research in Chapter VI, and for leading the research in Appendix B. I would like to thank Dr. Reuben Fan, Brian Lustig, Andrea Brock, Jeremy Winberry, and Lisa Chu of the Roe lab for their support of my research and their friendship. I want to acknowledge Matthew Bouchard, Dr. Brenda Chen and Lauren Grosberg for their assistance in experiments that comprised Chapter V. I want to thank Dr. Noel Tulipan for allowing me to do clinical trial research in his operating room, and Melba Isom for helping me consent patients and handling the administrative side of the study. Finally, I want to thank all my friends in the Biophotonics laboratory at Vanderbilt. They were always willing to help me with research, provide comic relief when needed, willing to help out when I dislocated my knee, and listened when I needed to vent. I will always be grateful for your support.

This dissertation would not have been possible without the love and support of my family. I first would like to thank my mom, Kim, brother, Nicholas, and my grandparents, Judy and Gary, who have always been there for me during the best and worst times of my life. They encouraged me to pursue my goals and did everything in their power to ensure I reached my goals. I also want to thank my mother-in-law, Priscilla Brazelton, and the rest of the Brazelton and Martin family for welcoming me into their family. They have loved and supported me as if I were a son. Most importantly, I would like to thank my beautiful wife, Elizabeth, for all of her love, patience, and support during my entire time as a graduate student. She was my rock of support during my entire time at Vanderbilt. I am forever grateful for the sacrifices she made so I could pursue my dream. Without her, this dissertation would not have been possible.

TABLE OF CONTENTS

LIST OF FIGURES

CHAPTER I

INTRODUCTION

1.1 Motivation

Neural stimulation has been a driving force in the advancement of neuroscience since Galvani first accidentally stimulated frog sciatic nerves using electrical charge [1]. Since Galvani's pioneering experiments, the field of neurostimulation has rapidly evolved over the course 220 years to include advanced neurostimulation techniques designed to further our understanding of neuroscience principles. Electrical, thermal, chemical, optical, magnetic and mechanical methods have been reported to generate action potentials in both the central nervous system and peripheral nervous system [2-6]. Clinical therapeutic and diagnostic applications of neurostimulation have seen major advances in the past 50 years. Therapeutic applications of neurostimulation include treatment of paralysis (reanimation of paralyzed limbs [7, 8], bladder incontinence [9] etc.), hearing loss, movement disorders (Parkinson's [10], Essential Tremor [11] etc), and treatment of chronic pain [12]. Furthermore, clinical diagnostic use of neurostimulation techniques have decreased incidence of neural damage during surgical procedures associated with inadvertent neural damage (laryngeal surgery [13], acoustic neuroma resection [14], hip surgery [15] etc). In total, there are over 100 million candidates worldwide that could benefit from clinical neurostimulation technologies, yet due to the infancy of this field and the limitations from existing stimulation technologies, the market is grossly underserved with less than 1% market penetration [16].

Infrared neural stimulation (INS) is a relatively new neurostimulation technique that has been well characterized in the peripheral nervous system [16-21]. The benefits of INS include high spatially precise stimulation, ability to deliver stimulating light in a contact free interface, and the technique does not generate an electrical stimulation artifact [16]. Furthermore, INS is compatible with magnetic resonance imaging because the technique does not induce electric field effects and the stimulating fiber optic is made of inert silica. These advantages make INS a viable alternative neurostimulation technique to traditional electrical stimulation for research and clinical applications. However, prior to this dissertation, INS had not been translated for stimulation of central nervous system (CNS) structures. Development of this technique for CNS applications will provide an additional tool for researchers and clinicians in furthering our understanding of the nervous system; therefore, the overall objective of this dissertation is to develop and characterize INS as a stimulation modality for *in vivo* stimulation of surface cortical structures using optical and electrical methods to detect INS evoked cortical activity.

1.2 Specific Aims

***Specific Aim (1): Determine feasibility of INS as a stimulation modality for activating cortical neurons in vitro and identify optimal laser parameters for stimulation*.** Rodent thalamocortical brain slices were stimulated with pulsed infrared light generated by the Vanderbilt Mark-III Free Electron Laser to establish feasibility of INS to evoke action potential in cortical neurons. Laser parametric investigations were performed to

determine effects of wavelength, repetition rate, and spot size on stimulation threshold. Ability to record intracellular potentials during INS was also demonstrated.

Specific Aim (2): Establish efficacy of INS for activating rat somatosensory cortex in vivo. Experiments in this aim were designed to utilize optical intrinsic signal imaging (OISI) under 632 nm illumination to characterize INS evoked changes in diffuse reflectance signal acquired from rat somatosensory cortex. The spatial and temporal aspects of INS evoked optical intrinsic signal (OIS) were characterized to assess spatial precision of INS for surface cortical stimulation and was compared to OIS evoked by peripheral vibrotactile stimulation of forepaw and whiskers. Effects of laser radiant exposure and repetition rate were assessed with OISI. Single unit recordings were used to determine functional viability of cortex before and after INS and how INS modulated the underlying neuronal activity evoked by INS.

Specific Aim (3): Investigate the cortical cellular components activated by INS with calcium dye imaging and evaluate INS parameters for evoking calcium signaling in cortical tissue. Experiments in this aim employed intracellular calcium-sensitive fluorescent dye to assess cortical cellular mechanisms activated by INS. Calcium signals evoked by INS were characterized spatially and temporally with wide field imaging and compared against calcium signals evoked by direct electrical stimulation of somatosensory cortex. Cellular contributions to INS evoked calcium signals were determined using the pharmacological agents fluoroacetate (an astrocyte poison) and CNQX (glutamate antagonist). *In vivo* 2-photon imaging was used to confirm findings of

pharmacological experiments. A parametric investigation on laser radiant exposure, repetition rate, pulse width, and stimulation duration was conducted to identify optimal parameters for evoking calcium signals with INS.

Specific Aim (4): Demonstrate feasibility of INS as a stimulation modality in non-human primate cortex. Non-human primate (NHP) cortex represents the closest animal model to human cortex. Implementation of INS in NHPs advances INS towards clinical implementation for cortical stimulation in humans. Optical intrinsic signal imaging and electrophysiology techniques were used to assess feasibility of INS for activation of cortical neurons located in primary visual (VI) cortex of non-human primates. Infrared neural stimulation was also assessed for modulating visually evoked OIS in VI cortex to establish ability of INS to perturb functionally relevant cortical responses. Effects of fiber size were also assessed in these experiments.

1.3 Dissertation Outline

The work in this dissertation is outlined in the following manner. Chapter I introduces the motivation for this research and establishes the significance of this work. The specific aims of the project are also summarized here.

Chapter II provides relevant background information on the topic of this dissertation. Topics include a brief overview of the central nervous system, a description of basic optical properties, an overview of optical imaging methods used in this work, a summary of neurostimulation methods including electrical stimulation, alternative neurostimulation methods, and optogenetics, a detailed discussion on INS including the

underlying mechanisms of stimulation, previous applications of INS, and an introduction to hybrid stimulation. The significance of this work is also discussed.

Chapter III presents the initial feasibility studies of applying INS for cortical stimulation in thalamocortical brain slices. This work was published in the June-July 2010 issue of *IEEE Journal of Selected Topics in Quantum Electronics* [22].

Chapter IV reports on the first *in vivo* CNS application of INS in rat somatosensory cortex as assessed by OISI and electrophysiology techniques. This publication also reports the first observation of inhibition of neural activity with INS. This work was published in the July 2011 issue of *Neuroimage* [23].

Chapter V characterizes the cellular components activated by pulsed infrared light through wide field and 2-photon imaging of calcium-sensitive dyes loaded into somatosensory cortex. Infrared neural stimulation was found to evoke a two component calcium signal that propagated across the surface of cortex. Pharmacological investigations related the evoked calcium transients to both astrocytes and neurons. This is the first report on INS activating non-excitable cells *in vivo*. This work will be submitted for publication to *Nature Communication* in January 2013.

Chapter VI establishes feasibility of INS for stimulating primary visual cortex in Non-human primates. Pulsed infrared light was shown to modulate functionally relevant domains using OISI, and single unit recordings indicated INS evoked excitatory neural activity. This work will be submitted for publication in *NeuroImage* in January 2013.

Chapter VII summarizes the major results discussed in chapters III – VI and the overall objectives of this dissertation. Future studies and societal impact are also discussed.

Appendix A contains supplemental data for Chapter V characterizing the spatial extent of INS evoked calcium signal as well as parametric data for evoking calcium signals with pulsed infrared light.

Appendix B reports on two additional non-human primate studies motivated by Chapter VI. The first study demonstrates that INS evokes cerebral blood volume (CBV) responses in functional magnetic resonance imaging (fMRI) in somatosensory cortex of squirrel monkeys. A manuscript is in preparation for *Nature Neuroscience* to report the fMRI findings. The second study reports on initial awake studies in Macaque monkeys where INS of visual cortex is shown to evoke a behavioral response.

Appendix C reports on the first clinical trial of INS in humans. Safety and efficacy are demonstrated in patients undergoing selective dorsal rhizotomy procedures for treatment of refractive spasticity. This work will be submitted to *Nature Medicine* in January 2013.

1.4 References

[1] Galvani, *Bon. Sci. Art. Inst. Acad. Comm.*, pp. 363-418, 1791.

[2] Fork, R. L., "Laser Stimulation of Nerve Cells in Aplysia," *Science*, vol. 171, pp. 907-908, 1971.

[3] Barker, A. T., "An introduction to the basic principles of magnetic nerve stimulation," *Journal of clinical neurophysiology: official publication of the American Electroencephalographic Society*, vol. 8, p. 26, 1991.

[4] Casey, K. L., Geisser, M., Lorenz, J., Morrow, T. J., Paulson, P., and Minoshima, S., "Psychophysical and cerebral responses to heat stimulation in patients with central pain, painless central sensory loss, and in healthy persons," *Pain*, 2011.

[5] Kim, H., Taghados, S. J., Fischer, K., Maeng, L.-S., Park, S., and Yoo, S.-S., "Noninvasive Transcranial Stimulation of Rat Abducens Nerve by Focused

Ultrasound," *Ultrasound in Medicine & Biology,* vol. 38, pp. 1568-1575, 2012.

[6] Azizi, F., Lu, H., Chiel, H. J., and Mastrangelo, C. H., "Chemical neurostimulation using pulse code modulation (PCM) microfluidic chips," *Journal of Neuroscience Methods,* vol. 192, pp. 193-198, 2010.

[7] Gan, L. S., Ravid, E., Kowalczewski, J. A., Olson, J. L., Morhart, M., and Prochazka, A., "First Permanent Implant of Nerve Stimulation Leads Activated by Surface Electrodes, Enabling Hand Grasp and Release The Stimulus Router Neuroprosthesis," *Neurorehabilitation and neural repair,* vol. 26, pp. 335-343, 2012.

[8] Schiefer, M., Polasek, K., Triolo, R., Pinault, G., and Tyler, D., "Selective stimulation of the human femoral nerve with a flat interface nerve electrode," *Journal of Neural Engineering,* vol. 7, p. 026006, 2010.

[9] Sievert, K. D., Amend, B., Gakis, G., Toomey, P., Badke, A., Kaps, H., and Stenzl, A., "Early sacral neuromodulation prevents urinary incontinence after complete spinal cord injury," *Annals of Neurology,* vol. 67, pp. 74-84, 2009.

[10] Kahn, E., D'Haese, P.-F., Dawant, B., Allen, L., Kao, C., Charles, P. D., and Konrad, P., "Deep brain stimulation in early stage Parkinson's disease: operative experience from a prospective randomised clinical trial," *Journal of Neurology, Neurosurgery & Psychiatry,* 2011.

[11] Kern, D. S. and Kumar, R., "Deep brain stimulation," *Neurologist,* vol. 13, pp. 237-52, 2007.

[12] Tasker, R. R. and Vilela Filho, O., "Deep brain stimulation for neuropathic pain," *Stereotact Funct Neurosurg,* vol. 65, pp. 122-4, 1995.

[13] Brennan, J., Moore, E. J., and Shuler, K. J., "Prospective analysis of the efficacy of continuous intraoperative nerve monitoring during thyroidectomy, parathyroidectomy, and parotidectomy," *Otolaryngology - Head and Neck Surgery,* vol. 124, pp. 537-543, 2001.

[14] Wilson, L., Lin, E., and Lalwani, A., "Cost-effectiveness of intraoperative facial nerve monitoring in middle ear or mastoid surgery," *The Laryngoscope,* vol. 113, pp. 1736-1745, 2003.

[15] Sutter, M., Hersche, O., Leunig, M., Guggi, T., Dvorak, J., and Eggspuehler, A., "Use of multimodal intra-operative monitoring in averting nerve injury during

complex hip surgery," *Journal of Bone & Joint Surgery, British Volume,* vol. 94, pp. 179-184, 2012.

[16] Wells, J., Kao, C., Mariappan, K., Albea, J., Jansen, E. D., Konrad, P., and Mahadevan-Jansen, A., "Optical stimulation of neural tissue in vivo," *Opt Lett,* vol. 30, pp. 504-6, 2005.

[17] Izzo, A. D., Richter, C.-P., Jansen, E. D., and Walsh, J. T., Jr., "Laser stimulation of the auditory nerve," *Lasers in Surgery and Medicine,* vol. 38, pp. 745-753, 2006.

[18] Teudt, I. U., Nevel, A. E., Izzo, A. D., Walsh, J. T., Jr., and Richter, C. P., "Optical stimulation of the facial nerve: a new monitoring technique?," *Laryngoscope,* vol. 117, pp. 1641-7, 2007.

[19] Fried, N. M., Lagoda, G. A., Scott, N. J., Su, L.-M., and Burnett, A. L., "Optical stimulation of the cavernous nerves in the rat prostate," p. 684213 2008.

[20] Jenkins, M. W., Duke, A. R., GuS, DoughmanY, Chiel, H. J., FujiokaH, WatanabeM, Jansen, E. D., and Rollins, A. M., "Optical pacing of the embryonic heart," *Nat Photon,* vol. 4, pp. 623-626, 2010.

[21] Rajguru, S. M., Richter, C.-P., Matic, A. I., Holstein, G. R., Highstein, S. M., Dittami, G. M., and Rabbitt, R. D., "Infrared photostimulation of the crista ampullaris," *The Journal of Physiology,* vol. 589, pp. 1283-1294, 2011.

[22] Cayce, J. M., Kao, C. C., Malphrus, J. D., Konrad, P. E., Mahadevan-Jansen, A., and Jansen, E. D., "Infrared Neural Stimulation of Thalamocortical Brain Slices," *Selected Topics in Quantum Electronics, IEEE Journal of,* vol. 16, pp. 565-572, 2010.

[23] Cayce, J. M., Friedman, R., Jansen, E. D., Mahadevan-Jansen, A., and Roe, A. W., "Pulsed infrared light alters neural activity in rat somatosensory cortex in vivo," *Neuroimage,* vol. 57, pp. 155-166, 2011.

CHAPTER II

BACKGROUND

2.1 Overview of the Nervous System

The nervous system is divided into two primary systems, the peripheral nervous system (PNS) and the central nervous system (CNS) [1]. The CNS is comprised of the brain and spinal cord; and is the primary processing center responsible for interpreting neural signals received from the PNS and generating appropriate responses. The nerves and ganglia (neural somas) located outside the brain and spinal cord comprises the PNS. The primary functions of the PNS is to transduce external stimuli (visual, auditory, touch, pain, etc.), into electrochemical signals before transmitting these signals to the CNS. Additionally, the PNS transmits motor response information from the CNS to effector organs. The autonomic nervous system is a subset of the PNS and CNS and is responsible for controlling bodily functions below the level of consciousness (i.e. heart rate, digestion, thermal regulation etc.). The purpose of this research is to develop infrared neural stimulation (INS) as neurostimulation modality for activating cortical neurons through surface stimulation of the cerebral cortex; therefore, this background on the nervous system will focus on the anatomy and physiology of the cerebral cortex and the cells that comprise it.

2.1.1 Anatomical organization of human cerebral cortex

The cerebral cortex is responsible for higher cognition, generating motor movement, and interpreting sensory information [1]. The cerebrum is composed of white matter that is overlaid with gray matter, the cortex of the brain, which is 1 to 4.5 millimeters thick in humans [2]. Gray matter contains neural cell bodies that are responsible for signal processing in the brain, and the white matter is mainly composed of myelinated axons that transmit information from the cortex to other areas of the brain or to the body to initiate a response. The cerebrum of the brain can be broken down in a series of modules that start grossly and decrease down to individual collection of neurons responsible for specific tasks. Grossly, the cerebrum is divided into two hemispheres and each hemisphere contain lobes with distinct functions. The frontal lobe is responsible for conscious thought, olfactory, generation of speech, and gross motor movements. The parietal lobe integrates sensory information and is responsible for written language. The occipital lobe interprets visual information, and the temporal lobe is responsible for hearing and interpretation of verbal language. Within each of these lobes, further modulation exists with the identification of primary and secondary processing areas. As an example, primary somatosensory cortex can be subdivided into distinct cortical units, including areas 3a/b, 1, and 2. Each of these areas within somatosensory cortex have specific functions. In areas 3a and 2, neurons interpret information concerning proprioception generated by movement of muscles tendons and joints, and in areas 3b and 1 information from cutaneous stimulation is processed allowing for discrimination of fine touch [3]. Furthermore, each of these somatosensory areas contain a representation of the body corresponding to where stimulation at specific locations on the body

generates neural responses and represent another level of modular units within cortex. An example of this high degree of organization is given in figure 2.1, which displays the detailed somatropic organization of Macaque monkey primary somatosensory cortex [4].

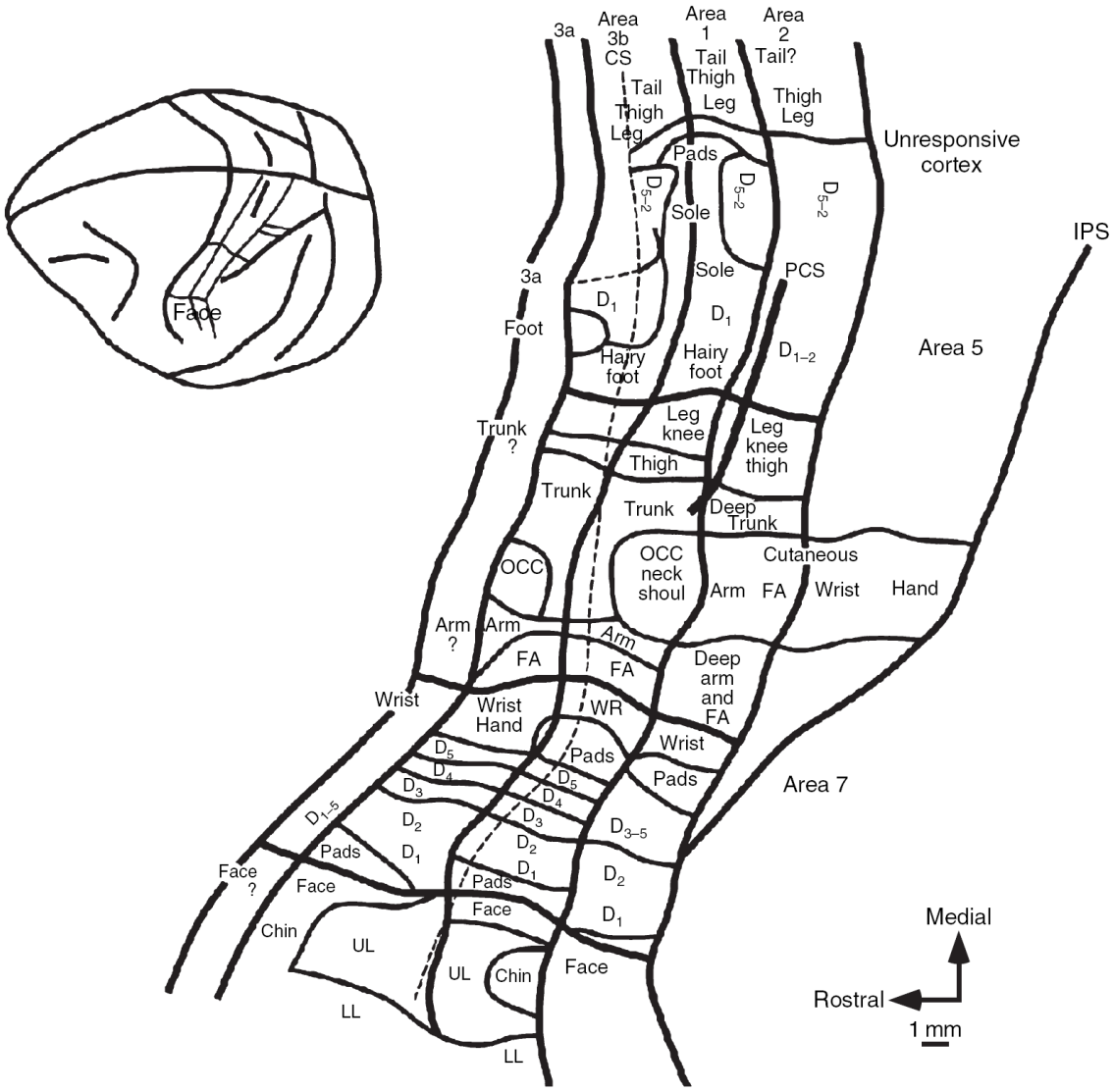

Figure 2.1: Somatotopic organization of anterior parietal cortex in the macaque monkey. Dashed line marks the location of central culcus (CS). D1-D5=digits of hand or foot, UL=upper lip, LL=lower lip, FA=forearm, Should=shoulder; OCC=occiput, Wr=wrist.(from [5]).

This high degree of organization demonstrated for somatosensory cortex is repeated throughout the cortex of the cerebrum. Motor cortex has a similar somatotopic organization to somatosensory cortex for controlling movement [6]. Other examples include the cochleotopic representation of sound frequencies present in auditory cortex and the presence of ocular dominance columns, orientation domains, and color domains in primary visual cortex [7-9]. Also, these highly specific functional modules can be as small as 200 μm in diameter [9, 10]. These highly organized structures observed throughout the cortex of the cerebrum presents an optimal target for developing INS as a stimulation modality for CNS applications.

2.1.2 Cellular anatomy and physiology

2.1.2.1 Neurons

The neuron is the functional unit in the nervous system and is responsible for interpretation of stimuli and communicating responses throughout the body. A basic neuron is comprised of two processes, dendrites and an axon, which are connected to a cell body. Dendrites are responsible for receiving input into a cell, and the axon is the conduit by which output signals from a neuron are transduced to the axon target, another neuron or effector organ. Neurons are classified into three different categories, multipolar, bipolar, and unipolar (Figure 2.2). A multipolar neuron has multiple dendrites that branch out from the cell body and synapse with many different axons from other neurons. Multipolar neurons are typically found in the cortex and are responsible for integration of stimuli received from the periphery and inputs from other neurons located in the brain. Examples of multipolar neurons include pyramidal cells and Purkinje

cells. A bipolar neuron has a single dendrite connected to the cell body on one pole, while the neuron's axon is connected to the cell body on the opposite pole. These cells are primarily responsible for transducing the special senses into electrochemical signals and for serving as inhibitory interneurons in cortex. A unipolar neuron connects the dendrite directly to the axon with the cell body being located at the connection of the two processes. These neurons are mainly found in dorsal ganglion [1].

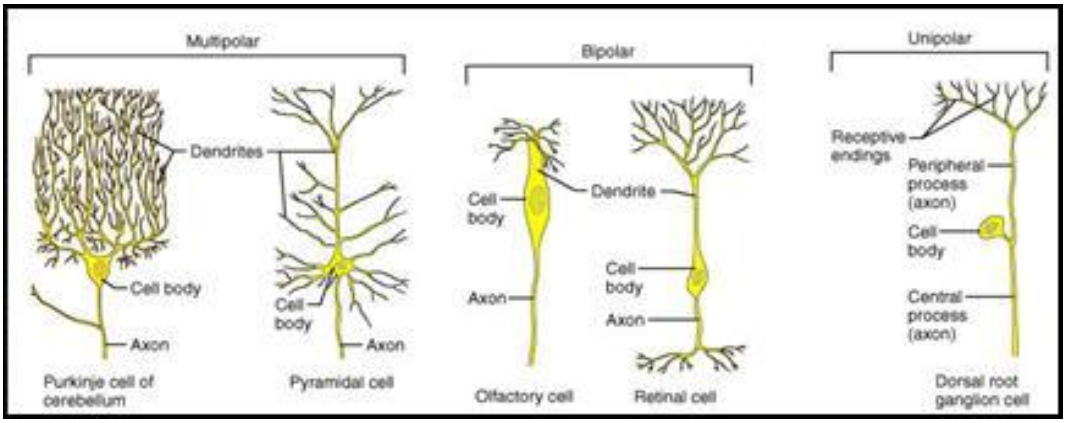

Figure 2.2: Representation of each type of neuron with example cell type [1].

Signals are transmitted to a neuron by depolarizing the membrane through a synapse on the dendrite or cell body by the release of a neurotransmitter [11, 12]. Neurotransmitter released at the synapse binds to a receptor protein on the postsynaptic membrane of the target neuron causing ion channels to open. The two primary neurotransmitters located in the brain are glutamate, for excitation, and GABA, for inhibition. Glutamate receptors can be characterized into two distinct catergories, ionotropic and metabotropic. Ionotropic glutamate receptors open to allow inflow of sodium and calcium (in small amounts) and outflow of potassium from the post-synaptic neuron depolarizing the cell membrane. Metabotropic glutamate receptors are G protein-

coupled proteins that can increase or decrease the excitability of the post synaptic cell through the signaling cascade initiated by the second messenger. Similarly, GABA acts on ionotropic and metabotropic GABA receptors. Activation of an ionotropic receptor ($GABA_A$ and $GABA_C$) allows for flow of chloride ions out of the cell resulting in hyperpolarization of the cell membrane. The metabotropic $GABA_B$ channel causes inhibition through the activation of potassium channels and blockage of calcium channels [13]. Depolarization at a synapse evokes a transient electro-chemical signal which propagates down the neuronal dendrite and cell body towards the axon hillock by opening voltage gated ion channels through temporal depolarization of adjacent sections of membrane [12, 14]. If the transient signal reaches the axon hillock without losing a significant amount of energy, then an action potential will result and propagate down an axon to the next synapse or effector organ. On the other hand, hyperpolarization of the membrane at a synapse inhibits the generation of action potentials. Inhibition only occurs in the brain to assist in higher order processing; however depolarization and action potential generation is seen throughout the nervous system. Some axons in the PNS and CNS have sections covered in myelin sheaths to serve as insulation to increase speed and efficiency of action potential propagation [12].

The neurons that comprise the cortical layers are typically considered either excitatory or inhibitory. Neurons that are classified as excitatory release glutamate and neurons that are classified as inhibitory typically release GABA. Pyramidal cells represent the one of the most common excitatory neurons in the cortex. These cells are characterized by multi-branching dendrites and axons allowing for pyramidal neurons to communicate with thousands of other neurons. Inhibitory neurons are more diverse and

collectively are typically referred to as interneurons as they mainly modulate intracortical signaling [13].

2.1.2.2 Astrocytes

Long considered to be simple support cells to neurons, recent research has indicated that astrocytes play an active role in many cortical metabolic processes [15, 16]. These cells have a complex cytoarchitecture with many processes that branch out into distinct domains with little overlap with adjacent cells. Astrocytes are connected to one another through gap junctions and communicate via calcium signaling [17, 18]. Astrocytes have been shown to maintain homeostasis of glutamate, ion, and water concentrations, assist in neurovascular coupling, energy storage for neurons, scar formation and tissue repair, synapse formation, and modulation of neural activity through neurotransmitter release [16]. This diverse set of functions performed by astrocytes in the cortex highlight their importance to neuronal function.

2.1.2.3 Other glia cells

In addition to astrocytes, a number of other support cells exist in the cortex of the brain. Oligodendrocytes are responsible for myelin generation to insulate axons in the CNS. Radial glial cells are important for serving as a scaffold neuron migration during development of the nervous system. Migrolia cells help to defend neurons from microorganisms and removes dead neuronal cells through phagocytosis. Each of these cells are crucial for proper CNS function [1].

2.1.2.4 Cortical Layers

While there are distinct differences in cellular architecture from region to region, cortex is generally organized into six distinct layer modules. Figure 2.3 summarizes the layers of cortex by illustrating basic neuron anatomy and indicated major layer inputs and outputs [13]. Layer I, the most superficial layer of cortex, is comprised of mainly apical dendritic tufts from underlying pyramidal neurons, astrocytes, and a few stellate (inhibitory) neurons [19]. Layer II is comprised of small pyramidal (excitatory) neurons and stellate neurons, and layer III is comprised of medium sized pyramidal neurons and fewer stellate neurons than layer II [20]. Together, layers I – III form the supragranular layers and are responsible for intracortical processing [21]. Layer IV, the internal granular layer, contains pyramidal and stellate neurons and is the primary input for sensory information coming from the PNS. Layer V is the internal pyramidal layer and contains large pyramidal cells, such as Betz cells in motor cortex, and represents the primary source for efferent signals originating from cortex. Layer VI is the multiform layer and is comprised of pyramidal and fusiform (inhibitory) neurons that send signals to the thalamus forming a closed loop circuit between cortex and thalamus allowing for feedback to the thalamus [21]. Together, these layers of cortex interpret and form responses to stimuli received from the PNS.

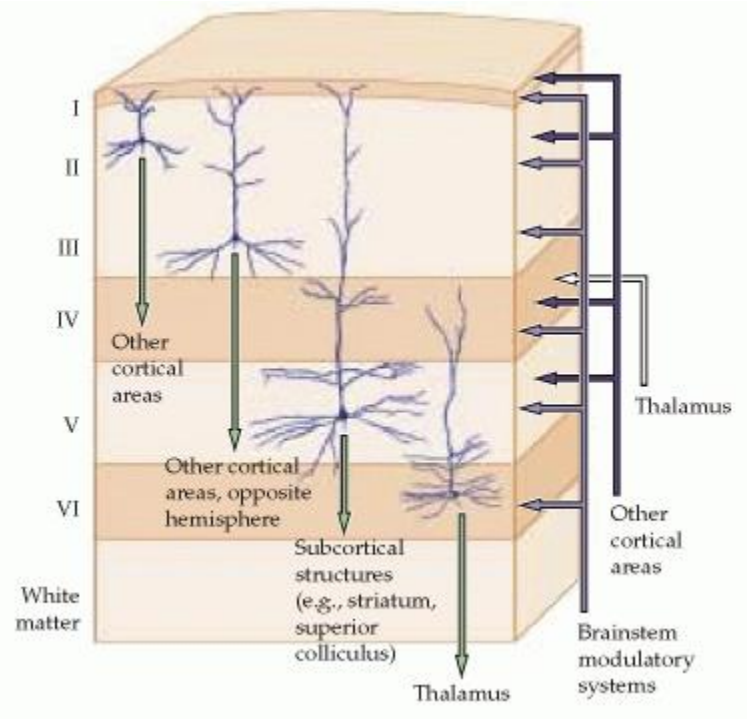

Figure 2.3: Summary of cortical layers illustrating location of neurons, layer inputs, and layer outputs. (from [13])

2.2 Tissue Optical Properties

Optical methods for evoking and detecting neural activity are at the center of this dissertation; therefore a basic understanding light tissue interaction is needed. Light tissue interaction principles in the brain determine how stimulating and imaging light interact with tissue. These factors ultimately determine if tissue will be stimulated (for INS) or signal will be generated (for optical imaging). Incident light on the brain is governed by three main optical properties, the refractive index (which governs specular reflection at tissue boundaries), absorption, and scattering.

2.2.1 Specular reflectance

Specular reflectance occurs when an incident photon strikes the surface of the brain is reflected at the same angle equal to the incident angle of light striking the tissue. This relationship is governed by Fresnel's laws which describes the behavior of light as it moves between different media with different index of refraction (i.e. n_{air}=1.00, $n_{silica=}$1.458 [22], and n_{brain}=1.35 in rats [23]). Specular reflection is a source of background noise in optical imaging data and is minimized through multiple averages and filtering of data [24]. Additionally, specular reflectance also causes losses in incident stimulation light; however these losses are minimal. For example, if we assume the fiber optic is in contact with the surface of the brain and consider the incident angle to be 0^{o}, then Fresnel's equation becomes:

$$R = \frac{n_i - n_t}{n_i + n_t}^2 \quad (1)$$

Where n_i represents the index of refraction of the fiber (n_{silica}) and n_t represents the index of refraction of the brain (n_{brain}), specular reflected loses are only 0.148%.

2.2.2 Absorption

When light enters the tissue, a photon can be absorbed, scattered, or transmitted. In turbid media like brain tissue, the wavelengths of light used in this dissertation for optical imaging and INS are dominated by absorption and scattering and the probability of transmitted photons is essentially zero. Absorption is governed by Beer's law that gives fluence rate as a function of depth in a given media. In cases where scattering is minimal, Beer's law is as follows:

$$E\ z\ = E_O e^{(-\mu_a z)} \quad (2)$$

Where E(z) is fluence rate at depth z [m], E_o is the incident irradiance at the surface [W/m^2], μ_a [1/m] is the absorption coefficient for tissue at a given wavelength. This equation can also be used to determine the penetration depth of incident light which is assumed to be equal to E(z)=1/e or ~ 37% of light irradiance at the surface. An absorbed photon will cause generation of heat, emission of fluorescence, or trigger a chemical reaction; therefore, wavelength choice and tissue properties must be considered when performing optical stimulation or imaging in cortex.

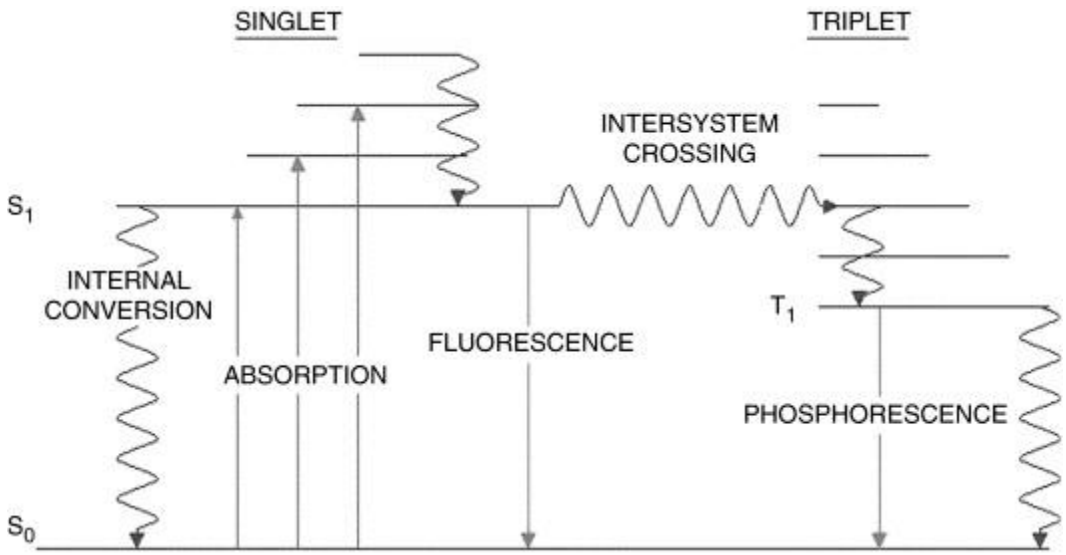

Figure 2.4: Jablonski diagram illustrating possible basic electron transitions that occur with absorption of a photon.[25]

Each absorbed photon has a set energy, $h\nu_a$ where h is Planc's constant and ν_a is the frequency of radiation that is transitioned to the absorbing chromophore through excitation of a ground state electron (S_0) to a higher unstable electron energy level (S1 or S_2). At this point, a Jablonski diagram can be used to better illustrate the possible transitions of an excited electron back to the ground state (Figure 2.4) [25]. In order to return the ground state, the excited electron will undergo one of the following processes: First, the electron will rapidly relax to the lowest energy level of $S_1(0)$ through internal conversion and energy is released in the form of heat. Once at $S_1(0)$, the electron will either undergo internal conversion to the ground state (S_0), transition from S_1 to S_0 with emission of photons (fluorescence), or intersystem crossing that can lead to phosphorescence [26].

2.2.2.1 Photothermal effects

Internal conversion of photon energy into heat is the most common process for dissipating the absorbed photon's energy. The rate of heat generation is defined as the rate and amount of energy deposited into the tissue per unit volume per unit time and is calculated by multiplying eq. 2 by the absorption coefficient (μ_a) where:

$$S\ z\ = \mu_a E_o e^{-\mu_a z} \tag{3}$$

The rate of heat generation S(z) [W/m^3] can then be used to determine the change in temperature due to absorption using the following equation:

$$\Delta T(z) = \frac{S\ z\ \Delta t}{\rho c} \tag{4}$$

Where ΔT is the change in temperature in degrees Celsius or Kelvin, Δt [secs] is the exposure duration to incident light, ρ [g/m^3] is the density of cortical tissue, and c [J/(g K)] is the specific heat constant of cortical tissue. Optically induced thermal gradients are governed by fundamental mechanisms of heat transport. It is important to note that subsequent biological effects (i.e. damage) are governed by rate processes and highlight the importance of exposure duration to incident light. Long duration or high intensity exposures to specific wavelengths of light can lead to tissue damage through a number of processes including, protein denaturation, coagulation, vaporization, melting, or carbonization [27]. Heat dissipation in tissue follows the laws of thermodynamics which

state, energy is conserved and heat flows from areas of high temperature to low temperature. Transport of heat is primarily accomplished through conduction, convection, radiation, and perfusion in cortical tissue [28].

2.2.2.2 Fluorescence

Fluorophores are molecules capable emitting fluorescence when excited by an appropriate wavelength of light. Fluorescence occurs following the absorption of a photon by a fluorophore molecule at its ground state and is excited. Due to internal conversion of an electron to the lowest excitable state of S_1, the emitted photons have a longer wavelength than the excitation photon. Therefore both the excitation and emission spectra of the fluorophore can be considered independent. The duration of fluorescence is typically between 10^{-9} to 10^{-6} seconds [26]. In cortical tissue, there are few endogenous fluorophores, including NADH, flavins, amino acids, elastin, collagen, and retinol, to name a few [29]. Intrinsic fluorescence, typically referred to as autofluorescence, has been used to functionally image cortical neural activation [30, 31], identify cancer margins *in vivo* [32], and image other metabolic pathways in the brain [33]. Exogenous fluorophores have also been developed to identify specific cell types and probe cellular processes. Examples of these applications include imaging neural activity [34, 35], identification of specific cell types [18], and identification of specific pathways in the brain [36].

Phosphorescence occurs when an excited electron undergoes intersystem crossing (Figure 2.4) before emitting a photon when returning to ground state. Intersystem crossing puts electrons in a classical “forbidden state” and this process is slow causing

increased lifetimes of photon emission. The lifetime of phosphorescence is typically 10^{-3} – 100 s; however, phosphorescence is rare and not common in biological tissue [26].

2.2.2.3 Photochemical interactions

Photochemistry employs the use of light as a catalyst to initiate chemical reactions or break molecular bonds. Naturally occurring examples of photochemical interactions include photosynthesis in plants and vitamin D production from sunlight in humans; however, research and medical applications have also benefited from photochemistry. A typical photochemical reaction requires low irradiances (1 W/cm^2) and long exposure times ranging from seconds to tens of minutes. The most successful clinical application of photochemistry is photodynamic therapy (PDT) for the treatment of cancer [37]. Optical uncaging and optogenetic stimulation represent applications of photochemistry in neuroscience research [38].

2.2.3 Scattering

Cortical tissue is highly scattering and complicates light transport in tissue at certain wavelengths. Scattering occurs due to incident light encountering change in index of refraction typically due to discrete particles (cells, organelles, membranes, etc.) in tissue. The scattering coefficient (μ_s) [1/m] explains the scattering properties of a given molecule and is dependent on the wavelength of light. The probability of a photon experiencing one scattering event over an infinitesimal distance (*dz*) [m] is given by the product of the scattering coefficient and *dz*, distance traveled by the photon. When a

photon is scattered, it is also important to know the direction of scatter which is defined by the anisotropy factor (g):

$$g = \text{average } (\cos \Theta) \tag{5}$$

where Θ is the scattering angle. The anisotropy factor ranges between -1 (back scattering) and 1 (forward scattering), and when g = 0 then scattering is isotropic. For cortical tissue, reported anisotropy values are 0.96 (white matter) and 0.88 (gray matter) indicating a predominately forward scatter situation [39]. To account for the direction of scattering, a reduced scattering coefficient is calculated using the following equation:

$$\mu_s' = \mu_s\ (1 - g) \tag{6}$$

The reduced scattering coefficient is typically used in tissue optics because the scattering coefficient and anisotropy factor are coupled preventing the determination of individual values.

2.3 Overview of Optical Imaging Methods

Optical imaging methods for detecting optical signals relevant to neuronal activity were a crucial component for characterizing INS evoked cortical signals discussed in this dissertation. In 1949, Hill and Kernes demonstrated the ability of optical methods to assess neural activity by measuring changes in scattering of white light (birefringence) to detect electrically evoked action potentials in crab nerves [40]. Since this seminal work, a

number of optical based technologies have been developed for probing cortical neural activity. Figure 2.5 summarizes these techniques in terms of spatial resolution, temporal resolution, and imaging depth [41]. As figure 2.5 demonstrates, optical methods can assess neuronal related activity with high temporal and spatial resolution, and certain techniques can resolve depth specific neural activity. These features are ideal for detecting INS evoked activity in the brain. The imaging modalities used during this dissertation will be briefly discussed which include optical intrinsic signal imaging (OISI), fluorescent dye imaging, and 2-photon microscopy.

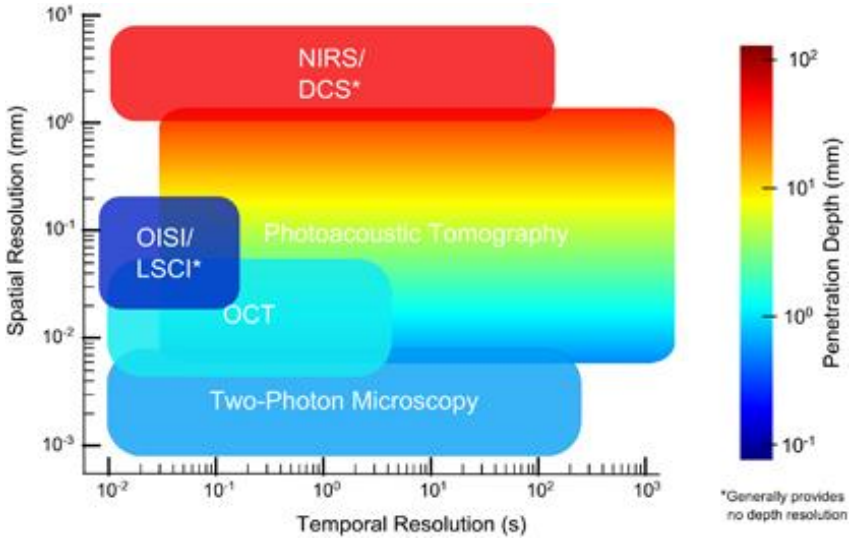

Figure 2.5 Comparison of spatial, temporal, and depth resolution of optical imaging techniques used to assess neural activity [41]

2.3.1 Optical intrinsic signal imaging

Optical intrinsic signal imaging is based on detecting changes in optical signal native to the cortex that is related to metabolic activity of the brain, which in turn can be used as an indirect measure of neural activity. Intrinsic sources useful for optical imaging

of cortex include autofluorescence of flavoprotein and NADH , scattering of light due to cellular or vascular swelling, and absorption of light by intrinsic chromophores (i.e. hemoglobin) [41, 42]. Spatial resolution of wide field OISI is on the order of tens of microns allowing for precise localization of increased metabolic activity and inferred neural activity [43]. In this research, diffuse reflectance imaging was used to visualize optical signals evoked by INS.

Increased neural activity in the brain causes a number of metabolic processes that can be detected by measuring changes in diffuse reflectance of light. These metabolic processes include cellular swelling, vasodilation, and hemodynamic changes, the variation in oxy and de-oxy hemoglobin concentrations, during periods of increased neural activity. Cellular swelling and vasodilation increases scattering of photons while hemodynamics primarily affect absorption of photons. Figure 2.6 displays the absorption spectrum of oxy and de-oxy hemoglobin and brain tissue scattering as a function of wavelength [42].

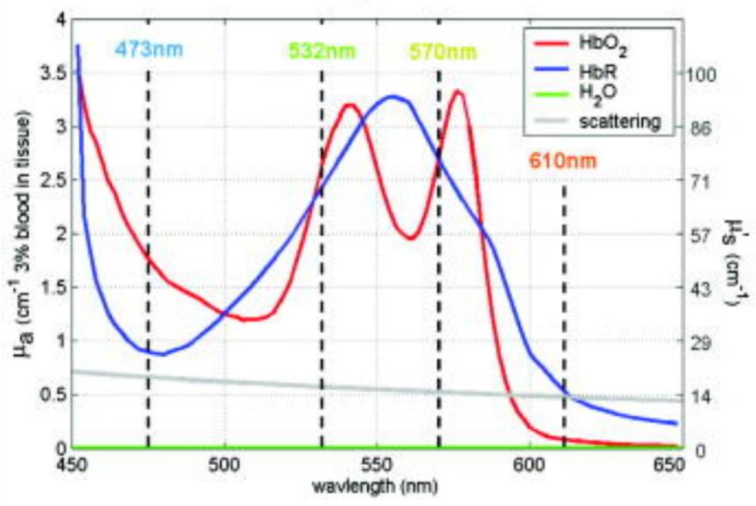

Figure 2.6: Absorption spectrum of oxy and de-oxy hemoglobin and approximate scattering spectrum of brain tissue (modified from [42])

Specific wavelengths can be chosen to image hemodynamic changes that are sensitive to either oxy (i.e. 473 nm) or de-oxy hemoglobin (i.e. 632 nm) or the total hemoglobin signal (i.e. 532 nm). Functionally relevant signal can be obtained with one wavelength or multi-wavelength imaging can be used to obtain each individual hemodynamic component to calculate an overall picture of the hemodynamic changes evoked by stimulation [41, 42]. Overall, a wide spectrum of visible wavelengths have been used to detect hemodynamic changes [44]. The change in diffuse reflectance signal evoked by increased neural activity is typically on the order of 0.1% and the duration of the signal is on the order of seconds. This duration is significantly slower than the fast firing rates of neurons which are measured in milliseconds; however, multiple studies have established strong correlations between changes in diffuse reflectance and increased neural activity [45-48].

The mechanisms describing neurovascular coupling responsible for generating the hemodynamic signal is complex and is still debated by the optical imaging and neuroscience communities. The traditional theory assumes that neurons directly generate a metabolic signal (i.e. decrease in O_2 or glucose concentrations) that triggers vasodilation in a negative feedback process [49]. A separate more accepted theory uses a feed-forward mechanism that assumes neurons signal directly to blood vessels or astrocytes to increase blood flow [50, 51]. Research supporting this theory has shown that neurons release vasodilators, such as nitric oxide, that dilates blood vessels [52-55]. Additionally, several studies have implicated astrocytes as being responsible for controlling vasodilation and vasoconstriction [56-59]. This vast array of vasodilation mechanisms that have been identified through research suggest that these mechanisms are

synergistic indicating both neurons and astrocytes directly modulate cortical blood flow further highlighting the complexity of neurovascular coupling.

The fine spatial scale of OISI methods and the absence of a requirement for exogenous agents represent the major strengths of this technique. Additionally, OISI instrumentation requires only a light source and a CCD camera sensitive to the illumination light to detect changes in diffuse reflectance signal, and optical imaging systems can be built relatively inexpensively [60]. These methods have been used to visualize the modular organization of cortex throughout the brain. Examples include somatotropic organization of primary somatosensory cortex [61-64], hemodynamic changes related to electrical stimulation in motor cortex [65, 66], topographic organization of auditory cortex [67, 68], and in visual cortex where OISI methods visualize the complex modular organization with fine spatial precision [8, 9, 64, 69, 70]. Additionally, OISI methods have been used to identify neuronal connectivity from primary cortex to higher order processing areas in a number of different applications [71-76]. These diverse applications of OISI highlight the importance of the tool in neuroscience for furthering our understanding of cortical function.

2.3.2 Fluorescent dye –based imaging

As described previously OISI only reports on increased metabolic activity and changing hemodynamics that can indirectly be related to neural activity. These methods require exogenous dyes that are sensitive to a specific biological marker, typically membrane voltage or ion concentrations, to be applied to cortex. These fluorescent dyes change their fluorescence due to changes in the specified biological marker and represent

a more direct measure of neural activity [77, 78]. Wide field optical imaging of these signals is similar to the methods used for OISI where the only additional instrumentation required is an emission filter to isolate fluorescence emission. The spatial resolution of these responses is on the same order as those for OISI; however, the temporal resolution is on the order of milliseconds, the same timescale as neural firing (Figure 2.7) [79, 80]. The primary classifications of fluorescent dyes used to optically image cortical tissue are voltage sensitive dyes (VSD) and ion sensitive dyes.

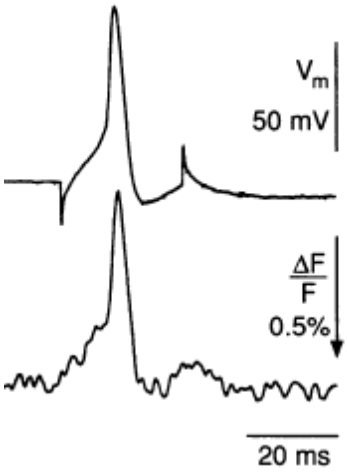

Figure 2.7: Intracellular recording of an evoked potential compared to change in fluorescence reported by voltage sensitive dye. (modified from [80])

Voltage sensitive dye imaging represents the oldest form of *in vivo* wide field optical imaging and predates OISI [79, 81]. Cortex is typically stained with VSD through topically application of the dyes on cortex. The dye molecules bind to the cell membranes without disrupting normal cellular function and report cell membrane potential changes through changes in emitted fluorescence when excited by appropriate wavelengths of light [79]. Voltage sensitive dye imaging methods have been used in a wide variety of

applications revealing the dynamics of cortical processing with high temporal resolution and have allowed for functional connectivity in greater spatial detail than what is possible with OISI [82-84].

Fluorescence imaging with ion sensitive dyes can be used to visualize both neural and astrocyte activity. Dye molecules that are loaded into cells, via direct injection or passive diffusion, report on intracellular ionic concentrations through changes in fluorescence [42]. Fluorescent dyes for detecting ion concentration gradients have been demonstrated for sodium [85], potassium [86], and chloride [87]; however the most widely applied fluorescent probe sensitive to ion gradients are calcium sensitive dyes [88]. The fluorescence signal associated with calcium sensitive dyes is generally stronger and are more reliable than VSDs [42, 79, 89]. Applications of calcium sensitive dyes include wide field imaging of cortex [60], selective detection of dendritic calciums signals [90, 91], and calcium dyes are routinely used to characterize astrocyte signaling [18, 92].

2.3.3 Two-photon microscopy

The development of two-photon microscopy allowed for individual cell processes and function to be visualized, and has had significant impact on the neuroscience community [93]. Two-photon microscopy relies on the concept of two-photon excitation where two photons excite a fluorophore simultaneously resulting in emission of fluorescence. The two photons used to excite the fluorophore have approximately half the energy of photons typically needed to evoke fluorescence emission. This feature of two-photon microscopy allows longer wavelengths of light that penetrate deeper into tissue, to

be used to evoke fluorescence signals in cortex. To evoke two-photon excitation, light from a femtosecond laser is focused through a high numerical aperture microscope objective down to a diffraction limited point where fluorescence generation is almost exclusive in a volume as small as $0.1\mu m^2$ [94, 95]. This highly localized two-photon fluorescence allows for 3-D microscopy of tissue with subcellular spatial resolution and measurement of cell specific signaling (figure 2.8) [96]. These features have proven useful in many neuroscience applications including imaging networked neural activity [97], dendritic spine development and dynamics [98], neurovascular coupling [99], and astrocyte signaling [18].

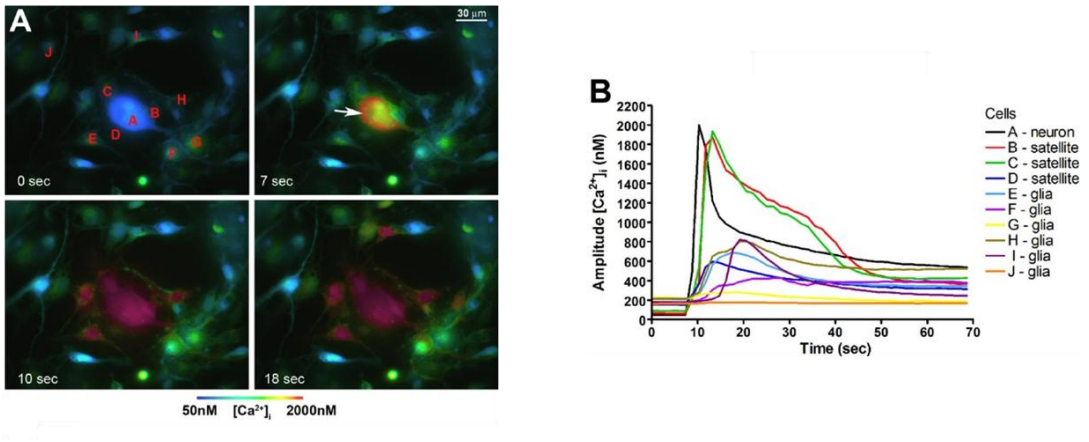

Figure 2.8 Two-photon calcium imaging of neural and astrocyte activity. A.) Individual neurons and glial cells are resolved with two photon imaging. B.) Calcium signal resolved from specific cells with two-photon microscopy (modified from [96]).

2.4 Overview of Neural Stimulation

2.4.1 Electrical stimulation

Electrical stimulation has been the gold standard for stimulating neurons for both clinical and basic research applications for nearly two centuries. Neurons are activated by electrical stimulation through the flow of current between a cathode and anode placed on or near the target neural tissue. The injected current depolarizes the cell membrane through induction of ionic current that flows across the membrane. Once the membrane potential of the neuron reaches its threshold potential voltage-gated ion channels open and generate action potentials that propagate down the axon of the stimulated neuron [11, 12, 100, 101]. Electrical stimulation parameters are well characterized and can be tailored to specific applications providing a robust methodology for neurostimulation; however, electrical stimulation can be limited by inherent electrical field spread activating unwanted neural tissue, generation of stimulation artifact that can mask relevant neuronal signals, and electrodes must contact or impale tissue increasing risks for damage [6, 7]. In order to address these limitations, researchers have developed innovative alternative neural stimulation modalities.

2.4.2 Alternative methods for neural control

Complementary neurostimulation techniques to electrical stimulation have been developed using ultrasound, magnetic, and optical approaches over the past 50 – 60 years. Ultrasound neural modulation has been investigated for over 60 years [102] and modulates neural activity through delivery of focused ultrasound to targeted neural tissue

non-invasively [103]. Focused ultrasound has been reported to both inhibit and excite neural tissue, and the mechanism behind ultrasound stimulation of neural tissue is thought to be a combination of a thermal mechanism and an unidentified secondary mechanism [104]. Magnetic stimulation of neural tissue has been studied for diagnostic and therapeutic applications for over two decades [105]. Neurostimulation with magnetic fields has primarily focused on transcranial stimulation using large magnetic coils positioned over the scalp that generate large time varying magnetic fields which induce a local electric field effect modulating neural activity [106]. Recent advances in the field of neuro-magnetic stimulation have demonstrated the ability of miniaturized magnetic coils (500 μm in size) to evoke action potentials in retina ganglion cells without physical contact; however the magnetic fields induce large stimulation artifacts on recording electrodes [107]. While these alternative neurostimulation modalities have shown promise in overcoming specific limitations of electrical stimulation, these techniques do not exhibit the same level of spatial and temporal precision that has been characterized for optical based neurostimulation methods.

The ability of light to stimulate or modulate neural activity has been known for several decades [108-111], but recent discoveries have established the potential of optical techniques to be viable neurostimulation methods for furthering our scientific understanding and highlight the potential preclinical use in diagnostic and therapeutic applications. In 2005, the first reports of optogenetic stimulation [112] and infrared neural stimulation [113] were presented and both techniques have rapidly developed into accepted neurostimulation modalities.

2.4.3 Optogenetics

The field of optogenetic stimulation was discovered by Boyden and colleagues when they demonstrated the ability to transfect genetic material for coding photosensitive channelrhodopsin-2 cation channels into cortical neurons and activate the transfected neurons using visible light [112, 114]. Figure 2.9 represents an example recording of neurons expressing channelrhodopsin-2 cation channels and demonstrates that pulsed visible light is capable of driving the genetically modified neuron in a pulse to pulse fashion for multiple repetition rates without generation of a stimulation artifact [114]. Optogenetic stimulation has revolutionized the field of neuroscience by allowing scientists to target individual populations of neurons to study specific disease processes or behaviors present in humans using animal models [115]. Additionally, targeting strategies for virus delivery using multiple opsins allow researchers to excite or inhibit individual neural circuit components in the same animal [116]. These techniques associated with optogenetics have allowed researchers to better understand the neural circuitry underlying fear and anxiety disorders [117, 118], addiction [119], autism [120], schizophrenia [121], Parkinson's disease [122], epilepsy [123], and sleep disorders [124].

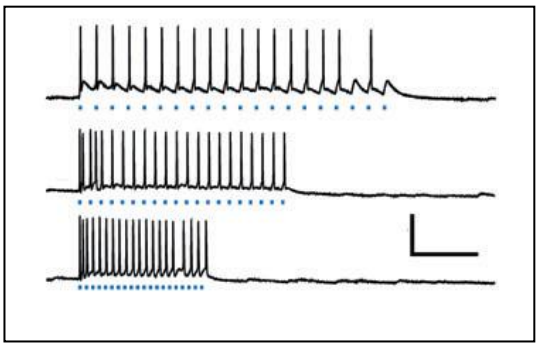

Figure 2.9: Optogenetics stimulation of rodent hippocampal neurons expressing channel rhodopsin 2 photosensitive ion channels at 20, 30, and 50 Hz (Scale bars: 50 mV and 200 ms). (Modified from [125])

Recent advances in human gene transfer indicate a promising future for applying optogenetic neural stimulation in humans. Pilot clinical trials have reported successful transfection of human cells with adeno-associated virus (AAV) to treat patients with vision deficiencies [126] and hemophilia [127]. Additionally, AAV was recently used to transfect human retinas *ex vivo* to express halorhodopsin, a light sensitive chloride pump, and demonstrate the ability to evoke photocurrents in transfected human photo receptors [128]. While these advances in human gene transfer and optogenetics is promising, a number of ethical and technical challenges must be addressed before widespread application of optogenetics in humans can be realized [129].

2.4.4 Infrared neural stimulation

Unlike optogenetics, infrared neural stimulation (INS) relies on intrinsic mechanisms to evoke action potentials in neural tissue with pulsed, low-intensity infrared light [113, 130]. Infrared neural stimulation has been shown to activate nerves with high spatial precision without generating a stimulation artifact. Additionally, INS can be performed with a contact free interface that eliminates risks of damaging tissue from direct contact with a stimulating fiber. These advantages of INS highlight the potential of the technique for CNS applications.

The seminal work characterizing the ability of infrared light to stimulate neural tissue was conducted in the rat sciatic nerve. In these studies, pulsed infrared light at a number of wavelengths was found to evoke compound nerve and muscle action when stimulation was applied to the nerve. The INS evoked potentials were found to be spatially precise routinely activating only one muscle group. Figure 2.10 compares INS

evoked signals to those evoked by electrical stimulation in sciatic nerve [131]. Electrical stimulation of the sciatic nerve was found to evoke action potentials in both the gastrocnemius and biceps femoris fascicles (Figure 2.10a); whereas INS at the same location only stimulated axons located in the gastrocnemius fascicle (Figure 2.10b). A primary characteristic to note between electrical and INS evoked responses is the magnitude of the evoked neural responses where the electrically evoked signal is ten times larger than the response evoked by INS. The lower magnitude of the INS evoked response indicates the pulsed infrared light activated fewer axons illustrating the high spatial precision of INS. Furthermore, an electrical stimulation artifact is noted in both recordings in figure 2.10a whereas, no stimulation artifact is observed in the recording acquired during INS (Figure 2.10b). Stimulation artifacts can mask relevant neural signal and prevents electrical stimulation and recording to take place at the same location. The lack of stimulation artifact associated with INS highlights the potential of this stimulation modality to stimulate and record evoked potentials at the same location, a potentially important tool for CNS applications [131].

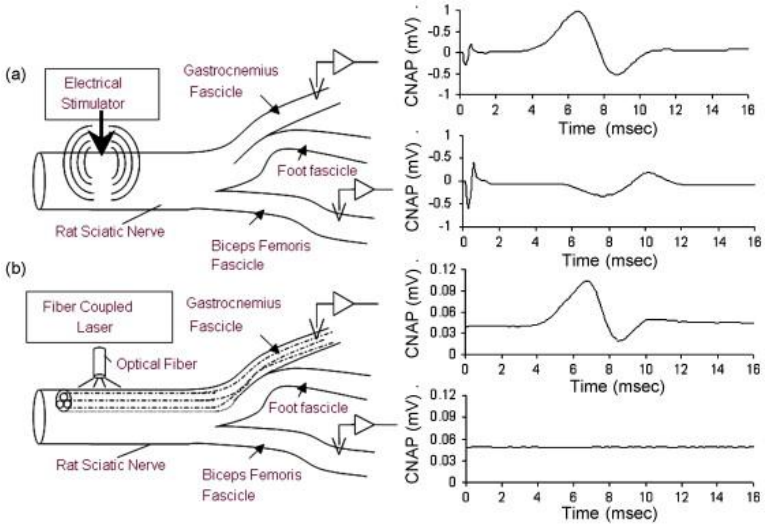

Figure 2.10: Demonstration of the advantages of INS as compared to electrical stimulation. (A.) Threshold electrical stimulation of the sciatic nerve activates axons in multiple sciatic nerve fascicles. (B.) Threshold INS at the same location of electrical stimulation where activation is seen only in the gastrocnemius fascicle (from [131]).

2.4.4.1 Mechanisms of INS

The initial studies for characterizing INS used the wavelength-tunable free electron laser (FEL) (2000-6000 nm) and the holmium:YAG laser (2120nm). These studies demonstrated that for extraneural stimulation of mammalian peripheral nerves INS was dependent on the water absorption spectrum, as water is the dominant tissue absorber in the infrared and light-tissue interactions become absorption dominated for these wavelengths [130]. Infrared neural stimulation has also been performed as shorter wavelengths including, diode lasers at 1850-1890 nm [132] and 1455 nm [133]. The common factor between all demonstrated wavelengths for INS of neural tissue is the similar absorption coefficients at each wavelength which correspond to an approximate penetration depth of 300 – 600 μm in tissue [134].

Wells et al. determined the underlying biophysical mechanism behind INS through a series of experiments and deductive reasoning that tested each of the four possible interactions between infrared light and axons that could evoke action potential propagation [135]. The four interactions considered were electric field, photochemical, photomechanical, and photothermal effects. Electric field effects were tested by first calculating the space varying electric field of light at 2120 nm which determined the maximum theoretical current induced by the light was l0.05 mA/mm^2, well below stimulation thresholds identified for the surface electrical stimulation (0.95±58 A/cm^2) [135]. Experimentally, electric field effects were ruled out by attempting stimulation with an alexandrite laser operating at 750 nm compared to a holmium:YAG laser (2120 nm) that was known to stimulate. All parameters were the same in these experiments with the exception of wavelength. The wavelength change to 750 nm decreased the absorption coefficient from 3 cm^{-1} to 10^{-4} cm^{-1} switching the process to a scattering dominated process. The alexandrite laser was found to not stimulate up to 150 times the stimulation threshold of the holmium:YAG; however once damage threshold was reached and changes in tissue optical properties began to promote absorption, the alexandrite laser began stimulating [135]. This finding supported an absorption driven process being responsible for INS evoked neural activity. Photochemical effects were eliminated based on the fact that infrared photons have low photon energy (<0.1 eV) which is too low to drive photochemical reactions, and photomechanical effects were eliminated by failure to stimulate with a piezoelectric actuator calibrated to deliver pressure waves equal to the minimal pressure waves induced during INS due to thermal expansion of the nerve.

Through process of elimination, the only remaining mechanism for INS evoked action potentials were photothermal interactions [135].

The photothermal mechanism behind INS was further characterized through a number of experiments by Wells et al. [135]. Action potential generation was found to occur only after the entire pulse of light had been delivered. This indicate that neural tissue must sustain a minimal thermal change before action potentials are generated and predicts that longer pulses will not evoke neural signals due to thermal diffusion [135]. In the sciatic nerve, the minimal thermal gradient needed to evoke an action potential was a change in temperature equal to 6 ^{o}C at the surface; however at the depth of the axons within the nerve, the minimal predicted temperature change for evoking neural activity is approximately 2 ^{o}C [135].

While the thermal basis for INS is well established, the exact mechanism by which the thermal energy is transduced into action potentials was initially not well understood. However, recent studies have identified specific mechanisms through which thermal energy modulates neural activity. Two groups have identified excitatory mechanisms where one group demonstrates INS depolarizes cell membranes through local membrane capacitance changes [136] and the other group demonstrates direct activation of heat sensitive transient receptor potential vanilloid-related (TRPV) channels [137]. A separate study has also proposed a thermal based mechanism that inhibits action potential propagation [138].

Shapiro and colleagues recently demonstrated the ability of pulsed infrared (1889 nm) to depolarize cell membranes through changing the membrane capacitance [136]. Pulsed infrared light was shown to evoke inward currents in wild-type *X. laevis oocytes,*

and in human HEK cells. This was an interesting finding as these cells are considered non-excitable. The INS evoked current was not blocked by a variety of pharmacological conditions including ion channel blockers, transport blockers, or changing the ionic content of the extracellular bath; however replacing the H_2O in the extracellular bath with heavy water (D_2O) decreased these inward intracellular currents by 65.3±4.1 % in oocytes and 75.8±12.6% in HEK cells. This finding led Shapiro and colleagues to investigate possible membrane based mechanisms and the experiment was repeated in artificial lipid bilayers demonstrating the same results with D_2O decreasing the inward currents by 79.3±12.6 %. These findings confirm the role of water absorption in the mechanism of INS as the decrease in current amplitudes was due to decreased absorption of light D_2O at 1889 nm and led to the hypothesis that infrared induced temperature gradients caused changes in membrane capacitance that are proportional to the inward current [136]. To test the hypothesis, capacitance changes were measured in both artificial lipid bilayers and HEK cells where a dose dependent capacitance change was observed. To further support these findings, the capacitance change was modeled with a modified version of the Gouy-Chapman-Stern theory of double layer capacitors where temperature terms are needed to explain membrane capacitance [139]. This model was used to reproduce experimental results confirming the ability of infrared light to depolarize lipid membrane bilayers by inducing changes in membrane capacitance [136]. This finding is important to INS overall as it suggests that any cell membrane can be depolarized regardless of innate "excitability" of a given cell.

Direct activation of TRPV channels I-IV offer another possible mechanism behind INS evoked action potentials. TRPV channels are thermally sensitive cation

(Ca^{2+}, Na^{+}) channels located throughout the nervous system [140-142], and have been shown to be activated by slow thermal gradients (120 seconds) applied to cultured neurons [143]. Recently, Albert and colleagues demonstrated that INS evoked action potentials in retinal and vestibular ganglion cells were generated through activation of TRPV IV channels [137]. Their findings showed that the INS evoked potential were dependent on presence of calcium and that the TRPV channel antagonist ruthenium red completely blocked INS evoked potentials. The involvement of TRPV channels is not surprising as the fast thermal gradient generated during INS raises the temperature to above threshold temperature for TRPV channel activation [135]. These findings are the first to confirm involvement of specific ion channels in generating infrared evoked neural activities

While two mechanisms have been identified to explain excitatory neural activity evoked by INS, a separate study has identified a theoretical method by which action potential propagation is inhibited in the presence of spatially localized heating. Mou and colleagues demonstrated local temperature increases induced by a 1550 nm diode laser increased electrical stimulation threshold in excised *Xenopus laevis* sciatic nerves [138]. The mechanism credited for action potentials block is known as “heat block” and was first characterized by Hodgkin and Katz in 1949 [144]. In this model, increases in temperature accelerates the rate of change in the gating-mechanisms responsible for action potential generation; however in heat block, the rate of acceleration for the inactivation of sodium channels and activation of potassium channels overtake the rate of sodium channel activation. This phenomenon will theoretically block action potential propagation. Modeling of the *Xenopus laevis* data showed that temperature increases at

individual nodes of Ranvier blocked action potential propagation and that the required temperature changes were in physiological safe ranges (30-40 ^{o}C); however Mou and colleagues did not provide experimental evidence of complete blockage of action potential propagation [138]. Recently, Duke et al. has demonstrated the ability to specifically block single unit propagation in *Aplysia* bucal nerves with high spatial precision and without effecting propagation of single units in neighboring axons [145]. This finding confirms the ability of pulsed infrared light to inhibit propagating neural activity.

The overall mechanism responsible for INS evoked potentials is complex. The capacitance mechanism indicates pulsed infrared light will depolarize any cell membrane regardless if ion channels are present or not. This mechanism can therefore be applied universally to all cells and suggests other "non-excitable" cell types can be depolarized. Confirmation of TRPV channel sensitivity identifies the first transmembrane gated ion channel that is sensitive to INS. This indicates that cells, i.e. neuron and astrocytes, expressing TRPV channels will be more sensitive to INS. The mechanisms of "heat block" show that action potential propagation can be inhibited by pulsed infrared light and further complicates the mechanistic picture. In the brain, all three of these mechanisms are likely involved in INS modulated activity.

2.4.4.2 Applications of INS

Since the seminal paper characterizing INS as a stimulation modality in the rat sciatic nerve, pulsed infrared light has been used to stimulate neural tissue in a wide variety of applications. In this section, applications of INS for neural stimulation will be

briefly summarized. Infrared neural stimulation has been applied to clinically relevant applications including neural monitoring, functional cochlear stimulation, and cardiac pacing.

Neural monitoring represents the first targeted clinical application for INS. Intraoperative neural monitoring with electrical stimulation can sometimes lead to misdiagnosis of neural tissue leading to neurological deficit postoperatively. The work that initially characterized INS for stimulation of peripheral nerves also demonstrated the ability to functionally map the rat sciatic identifying the topographic organization of individual fascicles [131]. This demonstration identified the potential of INS for neural monitoring. Since this study, others have developed INS techniques for stimulating the facial and cavernous nerves. Facial nerve monitoring with INS demonstrated the ability to selectively activate compound muscle potentials in individual nerve bundles showing the same selectivity demonstrated for the sciatic nerve. The facial nerve was stimulated at radiant exposures between 0.71 – 1.77 J/cm^2 and damage was not observed until 2.0 J/cm^2. Furthermore, INS was shown to stimulate through fascia covering the nerve using between 0.88 – 1.77 J/cm^2 which further reduces the invasiveness to the nerve by INS [146]. Extensive research for applying INS to identify cavernous nerves surrounding the prostate during prostatectomies has recently been reported. Fried et al. first demonstrated the ability of pulsed infrared light to evoke intracavernosal pressure changes using a wavelength between 1860 – 1870 and radiant exposures greater than 0.35 J/cm^2 at repetition rates of 10 Hz [147]. Additional work by this group has led to the development of a laparoscopic probe with a collimated output that have been shown to stimulate cavernous nerves over a 20 mm working distance effectively establishing feasibility for

clinical studies for neural monitoring during prostatectomies [148]. Fried's group has also recently demonstrated the ability to stimulate the cavernous nerve through overlaying fascia with a similar thickness to the connective tissue seen during human prostatectomies [149]. The successful application of INS for stimulating the sciatic, facial, and cavernous nerves suggests that neural monitoring can be performed on a wide array of peripheral nerves.

One of the most developed applications of INS aimed at clinical use is stimulation of auditory ganglion cells for improved cochlear implants [150]. In these studies, INS was shown to activate auditory spiral ganglion cells with high spatial precision comparable to low level acoustic tone evoked potentials. Optimal laser parameters for activation of auditory spiral ganglion cells require short pulse width (35 μs) and low radiant exposures (mJ/cm^2) [132]. Additionally, INS evoked responses were shown to propagate to the inferior colliculus verifying the optically induced signals reached higher processing areas of the auditory system and demonstrated that activation evoked by optical stimuli is comparable to that produced by acoustic tones [151]. Recently, successful implantation of a fiber optic in the cat cochlear and successful INS for ten hours a has shifted the research towards development of chronic optical based cochlear implants [152].

Cardiac pacing with pulsed infrared light represents another potential clinical application of INS techniques. Recently, Jenkins et al. demonstrated the ability of pulsed infrared light to pace embryonic quail hearts *in vivo* with a contact free interface [153]. Threshold for pacing the embryo heart was determined to be 0.81 ± 0.01 J/cm^2, and laser pulsed locked pacing was demonstrated at 2 and 3 Hz. Additionally, initial analysis of

damage associated with infrared irradiation indicated that stimulating radiant exposures (i.e. 0.88 J/cm^2) did not cause damage [153] indicating that pulsed infrared light can be safely used to stimulate embryo hearts [153]. These findings show that cardiac pacing is possible and identifies the possibility of optic based pacemakers for the adult human heart.

2.4.4.3 Hybrid stimulation

Hybrid stimulation is the combination of sub-threshold electrical stimulation with sub-threshold INS and aims to take advantage of the robustness of electrical stimulation techniques while preserving the high spatial precision of INS. This concept has recently been characterized in the rat sciatic nerve and *Aplysia* buccal nerves. Hybrid stimulation thresholds showed a three-fold decrease in radiant exposures needed to stimulate compared to INS alone [154]. The demonstrated three-fold decrease in radiant exposures significantly reduces the likelihood of damage from infrared irradiation. Further characterization of this technique to control for temporal and spatial variations improved the reliability of hybrid stimulation allowing for physiologically relevant studies to be performed [155]. Hybrid stimulation was recently demonstrated to evoke functionally relevant muscle contractions, signifying the first functionally relevant response in a peripheral nerve evoked by pulsed infrared light [156]. This finding demonstrates possible utility for inclusion in future neuroprosthetic devices as hybrid techniques offer higher degrees of spatial control than electrical stimulation alone.

These highlighted clinically relevant applications of INS and hybrid stimulation demonstrate the applicability of the technique for stimulating a vast array of excitable

tissue. The clinical potential of INS in the brain is high and motivates translation of INS to the central nervous system applications.

2.5 Significance

Development of INS as a stimulation modality for CNS applications will provide a new tool for neuroscientist and clinicians for perturbation of cortical neural circuitry. The associated high spatial precision of INS will allow for eloquent mapping of cortical areas. Artifact free stimulation indicates neural recordings can be acquired closer to the site of stimulation and may reveal previously masked neural signals; and the contact free interface allows INS to be less invasive than electrical stimulation for surface stimulation of cortical structures further supporting potential clinical utility. Additionally, the different mechanism of INS compared to electrical stimulation may allow for activating neural support cells (i.e. astrocytes) present in the CNS. This dissertation represents the first step in developing INS as a neurostimulation modality for activating structures located in the CNS.

2.6 References

[1] Guyton, A. C. and Hall, J. E., *Medical Physiology*, 11 ed. Philadelphia, 2006.

[2] Fischl, B. and Dale, A. M., "Measuring the thickness of the human cerebral cortex from magnetic resonance images," *Proceedings of the National Academy of Sciences*, vol. 97, pp. 11050-11055, 2000.

[3] Ruben, J., Schwiemann, J., Deuchert, M., Meyer, R., Krause, T., Curio, G., Villringer, K., Kurth, R., and Villringer, A., "Somatotopic organization of human secondary somatosensory cortex," *Cerebral Cortex*, vol. 11, pp. 463-473, 2001.

[4] Krubitzer, L. A. and Kaas, J. H., "The somatosensory thalamus of monkeys: cortical connections and a redefinition of nuclei in marmosets," *The Journal of Comparative Neurology*, vol. 319, pp. 123-140, 2004.

[5] Qi, H. and Kaas, J., "Somatosensory areas of the cerebral cortex: architectonic characteristics and modular organization," *The Senses: A Comprehensive Reference. London, Elsevier,* vol. 6, p. 143, 2008.

[6] Rao, S. M., Binder, J., Hammeke, T., Bandettini, P., Bobholz, J., Frost, J., Myklebust, B., Jacobson, R., and Hyde, J., "Somatotopic mapping of the human primary motor cortex with functional magnetic resonance imaging," *Neurology*, vol. 45, pp. 919-924, 1995.

[7] Sharma, J., Angelucci, A., and Sur, M., "Induction of visual orientation modules in auditory cortex," *Nature,* vol. 404, pp. 841-847, 2000.

[8] Lu, H. D. and Roe, A. W., "Optical imaging of contrast response in macaque monkey V1 and V2," *Cerebral Cortex,* vol. 17, pp. 2675-2695, 2007.

[9] Lu, H. D. and Roe, A. W., "Functional Organization of Color Domains in V1 and V2 of Macaque Monkey Revealed by Optical Imaging," *Cerebral Cortex,* vol. 18, pp. 516-533, 2008.

[10] Horton, J. C. and Hocking, D. R., "Intrinsic Variability of Ocular Dominance Column Periodicity in Normal Macaque Monkeys," *The Journal of Neuroscience*, vol. 16, pp. 7228-7339, 1996.

[11] Hille, B., *Ion Channels of Excitable Membranes*, 3 ed. Sunderland, MA: Sinaure Associates, 2001.

[12] Plonsey, R. and Barr, R., *Bioelectricity: A Quantitative Approach*, 2 ed.: Kluwer Academic, 2000.

[13] Purves, D., Augustine, G., and Fitzpatrick, D., *Neuroscience*, 2 ed. Sunderland, MA: Sinauer Associates, 2001.

[14] Cole, K., "Membranes, Ions, and Impulses: A Chapter of Classical Biophysics," ed Berkely: University of California Press, 1968, p. 569.

[15] Fiacco, T. A., Agulhon, C., and McCarthy, K. D., "Sorting out astrocyte physiology from pharmacology," *Annual review of pharmacology and toxicology*, vol. 49, pp. 151-174, 2009.

[16] Allaman, I., Bélanger, M., and Magistretti, P. J., "Astrocyte–neuron metabolic relationships: for better and for worse," *Trends in Neurosciences,* vol. 34, pp. 76-87, 2011.

[17] Riera, J., Hatanaka, R., Uchida, T., Ozaki, T., and Kawashima, R., "Quantifying the uncertainty of spontaneous Ca^{2+} oscillations in astrocytes: Particulars of Alzheimer's disease," *Biophysical Journal,* vol. 101, pp. 554-564, 2011.

[18] Takata, N. and Hirase, H., "Cortical layer 1 and layer 2/3 astrocytes exhibit distinct calcium dynamics in vivo," *PLoS One,* vol. 3, p. e2525, 2008.

[19] Shipp, S., "Structure and function of the cerebral cortex," *Current biology : CB,* vol. 17, pp. R443-R449, 2007.

[20] Holmgren, C., Harkany, T., Svennenfors, B., and Zilberter, Y., "Pyramidal cell communication within local networks in layer 2/3 of rat neocortex," *The Journal of Physiology,* vol. 551, pp. 139-153, 2003.

[21] Kandel, E. R., Schwartz, J. H., and Jessell, T. M., *Principles of Neural Science*, 4 ed. New York: McGraw Hill, 2000.

[22] Malitson, I. H., "Interspecimen Comparison of the Refractive Index of Fused Silica," *J. Opt. Soc. Am.,* vol. 55, pp. 1205-1208, 1965.

[23] Binding, J., Ben Arous, J., Léger, J. F., Gigan, S., Boccara, C., and Bourdieu, L., "Brain refractive index measured in vivo with high-NA defocus-corrected full-field OCT and consequences for two-photon microscopy," *Optics express,* vol. 19, pp. 4833-4847, 2011.

[24] White, B. R., Bauer, A. Q., Snyder, A. Z., Schlaggar, B. L., Lee, J. M., and Culver, J. P., "Imaging of functional connectivity in the mouse brain," *PLoS ONE,* vol. 6, p. e16322, 2011.

[25] Monici, M., "Cell and tissue autofluorescence research and diagnostic applications," in *Biotechnology Annual Review*. vol. Volume 11, M. R. El-Gewely, Ed., ed: Elsevier, 2005, pp. 227-256.

[26] Lakowicz, J. R., *Principles of fluorescence spectroscopy* vol. 1: Springer, 2006.

[27] Thomsen, S., "Qualitative and quantitative pathology of clinically relevant thermal lesions," *Critical Reviews of Optical Science and Technology CR,* vol. 75, pp. 425-459, 2000.

[28] Incropera, F. P., *Fundamentals of Heat and Mass Transfer*, 5th ed.: John Wiley and Sons, Inc, 2002.

[29] Zipfel, W. R., Williams, R. M., Christie, R., Nikitin, A. Y., Hyman, B. T., and Webb, W. W., "Live tissue intrinsic emission microscopy using multiphoton-excited native fluorescence and second harmonic generation," *Proceedings of the National Academy of Sciences,* vol. 100, pp. 7075-7080, 2003.

[30] Husson, T. R., Mallik, A. K., Zhang, J. X., and Issa, N. P., "Functional imaging of primary visual cortex using flavoprotein autofluorescence," *J Neurosci,* vol. 27, pp. 8665-75, 2007.

[31] Reinert, K. C., Gao, W., Chen, G., and Ebner, T. J., "Flavoprotein autofluorescence imaging in the cerebellar cortex in vivo," *J Neurosci Res,* vol. 85, pp. 3221-32, 2007.

[32] Gebhart, S. C., Thompson, R. C., and Mahadevan-Jansen, A., "Liquid-crystal tunable filter spectral imaging for brain tumor demarcation," *Appl. Opt.,* vol. 46, pp. 1896-1910, 2007.

[33] Mayevsky, A. and Rogasky, G., "Mitochondrial function of in vivo evaluated by NADH fluorescence: from animal models to human studies," *Am J Physiol Cell Physiol,* vol. 292, pp. 615-40, 2007.

[34] Schulz, K., Sydekum, E., Krueppel, R., Engelbrecht, C. J., Schlegel, F., Schröter, A., Rudin, M., and Helmchen, F., "Simultaneous BOLD fMRI and fiber-optic calcium recording in rat neocortex," *Nature Methods,* vol. 9, pp. 597-602, 2012.

[35] Peterson, C., Grinvald, A., and Sakmann, B., "Spatiotemporal Dynamics of Sensory Responses in Layer 2/3 of Rat Barrel Cortex Measured In Vivo by Voltage-Sensitive Dye Imaging Combined with Whole-Cell Voltage Recordings and Neuron Reconstructions " *Journal of Neuroscience,* vol. 23, pp. 1298-1309, 2002.

[36] Hama, H., Kurokawa, H., Kawano, H., Ando, R., Shimogori, T., Noda, H., Fukami, K., Sakaue-Sawano, A., and Miyawaki, A., "Scale: a chemical approach for fluorescence imaging and reconstruction of transparent mouse brain," *Nature neuroscience,* vol. 14, pp. 1481-1488, 2011.

[37] Dougherty, T. J., Henderson, B. W., Gomer, C. J., Jori, G., Kessel, D., Korbelik, M., Moan, J., and Peng, Q., "Photodynamic therapy," *Journal of the National Cancer Institute,* vol. 90, pp. 889-905, 1998.

[38] Adams, S. R. and Tsien, R. Y., "Controlling cell chemistry with caged compounds," *Annual review of physiology,* vol. 55, pp. 755-784, 1993.

[39] Cheong, W. F., Prahl, S. A., and Welch, A. J., "A review of the optical properties of biological tissues," *Quantum Electronics, IEEE Journal of,* vol. 26, pp. 2166-2185, 1990.

[40] Hill, D. K. and Keynes, R. D., "Opacity changes in stimulated nerve," *J. Phsyiology,* vol. 108, pp. 278-281, 1949.

[41] Anna Devor, S. S., Srinivasan, V. J., Yaseen, M. A., Nizar, K., Saisan, P. A., Tian, P., Dale, A. M., Vinogradov, S. A., and Maria Angela Franceschini, D. A. B., "Frontiers in optical imaging of cerebral blood flow and metabolism," *Journal of Cerebral Blood Flow & Metabolism,* 2012.

[42] Hillman, E. M. C., "Optical brain imaging in vivo: techniques and applications from animal to man," *Journal of Biomedical Optics,* vol. 12, pp. 051402-28, 2007.

[43] Roe, A. W., "Long-term optical imaging of intrinsic signals in anesthetized and awake monkeys," *Appl. Opt.,* vol. 46, pp. 1872-1880, 2007.

[44] Frostig, R. D., Lieke, E. E., Ts'o, D. Y., and Grinvald, A., "Cortical functional architecture and local coupling between neuronal activity and the microcirculation revealed by in vivo high-resolution optical imaging of intrinsic signals," *Proceedings of the National Academy of Sciences,* vol. 87, pp. 6082-6086, 1990.

[45] Devor, A., Dunn, A. K., Andermann, M. L., Ulbert, I., Boas, D. A., and Dale, A. M., "Coupling of total hemoglobin concentration, oxygenation, and neural activity in rat somatosensory cortex," *Neuron,* vol. 39, pp. 353-359, 2003.

[46] Martin, C., Martindale, J., Berwick, J., and Mayhew, J., "Investigating neural–hemodynamic coupling and the hemodynamic response function in the awake rat," *Neuroimage,* vol. 32, pp. 33-48, 2006.

[47] Offenhauser, N., Thomsen, K., Caesar, K., and Lauritzen, M., "Activity-induced tissue oxygenation changes in rat cerebellar cortex: interplay of postsynaptic activation and blood flow," *The Journal of Physiology,* vol. 565, pp. 279-294, 2005.

[48] Mathiesen, C., Caesar, K., Thomsen, K., Hoogland, T. M., Witgen, B. M., Brazhe, A., and Lauritzen, M., "Activity-dependent increases in local oxygen consumption correlate with postsynaptic currents in the mouse cerebellum in vivo," *The Journal of Neuroscience,* vol. 31, pp. 18327-18337, 2011.

[49] Attwell, D. and Laughlin, S. B., "An energy budget for signaling in the grey matter of the brain," *Journal of Cerebral Blood Flow & Metabolism*, vol. 21, pp. 1133-1145, 2001.

[50] Attwell, D., Buchan, A. M., Charpak, S., Lauritzen, M., MacVicar, B. A., and Newman, E. A., "Glial and neuronal control of brain blood flow," *Nature*, vol. 468, pp. 232-243, 2010.

[51] Cauli, B. and Hamel, E., "Revisiting the role of neurons in neurovascular coupling," *Frontiers in neuroenergetics*, vol. 2, 2010.

[52] Busija, D. W., Bari, F., Domoki, F., and Louis, T., "Mechanisms involved in the cerebrovascular dilator effects of< i> N</i>-methyl-d-aspartate in cerebral cortex," *Brain research reviews*, vol. 56, pp. 89-100, 2007.

[53] Northington, F. J., Matherne, G. P., and Berne, R. M., "Competitive inhibition of nitric oxide synthase prevents the cortical hyperemia associated with peripheral nerve stimulation," *Proceedings of the National Academy of Sciences*, vol. 89, pp. 6649-6652, 1992.

[54] Yaksh, T. L., Wang, J. Y., Go, V., and Harty, G. J., "Cortical vasodilatation produced by vasoactive intestinal polypeptide (VIP) and by physiological stimuli in the cat," *Journal of Cerebral Blood Flow & Metabolism*, vol. 7, pp. 315-326, 1987.

[55] Niwa, K., Araki, E., Morham, S. G., Ross, M. E., and Iadecola, C., "Cyclooxygenase-2 contributes to functional hyperemia in whisker-barrel cortex," *The Journal of Neuroscience*, vol. 20, pp. 763-770, 2000.

[56] Horiuchi, T., Dietrich, H. H., Hongo, K., and Dacey, R. G., "Mechanism of extracellular K+-induced local and conducted responses in cerebral penetrating arterioles," *Stroke*, vol. 33, pp. 2692-2699, 2002.

[57] Takano, T., Tian, G. F., Peng, W., Lou, N., Libionka, W., Han, X., and Nedergaard, M., "Astrocyte-mediated control of cerebral blood flow," *Nature neuroscience*, vol. 9, pp. 260-267, 2005.

[58] Peng, X., Carhuapoma, J. R., Bhardwaj, A., Alkayed, N. J., Falck, J. R., Harder, D. R., Traystman, R. J., and Koehler, R. C., "Suppression of cortical functional hyperemia to vibrissal stimulation in the rat by epoxygenase inhibitors," *American Journal of Physiology-Heart and Circulatory Physiology*, vol. 283, pp. H2029-H2037, 2002.

[59] Girouard, H., Bonev, A. D., Hannah, R. M., Meredith, A., Aldrich, R. W., and Nelson, M. T., "Astrocytic endfoot Ca2+ and BK channels determine both arteriolar dilation and constriction," *Proceedings of the National Academy of Sciences,* vol. 107, pp. 3811-3816, 2010.

[60] Bouchard, M. B., Chen, B. R., Burgess, S. A., and Hillman, E. M. C., "Ultra-fast multispectral optical imaging of cortical oxygenation, blood flow, and intracellular calcium dynamics," *Opt. Express,* vol. 17, pp. 15670-15678, 2009.

[61] Chen, L. M., Friedman, R. M., and Roe, A. W., "Optical imaging of SI topography in anesthetized and awake squirrel monkeys," *J Neurosci,* vol. 25, pp. 7648-59, 2005.

[62] Chen, L. M., Turner, G. H., Friedman, R. M., Zhang, N., Gore, J. C., Roe, A. W., and Avison, M. J., "High-resolution maps of real and illusory tactile activation in primary somatosensory cortex in individual monkeys with functional magnetic resonance imaging and optical imaging," *J Neurosci,* vol. 27, pp. 9181-91, 2007.

[63] Tsytsarev, V., Pope, D., Pumbo, E., and Garver, W., "Intrinsic optical imaging of directional selectivity in rat barrel cortex: Application of a multidirectional magnetic whisker stimulator," *Journal of Neuroscience Methods,* vol. 189, pp. 80-83, 2010.

[64] Grinvald, A., Lieke, E., Frostig, R. D., Gilbert, C. D., and Wiesel, T. N., "Functional architecture of cortex revealed by optical imaging of intrinsic signals," 1986.

[65] Stepniewska, I., Friedman, R. M., Gharbawie, O. A., Cerkevich, C. M., Roe, A. W., and Kaas, J. H., "Optical imaging in galagos reveals parietal–frontal circuits underlying motor behavior," *Proceedings of the National Academy of Sciences,* vol. 108, pp. E725–E732, 2011.

[66] Haglund, M. M., Ojemann, G. A., and Hochman, D. W., "Optical imaging of epileptiform and functional activity in human cerebral cortex," *Nature,* vol. 358, pp. 668-671, 1992.

[67] Dinse, H. R., Godde, B., Hilger, T., Reuter, G., Cords, S. M., Lenarzl, T., and Seelen, W., "Optical Imaging of Cat Auditory Cortex Cochleotopic Selectivity Evoked by Acute Electrical Stimulation of a Multi-channel Cochlear Implant," *European Journal of Neuroscience,* vol. 9, pp. 113-119, 1997.

[68] Harrison, R. V., Harel, N., Kakigi, A., Raveh, E., and Mount, R. J., "Optical imaging of intrinsic signals in chinchilla auditory cortex," *Audiology and Neurotology,* vol. 3, pp. 214-223, 1998.

[69] Grinvald, A., Lieke, E. E., Frostig, R. D., and Hildesheim, R., "Cortical point-spread function and long-range lateral interactions revealed by real-time optical imaging of macaque monkey primary visual cortex," *J. Neurosci.,* vol. 14, pp. 2545-2568, 1994.

[70] Toth, L. J., Rao, S. C., Kim, D. S., Somers, D., and Sur, M., "Subthreshold facilitation and suppression in primary visual cortex revealed by intrinsic signal imaging," *Proceedings of the National Academy of Sciences,* vol. 93, pp. 9869-9874, 1996.

[71] Chen, L. M., Friedman, R. M., and Roe, A. W., "Optical imaging of a tactile illusion in area 3b of the primary somatosensory cortex," *Science,* vol. 302, pp. 881-5, 2003.

[72] Fan, R. H., Baldwin, M. K. L., Jermakowicz, W. J., Casagrande, V. A., Kaas, J. H., and Roe, A. W., "Intrinsic signal optical imaging evidence for dorsal V3 in the prosimian galago (Otolemur garnettii)," *The Journal of Comparative Neurology,* 2012.

[73] Roe, A. W., Chelazzi, L., Connor, C. E., Conway, B. R., Fujita, I., Gallant, J. L., Lu, H., and Vanduffel, W., "Toward a unified theory of visual area V4," *Neuron,* vol. 74, pp. 12-29, 2012.

[74] Malach, R., Amir, Y., Harel, M., and Grinvald, A., "Relationship between intrinsic connections and functional architecture revealed by optical imaging and in vivo targeted biocytin injections in primate striate cortex," *Proceedings of the National Academy of Sciences,* vol. 90, pp. 10469-10473, 1993.

[75] Yoshioka, T., Blasdel, G. G., Levitt, J. B., and Lund, J. S., "Relation between patterns of intrinsic lateral connectivity, ocular dominance, and cytochrome oxidase-reactive regions in macaque monkey striate cortex," *Cerebral Cortex,* vol. 6, pp. 297-310, 1996.

[76] Nelken, I., Bizley, J. K., Nodal, F. R., Ahmed, B., Schnupp, J. W. H., and King, A. J., "Large-scale organization of ferret auditory cortex revealed using continuous acquisition of intrinsic optical signals," *Journal of Neurophysiology,* vol. 92, pp. 2574-2588, 2004.

[77] Grinvald, A., Fine, A., Farber, I. C., and Hildesheim, R., "Fluorescence monitoring of electrical responses from small neurons and their processes," *Biophys J,* vol. 42, pp. 195-8, 1983.

[78] Grinvald, A., Shoman, D., Shmuel, A., Glaser, D., Vanzetta, I., Shtoyermann, E., Slovin, H., Sterkin, A., Hildesheim, R., and Arieli, A., "In-Vivo optical imaging

of cortical architecture and dynamics," in *Modern Techniques in Neuroscience Research*, U. Windhorst and Johansson, Eds., ed: Springer Verlag, 1999.

[79] Chemla, S. and Chavane, F., "Voltage-sensitive dye imaging: Technique review and models," *Journal of Physiology-Paris,* vol. 104, pp. 40-50, 2010.

[80] Chien, C. B. and Pine, J., "Voltage-sensitive dye recording of action potentials and synaptic potentials from sympathetic microcultures," *Biophysical Journal,* vol. 60, pp. 697-711, 1991.

[81] Orbach, H. S., Cohen, L. B., and Grinvald, A., "Optical mapping of electrical activity in rat somatosensory and visual cortex," *The Journal of Neuroscience,* vol. 5, pp. 1886-1895, 1985.

[82] Jancke, D., Chavane, F., Naaman, S., and Grinvald, A., "Imaging cortical correlates of illusion in early visual cortex," *Nature,* vol. 428, pp. 423-426, 2004.

[83] Ahmed, B., Hanazawa, A., Undeman, C., Eriksson, D., Valentiniene, S., and Roland, P. E., "Cortical dynamics subserving visual apparent motion," *Cerebral Cortex,* vol. 18, pp. 2796-2810, 2008.

[84] Ferezou, I., Bolea, S., and Petersen, C. C. H., "Visualizing the cortical representation of whisker touch: voltage-sensitive dye imaging in freely moving mice," *Neuron,* vol. 50, pp. 617-629, 2006.

[85] Lamy, C. M. and Chatton, J. Y., "Optical probing of sodium dynamics in neurons and astrocytes," *Neuroimage,* vol. 58, pp. 572-578, 2011.

[86] Padmawar, P., Yao, X., Bloch, O., Manley, G. T., and Verkman, A., "K+ waves in brain cortex visualized using a long-wavelength K+-sensing fluorescent indicator," *Nature Methods,* vol. 2, pp. 825-827, 2005.

[87] Bregestovski, P. and Arosio, D., "Green Fluorescent Protein-Based Chloride Ion Sensors for In Vivo Imaging," *Fluorescent Proteins II,* pp. 99-124, 2012.

[88] Tsien, R. Y., "A non-disruptive technique for loading calcium buffers and indicators into cells," *Nature,* vol. 290, pp. 527-528, 1981.

[89] Homma, R., Baker, B. J., Jin, L., Garaschuk, O., Konnerth, A., Cohen, L. B., and Zecevic, D., "Wide-field and two-photon imaging of brain activity with voltage- and calcium-sensitive dyes," *Philosophical Transactions of the Royal Society B: Biological Sciences,* vol. 364, pp. 2453-2467, 2009.

[90] Murayama, M. and Larkum, M. E., "Enhanced dendritic activity in awake rats," *Proceedings of the National Academy of Sciences,* vol. 106, pp. 20482-20486, 2009.

[91] Murayama, M., Perez-Garci, E., Nevian, T., Bock, T., Senn, W., and Larkum, M. E., "Dendritic encoding of sensory stimuli controlled by deep cortical interneurons," *Nature,* vol. 457, pp. 1137-1141, 2009.

[92] Min, R. and Nevian, T., "Astrocyte signaling controls spike timing-dependent depression at neocortical synapses," *Nature neuroscience,* vol. 15, pp. 746-753, 2012.

[93] Denk, W., Strickler, J. H., and Webb, W. W., "Two-photon laser scanning fluorescence microscopy," *Science (New York, NY),* vol. 248, p. 73, 1990.

[94] Svoboda, K. and Yasuda, R., "Principles of Two-Photon Excitation Microscopy and Its Applications to Neuroscience," *Neuron,* vol. 50, pp. 823-839, 2006.

[95] Zipfel, W. R., Williams, R. M., and Webb, W. W., "Nonlinear magic: multiphoton microscopy in the biosciences," *Nature Biotechnology,* vol. 21, pp. 1369-1377, 2003.

[96] Suadicani, S. O., Cherkas, P. S., Zuckerman, J., Smith, D. N., Spray, D. C., and Hanani, M., "Bidirectional calcium signaling between satellite glial cells and neurons in cultured mouse trigeminal ganglia," *Neuron Glia Biology,* vol. 6, pp. 43-51, 2010.

[97] Göbel, W. and Helmchen, F., "In vivo calcium imaging of neural network function," *Physiology,* vol. 22, pp. 358-365, 2007.

[98] Lendvai, B., Stern, E. A., Chen, B., and Svoboda, K., "Experience-dependent plasticity of dendritic spines in the developing rat barrel cortex in vivo," *Nature,* vol. 404, pp. 876-881, 2000.

[99] Hillman, E., Devor, A., Bouchard, M. B., Dunn, A. K., Krauss, G., Skoch, J., Bacskai, B. J., Dale, A. M., and Boas, D. A., "Depth-resolved optical imaging and microscopy of vascular compartment dynamics during somatosensory stimulation," *Neuroimage,* vol. 35, pp. 89-104, 2007.

[100] Cohen, L. B. and Keynes, R. D., "Evidence for structural changes during the action potential in nerves from walking legs of Maia squinado," *Journal of Physiology,* vol. 194, pp. 85-86, 1968.

[101] Huang, C., Harootunian, A., Maher, M., Quan, C., Raj, C., McCormack, K., Numann, R., Negulescu, P., and Gonzalez, J., "Characterization of voltage-gated sodium channel blockers by electrical stimulation and fluorescence detection of membrane potential," *Nature Biotechnology*, vol. 24, pp. 439-446, 2006.

[102] Ballantine, H. T., Bell, E., and Manlapaz, J., "Progress and Problems in the Neurological Applications of Focused Ultrasound*," *Journal of Neurosurgery,* vol. 17, pp. 858-876, 1960.

[103] Kim, H., Taghados, S. J., Fischer, K., Maeng, L.-S., Park, S., and Yoo, S.-S., "Noninvasive Transcranial Stimulation of Rat Abducens Nerve by Focused Ultrasound," *Ultrasound in Medicine & Biology,* vol. 38, pp. 1568-1575, 2012.

[104] Colucci, V., Strichartz, G., Jolesz, F., Vykhodtseva, N., and Hynynen, K., "Focused Ultrasound Effects on Nerve Action Potential< i> in vitro</i>," *Ultrasound in medicine & biology,* vol. 35, pp. 1737-1747, 2009.

[105] Barker, A. T., Jalinous, R., and Freeston, I. L., "NON-INVASIVE MAGNETIC STIMULATION OF HUMAN MOTOR CORTEX," *The Lancet,* vol. 325, pp. 1106-1107, 1985.

[106] Barker, A. T., "An introduction to the basic principles of magnetic nerve stimulation," *Journal of clinical neurophysiology: official publication of the American Electroencephalographic Society,* vol. 8, p. 26, 1991.

[107] Bonmassar, G., Lee, S. W., Freeman, D. K., Polasek, M., Fried, S. I., and Gale, J. T., "Microscopic magnetic stimulation of neural tissue," *Nature Communications,* vol. 3, p. 921, 2012.

[108] Booth, J., Von Muralt, A., and Stampfli, R., "The photochemical action of ultra-violet light on isolated single nerve fibres," *Helvetica physiologica et pharmacologica acta,* vol. 8, p. 110, 1950.

[109] Allègre, G., Avrillier, S., and Albe-Fessard, D., "Stimulation in the rat of a nerve fiber bundle by a short UV pulse from an excimer laser," *Neuroscience Letters,* vol. 180, pp. 261-264, 1994.

[110] Fork, R. L., "Laser Stimulation of Nerve Cells in Aplysia," *Science,* vol. 171, pp. 907-908, 1971.

[111] Arvanitaki, A. and Halazonitis, N., "Excitatory and inhibiotry processes initiated by light and infra-red radiations in signle identifiable nerve cells," in *Nervous Inhibition*, E. Florey, Ed., ed Pergamon, New York, 1961.

[112] Boyden, E. S., Zhang, F., Bamberg, E., Nagel, G., and Deisseroth, K., "Millisecond-timescale, genetically targeted optical control of neural activity," *Nat Neurosci*, vol. 8, pp. 1263-1268, 2005.

[113] Wells, J., Kao, C., Mariappan, K., Albea, J., Jansen, E. D., Konrad, P., and Mahadevan-Jansen, A., "Optical stimulation of neural tissue in vivo," *Opt Lett*, vol. 30, pp. 504-6, 2005.

[114] Zhang, F., Wang, L. P., Boyden, E. S., and Deisseroth, K., "Channelrhodopsin-2 and optical control of excitable cells," *Nature Methods*, vol. 3, pp. 785-792, 2006.

[115] Tye, K. M. and Deisseroth, K., "Optogenetic investigation of neural circuits underlying brain disease in animal models," *Nature Reviews Neuroscience*, vol. 13, pp. 251-266, 2012.

[116] Yizhar, O., Fenno, L. E., Davidson, T. J., Mogri, M., and Deisseroth, K., "Optogenetics in neural systems," *Neuron*, vol. 71, pp. 9-34, 2011.

[117] Tye, K. M., Prakash, R., Kim, S. Y., Fenno, L. E., Grosenick, L., Zarabi, H., Thompson, K. R., Gradinaru, V., Ramakrishnan, C., and Deisseroth, K., "Amygdala circuitry mediating reversible and bidirectional control of anxiety," *Nature*, vol. 471, pp. 358-362, 2011.

[118] Haubensak, W., Kunwar, P. S., Cai, H., Ciocchi, S., Wall, N. R., Ponnusamy, R., Biag, J., Dong, H. W., Deisseroth, K., and Callaway, E. M., "Genetic dissection of an amygdala microcircuit that gates conditioned fear," *Nature*, vol. 468, pp. 270-276, 2010.

[119] Witten, I. B., Lin, S. C., Brodsky, M., Prakash, R., Diester, I., Anikeeva, P., Gradinaru, V., Ramakrishnan, C., and Deisseroth, K., "Cholinergic interneurons control local circuit activity and cocaine conditioning," *Science Signalling*, vol. 330, p. 1677, 2010.

[120] Yizhar, O., Fenno, L. E., Prigge, M., Schneider, F., Davidson, T. J., O'Shea, D. J., Sohal, V. S., Goshen, I., Finkelstein, J., and Paz, J. T., "Neocortical excitation/inhibition balance in information processing and social dysfunction," *Nature*, vol. 477, pp. 171-178, 2011.

[121] Sohal, V. S., Zhang, F., Yizhar, O., and Deisseroth, K., "Parvalbumin neurons and gamma rhythms enhance cortical circuit performance," *Nature,* vol. 459, pp. 698-702, 2009.

[122] Gradinaru, V., Mogri, M., Thompson, K. R., Henderson, J. M., and Deisseroth, K., "Optical deconstruction of parkinsonian neural circuitry," *Science,* vol. 324, pp. 354-359, 2009.

[123] Tønnesen, J., Sørensen, A. T., Deisseroth, K., Lundberg, C., and Kokaia, M., "Optogenetic control of epileptiform activity," *Proceedings of the National Academy of Sciences,* vol. 106, pp. 12162-12167, 2009.

[124] Adamantidis, A. R., Zhang, F., Aravanis, A. M., Deisseroth, K., and De Lecea, L., "Neural substrates of awakening probed with optogenetic control of hypocretin neurons," *Nature,* vol. 450, pp. 420-424, 2007.

[125] Zhang, F., Wang, L.-P., Boyden, E. S., and Deisseroth, K., "Channelrhodopsin-2 and optical control of excitable cells," *Nat Meth,* vol. 3, pp. 785-792, 2006.

[126] Maguire, A. M., Simonelli, F., Pierce, E. A., Pugh Jr, E. N., Mingozzi, F., Bennicelli, J., Banfi, S., Marshall, K. A., Testa, F., and Surace, E. M., "Safety and efficacy of gene transfer for Leber's congenital amaurosis," *New England Journal of Medicine,* vol. 358, pp. 2240-2248, 2008.

[127] Nathwani, A. C., Tuddenham, E. G. D., Rangarajan, S., Rosales, C., McIntosh, J., Linch, D. C., Chowdary, P., Riddell, A., Pie, A. J., and Harrington, C., "Adenovirus-associated virus vector–mediated gene transfer in hemophilia B," *New England Journal of Medicine,* vol. 365, pp. 2357-2365, 2011.

[128] Busskamp, V., Duebel, J., Balya, D., Fradot, M., Viney, T. J., Siegert, S., Groner, A. C., Cabuy, E., Forster, V., and Seeliger, M., "Genetic reactivation of cone photoreceptors restores visual responses in retinitis pigmentosa," *Science Signalling,* vol. 329, p. 413, 2010.

[129] Kimmelman, J., "The ethics of human gene transfer," *Nature Reviews Genetics,* vol. 9, pp. 239-244, 2008.

[130] Wells, J., Kao, C., Jansen, E. D., Konrad, P., and Mahadevan-Jansen, A., "Application of infrared light for *in vivo* neural stimulation," *J Biomed Opt,* vol. 10, p. 064003, 2005.

[131] Wells, J., Konrad, P., Kao, C., Jansen, E. D., and Mahadevan-Jansen, A., "Pulsed laser versus electrical energy for peripheral nerve stimulation," *J Neurosci Methods,* vol. 163, pp. 326-37, 2007.

[132] Izzo, A. D., Walsh, J. T., Jr., Jansen, E. D., Bendett, M., Webb, J., Ralph, H., and Richter, C. P., "Optical parameter variability in laser nerve stimulation: a study of pulse duration, repetition rate, and wavelength," *IEEE Trans Biomed Eng,* vol. 54, pp. 1108-14, 2007.

[133] Tozburun, S., Lagoda, G. A., Burnett, A. L., and Fried, N. M., "Continuous-Wave Laser Stimulation of the Rat Prostate Cavernous Nerves Using a Compact and Inexpensive All Single Mode Optical Fiber System," *Journal of Endourology,* vol. 25, pp. 1727-1731, 2011.

[134] Hale, G. M. and Querry, M. R., "Optical constants of water in the 200-nm to 200-μm wavelength region," *Appl. Opt.,* vol. 12, pp. 555-563, 1973.

[135] Wells, J., Kao, C., Konrad, P., Milner, T., Kim, J., Mahadevan-Jansen, A., and Jansen, E. D., "Biophysical mechanisms of transient optical stimulation of peripheral nerve," *Biophys J,* vol. 93, pp. 2567-80, 2007.

[136] Shapiro, M. G., Homma, K., Villarreal, S., Richter, C.-P., and Bezanilla, F., "Infrared light excites cells by changing their electrical capacitance," *Nat Commun,* vol. 3, p. 736, 2012.

[137] Albert, E. S., Bec, J., Desmadryl, G., Chekroud, K., Travo, C., Gaboyard, S., Bardin, F., Marc, I., Dumas, M., and Lenaers, G., "TRPV4 channels mediate the infrared laser-evoked response in sensory neurons," *Journal of Neurophysiology,* vol. 107, pp. 3227-3234, 2012.

[138] Zongxia, M., Triantis, I. F., Woods, V. M., Toumazou, C., and Nikolic, K., "A Simulation Study of the Combined Thermoelectric Extracellular Stimulation of the Sciatic Nerve of the Xenopus Laevis: The Localized Transient Heat Block," *Biomedical Engineering, IEEE Transactions on,* vol. 59, pp. 1758-1769, 2012.

[139] Henderson, D. and Boda, D., "Insights from theory and simulation on the electrical double layer," *Phys. Chem. Chem. Phys.,* vol. 11, pp. 3822-3830, 2009.

[140] Benfenati, V., Amiry-Moghaddam, M., Caprini, M., Mylonakou, M. N., Rapisarda, C., Ottersen, O. P., and Ferroni, S., "Expression and functional characterization of transient receptor potential vanilloid-related channel 4 (TRPV4) in rat cortical astrocytes," *Neuroscience,* vol. 148, pp. 876-892, 2007.

[141] Kauer, J. A. and Gibson, H. E., "Hot flash: TRPV channels in the brain," *Trends in Neurosciences,* vol. 32, pp. 215-224, 2009.

[142] Fischer, M. J. M., Reeh, P. W., and Sauer, S. K., "Proton-induced calcitonin gene-related peptide release from rat sciatic nerve axons, in vitro, involving TRPV1," *European Journal of Neuroscience,* vol. 18, pp. 803-810, 2003.

[143] Sharif-Naeini, R., Ciura, S., and Bourque, C. W., "TRPV1 Gene Required for Thermosensory Transduction and Anticipatory Secretion from Vasopressin Neurons during Hyperthermia," *Neuron,* vol. 58, pp. 179-185, 2008.

[144] Hodgkin, A. and Katz, B., "The effect of temperature on the electrical activity of the giant axon of the squid," *The Journal of Physiology,* vol. 109, p. 240, 1949.

[145] Duke, A. R., "Selective Control of Electrical Neural Activation using Infrared Light," Doctor of Philosophy Dissertation, Biomedical Engineering, Vanderbilt University, 2012.

[146] Teudt, I. U., Nevel, A. E., Izzo, A. D., Walsh, J. T., Jr., and Richter, C. P., "Optical stimulation of the facial nerve: a new monitoring technique?," *Laryngoscope,* vol. 117, pp. 1641-7, 2007.

[147] Fried, N. M., Lagoda, G. A., Scott, N. J., Su, L.-M., and Burnett, A. L., "Noncontact Stimulation of the Cavernous Nerves in the Rat Prostate Using a Tunable-Wavelength Thulium Fiber Laser," *Journal of Endourology,* vol. 22, pp. 409-414, 2008.

[148] Tozburun, S., Mayeh, M., Lagoda, G. A., Farahi, F. A., Burnett, A. L., and Fried, N. M., "A Compact Laparoscopic Probe for Optical Stimulation of the Prostate Nerves," *Selected Topics in Quantum Electronics, IEEE Journal of,* vol. 16, pp. 941-945, 2010.

[149] Tozburun, S., Lagoda, G. A., Burnett, A. L., and Fried, N. M., "Subsurface near infrared laser stimulation of the periprostatic cavernous nerves," *Journal of biophotonics,* 2012.

[150] Izzo, A. D., Richter, C.-P., Jansen, E. D., and Walsh, J. T., Jr., "Laser stimulation of the auditory nerve," *Lasers in Surgery and Medicine,* vol. 38, pp. 745-753, 2006.

[151] Richter, C., Rajguru, S., Matic, A., Moreno, E., Fishman, A., Robinson, A., Suh, E., and Walsh Jr, J., "Spread of cochlear excitation during stimulation with pulsed

infrared radiation: inferior colliculus measurements," *Journal of Neural Engineering,* vol. 8, p. 056006, 2011.

[152] Rajguru, S. M., Matic, A. I., Robinson, A. M., Fishman, A. J., Moreno, L. E., Bradley, A., Vujanovic, I., Breen, J., Wells, J. D., Bendett, M., and Richter, C.-P., "Optical cochlear implants: Evaluation of surgical approach and laser parameters in cats," *Hearing Research,* vol. 269, pp. 102-111, 2010.

[153] Jenkins, M. W., Duke, A. R., GuS, DoughmanY, Chiel, H. J., FujiokaH, WatanabeM, Jansen, E. D., and Rollins, A. M., "Optical pacing of the embryonic heart," *Nat Photon,* vol. 4, pp. 623-626, 2010.

[154] Duke, A. R., Cayce, J. M., Malphrus, J. D., Konrad, P., Mahadevan-Jansen, A., and Jansen, E. D., "Combined optical and electrical stimulation of neural tissue in vivo," *Journal of Biomedical Optics,* vol. 14, pp. 060501-3, 2009.

[155] Duke, A. R., Lu, H., Jenkins, M. W., Chiel, H. J., and Jansen, E. D., "Spatial and temporal variability in response to hybrid electro-optical stimulation," *Journal of Neural Engineering,* vol. 9, p. 036003, 2012.

[156] Duke, A. R., Peterson, E., Mackanos, M. A., Atkinson, J., Tyler, D., and Jansen, E. D., "Hybrid electro-optical stimulation of the rat sciatic nerve induces force generation in the plantarflexor muscles," *Journal of Neural Engineering,* vol. 9, p. 066006, 2012.

CHAPTER III

INFRARED NEURAL STIMULATION OF THALAMOCORTICAL BRAIN SLICES

Jonathan Matthew Cayce[1], Chris C Kao[2], Jonathan D Malphrus[1], Peter E. Konrad[1,2], Anita Mahadevan-Jansen[1,2], and E. Duco Jansen[1,2]

[1] Department of Biomedical Engineering, Vanderbilt University

Nashville Tennessee

[2] Department of Neurological Surgery, Vanderbilt University

Nashville Tennessee

This chapter was published in:

"Infrared neural stimulation of thalamocortical brain slices,"

IEEE Journal of Selected Topics in Quantum Electronics, vol 16, pp. 565-572, 2010

3.1 Abstract

Infrared neural stimulation (INS) has been well characterized in the peripheral nervous system, and has been shown to enable stimulation with high spatial precision and without causing the typical electrical stimulation artifact on recording electrode. The next step in the development of INS is to demonstrate feasibility to stimulate neurons located in the central nervous system (CNS). Thalamocortical brain slices were used to establish feasibility of INS in the CNS and to optimize laser parameters. Infrared light was used to evoke action potentials in the brain slice with no electrical stimulation artifact. This response was blocked by the application of tetrodotoxin demonstrating neurological origin of the recorded signal. Threshold radiant exposure decreased as the absorption coefficient of the wavelength of light increased. Higher repetition rates lead to a decrease in threshold radiant exposure, and threshold radiant exposure was found to decrease as the spot size diameter increased. Additionally, neuronal responses to INS were intracellularly recorded demonstrating artifact free electrical recordings. The results from this study lay the foundation for future *in vivo* studies to develop INS for CNS stimulation.

3.2 Introduction

Prior to this study, INS research has been confined to the peripheral nervous system (PNS), imploring the question of whether it is possible to directly stimulate neurons in the brain using this technique [1, 2]. The properties of INS present a unique tool for basic science studies aimed at understanding brain function, and possibly providing clinicians a tool to improve on current neurosurgical procedures. Possible applications of INS in the CNS include cortical mapping during awake craniotomies, tumor resection, and deep brain stimulation. All three potential applications stand to benefit from the lack of electrical field spread associated with INS, and cortical mapping and tumor resection procedures could benefit from contact free delivery of infrared light reducing the possibility of mechanical damage to healthy tissue. The high spatial precision of INS will offer researchers another tool to help understand the function of neural networks and possibly reveal neural signal which is masked by the stimulation artifact seen with electrical stimulation. Thus the next step in the development of INS is to achieve and optimize this method for the CNS, specifically the brain.

The differences in geometry and physiology of the brain compared to the PNS imply that a different wavelength of infrared light may be needed to achieve stimulation in the CNS. Unlike the PNS where axons of neurons are organized in parallel bundles in nerves, the brain is organized into a complex neuronal network. The thalamocortical brain slice model was chosen for an *in vitro* feasibility study. The thalamocortical brain slice model is a well understood and reproducible model that is commonly used in these types of studies [3-5]. It preserves a three neuron network between cortical and thalamic neurons that reproduce action potential activity similar to that seen with in vivo animal

studies making this model an ideal method for testing INS in the CNS [3, 5]. The purpose of this study was to prove feasibility and optimize the parameters of optical stimulation *in vitro* in the thalamocortical brain slice model.

3.3 Materials and Methods

3.3.1 Slice preparation

Spraque-Dawley rats (21 to 35 days, n=35) were anesthetized with inhalation of 4% isoflurane for 1-1.5 min and were immediately decapitated. The brain was rapidly dissected from the cranial cavity, and cerebellum was removed. A parasagittal cut was made at a 55 degree angle from the midline of the brain at 10 degree elevation to allow for correct orientation during slice preparation [3]. Thalamocortical slices were then cut to be between 400 ± 50 μm thick using a Vibratome 1000 (Vibratome, St Louis, MO). During slice preparation, the brain tissue was bathed in an artificial cerebral spinal fluid (ACSF) containing the following concentrations (in mM): 124 NaCl , 5 KCl , 1.25 NaH_2PO_4, 2 $CaCl_2$, 2 $MgCl_2$ 26 $NaHCO_3$ and 10 glucose. The ACSF was oxygenized using a 95% O_2 / 5% CO_2 gas concentration which maintained the tissue throughout slice preparation and experimentation [5]. The thalamocortical slices were then placed in a similar oxygenized ACSF solution which was magnesium deficient to induce hyperactivity and the slices were allowed to incubate for 1 hour. After incubation, the slice was placed in an interfaced perfusion chamber at room temperature (22 ^{o}C) and perfused by oxygenated, potassium deficient ACSF solution at a rate of 2.5 ml/min. Electrical recordings were made with glass patch electrodes (3-6 MΩ) pulled from

borosilicate glass capillaries (World Precision Instruments, Sarasota, FL) using a vertical Narishige PP-83, (Scientific Instrument Lab., Tokyo, Japan). The glass electrode was filled with a fluid containing the following constituent concentrations (in mM): 110 cesium-potassium gluconate, 2 $MgCl_2$, 1 Na-EGTA, 0.1 $CaCl_2$, 2 MgATP, 0.2 NaGTP and 10 HEPES. The glass electrode was placed onto the tissue using a micromanipulator to record extracellular potentials. Recordings of all electrical signals were made with an Axopatch-200B amplifier (Axon Instruments Inc., Foster City, CA) and the signal was digitized and analyzed using Axon Digidata 1322A data acquisition system and pCLAMP8 software (Axon Instruments Inc., Foster City, CA). Electrical stimulation was performed using a platinum-iridium tipped bipolar microelectrode (insolated by glass) separated by 100 μm and an impedance ~2000 Ω placed on the slice using a micromanipulator. Electrical pulses were generated using an IsoSTIM A320 (World Precision Instruments, Sarasota, FL) at 2 - 30 Hz and a pulse width of 5 μs with an amplitude of 1-10 mA. Electrical stimulation was used to verify viable tissue within the slice before INS was performed.

3.3.2 Laser source and delivery

All experiments were performed using the Mark-III Free Electron Laser (FEL) at Vanderbilt University. The FEL is a tunable pulsed laser source with a wavelength range between 2.51 μm and 10 μm (wavelength bandwidth ± 0.5%). The beam generated by the FEL consists of a macro pulse width that is 5 μs (FWHM) which is the sum of a train of 1 ps pulses of laser light at 2.85 GHz. The maximum macro pulse rate of the FEL was 30 Hz. The Gaussian beam generated by the FEL was delivered to the tissue using a

series of relay optics and focused through a 50 mm diameter converging CaF_2 lens with a 200 mm focal length to a variable spot size diameter between 100 μm – 510 μm. For each experiment, the spot size was determined using the knife edge method to establish an accurate measure for the radiant exposure [6]. The accuracy of the knife edge spot size measurement was determined to be ± 50μm.

3.3.3 Feasibility

Initial feasibility studies used the FEL at a wavelength of 4.00 μm. At this wavelength, the absorption coefficient (146 cm^{-1}) ensures that adequate light was delivered to viable tissue in the slice [7]. The initial pulse repetition rates used were 15 and 30 Hz, and the spot size was maintained at 300±50 μm.

3.3.4 Wavelength study

Wavelength optimization was performed using the following wavelengths: 2.51 μm, 3.65 μm, 4.00 μm, 4.40 μm, and 5.30 μm, and the radiant energy per pulse was varied to determine threshold at each wavelength. Each wavelength was picked for its unique absorption coefficient in water ranging from approximately 96 - 294 cm^{-1} [8]. INS at each wavelength was performed using a repetition rate of 30 Hz, a spot size between 350±50 μm on at least 3 separate viable slices at 4-6 locations (n=12-16). Laser stimulation was applied to the cortical area of the brain slice and the glass recording electrode was placed at least 2 mm away in the cortex. Threshold was determined when a visual change (~0.2 mV) in the baseline signal of the recording from the glass pipette electrode was observed and could be eliminated by the application of the sodium channel

blocker 3 μM tetrodotoxin (TTX), but not by applying a similar physiological solution without TTX (negative control). A recording was made of the signal with a reference trace generated by the FEL corresponding to laser pulse generation.

3.3.5 Repetition rate and spot size study

The effects of different repetition rates on threshold radiant energy were determined using light at λ=3.65 μm and a spot size diameter of 320±50 μm at the following repetition rates: 30 Hz, 15 Hz, 10 Hz, 7.5 Hz, and 6 Hz. Three separate slices were stimulated at each repetition rate with 4-6 stimulation sites dependent on slice quality. Consistent orientation was maintained by irradiating tissue 2 mm away from the recording electrode using the different repetition rates identified above. Again, TTX was used to validate the physiological nature of the recorded response. The effects of spot size on threshold radiant energy were studied using light at λ=3.65 μm with a repetition rate of 30 Hz and a spot size diameter ranging between 140 μm to 510 μm. Infrared neural stimulation was performed using the same protocol outlined for the repetition rate dependence study.

3.3.6 Intracellular recordings

In order to demonstrate the benefits of INS, specifically the ability to stimulate neurons with high spatial precision and without inducing a stimulation artifact, and intracellular recordings were performed during laser stimulation (λ=3.65 μm) in the ventrobasal thalamus and cortical sections of the brain slice using a glass pipette [4]. Once a whole cell patch was established, the tissue was irradiated with infrared light 2

mm away from the recording site and the signal resulting signal was recorded. Tetrodotoxin was used to verify biological origin of the signal.

3.3.7 Determination of dead layer thickness

It is known that the brain slice methodology results in significant damage to the outer layer of tissue with a thickness ranging from 50 – 200 μm [9-11]. Since this layer does not participate in electrical activity but will account for absorption of optical energy, it is imperative that we establish the exact extent of this layer in our experiments to determine the radiant exposure at the depth where living neurons reside within the slice. To verify the existence of the damaged layer of tissue, freshly cut slices were incubated for three hours with an ACSF media containing a 0.1 mM concentration of propidium iodide (PI). The PI molecule is positively charged which prevents it from crossing the cellular membrane of neurons; therefore PI will only enter neurons with damaged membranes [12]. The brain slices stained with PI were flash frozen and sectioned orthogonal to original cutting plane and analyzed with a fluorescence microscope to determine the thickness of the damaged layer of tissue. The result from the staining determined the damaged layer of tissue to be at least 150 μm thick and was used to adjust the surface radiant exposure to the apparent radiant exposure seen by the viable tissue within the slice.

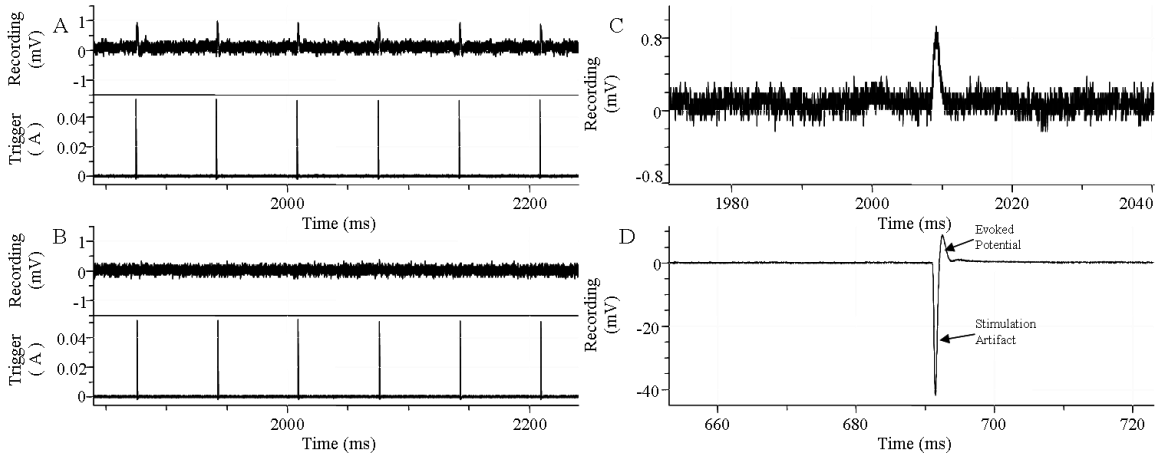

Figure 3.1: Infrared neural stimulation evokes neural spike activity in the thalamocortical slice as seen in extracellular recordings. A&B. Top trace displays recorded extracellular potentials; bottom trace represents timing of each laser pulse. A. Infrared light evoked action potentials. B. Lack of infrared evoked spike activity after TTX application. C. Single evoked response to infrared light. [Laser parameters: 1.46 J/cm^2, 15 Hz, 300±50 μm spot size] D. Single evoked response to electrical stimulation at 0.8 mA, 15 Hz, delivered 2 mm away from recording electrode. Note the large difference in voltage from electrical stimulation

3.4 Results

Initial feasibility of infrared neural stimulation was established using λ=4.00 μm at 15 Hz and 30 Hz with a spotsize of 300±50 μm. Figure 3.1 represents a resulting recorded signal of electrical activity. It can be seen that electrical spiking was frequency locked with the laser pulses. A zoomed view of the INS induced action potential (Figure 3.1C) reveals the lack of a stimulation artifact that is commonly seen with electrical stimulation (Figure 3.1D). Figure 3.1D represents a single action potential from electrical stimulation. Note the large stimulation artifact which is present during electrical stimulation (Figure 3.1D), but not present during INS (Figure 3.1C). The signal induced by infrared light was eliminated once TTX was applied to the tissue (Figure 3.1B). This suggests that the signal was not due to laser induced electrical noise or a direct thermal or irradiation effect from the laser on the recording electrode. Attempts to

stimulate the thalamus, hippocampus, and other deep structures contained in the slice produced similar extracellular recordings as seen in Figure 3.1.

Based on these results, wavelength dependence of INS was determined. Each of the wavelengths used (2.51 μm, 3.65 μm, 4.00 μm, 4.40 and 5.30 μm) was found to successfully stimulate a brain slice and the resulting signal was eliminated by the application of TTX. Figure 3.2 shows that the stimulation threshold is wavelength dependent and has a logarithmic correlation to the absorption coefficient of each wavelength (Figure 3.2). A wavelength with a higher absorption coefficient will require less energy to be

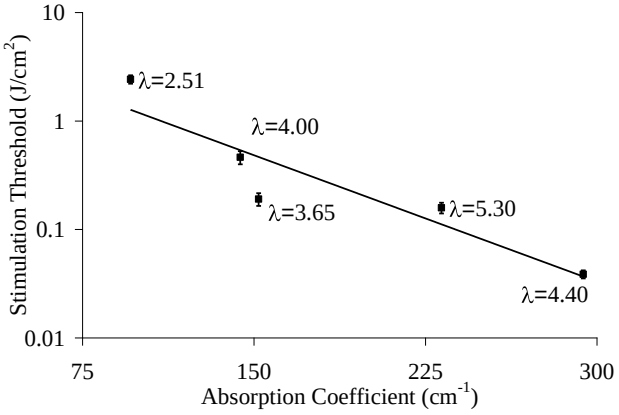

Figure 3.2: Semilog plot of stimulation threshold radiant exposure as a function of absorption coefficient (R^2=0.85). Laser parameters: λ=2.51 μm, 3.65 μm, 4.00 μm, 4.40 μm, and 5.30 μm. Spot size diameter = 350±50 μm, Pulse repetition rate = 30 Hz.

deposited at the viable neuron of 30 Hz produced the lowest radiant exposure per pulse (0.19 J/cm^2) needed for stimulation. Figure 3.3 illustrates that threshold radiant exposures increased as the repetition rate decreased following an exponential distribution. Here the optimal repetition rate was determined to be 30 Hz as indicated by the repetition rate which produced the lowest stimulation threshold.

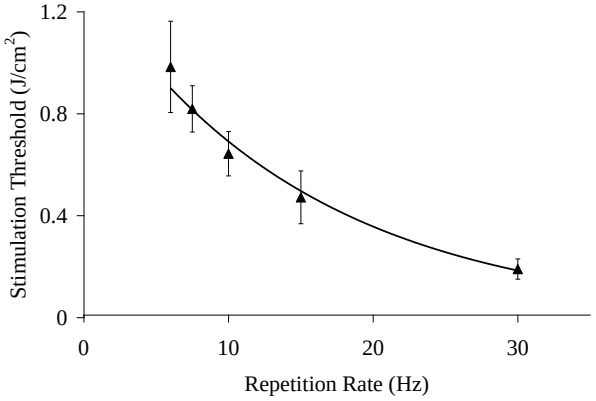

Figure 3.3: Increasing pulse repetition rate reduces the stimulation threshold radiant exposure (R^2=0.98). Laser parameters: λ=3.65 μm, 30 Hz, Spot Size= 320±50 μm.

To study the effect of spotsize on stimulation threshold, the repetition rate was fixed at 30 Hz and the spot size was varied. Results show a larger spot size reduces the radiant exposure needed to evoke action potentials (Figure 3.4). The resultant curve exhibited an exponential relationship.

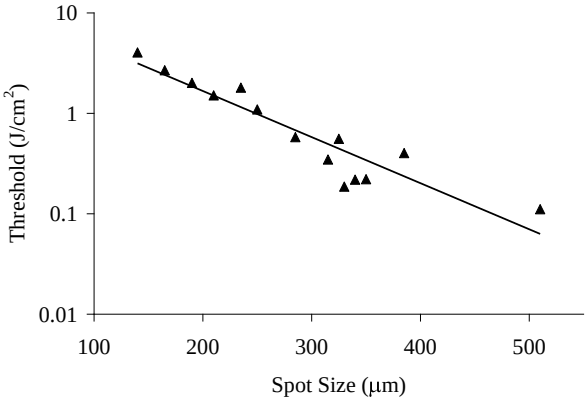

Figure 3.4: Semilog plot of stimulation threshold radiant exposure as a function of spot size (R^2=0.86). Increasing spot size diameter reduces radiant energy levels at neuronal activation thresholds. Laser parameters: λ=3.65 μm, 30 Hz.

Figure 3.5 represents an intracellular recording of neural activity induced by INS at a wavelength of 3.65 μm at 30 Hz. The trace shows an initial fast component followed by additional peaks in the intracellular potential trace. Tetrodotoxin was used to eliminate the signal to ensure no mechanical or thermal artifact existed in the signal.

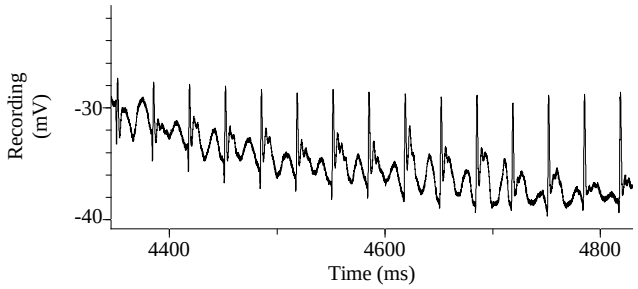

Figure 3.5: Infrared stimulation evokes neural action potentials as seen in intracellular recordings. Laser parameters: λ=3.65 μm, 30 Hz, Spot size=320±20 μm, Pulse width=5μs, 0.49 J/cm^2.

3.5 Discussion

This study presents the first results on the application of infrared neural stimulation (INS) for the central nervous system, an area where high spatial precision of stimulation is often desired. Wininger et al. reported *in vitro* infrared stimulation of lobster nerves, but they were unable to maintain constant stimulation after one or two pulses of infrared light was applied to the tissue [13]. The results of this study showed that we were able to stimulate thalamocortical brain slices using pulsed infrared laser light to generate action potentials at the repetition rate of the laser. The application of TTX to the perfusion chamber blocked the recorded electrical signal generated by INS and confirmed the signal to be of physiological origin. Application of physiological saline without TTX did not block signal induction. Stimulation was accomplished

without physical contact with the tissue and no stimulation artifact was evident on the electrical recording trace (Figure 3.1).

The surface radiant exposures at the surface of the brain slice needed to evoke an extracellular potential resulted in ablation of the tissue for all wavelengths tested. An inherent limitation of the thalamocortical brain slice model is the presence of dead and damaged tissue layers which result from trauma caused by the cutting process to make the slice. The dead and damaged layer thickness ranges between 50 – 200 μm and is dependent on slice thickness and cutting method [9-11, 14-16]. In this study, PI staining of living brainslices showed an averaged dead/damaged layer thickness of 150 μm which is in agreement with previous studies that characterized the dead/damaged layer using a variety of techniques [9-11]. To stimulate the brain slice, infrared light had to penetrate the damaged layer of tissue, which acted as an attenuator since water in the damaged layer absorbs the infrared energy. Additionally, the relatively low repetition rates allowed ACSF to fill the shallow crater caused by ablation essentially replacing the damaged tissue. Therefore the stimulation radiant exposures were reported as the amount of light remaining at 150 μm deep into the slice using Beer's law to calculate the adjusted radiant exposures. The adjustment of the radiant exposures from surface radiant energy to the radiant energy at the depth of viable tissue revealed stimulation thresholds that were similar to thresholds identified for INS in the peripheral nervous system at the axonal level [2, 17]. Wells et al. showed that 64% (~0.256 J/cm^2) of the surface radiant energy at a wavelength of 2.12 μm remained at the level of the axons in the nerve [9].

Stimulation threshold was significantly lower than the studies of INS in the rat sciatic nerve for all wavelengths tested except λ=2.51 μm. There are several factors that

contribute to the lower stimulation threshold radiant exposures seen in this study. First, in the brain slice INS was able to stimulate gray matter (mainly cell bodies and dendrites) and white matter (mainly axons); whereas in the PNS only the axons are targeted [18, 19]. The CNS also contains less connective tissue compared to the PNS, which reduces the amount of energy that is absorbed in the connective tissue surrounding the neurons. These two factors indicate more excitable tissue exists in a given volume of CNS tissue when compared to nerves in the PNS and helps to explain the lower stimulation thresholds seen in the brain slice.

As was shown previously for the sciatic nerve, wavelength was a crucial parameter for performing INS without damaging tissue [1, 19, 20]. The laser wavelength determines the volume of tissue that is stimulated. The absorption and reduced scattering coefficient in tissue at a given wavelength determines the penetration depth of the light and dictates the spatial distribution of light absorption in the tissue and the FEL provided a wide range of wavelengths with unique optical properties to probe different depths in tissue. It should be noted that other wavelengths not in the range of the FEL could provide the same optical properties as those tested in this study. The studies in the sciatic nerve demonstrated that shorter wavelengths (2.12 μm (holmium:YAG) and 1.85 μm (diode laser, Lockheed Martin Aculight)) produced similar neural activation characteristics to those seen in the FEL [1, 2, 19, 20]. Figure 3.2 shows a logarithmic relationship between absorption coefficient and stimulation threshold. As the absorption coefficient increases, less energy is needed to stimulate in the brain slice; however a higher absorption coefficient also indicates it is easier to damage and ablate tissue. Conversely, wavelengths with lower absorption coefficients require more energy to

stimulate neurons, but with a lower probability that thermal damage will occur. To optimize the wavelength of INS, efficiency of stimulation must be weighed against the risk of damage. In this study, λ=3.65 μm light had an absorption coefficient which was at the midpoint of the wavelengths tested and was selected as the wavelength to conduct the experiments for repetition rate dependence and spot size dependence.

The central nervous system processes information at a higher rate when compared with the peripheral nervous system requiring higher repetition rates when performing electrical stimulation [21-23]. Izzo et al. showed the need for higher repetition rates when using INS in the cochlea and the auditory vestibular nerve to transfer stimulated sensory information to the brain [17, 20]. Therefore, INS should function optimally at a higher repetition rate in the central nervous system than what was used in the sciatic nerve during the original development of INS [2, 17]. The results show that as the laser repetition rate increased the threshold radiant energy decreased (Figure 3.3). At each repetition rate tested, the recorded response was frequency locked with the pulses generated by the laser. The FEL could only generate infrared light up to a pulse rate of 30 Hz. It is conceivable that even lower radiant exposures may be needed to stimulate TC slices with higher frequencies. There are two possible explanations which could be attributed to the decrease in stimulation threshold with increasing pulse repetition rate. The first considers that the neurons in the brain slice have an intrinsic firing rate where all neurons will depolarize at the same time. The argument can be made that an increased stimulation rate would make it easier to desynchronize the intrinsic firing of neurons in the brain slice. This explanation accounts for the decrease in threshold radiant energy seen with INS. The second explanation considers that the higher repetition rates deposits

more energy where some thermal superposition may occur which reduces the amount of energy needed by the next pulse to stimulate.

The number of neurons recruited by INS affects the magnitude of the evoked signal measured using extracellular recording techniques. The last major parameter for INS in the TC slice was determining the optimal spot size of the laser beam. The results show a larger spot size yields a lower threshold radiant exposure needed to stimulate (Figure 3.4). The number of stimulated neurons is dependent on spot size where only the neurons exposed to the infrared light are directly activated. As the spot size decreases, the resulting electrical signal magnitude is smaller since the number of neurons contributing to the signal is decreased making it more difficult to detect the signal with a recording electrode (Figure 3.4); however if a detection modality with the capability to detect over a wide area with high sensitivity (i.e. optical imaging or fMRI) was used, then activity may be detected using the same threshold radiant exposures used with larger spot sizes in smaller spot sizes. Clearly, a more versatile detection system is needed to fully understand the limitations of the spatial precision associated with INS in the CNS.

The final parameter which could influence the INS stimulation threshold in the brain slice was the pulse width of the laser beam. As was mentioned previously, the FEL laser had a fixed macropulse width of 5 μs; however previous studies in the sciatic nerve suggest that stimulation threshold for INS is not effected by the pulse width of light as long as the pulse width is less than the thermal relaxation constant of tissue [2]. Pulse widths between 5 μs and 5 ms have been used to stimulate the sciatic nerve without significantly changing the INS stimulation threshold [1, 2, 19, 20]. It is hypothesized

that future studies will show the pulse width of infrared light will have minimal effect on the stimulation threshold of INS in the CNS.

INS intracellular recordings allowed for the viewing of the induced signal as it traveled through the neuronal networks**.** Using INS as the stimulation modality in intracellular recording experiments has the potential to expand the current knowledge on how neurons process information and relay instructions to different regions of the body. A major advantage of INS over electrical stimulation is the lack of an electrical stimulation artifact seen by the recording electrode. The stimulation artifact associated with electrical stimulation could mask a portion of the physiological signal hindering the interpretation of such signals which are essential for our understanding of the biology associated with the neuron. We successfully conducted a small number of intracellular recordings at 3.65 μm (Figure 3.5). These recordings demonstrate the feasibility of performing INS with electrical intracellular recording techniques

3.6 Conclusions

In summary, we have given a brief overview of the state of the work of INS in the peripheral nervous system and we have shown that infrared neural stimulation is feasible in the central nervous system. Results show consistent frequency locked stimulation and the ability to stimulate continuously. INS in the central nervous systems maintains the contact free, artifact free, and spatial precision characteristics demonstrated by researchers using INS in the peripheral nervous system [13, 19, 24- 26]. These results present a strategy for future studies that will focus on advancing the technique to an *in vivo* preparation. With the completion of the *in vivo* studies, more specific application

based studies can advance INS to deep brain stimulation applications, high spatial precision cortical mapping, and eventual implementation in designs for closed loop neural-machine prosthetics

3.7 Acknowledgements

The authors would like to thank John Kozub, PhD. and the FEL staff for ensuring the Mark-III FEL laser was tuned to the appropriate wavelengths and functioned properly for this study. This work was supported by the National Institutes of Health (NIH R01 NS052407-01) and DOD-MFEL Program (DOD/AFOSR F49620-01-1-4029).

3.8 References

[1] J. Wells, C. Kao, K. Mariappan, J. Albea, E. D. Jansen, P. Konrad, and A. Mahadevan-Jansen, "Optical stimulation of neural tissue in vivo," *Opt Lett,* vol. 30, pp. 504-6, Mar 1 2005.

[2] J. Wells, C. Kao, P. Konrad, T. Milner, J. Kim, A. Mahadevan-Jansen, and E. D. Jansen, "Biophysical mechanisms of transient optical stimulation of peripheral nerve," *Biophys J,* vol. 93, pp. 2567-80, Oct 1 2007.

[3] A. Agmon and B. W. Connors, "Thalamocortical responses of mouse somatosensory (barrel) cortex in vitro," *Neuroscience,* vol. 41, pp. 365-79, 1991.

[4] M. G. Blanton, J. J. Lo Turco, and A. R. Kriegstein, "Whole cell recording from neurons in slices of reptilian and mammalian cerebral cortex," *Journal of Neuroscience Methods,* vol. 30, pp. 203-210, 1989.

[5] C. Q. Kao and D. A. Coulter, "Physiology and pharmacology of corticothalamic stimulation-evoked responses in rat somatosensory thalamic neurons in vitro," *J Neurophysiol,* vol. 77, pp. 2661-76, May 1997.

[6] J. M. Khosrofian and B. A. Garetz, "Measurement of a Gaussian laser beam diameter through the direct inversion of knife-edge data," *Appl Opt,* vol. 22, p. 3406, Nov 1 1983.

[7] D. Wieliczka, S. Weng, and M. Querry, "Wedge shaped cell for highly absorbent liquids: infrared optical constants of water," *Appl Opt,* vol. 28, pp. 1712-1219, 1989.

[8] G. M. Hale and M. R. Querry, "Optical Constants of Water in the 200-nm to 200-µm Wavelength Region," *Appl. Opt.,* vol. 12, pp. 555-563, 1973.

[9] I. J. Bak, U. Misgeld, M. Weiler, and E. Morgan, "The preservation of nerve cells in rat neostriatal slices maintained in vitro: A morphological study," *Brain Research,* vol. 197, pp. 341-353, 1980.

[10] K. H. Reid, H. L. Edmonds Jr, A. Schurr, M. T. Tseng, and C. A. West, "Pitfalls in the use of brain slices," *Progress in Neurobiology,* vol. 31, pp. 1-18, 1988.

[11] P. W. Burgoon, R. W. Burry, and J. A. Boulant, "Neuronal thermosensitivity and survival of rat hypothalamic slices in recording chambers," *Brain Research,* vol. 777, pp. 31-41, 1997.

[12] J. H. Laake, F. M. Haug, T. Wieloch, and O. P. Ottersen, "A simple in vitro model of ischemia based on hippocampal slice cultures and propidium iodide fluorescence," *Brain Res Brain Res Protoc,* vol. 4, pp. 173-84, Jul 1999.

[13] F. A. Wininger, J. L. Schei, and D. M. Rector, "Complete optical neurophysiology: toward optical stimulation and recording of neural tissue," *Appl. Opt.,* vol. 48, pp. D218-D224, 2009.

[14] H. B. Yuan, Y. Huang, S. Zheng, and Z. Zuo, "Hypothermic preconditioning reduces Purkinje cell death possibly by preventing the over-expression of inducible nitric oxide synthase in rat cerebellar slices after an in vitro simulated ischemia," *Neuroscience,* vol. 142, pp. 381-389, 2006.

[15] A. U. Larkman, A. Mason, and C. Blakemore, "The in vitro slice preparation for combined morphological and electrophysiological studies of rat visual cortex," *Neuroscience Research,* vol. 6, pp. 1-19, 1988.

[16] G. W. Hesse and V. E. Shashoua, "Protein synthesis as a function of depth in slices of rat hippocampus," *Neuroscience Letters,* vol. 109, pp. 186-190, 1990.

[17] J. Wells, S. Thomsen, P. Whitaker, E. D. Jansen, C. C. Kao, P. E. Konrad, and A. Mahadevan-Jansen, "Optically mediated nerve stimulation: Identification of injury thresholds," *Lasers Surg Med,* vol. 39, pp. 513-26, Jul 2007.

[18] A. D. Izzo, C.-P. Richter, E. D. Jansen, and J. Joseph T. Walsh, "Laser stimulation of the auditory nerve," *Lasers in Surgery and Medicine,* vol. 38, pp. 745-753, 2006.

[19] J. Wells, P. Konrad, C. Kao, E. D. Jansen, and A. Mahadevan-Jansen, "Pulsed laser versus electrical energy for peripheral nerve stimulation," *J Neurosci Methods,* vol. 163, pp. 326-37, Jul 30 2007.

[20] A. D. Izzo, J. T. Walsh, Jr., E. D. Jansen, M. Bendett, J. Webb, H. Ralph, and C. P. Richter, "Optical parameter variability in laser nerve stimulation: a study of pulse duration, repetition rate, and wavelength," *IEEE Trans Biomed Eng,* vol. 54, pp. 1108-14, Jun 2007.

[21] C. D. Salzman, K. H. Britten, and W. T. Newsome, "Cortical microstimulation influences perceptual judgements of motion direction," *Nature,* vol. 346, pp. 174-177, 1990.

[22] I. Stepniewska, P. C. Fang, and J. H. Kaas, "Microstimulation reveals specialized subregions for different complex movements in posterior parietal cortex of prosimian galagos," *Proc Natl Acad Sci U S A,* vol. 102, pp. 4878-83, Mar 29 2005.

[23] E. J. Tehovnik, A. S. Tolias, F. Sultan, W. M. Slocum, and N. K. Logothetis, "Direct and indirect activation of cortical neurons by electrical microstimulation," *J Neurophysiol,* vol. 96, pp. 512-21, Aug 2006.

[24] A. D. Izzo, J. T. Walsh, H. Ralph, J. Webb, M. Bendett, J. Wells, and C.-P. Richter, "Laser stimulation of auditory neurons: effect of shorter pulse duration and penetration depth," *Biophys. J.,* p. biophysj.107.117150, January 11, 2008 2008.

[25] I. U. Teudt, A. E. Nevel, A. D. Izzo, J. T. Walsh, Jr., and C. P. Richter, "Optical stimulation of the facial nerve: a new monitoring technique?," *Laryngoscope,* vol. 117, pp. 1641-7, Sep 2007.

[26] N. M. Fried, G. A. Lagoda, N. J. Scott, L.-M. Su, and A. L. Burnett, "Noncontact Stimulation of the Cavernous Nerves in the Rat Prostate Using a Tunable-Wavelength Thulium Fiber Laser," *Journal of Endourology,* vol. 22, pp. 409-414, 2008.

CHAPTER IV

PULSED INFRARED LIGHT ALTERS NEURAL ACTIVITY IN RAT SOMATOSENSORY CORTEX IN VIVO

Jonathan M. Cayce[1], Robert M Friedman[2], E. Duco Jansen[1,3],

Anita Mahadevan-Jansen[1,3], and Anna W. Roe[1,2]

[1] Department of Biomedical Engineering, Vanderbilt University

Nashville Tennessee

[2] Department of Psychology, Vanderbilt University

Nashville Tennessee

[3] Department of Neurological Surgery, Vanderbilt University

Nashville Tennessee

This chapter was published in:

"Pulsed infrared light alters neural activity in rat somatosensory cortex *in vivo*,"

Neuroimage, vol 57, issue 1, July 2011, pp. 155-166

4.1 Abstract

Pulsed infrared light has shown promise as an alternative to electrical stimulation in applications where contact free or high spatial precision stimulation is desired. Infrared neural stimulation (INS) is well characterized in the peripheral nervous system; however, to date, research has been limited in the central nervous system. In this study, pulsed infrared light (λ=1.875 μm, pulse width=250 μs, radiant exposure=0.01-0.55 J/cm^2, fiber diameter =400 μm, repetition rate=50-200 Hz) was used to stimulate the somatosensory cortex of anesthetized rats, and its efficacy was assessed using intrinsic optical imaging and electrophysiology techniques. INS was found to evoke an intrinsic response of similar magnitude to that evoked by tactile stimulation (0.3-0.4% change in intrinsic signal magnitude). A maximum deflection in the intrinsic signal was measured to range from 0.05% to 0.4% in response to INS, and the activated region of cortex measured approximately 2 mm in diameter. The intrinsic signal magnitude increased with faster laser repetition rates and increasing radiant exposures. Single unit recordings indicated a statistically significant decrease in neuronal firing that was observed at the onset of INS stimulation (0.5 s stimulus) and continued up to 1s after stimulation onset. The pattern of neuronal firing differed from that observed during tactile stimulation, potentially due to a different spatial integration field of the pulsed infrared light compared to tactile stimulation. The results demonstrate that INS can be used safely and effectively to manipulate neuronal firing.

4.2 Introductions

Infrared neural stimulation (INS) represents a relatively new stimulation modality that exhibits high spatial precision and can be delivered in a contact free method for the stimulation of neural tissue [1]. Investigations into the use of pulsed infrared light to stimulate neural tissue by our group began in the peripheral nervous system (PNS) where we, and others, have demonstrated the ability of INS to reliably evoke action potentials in peripheral nerves [2-4]. Pulsed infrared light can also stimulate auditory ganglion cells in the cochlea with high spatial precision establishing INS as a possible alternative to electrical stimulation for cochlear implants [5-7]. Most recently, embryonic quail hearts were paced by pulsed infrared light, suggesting the possibility of optically based pacemakers [8]. In the central nervous system (CNS) the first application of INS was demonstrated by our group in thalamocortical brain slices [9].

For each of these applications, the parameter set for INS had to be established. Stimulation of the sciatic and facial nerve required low frequency stimulation (maximum of 5 Hz) to evoke stimulus locked compound muscle action potentials; the threshold radiant exposures were 0.4 J/cm^2 and 0.7 J/cm^2 for the sciatic and facial nerves, respectively [3, 4]. Stimulation of rat cavernous nerves with infrared light at a radiant exposure of 1 J/cm^2 at 10 Hz for 60s produced a complex intracavernosal pressure response with no functional loss [2]. In cochlear studies, effective non-damaging stimulation parameters, consisting of high frequency (at least 200 Hz), short pulse width stimulation, evoked potentials in the inferior colliculus [5-7]. The pacing of embryonic hearts required radiant exposures of 0.8 J/cm^2 at 2 Hz [8]. The different stimulation

parameters across each of these studies illustrates that each new INS application requires the identification of unique laser parameters to best activate a new target tissue.

The differences in anatomy and physiology of the CNS compared to the PNS presents a new set of challenges in applying INS to activate neural tissue. Unlike the PNS where axons of both afferent and efferent neurons are organized in parallel bundles in fascicles of nerves, the brain contains complex neuronal networks with interwoven architectures. In addition, cellular composition of the CNS (e.g. neurons, support cells such as astrocytes, ogliodendrocytes, and microglia) may affect neuronal responses in ways not seen in PNS studies. Thus, even though INS is an effective means of stimulation in the PNS, fully realizing the potential of INS to activate CNS tissue will require complete characterization of stimulation parameters for each CNS structure. This study represents a further step towards this goal.

To approach *in vivo* cortical application, feasibility of CNS stimulation was first investigated with infrared light by applying INS to thalamocortical brain slices *in vitro* [9]. The thalamocortical brain slice model preserves a three-neuron network between cortical and thalamic neurons present *in vivo* [10-12]. In the slice study, pulsed infrared light was shown to stimulate CNS neurons and evoked potentials that could be blocked with tetrodotoxin (TTX). Parametric studies demonstrated that the absorption coefficient of a given wavelength determined stimulation threshold. An increase in spot size and higher repetition rates also reduced stimulation threshold. The results from this study supported previous findings that suggest a temperature gradient (dT/dz or dT/dt) is the most likely mechanism by which pulsed infrared light induces neural activation [13].

While the brain slice model was ideal for establishing feasibility, there are fundamental differences between an *in vitro* brain-slice and an *in* vivo application.

The purpose of this study was to examine whether pulsed infrared light could be used to regulate cortical neuronal activity *in vivo* and to investigate laser parameters that activated cortex without causing damage. Both electrophysiological and optical intrinsic signal imaging (OISI) techniques were used to characterize signals generated by INS. Because OISI offers a large field of view (~10 mm) and high spatial resolution (10 μm), it has been an effective way to examine functional organization in cerebral cortex and to guide microelectrode placement to characterize neuronal responses [14, 15]. In this study, rat somatosensory cortex corresponding to the forepaw and barrel fields was chosen because these areas have been well characterized with OISI methods [16-19] and lends themselves well to assessment of INS effects. We report that INS can manipulate somatosensory cortex activity without apparent detriment to cortical function. This study represents the first successful application of INS to cortical structures *in vivo,* where INS has potential clinical use and shows promise to be a useful tool for future studies of neuronal circuitry.

4.3 Methods

4.3.1 Surgical procedures

All procedures were performed in accordance with protocols approved by the Vanderbilt University IACUC. Briefly, male Long Evan rats (n = 15; 300 – 500 g) were anesthetized with a 50% urethane (Sigma, St. Louis MO) solution (I.P. 1.4 g/kg). The toe-pinch test was used to ensure the animal was in an adequate state of anesthesia. A tracheotomy was performed to allow for ventilation (Harvard Model 683 Small Animal Ventilator, Harvard Apparatus Holliston, MA) of the animal during the experiment. The animal was placed in a stereotactic frame and a craniotomy and durotomy were conducted to expose somatosensory cortex (+2 to -5 mm anterior/posterior, and 7 mm lateral to bregma) [16, 20]. Mannitol (1.0 ml, 20% concentration) was given I.P. to prevent potential brain swelling. Warm (~ 37 Celsius) 3% agar (Sigma, St. Louis MO) in saline was used to stabilize the cortex and a glass coverslip was placed on the agar to create an imaging window for optical imaging. A small portion of agar was dissected away to create an access port for placement of the optical fiber for application of INS.

4.3.2 Optical imaging

Ten animals were used in experiments involving optical imaging. Intrinsic signal optical imaging was performed using a CCD camera (NeuroCCD-SM256, SciMeasure Analytical Systems, Inc. Decatur, GA) positioned over the craniotomy. Cortex was illuminated by 632 nm bandpass filtered light from a halogen light source and focused onto the brain using fiber optics. Light reflected from cortex was collected onto the CCD

chip using a Dark Invader 50 mm f/1.3 lens (B.E. Meyers & Co., Inc., Redmond WA) and a Ex2C Computar C-mount extender (CBC (AMERICA) Corp., Commack, NY) to provide a working distance of 20 cm and a FOV of approximately 5 X 5 mm. This working distance allowed for easy placement of the optical fiber used for laser stimulation.

The Redshirt Imaging System running Cortiplex software (Redshirt Imaging, Decatur, GA) controlled the sequence of the entire experiment. The software collected images from the CCD camera and controlled the stimulus presentation (Figure 4.1). At the beginning of each imaging trial, Redshirt software started collecting image frames and sent a binary code specifying a stimulus condition to a stimulus computer running LabVIEW software and National Instruments hardware (National Instruments, Austin, TX). The LabVIEW program sent TTL pulses to the laser and the driver of the piezoelectric stimulators at the desired repetition rate for a given experiment. Radiant exposure, pulse width, and wavelength were all preset on the laser. Voltage and pulse width were preset on the piezoelectric controller. Stimuli were presented 300 ms after trial onset. After image acquisition the intertrial interval was 8-15 s. Figure 4.1B outlines the imaging protocol used to collect images.

We designed two types of imaging runs. For runs with only cutaneous stimulation, images were typically collected for 3 s at a frame rate of 5 Hz. For experiments with at least one INS condition, images were collected for 10 to 15 s at a frame rate of 10 Hz. In all experiments there were at least two conditions for a given imaging run: one stimulus condition (i.e. tactile or INS) and one blank (no stim) condition. In most cases there were multiple stimulation conditions (i.e. one tactile and 3

laser conditions). Conditions were grouped into blocks where each condition was presented in an interleaved and pseudorandom manner. Between 25 and 50 blocks of each condition were collected for one imaging run.

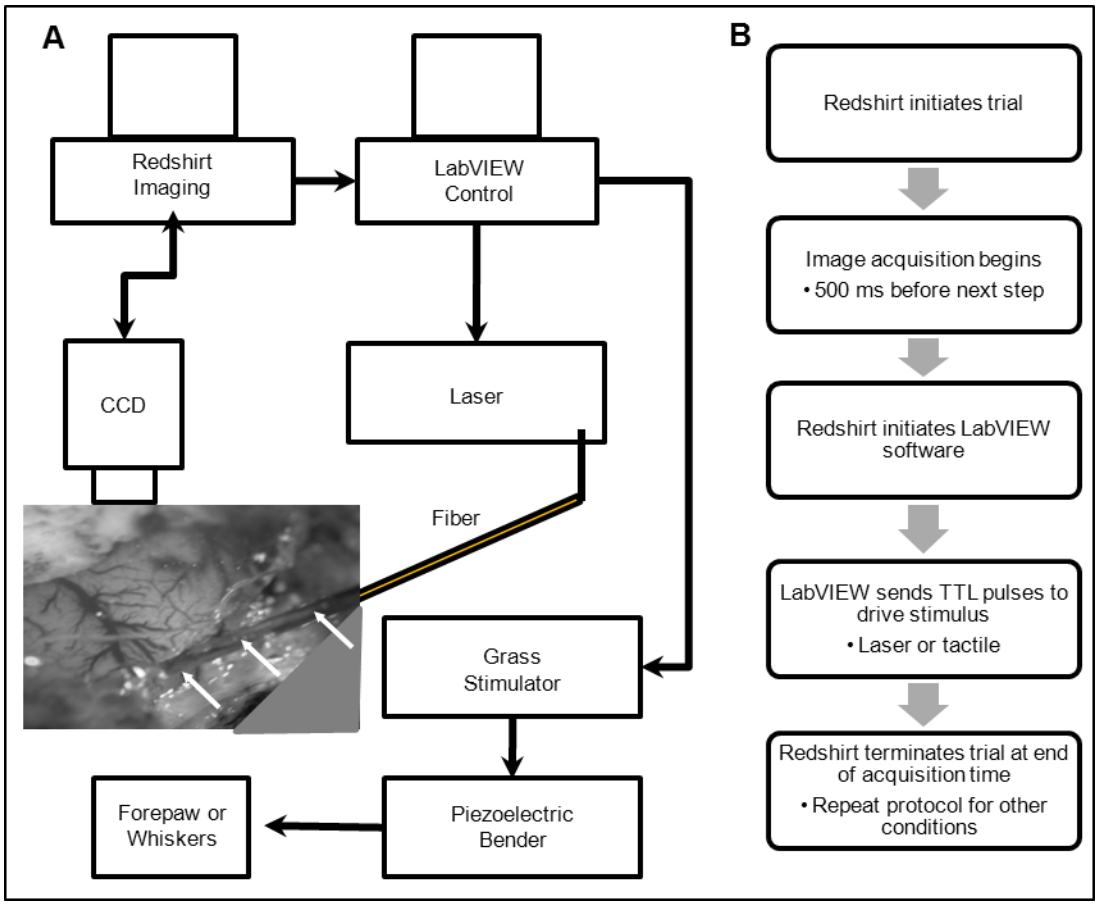

Figure 4.1: Experimental setup for infrared neural stimulation and optical imaging. (A) Schematic diagram of the experimental setup. Experiment is controlled by Redshirt imaging software that acquires images and determines when stimuli are presented by signaling a separate computer running LabVIEW software that is responsible for stimulus presentation. The LabVIEW control computer triggers stimuli by sending TTL pulses to either the piezoelectric controller or the laser. The optical fiber used to deliver infrared light is positioned on cortex or just above cortex through a window created through agar and the piezoelectric bender is positioned on targeted forepaw digit or whiskers. Image shows an example of a fiber positioned on cortex through a port created in the agar. (B) Imaging protocol flow chart of one trial for a given condition.

4.3.3 Laser stimulation parameters

Wavelength selection for performing infrared neural stimulation was based on the optical penetration depth of light in tissue which was estimated using absorption data for water since biological soft tissue is 70% water [21]. Previous studies using infrared light to stimulate neural tissue have indicated that an optical penetration depth of 300 – 600 μm is optimal for stimulating neural tissue [1, 7, 22]. This optical penetration depth range corresponded to a wavelength of 1.875 μm. Infrared neural stimulation was performed using a 1.875 μm ± 0.02 μm Capella neural stimulator (Lockheed Martin Aculight, Bothel WA). Light was delivered to the cortex through a 400 μm diameter Ocean Optics fiber (St. Petersburg, FL) with a numerical aperture (NA) of 0.22. The fiber was placed between 0 – 1000 μm from cortex using a hydraulic micromanipulator (Narishige, Tokyo, Japan). Laser repetition rate ranged between 50 – 200 Hz, and pulse duration was held constant at 250 μs. The average power from the laser was measured at the fiber tip using a Power Max 500D laser power meter with a PM3 detector head (Coherent, Santa Clara, CA). Radiant exposure was calculated based on the NA of the fiber and the distance of the fiber tip from cortex [1]. The radiant exposure varied between 0.01 – 0.55 J/cm^2 and was dependent on the stimulation parameters used for a given experiment. Pulse train duration for all INS experiments was 500 ms. Laser triggering was controlled via a LabVIEW software interface (Figure 4.1).

4.3.4 Tactile stimulation parameters

Piezoelectric benders (Noliac, Kvistgaard, Denmark) were used to present vibratory stimuli to the forepaw digits or the whiskers contralateral to the cortical

recording site. Each piezoelectric stimulator was driven using DC pulses from a GRASS stimulator (S88 Astro-Med Inc, West Warwick, RI) that was triggered by LabVIEW software to control stimulation (Figure 4.1). For optical imaging, square wave pulses at 8 Hz for 3 seconds were delivered to the piezoelectric; for electrophysiology, pulses were delivered to the piezoelectric at 1 Hz for 3 seconds. Neurophysiological responses to palpation were used to map somatosensory cortex and to assess the health and functionality of cortex before, during and after INS presentation.

4.3.5 Optical imaging data analysis

Analysis of optical imaging data was performed with software written in Matlab (Mathworks, Natick, MA). All conditions (blank and experimental) were first frame subtracted and then summed across trials to maximize signal to noise ratio. Experimental conditions were then blank-subtracted to measure changes in the intrinsic signal from baseline [15]. Trial by trial assessment of image quality was conducted to remove any bad trials due to lighting abnormalities, large physiological movement, or camera acquisition errors. As determined by the signal to noise ratio for a given experiment, image maps were optimized for display by clipping the range (0.8 - 2.5 standard deviations) of pixel values around the mean. In some cases, a blood vessel mask was used to reduce artifact signal related to surface vasculature. Standard Gaussian low-pass and median high-pass filtering were used to remove contamination from uneven illumination and from other physiological noise sources. A student's t-test was used to compare stimulation conditions to blank conditions to identify significant pixels and create t-maps. This analysis aided in identifying regions of interest for time course analysis. The time

course of the intrinsic signal was examined at selected sites by averaging the values of pixels within the region of interest. The summed pixel value from the first image frame was subtracted from each subsequent sequence of frames in a condition's sequence and then used as a divisor to measure the change in reflectance over background reflectance (dR/R). The blank time course was then subtracted from each experimental condition to remove non-stimulus associated changes in reflectance. In a given experiment, the maximum deflection magnitude of the signal was used to determine the peak of the intrinsic response and was used to compare the ability of each stimulation condition to induce intrinsic responses.

4.3.6 Electrophysiology recordings

Five additional animals were used to study the electrophysiology associated with INS. Single unit electrophysiology was used to assess the cortical neuronal responsiveness before, during, and after INS. Tungsten microelectrodes (1 – 3 MΩ, World Precision Instruments, Sarasota, FL) were inserted into cortex at depths of 50 – 500 μm in regions of interest identified from piezoelectric tactile stimulation. Single units were isolated with high spontaneous activity to study the effects of INS on neuronal activity. The fiber optic was placed approximately 1 mm away from the electrode. Signals were filtered and digitized using a 16 channel AM-Systems (Sequim, WA) differential amplifier using a 300 – 5K bandpass filter. The LabVIEW interface was used to control presentation of tactile and laser stimulation, and Datawave software (Loveland, CO) was used to collect single unit data. Peristimulus time histograms (PSTH) were

generated using Dataview software. A paired Student's t-test analysis was used to determine the significance of changes observed in the PSTH related to laser stimulation.

4.4 Results

The experiments described below were conducted in rat somatosensory cortex, either in barrel cortex in response to whisker stimulation or in forepaw cortex in response to tactile stimulation of the digits.

4.4.1 Intrinsic optical imaging of vibrotactile stimulation

Baseline functionality and viability of somatosensory cortex prior to the application of INS was assessed through optical imaging of hemodynamic responses in somatosensory cortex. Figure 4.2 illustrates a normal functional response to vibrotactile stimulation of D2 and D4 of the contralateral forepaw in response to taps delivered by a piezoelectric stimulator (8 Hz, 3 s). Darker pixels in the functional maps indicate activation (Figure 4.2B, C, and D). Cortical activation to D4 stimulation was medial and posterior to D2 as emphasized by the dark (D4, ROI 2) and light (D2, ROI 1) ROIs in the subtraction map between the two conditions (Figure 4.2D). Figure 4.2E, F and G illustrate signal time courses taken from the D2 (ROI 1), D4 (ROI 2), and control (edge of craniotomy, ROI 3) locations, respectively. Optical responses to D2 stimulation, D4 stimulation, and the no stimulation conditions are plotted in green, blue, and red traces, respectively. As indicated by the larger negative deflections in intrinsic signal magnitude, the time courses of activation (Figure 4.2E-G) demonstrated preferential activation for stimulation of D2 at the D2 site (ROI 1) and for stimulation of D4 at the D4 site (ROI 2).

The optical intrinsic signals were not focal within the forepaw representation as D2 stimulation activated the D4 ROI and D4 stimulation activated the D2 ROI. The blank condition (no stimulation) produced little response at the D2 and D4 sites, which was comparable to the lack of signal obtained at the control site for all three conditions (Figure 4.2G). These activation maps are representative of the optical responses obtained in rat barrel cortex and rat forepaw cortex generated by tactile stimulation in these experiments.

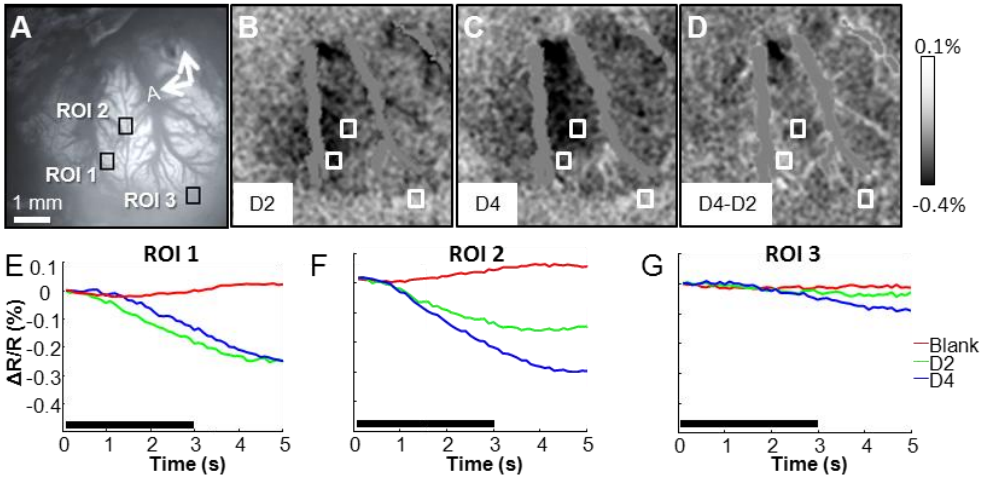

Figure 4.2: Typical intrinsic imaging response to vibrotactile stimulation of contralateral forepaw digits. (A) Blood vessel map. Black boxes are region of interests where time course data was calculated for D2, D4, and no stimulation conditions. (B & C) Activation maps in response to stimulation of D2 and D4 respectively. Darkening in image indicates activation. (D) D4 – D2 subtraction map, darkened area represents selective D4 and lightened area selective D2 activation. (E-G) Time courses of intrinsic signals taken from region of interests demarcated by black and white boxes in (A-D). Traces in green, blue, and red indicate responses to D2, D4, and no stimulation conditions. ROI 1 corresponds to a D2 region of cortex, ROI 2 corresponds to a D4 region of cortex and ROI 3 corresponds to a non-activated region of cortex. Black bar represents the timing of the stimulus. Stimulation parameters: 3 sec train, 8 Hz. Imaging Parameters: 10 fps, 21 trials. A = anterior, M = medial. Scale bar next to (D) indicates clipping range of % change in signal in respective images.

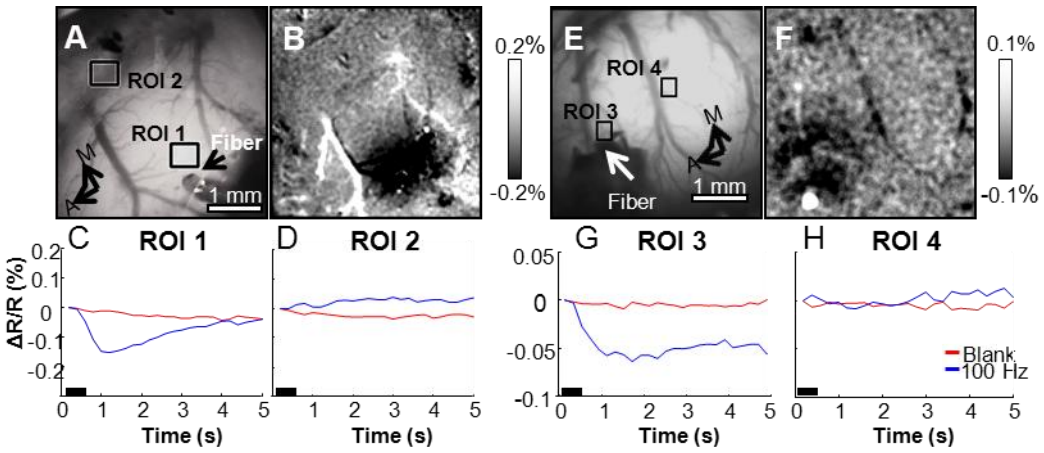

Figure 4.3: INS evoked intrinsic optical signals in somatosensory cortex. INS evokes intrinsic optical signals in somatosensory barrel field (A-D) and forepaw cortex (E-H) in separate experiments (632 nm). (A & E) Blood vessel maps indicating ROI locations (ROI 1&3 = site near INS stimulation, ROI 2&4 = site distant from INS stimulation) and fiber location (Fiber). (B & F) Activation maps obtained to laser stimulation in barrel field cortex (B) and forepaw cortex (F). (C & G) Time course of signals in region near laser stimulation (ROI 1 and ROI 3). (D & H) Time course of signals distant from laser stimulation site (ROI 2 and ROI 4). Blue line reflects signal evoked by laser stimulation. Red line shows control (no stim) time course. There is no appreciable optical response at this distance from laser stimulation. Laser parameters: λ = 1.875 µm, repetition rate = 100 Hz, pulse train duration = 500 ms, pulse width = 250 µs, radiant exposure = 0.55 J/cm2, spot size diameter = 400 µm. Imaging Parameters: 5 fps, ITI = 8 s, Trials = 40. A = anterior, M = medial. Black bar in (C-H) represents the timing of the stimulus. Scale bars next to (B & F) indicate clipping range of respective images.

4.4.2 Demonstration of INS induced optical intrinsic signals

Infrared neural stimulation was then examined to determine if pulsed infrared light could induce an optical response in cerebral cortex comparable to that induced by natural sensory stimulation. Figure 4.3 demonstrates that INS of cortical tissue induces changes in optical reflectance signal of somatosensory cortex. A fiber optic was placed over somatosensory cortex corresponding to the barrel fields (Figure 4.3A). Stimulation of the cortex with INS (100 Hz, 0.55 J/cm^2, λ=1.875 µm, 250 µs pulse width, 500 ms pulse train) evoked changes in optical reflectance at and near the fiber optic location, as illustrated by the activation map shown in Figure 4.3B. The activated region of cortex

(dark pixels) in response to these INS parameters produced a focal region of activation, approximately 1.5 - 2 mm in diameter. As shown in Figure 4.3C, the time course reaches a peak after 1 s and has a duration of 3 s. The magnitude of the change in reflectance peaked at approximately 0.15%. No such optical reflectance change was obtained during the Blank condition. Optical signal changes were not observed at sites distant from the INS location (Figure 4.3D), indicating that the INS-induced signal has high spatial selectivity. In a separate experiment, the same laser conditions used in Figure 4.3A were used to generate a response in forepaw cortex to demonstrate that INS can evoke optical responses in different cortical areas (Figure 4.3E-H). These experiments demonstrated that INS is capable of inducing optical responses in somatosensory cortex, some of which are similar to those obtained with natural tactile stimulation.

4.4.3 Effects of laser repetition rate on INS evoked intrinsic signal

To further establish that the optical signal was indeed induced by INS, varied repetition rate was varied to study how the reflectance signal changed in relation to the repetition rate of the laser (Figure 4.4). The expectation for these experiments was that the greater the total light energy applied to the cortex, the stronger the optical reflectance change. Using a 500 ms duration pulse train and 250 μs pulse width, we applied repetition rates of 50, 100, 150, and 200 Hz (Figure 4.4B-E). Figure 4.4A illustrates the location of the fiberoptic (Fiber) as well as a t-map generated via pixel-by-pixel t-tests ($p < 0.001$) between the 100 Hz laser stimulation and blank conditions (orange colored pixels). As can be seen qualitatively in Figure 4.4B-E, an increase in laser repetition rate increased the size of the activation region. Quantitatively, the 200 Hz laser stimulus (aqua

blue line) produced the largest optical reflectance change, while a 50 Hz stimulus (pink line) produced the smallest response (Figure 4.4F). As shown in Fig 4G, the magnitude of the intrinsic signal exhibits an exponential fit with repetition rate.

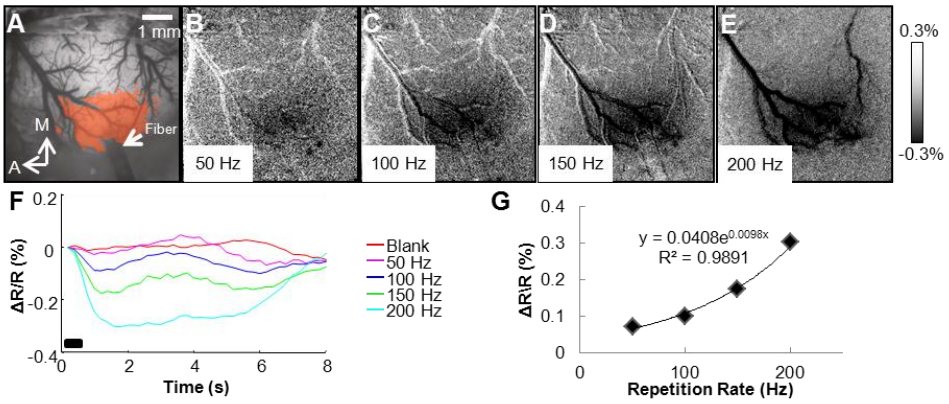

Figure 4.4: Intrinsic signals produced by different rates of INS. (A) Blood vessel map. Location of fiberoptic is indicated by arrow. Orange pixels indicate significant pixels in t-test between 100 Hz stimulation and blank condition. (B-E) Activation maps of laser repetition rates: 50 Hz (B), 100 Hz (C), 150 Hz (D), 200 Hz (E). (F) Time course of response resulting from laser stimulation conditions 50 Hz (red), 100 Hz (blue), 150 Hz (greenF), and 200 Hz (aqua blue) and blank conditions. (G) Laser repetition rate versus the peak amplitude of the intrinsic signal. Relationship fit with an exponential equation. Laser parameters: λ = 1.875 µm, repetition rates = 50, 100, 150, 200 Hz, pulse train duration = 500 ms, pulse width = 250 µs, radiant exposure = 0.55 J/cm^2, spot size = 400 µm. Imaging parameters: 40 Trials, 5 f/s. A = anterior, M = medial. Black bar in (F) represents the timing of the stimulus. Scale bar next to (E) indicates clipping range of images (B-E).

4.4.4 Effects of radiant exposure on intrinsic signal

Threshold is an important aspect of INS to consider when developing the modality as an alternative to electrical stimulation. Figure 4.5 displays the functional response when the radiant exposure of each pulse was adjusted across imaging runs, and examines the time course of activation for the ROI (red box) shown in Figure 4.5A. The laser parameters of stimulation used to generate these time courses were 200 Hz, 500 ms

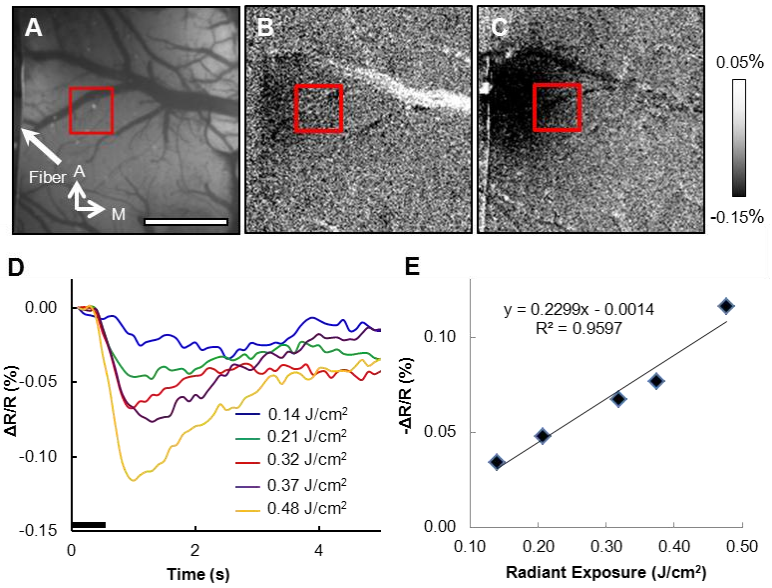

Figure 4.5: Increased INS radiant exposure leads to an increase in intrinsic signal magnitude. (A) Blood vessel map showing location of ROI (red box) and fiber location (tip barely in FOV). (B & C) Activation maps from stimulation with 0.14 J/cm^2 and 0.48 J/cm^2. (D) Time course of signal for different radiant exposures. (E) Radiant exposure versus peak amplitude of the intrinsic signal. Relationship fit with a linear equation. Laser parameters: λ = 1.875 µm, repetition rate = 200 Hz, pulse train duration = 500 ms, pulse width = 250 µs, spot size = 400 µm, radiant 0.14 (blue), 0.21 (green), 0.32 (red), 0.37 (purple), 0.48 J/cm^2 (orange). A = anterior, M = medial. Black bar in (D) represents the timing of the stimulus. Scale bar next to (C) indicates clipping range of images.

duration pulse train of 250 µs pulses at the five different radiant exposures indicated in the figure legend. Figure 4.5B&C show the functional maps to 0.14 J/cm^2 and 0.48 J/cm^2 radiant exposures. As expected, the smallest radiant exposure (0.14 J/cm^2 Figure 4.5D, blue line) resulted in the smallest intrinsic signal magnitude. Intermediate radiant exposures (0.21 and 0.32 and J/cm^2, green and red lines) produced intermediate signal size, and the largest radiant exposures tested (0.37 and 0.48 J/cm^2, purple and orange lines) resulted in the largest signal amplitudes. The magnitude of the intrinsic signal exhibits a linear fit with radiant exposure (Figure 4.5E). The area of activation also increased with radiant exposure energy, as shown qualitatively (Figure 4.5B&C).

Thus, within the ranges tested, both increases in laser stimulation rate and radiant exposures resulted in greater optical activation signal, suggesting a consistent and specific effect of laser stimulation on cortical response.

4.4.5 Effective distance of INS induced effect

The spatial selectivity of INS in cortical tissue was characterized by calculating the time course of the intrinsic signal at five distinct locations. Figure 4.6 displays the time courses based on distance from the laser stimulation site (200 Hz, 0.55 J/cm^2, pulse width 250 μs, pulse train 500 ms). In Figure 4.6A, the red box represents the region of interest closest to the optical fiber; the orange and magenta boxes are the most distant regions of interest. The peak signal is largest for the location closest to the fiber optic (Fig 4.6B, red line) and decreases in amplitude with distance from the stimulation location. This decline in signal size with distance also occurred in other directions as indicated by the comparable signal amplitude of magenta and orange ROIs in Figure 4.6A. As also shown in Figure 4.3, the prominent effects of INS stimulation lies within 1-2 mm of the stimulation site and declines rapidly as a function of distance from the stimulation site (Figure 4.6C). The spatial temporal aspects of the signal are illustrated in Figure 4.6D through a time series of optical images taken during the imaging run. The data was temporally binned by 2 to decrease the number of images displayed in the mosaic; therefore, each frame represents 400 ms in time. The stimulus came on at 200 ms and was off at 700 ms after trial start, which indicates frames 1-2 represent the time the laser was turned on. The signal peaks between frames 7 and 8 which corresponds to the time courses displayed in figure 4.6B. Furthermore, figure 4.6D demonstrates that

laser induced intrinsic signal is focal in an area measuring approximately 1 mm in diameter at its peak demonstrating the spatial precision of INS. This spatially limited characteristic makes INS a potentially useful method for studies requiring focal stimulation. The time series of images for 50, 100, 150, and 200 Hz were included as a supplemental figure to further demonstrate the effects of repetition rate on the evoked signal and to demonstrate the spatial precision of INS.

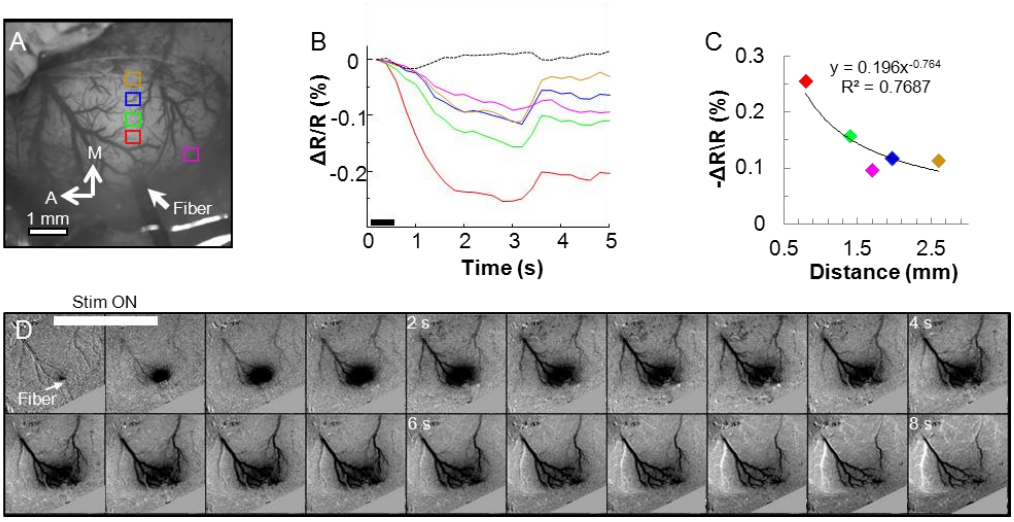

Figure 4.6: Spatial distribution of intrinsic signal in response to INS. (A) Blood vessel map with sampled ROIs overlaid. Color of box in map corresponds to color of time course trace displayed in (B). (B) Intrinsic signal time courses at different distances from the INS stimulation location. Dashed black line corresponds to the no stimulation condition collected from the red-boxed ROI. (C) Peak amplitude of the intrinsic signal as a function of distance from the fiber. Relationship fit with an exponential equation. (D) Time mosaic of optical images to illustrate the spatiotemporal aspects of the INS induced intrinsic signal. Images were temporally binned by two decreasing the effective frames per second to 2.5 Hz. Laser parameters: λ = 1.875 µm, repetition rate: 200 Hz, pulse train duration = 500 ms, pulse width = 250 µs, radiant exposure = 0.55 J/cm^2, spot size = 400 µm. Imaging parameters: 40 Trials, 5 f/s. Black bar in (B) represents the timing of the stimulus. A= anterior, M = medial.

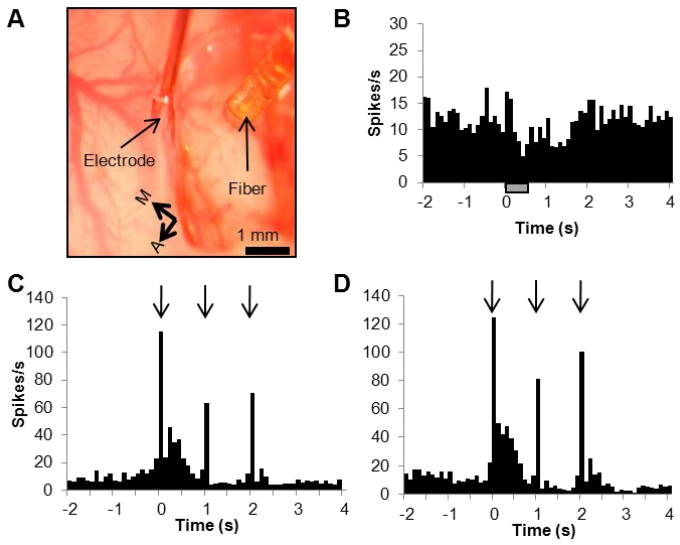

Figure 4.7: INS induces an inhibitory neural response and does not alter neuronal response to tactile stimulation. (A) Image of somatosensory cortex corresponding to barrel field showing electrode and fiber placement. Fiber stimulation site to electrode distance was approximately 1 mm. Electrode tip was placed 50 µm into cortex. (B) PSTH showing modulation of neural response to INS (30 trials). The laser-induced inhibition of neural activity had a duration of approximately 1.5 s and was followed by a rebound. (C) PSTH of vibrotactile stimulation generated by a piezoelectric bender deflecting contralateral whiskers once at each arrow. Laser and whisker stimulation were interleaved. (D) PSTH of vibrotactile stimulation after INS. (C & D) Demonstrate INS did not cause a loss of cortex functionally responding to sensory stimulation. Laser parameters: λ = 1.875 µm, repetition rate = 100 Hz, pulse train duration = 500 ms, pulse width = 250 µs, radiant exposure = 0.019 J/cm^2, spot size = 1200 µm. Hatched bar in (B) represents the timing of the stimulus. A= anterior, M = medial.

4.4.6 Inhibitory effect of INS stimulation in somatosensory cortex

In addition to optical imaging, electrophysiological techniques were used to study the effects of INS on neuronal activity. Figure 4.7A displays the positioning of the electrode and fiber, approximately 1 mm apart. This arrangement was similar for each experiment involving electrophysiological measurements. Units that were responsive to tactile stimulation were isolated to assess cortical function during INS. Figure 4.7B displays the results of laser stimulation on spontaneous neural activity. Illustrated is a peristimulus time histogram (PSTH) resulting from the irradiation of somatosensory cortex (186 trials with intertrial intervals of 15 s; radiant exposure of 0.019 J/cm^2, pulse

width of 250 μs, pulse train length of 500 ms). Stimulus onset occurred at time zero and lasted for 500 ms (hashed bar on PSTH). Infrared neural stimulation was observed to reduce the neural firing rate that lasted approximately 1.5-2.0 s, followed by a return to baseline levels. This reduction in firing rate was statistically significant, as evaluated by comparing the two seconds prior to stimulation and the two seconds post stimulation onset (paired t-test, α=0.05, -2000ms to 0 ms: $p < 0.0046$, 2000ms to 4000 ms $p<9.6E-5$). No statistical difference was observed between the two seconds before stimulation and the time region corresponding to 2 – 4 seconds after stimulation offset.

4.4.7 Cortex remains responsive during INS

The physiologic health of the cortex was assessed through electrophysiological recordings of neuronal responses to tactile stimulation. In Figure 4.7C&D, tactile stimulation was delivered by a piezoelectric stimulator that deflected contralateral whiskers once at each arrow in the PSTH. During runs in which INS was interleaved with tactile stimulation, consistent, normal neural responses to tactile stimulation were recorded (Figure 4.7C). The PSTH in Figure 4.7D represents tactile stimulation alone after INS had been applied demonstrating no loss in functionality. These recordings from tactile stimulation demonstrate that the normal excitatory and inhibitory periods of post-stimulation responses were present. Thus, even after repeated presentation of INS for a period of over 2 hours, normal neuronal tactile responses remained intact indicating that INS does not cause damage to cortex which compromises neuronal activity.

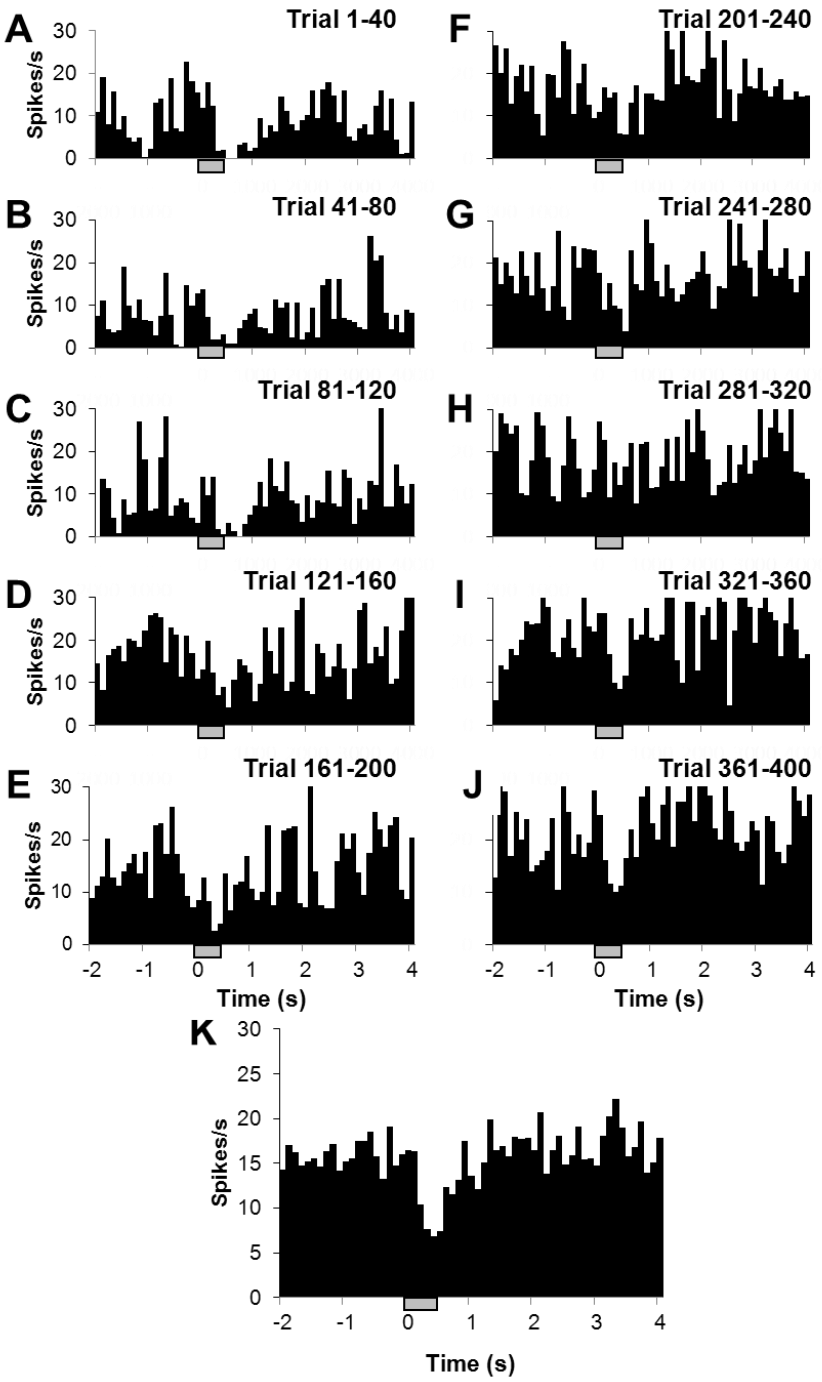

Figure 4.8: Inhibitory effect of INS on neural activity is consistent over many trials. (A-J) PSTH mosaic of ten segments (40 trials per segment). The laser induced inhibition is strongest in the first 120 trials, then weakens but is evident through trials 361-400. (K) PSTH summation of all segments (A – J). Laser parameters: λ=1.875µm, repetition rate = 200 Hz, pulse train duration = 500 ms, pulse width = 250 µs, radiant exposure = 0.0549 J/cm^2, spot size = 850 µm. Hatch bars represent the timing of the stimulus.

4.4.8 Stability of INS induced responses

Stability of INS induced responses is important to consider when assessing the stimulation modality's efficacy for neuroscience applications and eventual translation to clinical studies. To examine the stability of INS induced responses, a sequence of PSTHs were produced by dividing the total number of INS trials into sequential 40 trial epochs. Figure 4.8 displays a sequence of PSTHs recorded from a single unit in response to INS (radiant exposure 0.055 J/cm^2, spot size 850 μm , repetition rate of 200 Hz, pulse width 250 μs, train length 500 ms, 15 s intertrial interval). In most of the histograms, inhibition is most evident during the period from stimulus onset (time = 0 s) to approximately 1 s. In this example, it can be seen that INS induced inhibition is readily apparent from trial 1 to at least trial 120, and although appears to weaken slightly subsequently, the signal is still evident as late as trials 360-400. Paired t-tests between the two seconds following stimulus onset and prestimulus periods indicate that the difference in spike rate is statistically significant (α=0.05) for the summation of all trials (Figure 4.8K) indicating that INS in rat somatosensory cortex has an immediate inhibitory effect on neuronal response, one which appears to remain present over many trials

A separate experiment was conducted to assess the stability of this effect at two separate time points during an experiment. Figure 4.9A represents an initial PSTH taken over 30 trials separated by ITIs of 30 s. Again a period of statistically significant (paired t-test, -1 s to 0 s: $p < 0.01$, 1 s to 2 s $p<4.08E-5$) inhibition of baseline activity was observed within the first 1 s after INS onset (spot size diameter 850 μm, pulse train length 500ms, pulse width 250 μs, radiant exposure of approximately 0.078 J/cm^2). The laser was then turned off and the cortex was allowed to rest for 30 minutes after which

the experiment was repeated. Figure 4.9B illustrates the PSTH recorded from single unit activity at the same location using the same laser parameters used to generate figure 4.9A. Again, a period of inhibition was obtained within the first 1 s following INS (paired t-test, -1 s to 0 ms: $p < 0.03$, 1 s to 2 s $p<0.00038$). This further demonstrates the repeatability of the inhibitory effect.

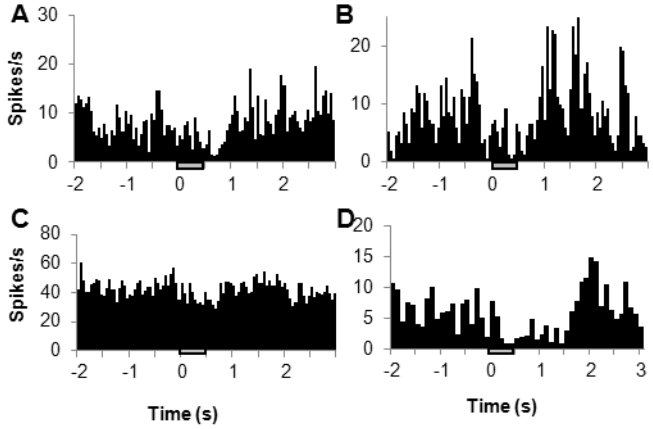

Figure 4.9: Repeatability of the neural INS inhibitory effect. (A) PSTH of single unit in response to INS. (B) A second PSTH from the same unit taken approximately 30 minutes later. Laser parameters: λ = 1.875 µm, repetition rate= 200 Hz , pulse train duration = 500 ms, pulse width = 250 µs, radiant exposure = 0.078 J/cm^2, spot size= 850 µm . (C,D) PSTHs from other experiments showing inhibition from different cells. Laser parameters: λ = 1.875 µm, repetition rate =100 Hz, pulse train duration = 500 ms, pulse width = 250 µs, radiant exposures: 0.043 J/cm^2 and 0.12 J/cm^2, spot sizes= 880 µm and 840 µm. Inhibition was observed regardless of baseline activity of a single unit. Hatch bars in represent the timing of the stimulus.

Figure 4.9 C&D illustrate two separate single units from experiments performed on individual animals where INS generated an inhibitory response in each PSTH. The repetition rate was set at either 100 and 200 Hz for each PSTH and the radiant exposure was 0.078 J/cm^2 and 0.019 J/cm^2 respectively, using a 500 ms pulse train and a pulse width of 250 µs. INS induced inhibition was significant (paired t-tests: Figure 4.9C, 0 to 1 s vs. -1 to 0 s: $p < 0.0037$, or vs. 1 to 2 s; $p < 0.000185$; Figure 4.9D 0 to 2 s vs. -2 to 0 s: $p < 0.0188$, or 2 to 4 s $p<0.0047$). In total, statistically significant inhibitory responses

were observed in all five animals studied in this fashion; excitatory responses were not observed. Thus, the effect of direct INS stimulation in rat somatosensory cortex appears to be inhibitory, as this effect was seen across all animals, different stimulation parameters, within different epochs of repeated INS stimulation, and during different recording periods within an experiment.

4.5 Discussion

4.5.1 Summary

We have previously demonstrated that in brain slices CNS neurons can be excited using pulsed infrared light [9]. Almost all previously published studies on INS of neural tissue have focused on the PNS [2, 5-8, 23-25]. This study is the first to examine the effects of INS on cortical tissue *in vivo*. Using OISI, INS induced changes in optical reflectance can show similarities to intrinsic signal responses previously reported for sensory stimuli presented to somatosensory or visual cortex [15, 19, 26-29]. As assessed by optical imaging, the spatial extent of the INS stimulus revealed a roughly 2 mm region of effect, demonstrating a localized response to INS in cortical tissue that is similar to the high spatial precision that has been well characterized in PNS applications [2-5, 23]. The amplitude of the intrinsic response increased with increasing infrared light energy, produced either by increasing the stimulation frequency or by increasing the radiant energy of the laser (Figs. 4&5). Changing the radiant exposure induced a linear response in peak signal magnitude compared to an exponential response demonstrated by changing the repetition rate. An exponential relationship was also observed in thalamocortical

slices where stimulation threshold decreased with increasing repetition rate [9]. That INS repetition rate affects cortical activity differently than radiant exposures suggests total radiant exposure alone cannot fully explain the functional results.

Infrared irradiation of the cortex did not appear to harm tissue, as both optical and neuronal signals were maintained, as shown with interleaved INS and tactile stimulation trials and normal subsequent measurements of tactile activation following 2-hour periods of repeated INS stimulation. Interestingly, cortical neuronal activity was significantly inhibited during the 1 s period post INS onset. This inhibition was consistently observed across animals, different laser stimulation parameters, and sustained epochs of neuronal recording. This is the first report of INS evoking neuronal inhibition [3, 4, 7, 9, 30, 31].

4.5.2 What underlies the INS evoked response?

Although the mechanism underlying INS induced optical changes is unknown, the effect is believed to be a transient heat-induced effect [13]. While temperature change was not measured in this study, other studies have looked at temperature change using similar stimulation parameters [5, 7]. In these studies, the average surface temperature change was estimated to be between 3 – 5 ^{o}C, and was shown to be non-damaging. The mechanism by which the heat gradient is transduced into neural signal is currently thought to be via heat-sensitive TRP receptors or via thermally mediated changes in ion channels [7, 13]. However, many potential sources, other than neural activity, could have led to the observed INS changes in optical reflectance (reduction of diffusely reflected light) [15, 32]. An argument can be made that the source of the intrinsic signal induced by the laser is simply the result of heat-induced vasodilation or heat-induced cellular

changes, such as cellular swelling or changes in cellular chromophores. However, we find this unlikely to be a primary effect, as the time course of the intrinsic signals evoked by infrared light reached its peak at approximately 2 s after laser offset (Figures 4.3-6), a time at which all heat associated with the laser would have dissipated (τ_{therm}= 112 ms, heat dissipated at 10*τ_{therm}; [5, 33]). Another possibility for the observed OIS response is an immediate heat response. If the laser evoked intrinsic signal was simply an immediate heat response, then the signal would be expected to decay exponentially. Instead our results indicate a long sustained response similar to that seen in sensory-induced intrinsic signals, suggestive of a neuronal related response. Additionally, studies that have used electrical stimulation to stimulate either the whisker pad or the fore/hindpaw demonstrated similar timecourses. Jones et al. demonstrated that a 1 sec electrical stimulus (15 Hz, 1.6 mA) of the whisker pad produced a timecourse with a 6 second duration [34], and Bouchard et al. demonstrated that the timecourse of the reduced oxy-hemoglobin signal does not return to baseline until ~5 secs post stimulation when electrical stimulation (3 Hz, 1 mA, for 4 s stimulation) is applied to the hind-paw [32]. While this study is not able to exclude heat-induced cellular changes or vasodilation as contributing factors, the strongest support for a neural response are the electrophysiology results which demonstrate clear, consistent inhibitory neuronal response, lasting approximately 1 s after laser stimulation onset (Figs. 7–9). We support the idea that INS, like sensory induced changes, led to changes in reflectance through such factors as changes in blood volume, blood oxygenation, and light scattering. The 632 nm illuminant used in this study targets the de-oxy hemodynamic component and has been shown to correlate strongly with neuronal responses.

The physiologic and anatomical differences between the PNS and the CNS can be used to help identify possible sources for the observed inhibitory response. In the PNS, all structures stimulated by infrared light have involved a nerve where stimulation could be applied and monitored downstream from the stimulation site. Conversely, the cerebral cortex of the brain consists of a neural network and contains inhibitory interneurons, and glial cells, astrocytes, ogliodendrocytes, and microglia, in a greater concentration than excitatory neurons. Direct stimulation of cortex with light could evoke responses in excitatory neurons that would then propagate in numerous directions making it difficult to detect evoked excitatory responses or INS could evoke direct responses in the smaller inhibitory neurons or glial cells. A confounding issue is the depth at which the infrared light penetrates into the tissue. In this study, the wavelength of light (1.875 μm) penetrates approximately 300 – 600 μm into tissue, where intensity decays exponentially following Beer's law [9, 21]. This indicates that mainly layers I and II of cortex are stimulated with only a small percentage of photons reaching layer III. A higher number of inhibitory neurons and astrocytes are present in layers I and II than excitatory neurons which are mainly located in layers III/IV [35, 36]. However, the dendritic tree of the pyramidal cells located in deeper layers project up to the superficial layers of cortex and will contribute to the absorption of infrared energy. Astrocytes present another possible component underlying the INS-induced response. Several groups have suggested that astrocytes have a role in generating hemodynamic responses [14, 37-39]. Other groups have demonstrated that astrocytes have an active role in modulating neuronal transmission [40-44]. Future studies are needed to determine the primary contributors to INS-induced cortical effects.

4.5.3 Correlation of intrinsic optical signal and neuronal inhibition

This is the first example of INS causing inhibition whereas all other INS studies evoked excitation [2-4, 9, 30]. Although our neuronal sample is small, we do not believe our results are purely due to sampling bias. Our electrodes were those typically used for extracellular recordings and isolate excitatory neuronal activity quite readily (e.g. Figure 4.7C&D). Although we typically sampled neurons from the superficial cortical layers, some recordings were also taken from deeper layers. We observed that the INS related neural activity was not limited to a specific depth or region of somatosensory cortex. In our recordings, we were more likely to sample cells with detectable spontaneous activity or clear tactilely driven response. Thus, there was nothing particularly unusual or unique about our sampling methods. It should be noted that tungsten microelectrodes likely bias towards sampling large pyramidal neurons and not responses from smaller inhibitory neurons.

While it is possible that INS had a suppressive effect on apical pyramidal cell dendrites in the superficial layers, it is also possible that INS has an excitatory effect on inhibitory neurons in superficial layers, resulting in the suppressed pyramidal neuronal responses that were detected. Feng et al. recently demonstrated that infrared light can increase the GABA current in isolated single cell recordings using cultured rat neurons [45], raising the possibility that some of the effects observed here may be direct effects on inhibitory neurons. Given the robust optical signals obtained with INS and the fact that our electrodes are biased towards larger neurons, it is likely that the predominant INS effect is preferential activation of inhibitory neurons. This is consistent with the effective penetration depth of the INS wavelength and stimulation parameters used here, which is

likely to reach primarily Layers I-II where inhibitory neurons are a predominant cellular component. We plan to conduct similar experiments in other cortical areas and other species to examine whether this is a general effect or whether it might be unique to rat somatosensory cortex.

This study underscores the fact that the neural basis of optical intrinsic signals is complex. Although many studies of cortical function emphasize the correlation of intrinsic signal magnitude with excitatory (presumably pyramidal) neuronal response, this is clearly not always the case. Subthreshold neuronal responses also have been highlighted as significant components of intrinsic cortical signals [46-48]. However, association of optical intrinsic signals with inhibitory neuron activation is less well documented. Although we have only inferred this relationship indirectly and thus further study is required, in this respect, this study is one of the first to highlight such a relationship.

Another possibility we have considered relates to the size of the laser stimulation fiber. We used a 400 μm diameter fiber positioned at distances up to 1.1 mm from the cortex, resulting in a spot size of up to 800 μm. The large size of the activation spot may have the effect of recruiting additional inhibitory circuits in somatosensory cortex. There are many examples of inhibitory effect of nearby barrels on the whisker barrel of interest [49, 50]. In visual cortex, larger size stimulation very frequently leads to inhibition [51, 52]. This is due to additional inhibitory circuits that are activated when the spot size goes beyond the receptive field size. This is a common feature of cortical circuitry and could underlie the basis for the observed inhibitory responses. Whether excitatory/inhibitory

effect is related to laser spot size would best be addressed in INS experiments using fibers of different diameter.

4.5.4 Future Directions

Many applications in the field of neuroscience could benefit from the high spatial selectivity of INS. For instance, INS could be used to study functional neural circuitry. While electrical stimulation is an established stimulation method in the field of neuroscience [53, 54], inherent electrical field spread makes it difficult to contain the area of neural activation. Infrared energy is governed by its optical penetration depth and can be engineered to target a specific volume of tissue. Consequently, neural activation by INS has been shown to be more spatially precise than electrical stimulation [55] and has the potential to stimulate a single neuron [45]. Infrared neural stimulation also has the advantage of being minimally invasive, reducing the risk of damaging neural tissue by physical contact, and could be a useful high spatial resolution brain mapping method during intraoperative procedures during neurosurgery [56, 57]. Potential application for deep brain stimulation is also a future possibility. The work presented here represents the first step towards realization of these goals and provides a promising stepping-stone towards future more advanced applications.

4.6 Acknowledgements

We thank Mike Remple for discussions on design of original experimental paradigm. This work was supported by the National Institutes of Health (NIH R01 NS052407-01 and NS44375), DOD-MFEL Program (DOD/AFOSR F49620-01-1-4029), and the Human Frontiers Science Program.

4.7 References

[1] Wells, J., Kao, C., Mariappan, K., Albea, J., Jansen, E. D., Konrad, P., and Mahadevan-Jansen, A., "Optical stimulation of neural tissue in vivo," *Opt Lett,* vol. 30, pp. 504-6, 2005.

[2] Fried, N. M., Lagoda, G. A., Scott, N. J., Su, L.-M., and Burnett, A. L., "Noncontact Stimulation of the Cavernous Nerves in the Rat Prostate Using a Tunable-Wavelength Thulium Fiber Laser," *Journal of Endourology,* vol. 22, pp. 409-414, 2008.

[3] Teudt, I. U., Nevel, A. E., Izzo, A. D., Walsh, J. T., Jr., and Richter, C. P., "Optical stimulation of the facial nerve: a new monitoring technique?," *Laryngoscope,* vol. 117, pp. 1641-7, 2007.

[4] Wells, J., Konrad, P., Kao, C., Jansen, E. D., and Mahadevan-Jansen, A., "Pulsed laser versus electrical energy for peripheral nerve stimulation," *J Neurosci Methods,* vol. 163, pp. 326-37, 2007.

[5] Izzo, A. D., Walsh, J. T., Ralph, H., Webb, J., Bendett, M., Wells, J., and Richter, C.-P., "Laser stimulation of auditory neurons: effect of shorter pulse duration and penetration depth," *Biophys. J.,* p. 107.117150, 2008.

[6] Rajguru, S. M., Matic, A. I., Robinson, A. M., Fishman, A. J., Moreno, L. E., Bradley, A., Vujanovic, I., Breen, J., Wells, J. D., Bendett, M., and Richter, C.-P., "Optical cochlear implants: Evaluation of surgical approach and laser parameters in cats," *Hearing Research,* vol. 269, pp. 102-111, 2010.

[7] Richter, C. P., Matic, A. I., Wells, J. D., Jansen, E. D., and Walsh, J. T., "Neural stimulation with optical radiation," *Laser & Photonics Reviews,* vol. 5, pp. 68-80, 2010.

[8] Jenkins, M. W., Duke, A. R., GuS, DoughmanY, Chiel, H. J., FujiokaH, WatanabeM, Jansen, E. D., and Rollins, A. M., "Optical pacing of the embryonic heart," *Nat Photon,* vol. 4, pp. 623-626, 2010.

[9] Cayce, J. M., Kao, C. C., Malphrus, J. D., Konrad, P. E., Mahadevan-Jansen, A., and Jansen, E. D., "Infrared Neural Stimulation of Thalamocortical Brain Slices," *Selected Topics in Quantum Electronics, IEEE Journal of,* vol. 16, pp. 565-572, 2010.

[10] Agmon, A. and Connors, B. W., "Thalamocortical responses of mouse somatosensory (barrel) cortex in vitro," *Neuroscience,* vol. 41, pp. 365-79, 1991.

[11] Blanton, M. G., Lo Turco, J. J., and Kriegstein, A. R., "Whole cell recording from neurons in slices of reptilian and mammalian cerebral cortex," *Journal of Neuroscience Methods,* vol. 30, pp. 203-210, 1989.

[12] Kao, C. Q. and Coulter, D. A., "Physiology and pharmacology of corticothalamic stimulation-evoked responses in rat somatosensory thalamic neurons in vitro," *J Neurophysiol,* vol. 77, pp. 2661-76, 1997.

[13] Wells, J., Kao, C., Konrad, P., Milner, T., Kim, J., Mahadevan-Jansen, A., and Jansen, E. D., "Biophysical mechanisms of transient optical stimulation of peripheral nerve," *Biophys J,* vol. 93, pp. 2567-80, 2007.

[14] Hillman, E. M. C., "Optical brain imaging in vivo: techniques and applications from animal to man," *Journal of Biomedical Optics,* vol. 12, pp. 051402-28, 2007.

[15] Roe, A. W., "Long-term optical imaging of intrinsic signals in anesthetized and awake monkeys," *Appl. Opt.,* vol. 46, pp. 1872-1880, 2007.

[16] Chapin, J. K. and Lin, C. S., "Mapping the body representation in the SI cortex of anesthetized and awake rats," *J Comp Neurol,* vol. 229, pp. 199-213, 1984.

[17] Dunn, A. K., Devor, A., Dale, A. M., and Boas, D. A., "Spatial extent of oxygen metabolism and hemodynamic changes during functional activation of the rat somatosensory cortex," *Neuroimage,* vol. 27, pp. 279-290, 2005.

[18] Petersen, C. C. H., "The Functional Organization of the Barrel Cortex," *Neuron,* vol. 56, pp. 339-355, 2007.

[19] Tsytsarev, V., Pope, D., Pumbo, E., and Garver, W., "Intrinsic optical imaging of directional selectivity in rat barrel cortex: Application of a multidirectional

magnetic whisker stimulator," *Journal of Neuroscience Methods,* vol. 189, pp. 80-83, 2010.

[20] Paxinos, G. and Watson, C., *The rat brain in stereotaxic coordinates / George Paxinos, Charles Watson*. Amsterdam:: Elsevier, 2007.

[21] Hale, G. M. and Querry, M. R., "Optical constants of water in the 200-nm to 200-µm wavelength region," *Appl. Opt.,* vol. 12, pp. 555-563, 1973.

[22] Cohen, L. B., Salzberg, B. M., and Grinvald, A., "Optical Methods for Monitoring Neuron Activity," *Annual Review of Neuroscience,* vol. 1, pp. 171-182, 1978.

[23] Duke, A. R., Cayce, J. M., Malphrus, J. D., Konrad, P., Mahadevan-Jansen, A., and Jansen, E. D., "Combined optical and electrical stimulation of neural tissue in vivo," *Journal of Biomedical Optics,* vol. 14, pp. 060501-3, 2009.

[24] Wells, J., Thomsen, S., Whitaker, P., Jansen, E. D., Kao, C. C., Konrad, P. E., and Mahadevan-Jansen, A., "Optically mediated nerve stimulation: Identification of injury thresholds," *Lasers Surg Med,* vol. 39, pp. 513-26, 2007.

[25] Wininger, F. A., Schei, J. L., and Rector, D. M., "Complete optical neurophysiology: toward optical stimulation and recording of neural tissue," *Appl. Opt.,* vol. 48, pp. D218-D224, 2009.

[26] Chen, L. M., Turner, G. H., Friedman, R. M., Zhang, N., Gore, J. C., Roe, A. W., and Avison, M. J., "High-resolution maps of real and illusory tactile activation in primary somatosensory cortex in individual monkeys with functional magnetic resonance imaging and optical imaging," *J Neurosci,* vol. 27, pp. 9181-91, 2007.

[27] Grinvald, A., "Real-Time Optical Mapping of Neuronal Activity: From Single Growth Cones to the Intact Mammalian Brain," *Annual Review of Neuroscience,* vol. 8, pp. 263-305, 1985.

[28] Ts'o, D. Y., Frostig, R. D., Lieke, E. E., and Grinvald, A., "Functional organization of primate visual cortex revealed by high resolution optical imaging," *Science,* vol. 249, pp. 417-420, 1990.

[29] Vanzetta, I., Hildesheim, R., and Grinvald, A., "Compartment-Resolved Imaging of Activity-Dependent Dynamics of Cortical Blood Volume and Oximetry," *J. Neurosci.,* vol. 25, pp. 2233-2244, 2005.

[30] Izzo, A. D., Richter, C.-P., Jansen, E. D., and Walsh, J. T., Jr., "Laser stimulation of the auditory nerve," *Lasers in Surgery and Medicine,* vol. 38, pp. 745-753, 2006.

[31] Fried, N. M., Lagoda, G. A., Scott, N. J., Su, L.-M., and Burnett, A. L., "Optical stimulation of the cavernous nerves in the rat prostate," in *Photonic Therapeutics and Diagnostics IV,* San Jose, CA, USA, pp. 684213-6 2008.

[32] Bouchard, M. B., Chen, B. R., Burgess, S. A., and Hillman, E. M. C., "Ultra-fast multispectral optical imaging of cortical oxygenation, blood flow, and intracellular calcium dynamics," *Opt. Express,* vol. 17, pp. 15670-15678, 2009.

[33] van Gamert, M. J. C. and Welch, A. J., "Approximate solutions for heat conduction: time constants," in *Optical - Thermal Response of Laser-Irradiated Tissue,* A. J. Welch, Ed., ed New York: Plenum Press, 1995.

[34] Jones, M., Berwick, J., Johnston, D., and Mayhew, J., "Concurrent Optical Imaging Spectroscopy and Laser-Doppler Flowmetry: The Relationship between Blood Flow, Oxygenation, and Volume in Rodent Barrel Cortex," *Neuroimage,* vol. 13, pp. 1002-1015, 2001.

[35] Helmstaedter, M., Staiger, J. F., Sakmann, B., and Feldmeyer, D., "Efficient Recruitment of Layer 2/3 Interneurons by Layer 4 Input in Single Columns of Rat Somatosensory Cortex," *J. Neurosci.,* vol. 28, pp. 8273-8284, 2008.

[36] Takata, N. and Hirase, H., "Cortical layer 1 and layer 2/3 astrocytes exhibit distinct calcium dynamics in vivo," *PLoS One,* vol. 3, p. e2525, 2008.

[37] Schummers, J., Yu, H., and Sur, M., "Tuned responses of astrocytes and their influence on hemodynamic signals in the visual cortex," *Science,* vol. 320, pp. 1638-1643, 2008.

[38] Takano, T., Tian, G.-F., Peng, W., Lou, N., Libionka, W., Han, X., and Nedergaard, M., "Astrocyte-mediated control of cerebral blood flow," *Nat Neurosci,* vol. 9, pp. 260-267, 2006.

[39] Wang, X., Lou, N., Xu, Q., Tian, G.-F., Peng, W. G., Han, X., Kang, J., Takano, T., and Nedergaard, M., "Astrocytic Ca2+ signaling evoked by sensory stimulation in vivo," *Nat Neurosci,* vol. 9, pp. 816-823, 2006.

[40] Bowser, D. N. and Khakh, B. S., "ATP Excites Interneurons and Astrocytes to Increase Synaptic Inhibition in Neuronal Networks," *J. Neurosci.,* vol. 24, pp. 8606-8620, 2004.

[41] Cunha, R. A., "Different cellular sources and different roles of adenosine: A1 receptor-mediated inhibition through astrocytic-driven volume transmission and synapse-restricted A2A receptor-mediated facilitation of plasticity," *Neurochemistry International,* vol. 52, pp. 65-72, 2008.

[42] Koizumi, S., Fujishita, K., Tsuda, M., Shigemoto-Mogami, Y., and Inoue, K., "Dynamic inhibition of excitatory synaptic transmission by astrocyte-derived ATP in hippocampal cultures," *Proceedings of the National Academy of Sciences of the United States of America,* vol. 100, pp. 11023-11028, 2003.

[43] Kozlov, A. S., Angulo, M. C., Audinat, E., and Charpak, S., "Target cell-specific modulation of neuronal activity by astrocytes," *Proceedings of the National Academy of Sciences,* vol. 103, pp. 10058-10063, 2006.

[44] Perea, G., Navarrete, M., and Araque, A., "Tripartite synapses: astrocytes process and control synaptic information," *Trends in Neurosciences,* vol. 32, pp. 421-431, 2009.

[45] Feng, H.-J., Kao, C., Gallagher, M. J., Jansen, E. D., Mahadevan-Jansen, A., Konrad, P. E., and Macdonald, R. L., "Alteration of GABAergic neurotransmission by pulsed infrared laser stimulation," *Journal of Neuroscience Methods,* vol. 192, pp. 110-114, 2010.

[46] Das, A. and Gilbert, C. D., "Long-range horizontal connections and their role in cortical reorganization revealed by optical recording of cat primary visual cortex," *Nature,* vol. 375, pp. 780-784, 1995.

[47] Grinvald, A., Lieke, E. E., Frostig, R. D., and Hildesheim, R., "Cortical point-spread function and long-range lateral interactions revealed by real-time optical imaging of macaque monkey primary visual cortex," *J. Neurosci.,* vol. 14, pp. 2545-2568, 1994.

[48] Toth, L. J., Rao, S. C., Kim, D. S., Somers, D., and Sur, M., "Subthreshold facilitation and suppression in primary visual cortex revealed by intrinsic signal imaging," *Proceedings of the National Academy of Sciences of the United States of America,* vol. 93, pp. 9869-9874, 1996.

[49] Derdikman, D., Hildesheim, R., Ahissar, E., Arieli, A., and Grinvald, A., "Imaging Spatiotemporal Dynamics of Surround Inhibition in the Barrels Somatosensory Cortex," *The Journal of Neuroscience,* vol. 23, pp. 3100-3105, 2003.

[50] Simons, D. J. and Carvell, G. E., "Thalamocortical response transformation in the rat vibrissa/barrel system," *Journal of Neurophysiology,* vol. 61, pp. 311-330, 1989.

[51] Ghose, G. M., "Attentional Modulation of Visual Responses by Flexible Input Gain," *Journal of Neurophysiology,* vol. 101, pp. 2089-2106, 2009.

[52] Levitt, J. B. and Lund, J. S., "Contrast dependence of contextual effects in primate visual cortex," *Nature,* vol. 387, pp. 73-76, 1997.

[53] Fritsch, G. and Hitzig, E., "Ueber die elektrische Erregbarkeit der Grosshirns.," *Archiv Anatomie, Physiologie, und Wissenschaftlische Medicin,* vol. 37, pp. 300-32, 1870.

[54] Galvani, *Bon. Sci. Art. Inst. Acad. Comm.,* pp. 363-418, 1791.

[55] Wells, J., Kao, C., Jansen, E. D., Konrad, P., and Mahadevan-Jansen, A., "Application of infrared light for in vivo neural stimulation," *J Biomed Opt,* vol. 10, p. 064003, 2005.

[56] Roux, F.-E. and TrÃ©moulet, M., "Organization of language areas in bilingual patients: a cortical stimulation study," *Journal of Neurosurgery,* vol. 97, pp. 857-864, 2002.

[57] Starr, P. A., Christine, C. W., Theodosopoulos, P. V., Lindsey, N., Byrd, D., Mosley, A., and Marks, W. J., "Implantation of deep brain stimulators into subthalmic nucleus: technical approach and magnetic imaging verified electrode locations," *Journal of Neurosurgery,* vol. 97, pp. 370-387, 2002.

CHAPTER V

CALCIUM IMAGING OF INFRARED-STIMULATED ACTIVITY IN RODENT BRAIN

Jonathan M. Cayce[1], Matthew B. Bouchard[2], Mykata Chernov[1],

Brenda R. Chen[2], Lauren E. Grosberg[2], E. Duco Jansen[1,3],

Elizabeth M. C. Hillman[2] and Anita Mahadevan-Jansen[1,3]

[1] Department of Biomedical Engineering, Vanderbilt University

Nashville Tennessee

[2] Laboratory for Functional Optical Imaging, Departments of Biomedical Engineering and Radiology, Columbia University, New York, New York

[3] Department of Neurological Surgery, Vanderbilt University

Nashville Tennessee

This chapter is prepared for submission to *Nature Communications*

5.1 Abstract

Infrared neural stimulation (INS) is a promising neurostimulation technique that can activate neural tissue with high spatial precision. However, little is understood about how infrared light interacts with neural tissue on a cellular level, particularly within the living brain. In this study, we use calcium sensitive dye imaging on macroscopic and microscopic scales to explore the spatiotemporal effects of INS on cortical calcium dynamics. The INS-evoked calcium signal that was observed exhibited a fast and slow component suggesting activation of multiple cellular mechanisms. Additionally, the slow component of the evoked signal exhibited wave-like properties suggesting network activation and was verified to originate from astrocytes through pharmacology and 2-photon imaging. We also provide evidence that the fast calcium signal may have been evoked through modulation of glutamate transients in apical dendrites. This study demonstrates that pulsed infrared light can induce intracellular calcium modulations in both astrocytes and neurons, providing new insights into the mechanisms of action of INS in the brain.

5.2 Introduction

Infrared neural stimulation (INS) has been demonstrated to be capable of activating peripheral nerves [1-4], auditory ganglion cells in the cochlear [5-7], the cristas ampullaris in the vestibular system [8], and can be used as a method for cardiac pacing [9]. The high spatial precision of INS suggests that this technique has the potential to improve upon current clinical care in a range of settings. However, one area that has been underexplored is the potential application of INS for stimulation of the central nervous system, for example for deep brain stimulation (DBS) in Parkinson's disease, or for mapping eloquent cortex during brain tumor resection. An all-optical method that does not require exogenous agents could have numerous advantages in clinical settings.

Our group first demonstrated INS in the central nervous system by evoking compound action potentials in thalamocortical brain slices *in vitro* [10]. In a separate study, we also discovered that pulsed infrared light increases GABA release in cultured neurons, suggesting that INS can modulate inhibitory synaptic activity [11]. The first *in vivo* application of INS in somatosensory cortex employed optical intrinsic signal imaging (OISI) to detect a decrease in the optical reflectance of 632 nm light in response to INS that appears similar to cortical reflectance changes evoked by peripheral tactile stimulation. However, single unit recordings during cortical INS revealed inhibition of spontaneous firing rates of cortical neurons, contradicting the apparently excitatory responses typically observed in OISI [12]. This result prompts the question of what effects INS has at the cellular level in the living brain, a question that must be answered if the utility of INS for clinical use in the brain is to be determined.

INS is known to evoke action potentials through a thermal gradient that causes depolarization [13]. Shapiro and colleagues provided evidence that INS depolarizes lipid membrane bilayers via a thermally mediated change in membrane capacitance that requires no specific ion channels. This suggests that any cell membrane can be depolarized by pulsed infrared light, which is consistent with responses seen in oocytes and mammalian HEK cells [14]. It is reasonable to expect therefore, in addition to neurons, that other cell types abundant in the brain, such as astrocytes could influence the cortical response to INS in ways not seen in the peripheral nervous system.

Optical intrinsic signal imaging measurements during normal stimulation are widely accepted to represent increases in local blood flow induced by local neuronal activity. However, the cellular mechanisms driving this neurovascular coupling are unresolved, and may involve astrocytes or myriad other cellular signaling [15]. While our earlier OISI measurements during INS stimulation likely corresponded to changes in blood volume and oxygenation within the interrogated region, these hemodynamic responses were only an indirect measure of the effects of INS. In the current study, calcium sensitive dye imaging was utilized as a direct measure of cellular responses. Calcium sensitive dyes exhibit an increase in fluorescence in the presence of increased calcium, so when loaded into a cell, the change in fluorescence can be used as a direct measure on intracellular calcium signaling. Calcium sensitive dyes can be imaged on an ensemble level using wide-field optical imaging methods similar to OISI, or on a cellular level using in-vivo two-photon microscopy [16-19]. Here, both imaging methods are used in addition to pharmacology to identify the predominant cell types responding to INS in the living brain.

Wide-field calcium responses to INS were found to exhibit a fast and slow component. Wave-like properties were also observed, suggesting possible network activation. Cellular imaging and pharmacology confirmed that the predominant cellular mechanisms responsible for INS-evoked calcium signals are primarily astrocytic; however, small underlying neuronal influences are present. The relationship between the INS parameters and the evoked calcium signals were characterized to obtain a complete picture of the observed response. This study demonstrates that INS influences cellular calcium signaling in both glial cells and neurons.

5.3 Methods

5.3.1 Surgical procedures

All procedures were performed in accordance with protocols approved by the Vanderbilt University or Columbia University (two-photon experiments only) IACUC. Briefly, male Sprague-Dawley rats (n = 32; 300 – 500 g) were anesthetized with a 50% urethane (Sigma-Aldrich, St. Louis MO) solution (I.P. 1.4 g/kg). Toe-pinch was used to ensure that the animal was in an adequate state of anesthesia. The animal was placed in a stereotactic frame and a craniotomy and durotomy were conducted to expose somatosensory cortex (+2 to -5 mm anterior/posterior, and 7 mm lateral to bregma) [20, 21]. Mannitol (1.0 ml, 20% concentration) was given I.P. to prevent potential brain edema. Oregon Green 488 BAPTA-1 AM calcium dye (O-6807, Life Technologies, Grand Island NY) was mixed with 8 µl pluronic acid in DMSO and 32 µl of Ringer's solution. This dye was loaded into a pulled glass capillary pipette and a microinjector

(Picospritzer, Parker, Cleveland OH) was used to inject the dye into the cortex throughout the craniotomy (5 - 10 locations, 20 - 40 psi, 200 – 1000 ms) at depths up to 1000 µm. A 400 µm diameter optical fiber (Ocean Optics, St. Petersburg FL) to deliver INS light was placed directly onto the cortex, and warm (~ 37 ^{o}C) 3% agar (Sigma-Aldrich) in saline and a glass coverslip were used to stabilize the cortex and create an imaging window (Figure 5.1A). Imaging began 30 – 60 minutes after dye loading to ensure proper labeling of cells.

5.3.2 Optical imaging methods

A multispectral imaging system based on the design of Bouchard et al. and Sun et al. was used to perform calcium sensitive dye imaging [16, 22]. Briefly, a high-power light emitting diode (LED) centered at 488 nm with a 460 ± 30 nm bandpass filter (Thorlabs, MCLED, Newark NJ, Semrock, FF01-460/60-20, Rochester NY) was focused onto the cortex with a bi-convex lens (Thorlabs, BK7, focal length = 10.0 mm). Images of the cortex were acquired using a 480x640 pixel Pike fire-wire camera (AVT, Newburyport MA) using a Zoom 7000 macro lens (Navitar, Rochester NY). A 500 nm longpass filter (BLP01-488R-25, Semrock) was placed between the lens and camera to reject the excitation light. The camera and LED were controlled by the SPLASSH software package [22].

For each experiment, one imaging run was composed of multiple (5 – 10) imaging trials, where a stimulus was presented once in each trial. Each imaging trial consisted of 30 seconds of imaging at 30 fps, with 6-10 seconds of baseline acquired before stimulation and images were binned 2x2. Image acquisition was synchronized with the

start of INS (or electrical) stimulation, and LED illumination was driven from the camera's 'expose' output signal to minimize photobleaching and exposure of the camera during read-out.

5.3.3 Laser stimulation parameters

Infrared neural stimulation was performed using a 1.875 μm ± 0.02 μm diode laser (Capella neural stimulator, Lockheed Martin Aculight, Bothel WA). This laser was chosen because previous studies indicated that the optical penetration depth (300 – 600 μm) was optimal for stimulation of neural tissue [2, 10]. Light was delivered to cortex via a 400 μm diameter low OH fiber optic (Ocean Optics, St. Petersburg FL) with a numerical aperture (NA) of 0.22. The fiber was positioned onto somatosensory cortex with a micromanipulator (Stoelting, Wood Dale IL). Average power was measured using a PM3 detector head attached to a Power Max 500 laser power meter (Coherent, Santa Clara CA) from the tip of the fiber after the completion of each experiment. Radiant exposure was calculated by assuming the spot size was the diameter of the fiber optic (400 μm). Radiant exposure varied for each experiment dependent on individual experimental parameters but ranged between 0.1 – 0.88 J/cm^2. Stimulation with infrared light was primarily applied at 200 Hz for a stimulation duration of 500 ms with a pulse width of 250 μs. Any variations in laser parameters are indicated in the descriptions of results and figure legends.

5.3.4 Electrical stimulation parameters

Electrical stimulation of cortex was performed with 3 MΩ tungsten microelectrodes (FHC, Bowdoin ME). The tip of the electrode was inserted into somatosensory cortex ($d \leq 100$ μm) using a micromanipulator (Stoelting, Wood Dale IL). Electrical pulses were generated using an IsoSTIM A320 (World Precision Instruments, Sarasota FL) isolator. Electrical stimulation parameters were set to match INS parameters for repetition rate (200 Hz), pulse width (250 μs), and pulse train length (500 ms). Current amplitude was constant at 0.3 mA.

5.3.5 Data Analysis

Image processing was performed using Matlab™ (Mathworks, Natick MA). The frames encompassing the first second before stimulation in each trial were averaged together to establish a baseline image before stimulation was applied. The baseline image was used to visualize differences in images acquired during and after stimulation through difference maps and time-course analysis. Activation maps were calculated by dividing images at particular times post-stimulation by images from 1 second before stimulation began (and converting to % change). The time course of the signal was analyzed using blockview visualization (Figure 5.1D) and average pixel value in a region of interest (ROI) versus time. Blockview analysis was performed by binning images for each half second. These images were averaged together and an activation map was calculated for each bin to show the spatiotemporal components of the INS evoked calcium signal. Regions of interest were selected automatically by first identifying the pixel with the greatest percent change in the calculated activation map and centering a 3x3 pixel ROI

around the identified pixel. The pixels in the ROI were averaged together for each timepoint and plotted against time. To analyze the spatial and temporal components of the evoked calcium signal, an ROI was translated in the anterior/posterior and medial/lateral directions. Time to peak signal was plotted as a function of distance for temporal analysis, and peak signal was plotted as a function of distance for spatial analysis.

5.3.6 Pharmacological studies

Fluoroacetate and CNQX were obtained from Sigma (St. Louis MO). Fluoracetate was prepared with a concentration of 1 mM and CNQX was prepared with a concentration of 50 µM in PBS. In these experiments, a water tight imaging chamber was constructed using a small plastic ring (diameter: 10 mm, height: 5 mm) and 4% agar solution. Baseline imaging was acquired with ACSF in the chamber using the following laser parameters: repetition rate = 200 Hz, pulse width = 250 µs, pulse train length = 500 ms, and radiant exposure = 0.51 - 0.65 J/cm^2. The ACSF was replaced by FAC or CNQX after acquisition of baseline imaging and incubated for 30 - 60 minutes. Changes in the fast component due to application of CNQX and FAC were assessed by comparing the peak signal corresponding to 0 - 1 seconds after start of stimulation for the control condition against the peak signal evoked by INS after application of pharmacological agents. Pharmacological effects on the slow component were assessed by comparing the average control signal corresponding 2 - 7 seconds after start of stimulation to the signal evoked by INS after application of CNQX or FAC. Data from each animal was normalized to compare data across animals. A single sample two tailed student's t-test

was used to determine if application of pharmacological agents significantly changed fluorescence signal strength evoked by INS, and a two-tailed paired student's t-test was used to establish statistical significance between experimental conditions.

5.3.7 Two-photon imaging

All two-photon imaging experiments (n=3) were performed using a custom two-photon microscope [23]. The exposed somatosensory cortex was labeled with Oregon Green 488 BAPTA-1 AM calcium sensitive dye using methods previously discussed. Sulforhodamine 101 (0.04 mM in ACSF, Invitrogen, Grand Island NY) was dropped onto the surface of the exposed cortex to selectively label astrocytes. After 30 minutes, the cortex was rinsed with ACSF and a cranial window was built using agar and a glass coverslip as described above. The animal was carefully positioned under the microscope's upright objective lens, and the INS delivery fiber optic was positioned to allow stimulation of cortex adjacent to the imaging field of view. Imaging was performed using 800-850 nm light generated with a Ti:Sapphire laser (Mai Tai HP Deep-See, Spectra Physics, Mountain View CA). Emitted fluorescent light was collected in three emission channels (350 to 505 , 505 to 560, and 560 to 650 nm). A 20x objective lens (XLUMLanFL 20x 0.95W; Olympus, Tokyo Japan) was used to image cortex at a depth between 100 – 300 μm. Depths greater than 300 μm could not be imaged due to the position of the INS fiber optic. Dynamic images of a selected 2D plane were acquired at 7.5 fps for 30 seconds during synchronized delivery of INS. Control measurements were performed where images were acquired with no INS. Image analysis was performed using Matlab™. Regions of interest were selected over astrocytes and the surrounding

neuropil to permit extraction of the time-course of intracellular calcium in response to INS.

5.4 Results

5.4.1 Infrared neural stimulation activates complex calcium waves *in vivo*

Our initial experiments aimed to demonstrate that pulsed infrared light evokes intracellular calcium changes in rat somatosensory cortex *in vivo*. Male Sprague-Dawley rats under urethane anesthesia were surgically prepared as described in the Methods section to unilaterally expose and load the somatosensory cortex with Oregon Green 488 BAPTA-1 AM (OGB) calcium sensitive dye [20, 21]. High-speed fluorescence images were then acquired at 30 frames per second during INS, delivered through a stimulating optical fiber placed on the cortical surface. As shown in figure 5.1B, focal activation was clearly observed. For all experiments, the peak percent change in fluorescence signal ranged from 0.2-1.7% and was dependent on the laser parameters used during the experiment. Calcium signals evoked by INS had an average duration of 7.54±1.39 seconds following stimulus onset and an averaged peak signal at 2.40±1.01 seconds for INS at 200 Hz for 500 ms (n=12) (Figures 5.1C&D). It should be noted that the brief decrease in fluorescence observed at the onset of laser stimulation was determined to be thermal artifact caused by thermal lensing and temperature dependent quenching of fluorescence, and was confirmed in calcium rich agar based phantoms and euthanized animals [24, 25]. Detailed characterization of the spatial extent of the signal and a parametric investigation of the effects of INS laser parameters on response amplitudes are described in Appendix A of this dissertation.

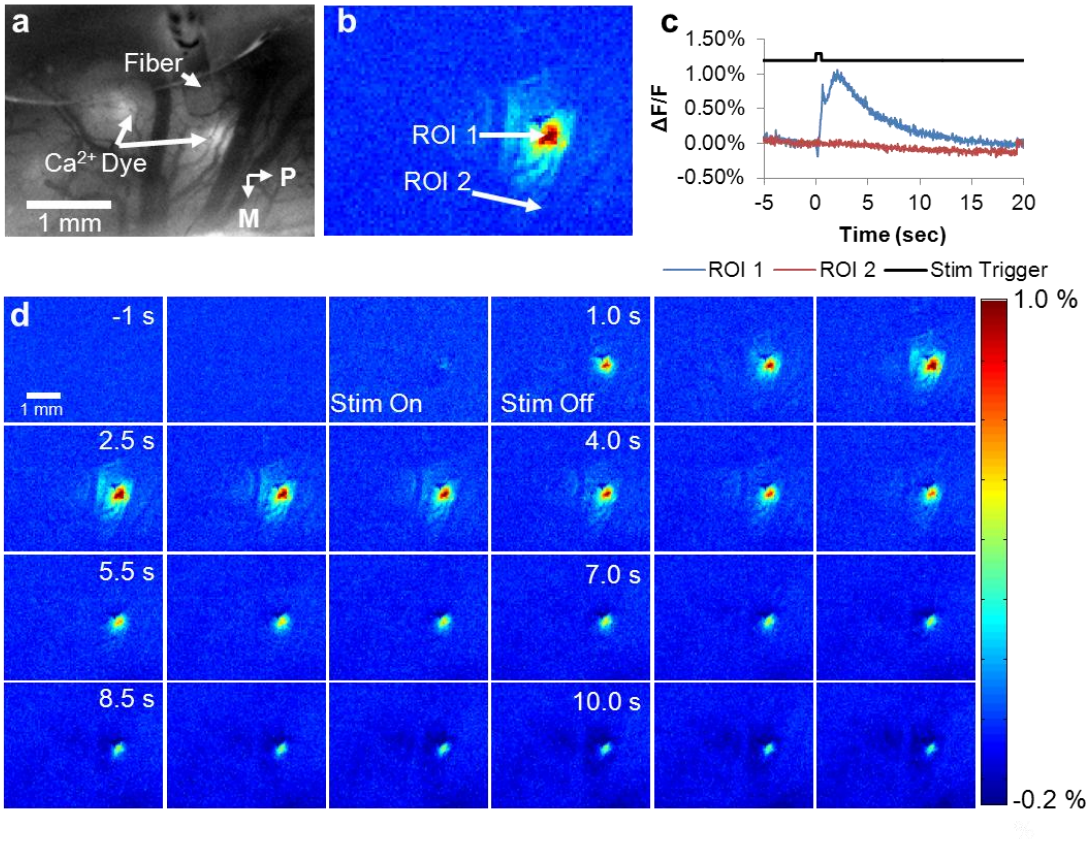

Figure 5.1: Pulsed infrared light evokes calcium activity in cortex. (A) Reference image displaying fiber position and location of calcium dye in cortex. (B) Activation map of INS evoked calcium signal and region of interest locations for timecourse analysis (C) Timecourse of INS evoked signal (D) Spatiotemporal components of INS evoked signal

Interestingly, a two component calcium signal was observed in 75% (19/25) of the animals that can be classified into two distinct temporal components (Figure 5.1B), suggesting activation of multiple cellular pathways. The first, fast temporal component is characterized by a rapid rise in fluorescence signal at the start of laser stimulation, and peaks 716±33 ms after the start of laser stimulation. This fast component of the INS evoked calcium signal is similar to spiking activity associated with neuronal activation [18, 26, 27]. The second, slow temporal component of the INS evoked intracellular calcium signal is generally greater in magnitude than the fast component and corresponds

to the overall peak signal (2.40±1.01 s) and total duration (7.54±1.39 s) of the calcium signal. Slow calcium responses have been reported to occur in astrocytes and other glial cells [18, 19, 28, 29]. Several studies have also demonstrated that intracellular calcium signals generated by astrocytes, interneurons, and dendrites can contain both fast and slow temporal components similar to those evoked by INS [18, 30, 31]. The presence of the fast and slow components and the overall long duration of the calcium response in relation to the short duration of INS (500 ms) was a surprising result, forcing the consideration of other involved cellular mechanisms in addition to neuronal firing.

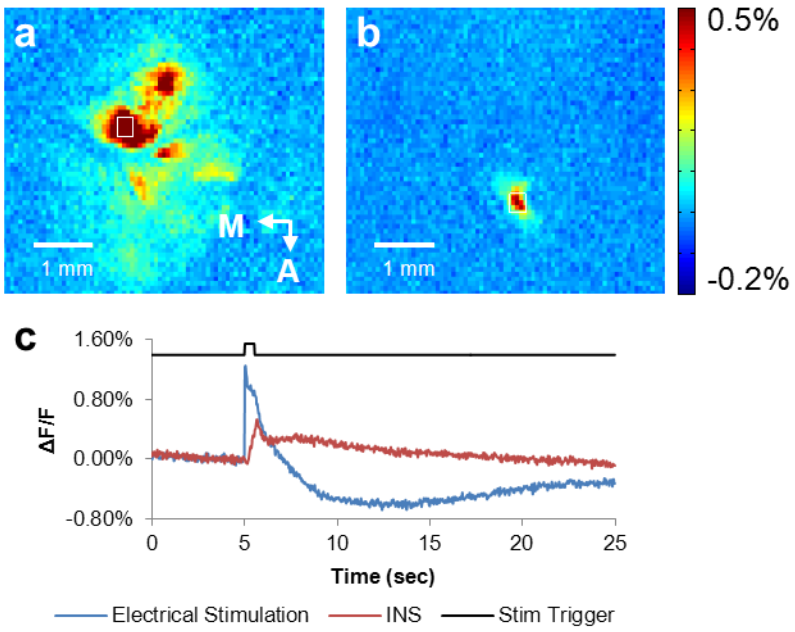

Figure 5.2: Direct comparison of electrical and INS-evoked calcium signals. (A) Activation map of calcium signal evoked by direct electrical stimulation of cortex. Image corresponds to 5 – 6 seconds on timecourse for electrical timulation. Electrical stimulation parameters: Current Amplitude: 0.3 mA, repetition rate: 200 Hz, pulse width: 250 us, pulse train length: 500 ms. (B) Activation map of calcium signal evoked by infrared stimulation in same animal. Image corresponds to 6 – 11 seconds on timecourse for INS. Laser parameters: λ: 1.875 um, repetition rate: 200 Hz, pulse width: 250 us, pulse train length: 500 ms, radiant exposure: 0.68 J/cm^2. (C) Timecourses of electrical and INS-evoked calcium signals

5.4.2 Comparison of INS calcium response to direct electrical stimulation

Direct electrical stimulation of the cortex is expected to primarily excite neuronal firing. We therefore sought to compare the intracellular calcium response to INS with the response to electrical cortical stimulation in the same animal (with matched parameters as described in Methods). Electrical stimulation (0.3 mA, 200 Hz for 500 ms) was found to generate a more spatially distributed calcium response than INS (radiant exposure: 0.68 J/cm^2, 200 Hz for 500 ms), 2 mm x 3 mm versus 0.5 x 1 mm respectively (Figure 5.2). Calcium responses to electrical stimulation peaked, on average, at 168±118 ms and returned to 0% at 2.15±0.26 seconds after start of stimulation (n=4), whereas the fast component of the INS-evoked calcium signal peaked later at 716±33 ms and had a secondary slow component peak at 2.4±1.01 secs. The total duration of the INS-evoked signal was five seconds longer in duration than the electrically evoked calcium signal. The peak amplitude of the change in fluorescence for electrical stimulation was generally twice that of INS, as shown in Figure 5.2C. The difference between peak times and durations of the INS and the electrically evoked signal indicate that different primary cellular mechanisms are responsible for generating calcium signals. The lack of a slow component in the electrically evoked signal provides evidence that two separate cellular mechanisms are involved in generation of INS evoked signals.

5.4.3 Calcium signals evoked by INS propagate across cortex.

Temporal analysis of INS-evoked calcium signals identified propagation of the calcium signal radiating out from the center of activation in cortex (n=8 out of 12). Figure 5.3B-C displays the response time-course for different locations medial and anterior to

the stimulation point. Figure 5.3D shows the time taken for these calcium signals to reach their maximum amplitude, plotted against distance for each 3x3 pixel region of interest along the anterior/posterior and medial/lateral directions, revealing a linear slope. To compare results across all eight animals, distance points were binned together to obtain seven averaged distance bins from the center of activation, and the corresponding time to peak values, in each bin, were averaged together (Figure 5.3D). The resulting average linear curve approximates the propagation velocity of the response to be 313±130 μm/s across the surface of cortex, which is slower than calcium waves associated neuronal signaling (0.01-0.02 m/s) [32] but faster than velocities associated with astrocyte signaling (10 – 60 μm/s) [19]. The observed velocity of the INS evoked calcium wave, and the differences in velocity associated with neurons and astrocytes motivates further investigation into the cellular processes activated by the infrared light.

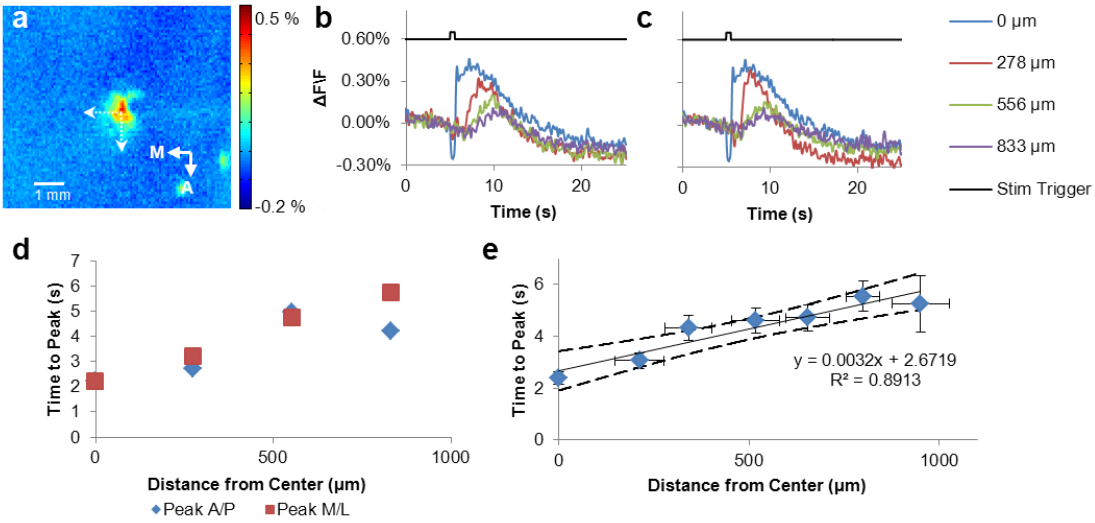

Figure 5.3: Pulsed infrared light evokes propagating calcium wave in cortex. (A) Activation map of INS evoked calcium signal. Arrows indicate direction of ROI translation using 3X3 pixel box spaced 2 pixels apart in medial and anterior directions. (B&C.) Smoothed timecourse signals for each positional ROI in the medial and anterior directions signifying a shift in time to peak of the calcium signal as distance increases from the stimulation site. (D) Time to peak signal as a function of distance for data displayed in b&c. Laser parameters: λ: 1.875 um, repetition rate: 200 Hz, pulse width: 250 us, pulse train length: 500 ms, radiant exposure: 0.86 J/cm^2. (E) Averaged time to peak signal as a function of distance for all animals (n = 8). Wave propagates linearly from center of activation with an approximate velocity of 313±130 µm/s. Error bars are ±s.e.m.

5.4.4 Cellular contributions to INS evoked calcium signals.

To further investigate the primary cellular components activated by INS, we conducted pharmacological studies using fluoroacetate (FAC), an astrocyte poison, and CNQX, a glutamate antagonist. The goal of these experiments was to isolate the roles of astrocytes and neurons in generating INS evoked calcium signals. For these experiments (n=8), a watertight imaging chamber was used to allow application of pharmacological agents to the surface of cortex. Control measurements of the calcium sensitive dye fluorescence response to INS with artificial cerebral spinal solution in the chamber were acquired first, to establish baseline signal (Figure 5.4A and E). A solution containing

either CNQX (50 µM in PBS) or FAC (1 mM in PBS) was then introduced into the imaging chamber and allowed to incubate for 30 – 60 minute.

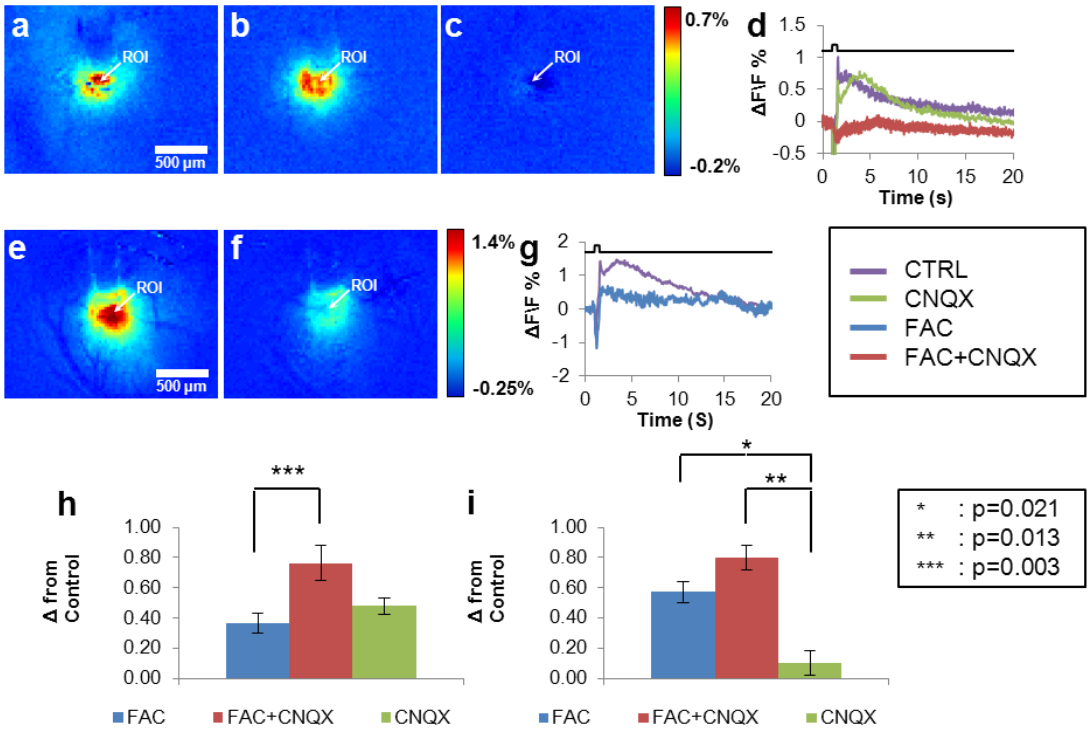

Figure 5.4: Pharmacological analysis demonstrates INS-evoked calcium signal is generated by combination of astrocytes and neurons. (a – c.) Activation maps evoked by INS for (a.) control, (b.) CNQX, and (c.) combined FAC and CNQX. (d.) Timecourse of signal after application of pharmacological agents (60 minutes). (e-f.) Activation maps evoked by INS in separate experiment for (e.) control and (f.) FAC alone. (g.) Timecourse of signals comparing control signal to signal after FAC application (60 minutes). (h) Difference between peak signal corresponding to the fast component (0 – 1.0 seconds on timecourse in d&g) for control signal and signal during pharmacological conditions. The combination of FAC and CNQX decreases the fast component calcium signal more than FAC alone (p=0.003) (i.) Difference between averaged signal (2 – 7 secs on timecourse in d&g) corresponding to the slow component for control and pharmacological conditions. The combination of FAC+CNQX (p=0.013) and FAC alone (p=0.021) decreases calcium signal more than CNQX alone (all error bars=s.e.m.)

Glutamate antagonist CNQX reduced the amplitude of the fast component (identified by peak signal between 0-1 seconds following start of stimulation) by 41.09±7.65% (n=3 rats, p=0.033, single sample t-test), but reduced the slow component signal (averaged signal between 1 – 5 seconds post stimulation) by only 10.0±8.5% a

decrease that was not statistically significant (n=3 rats, p=0.35, single sample t-test) (Figure 5.4A, B, D, H, I). This finding suggests that the fast component of the INS evoked calcium signal is related to excitatory glutametergic neuronal activity while the slow component has minimal contributions from glutametergic activity. Application of sodium fluoroacetate reduced the fast component by 36.67±6.6% (n=4 rats, p=0.01, single sample t-test) and reduced the slow component by 57.2 ±6.9% (n=4 rats, p=0.004, single sample t-test). The reduction seen in the fast component due to FAC was likely a result of the overall reduction of INS evoked calcium signal as the poisoning of astrocytes by FAC prevents normal regulation of neurotransmitter concentrations in the extracellular environment [33, 34]. The reduction of signal in slow component caused by FAC was also determined to be significantly greater than the reduction of slow component signal caused by CNQX alone (p=0.021, paired t-test). These findings are consistent with astrocytes being a major cellular contributor to the INS-evoked calcium signal (Figure 5.4E-I). Combined effects of CNQX and FAC (studied by adding FAC to the cortical bath after CNQX imaging) decreased the fast component by 71.9±9.37% (n=4 rats, p=0.005, single sample t-test) and the slow component by 80.0±8.2% (n=4 rats, p=0.002, single sample t-test) (Figure 5.4C, D, H, I). A paired t-test was performed between each pharmacological condition to determine statistically significant differences between conditions. For the fast component of the calcium signal, the additional decrease in observed fluorescence for combined CNQX+FAC was found to be significantly different when compared to FAC alone (p=0.003); however, no significant differences were observed when compared to CNQX alone (p=0.15). Combined CNQX+FAC significantly decreased the magnitude of the calcium response when compared to CNQX

alone (p=0.013), and near significant differences were observed between FAC alone and CNQX+FAC (p=0.093). This further decrease in fluorescence signal observed under CNQX+FAC conditions when compared to the effects of FAC and CNQX alone for both the slow and fast components indicate that a complementary mechanism, involving astrocytes and neurons, is responsible for producing the calcium response to INS.

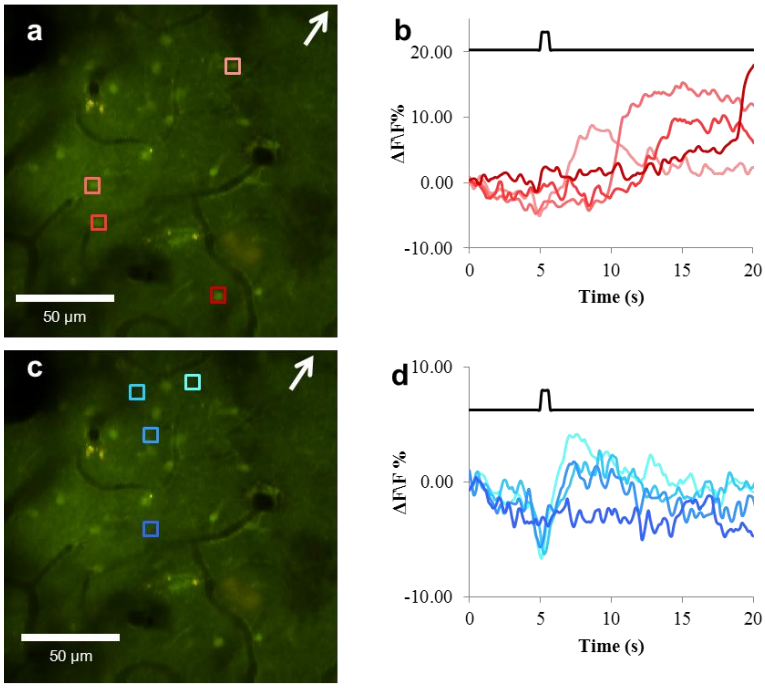

Figure 5.5: Two-photon imaging of INS-evoked calcium signals. (A&C.) Two photon image in cortex corresponding to a depth of 100 µm with ROI over responsive (A) astroctyes and (C) neuropil. White arrow indicates location of stimulation (fiber off screen). (B.) Timecourse of calcium signal in astrocytes highlighted by colored ROI demonstrating propagating calcium signal in astrocytic network evoked by infrared stimulation. (D.) Calcium activity in neuropil surrounding activated astrocytes. Red ROI indicates localized neuropil response. Laser Parameters: λ: 1.875 um, repetition rate: 200 Hz, pulse width: 250 us, pulse train length: 500 ms, radiant exposure: 0.8 J/cm2

To directly examine the cellular manifestations of the INS-evoked intracellular calcium response, in-vivo two-photon microscopy was used (n=3). In addition to the OGB calcium indicator, the cortex was labeled with astrocyte indicator Sulforhodamine

101 (0.04 mM in ACSF) [26, 35]. After confirming wide-field calcium responses to INS, 2-photon imaging was performed using a custom-built in-vivo 2-photon microscope [23] capable of resolving astrocytes, neurons and the microvasculature (Figure 5.5A, C). Figure 5.5A, shows a region of the somatosensory cortex 100 μm below the surface, with regions of interest selected to correspond to astrocytes. Figure 5.5B shows the time-courses of OGB fluorescence recorded from each of these astrocyte-specific ROIs during INS. The sequential increase in intracellular calcium seen in each cell body, in order of their distance from the site of INS excitation is consistent with the propagation of a calcium wave within the astrocyte network (Figure 5.5B). When regions of interest are selected to correspond to the surrounding neuropil, for the same data set (Figure 5.5C), a more uniform response to INS-stimulation is observed, consisting of a small increase in OGB fluorescence (Figure 5.5D). The neuropil response does not exhibit the wave propagation-like properties as seen in individual astrocytes. The INS evoked propagating calcium wave seen in the astrocyte network confirms sensitivity of astrocytes to pulsed infrared light; however, the local response seen in the neuropil supports the hypothesis that multiple cellular processes are involved in generating INS evoked calcium signals as the neuropil response is a confluence of signals generated by apical dendrites, interneurons, and astrocyte processes.

5.5 Discussion

The goal of this study was to evaluate and identify the cellular mechanisms activated by INS of cortex through the investigation of intracellular calcium dynamics *in vivo.* Infrared neural stimulation was demonstrated to evoke spatially localized calcium signals that propagate across the surface of cortex. In 76% of the experiments, INS evoked calcium signals contained a fast component and a slow component suggesting multiple cellular types are involved in generating INS calcium responses. A side by side comparison of INS to electrical stimulation revealed that INS evoked calcium signals were different, spatially and temporally, from calcium signals evoked by electrical stimulation indicating that different primary cellular sources were activated by each stimulation modality. Pharmacological studies demonstrated that CNQX significantly decreased the magnitude of the fast component of the calcium signal while FAC significantly reduced the averaged signal associated with the slow component. Combined effects of CNQX and FAC further reduced the averaged calcium signal demonstrating a complimentary mechanism involving both astrocytes and neurons. Two-photon microscopy experiments confirm activation of astrocyte networks and identified a local response in the neuropil that possibly signifies calcium activation in dendrites, axons, and glial processes in response to INS. The results of this study validate the ability of pulsed infrared light to evoke intracellular calcium transients in both astrocytes and neurons *in vivo.*

Astrocytes are the main support cell to neuronal activity in cortex and have been well characterized for generating spontaneous and evoked intracellular calcium signals [36]. The time-course of the INS-evoked calcium response observed with both wide-field

and two-photon imaging closely resembled the propagating calcium waves observed in astrocytes using in-vivo two-photon microscopy [19, 28]. Our pharmacological results with FAC and 2-photon imaging confirm that calcium signals evoked by infrared light are a result from directly activating astrocyte calcium transients *in vivo*. Additionally, recent reports of astrocyte photosensitivity to near infrared light further support our findings. Kuga et al., reported an increase in spontaneous synchronized astrocytic calcium waves under 800 nm light in a 2–photon system [19]. A similar *in vitro* experiment on plated astrocytes demonstrated that 800 nm light from a femtosecond laser could illicit an astrocyte calcium response, and in turn evoked a calcium response in a neighboring neurons [37, 38]. Both Kuga and Zhao report bidirectional calcium signaling between astrocytes and neurons [19, 37]. These observations supports the hypothesis that the observed INS-evoked calcium signals originate in astrocytes and influence neuronal responses secondarily indicating a possible astrocyte specific stimulation modality.

Calcium transients in apical dendrites located in the superficial layers of cortex represent the most likely source for neuronal contribution to the observed INS-evoked calcium signal. The results in this study show that CNQX inhibited the fast component of the INS evoked calcium signal suggesting pulsed infrared light evokes neuronal activity through modulation of excitatory glutametergic currents. Previous studies using imaging methods sensitive to dendritic calcium activity have demonstrated dendritic calcium signals evoked by hindpaw stimulation exhibit fast and slow components similar to the fast and slow components observed in INS-evoked signals [30, 31]. In these studies, researchers demonstrated a two component calcium signal with a total duration of 1 - 2 seconds in response to a 50 ms air puff or 10 ms electrical stimulus delivered to the

hindpaw. While the total duration of the calcium signal evoked by hindpaw stimulation is shorter than INS-evoked calcium signals (7.54±1.39 secs), the fast component evoked by the two stimulation methodologies is similar in duration (73 – 120 ms for hindpaw stimulation and 132±68 ms for INS) [30, 31]. The similarities between the fast temporal components of calcium signals evoked by hindpaw and infrared stimulation support apical dendritic glumate activity as the plausible primary neural source of INS-evoked calcium signals.

To understand how astrocytes and apical dendrites are likely responsible for the INS-evoked calcium signals we must consider the cell content of cortex activated by pulsed infrared light and the underlying mechanisms of INS. In this study, the wavelength of light (1.875 μm) penetrates approximately 300 – 600 μm into tissue, where intensity decays exponentially following Beer's law, indicating light is mainly absorbed in layers I and II of cortex with few photons reaching layer III [10, 39]. The predominant cell types/processes located in layers I and II of cortex are astrocytes and apical dendrites, and were identified as being the primary sources for INS evoked calcium transients [28, 31]. Additionally, our evidence of astrocyte and apical dendrite involvement in INS evoked calcium transients agrees with the recently discovered non cell specific capacitance mechanism as INS evoked calcium signals in both excitable apical dendrites and non-excitable astrocytes [14].

With these results, we demonstrate that INS directly evokes calcium transients in astrocytes and likely evokes calcium transients in apical dendrites through modulation of glutamate transients. We propose the hypothesis that these two methods of calcium signal generation interact giving rise to the confluence of calcium signals documented here.

Further detailed cellular physiology studies are needed to fully understand the mechanisms behind INS evoked calcium transients and how neuronal and astrocytic calcium signals interact. This study also highlights the potential of INS as a minimally invasive method to study astrocyte signaling to increase our understanding of how astrocytes interact with neurons and vasculature in the cortex; and therefore, improve our understanding of the disease processes associated with epilepsy [40], Alzheimer's disease [41], Parkinson's disease [42], and other movement disorders [43]

5.6 Acknowledgements

This work was supported by the National Institutes of Health (NIH R01 NS052407-01), DOD-MFEL Program (DOD/AFOSR F49620-01-1-4029), and the Human Frontiers Science Program.

5.7 References

[1] Teudt, I. U., Nevel, A. E., Izzo, A. D., Walsh, J. T., Jr., and Richter, C. P., "Optical stimulation of the facial nerve: a new monitoring technique?," *Laryngoscope,* vol. 117, pp. 1641-7, 2007.

[2] Wells, J., Kao, C., Mariappan, K., Albea, J., Jansen, E. D., Konrad, P., and Mahadevan-Jansen, A., "Optical stimulation of neural tissue in vivo," *Opt Lett,* vol. 30, pp. 504-6, 2005.

[3] Fried, N. M., Lagoda, G. A., Scott, N. J., Su, L.-M., and Burnett, A. L., "Noncontact Stimulation of the Cavernous Nerves in the Rat Prostate Using a Tunable-Wavelength Thulium Fiber Laser," *Journal of Endourology,* vol. 22, pp. 409-414, 2008.

[4] Katz, E. J., Ilev, I. K., Krauthamer, V., Kim, D. H., and Weinreich, D., "Excitation of primary afferent neurons by near-infrared light in vitro," *NeuroReport,* vol. 21, pp. 662-666, 2010.

[5] Izzo, A. D., Richter, C.-P., Jansen, E. D., and Walsh, J. T., Jr., "Laser stimulation of the auditory nerve," *Lasers in Surgery and Medicine,* vol. 38, pp. 745-753, 2006.

[6] Rajguru, S. M., Matic, A. I., Robinson, A. M., Fishman, A. J., Moreno, L. E., Bradley, A., Vujanovic, I., Breen, J., Wells, J. D., Bendett, M., and Richter, C.-P., "Optical cochlear implants: Evaluation of surgical approach and laser parameters in cats," *Hearing Research,* vol. 269, pp. 102-111, 2010.

[7] Richter, C. P., Rajguru, S. M., Matic, A. I., Moreno, E. L., Fishman, A. J., Robinson, A. M., Suh, E., and J. T. Walsh, J., "Spread of cochlear excitation during stimulation with pulsed infrared radiation: inferior colliculus measurements," *Journal of Neural Engineering,* vol. 8, p. 056006, 2011.

[8] Rajguru, S. M., Richter, C.-P., Matic, A. I., Holstein, G. R., Highstein, S. M., Dittami, G. M., and Rabbitt, R. D., "Infrared photostimulation of the crista ampullaris," *The Journal of Physiology,* vol. 589, pp. 1283-1294, 2011.

[9] Jenkins, M. W., Duke, A. R., GuS, DoughmanY, Chiel, H. J., FujiokaH, WatanabeM, Jansen, E. D., and Rollins, A. M., "Optical pacing of the embryonic heart," *Nat Photon,* vol. 4, pp. 623-626, 2010.

[10] Cayce, J. M., Kao, C. C., Malphrus, J. D., Konrad, P. E., Mahadevan-Jansen, A., and Jansen, E. D., "Infrared Neural Stimulation of Thalamocortical Brain Slices,"

Selected Topics in Quantum Electronics, IEEE Journal of, vol. 16, pp. 565-572, 2010.

[11] Feng, H.-J., Kao, C., Gallagher, M. J., Jansen, E. D., Mahadevan-Jansen, A., Konrad, P. E., and Macdonald, R. L., "Alteration of GABAergic neurotransmission by pulsed infrared laser stimulation," *Journal of Neuroscience Methods*, vol. 192, pp. 110-114, 2010.

[12] Cayce, J. M., Friedman, R., Jansen, E. D., Mahadevan-Jansen, A., and Roe, A. W., "Pulsed infrared light alters neural activity in rat somatosensory cortex in vivo," *Neuroimage*, vol. 57, pp. 155-166, 2011.

[13] Wells, J., Kao, C., Konrad, P., Milner, T., Kim, J., Mahadevan-Jansen, A., and Jansen, E. D., "Biophysical mechanisms of transient optical stimulation of peripheral nerve," *Biophys J*, vol. 93, pp. 2567-80, 2007.

[14] Shapiro, M. G., Homma, K., Villarreal, S., Richter, C.-P., and Bezanilla, F., "Infrared light excites cells by changing their electrical capacitance," *Nat Commun*, vol. 3, p. 736, 2012.

[15] Anna Devor, S. S., Srinivasan, V. J., Yaseen, M. A., Nizar, K., Saisan, P. A., Tian, P., Dale, A. M., Vinogradov, S. A., and Maria Angela Franceschini, D. A. B., "Frontiers in optical imaging of cerebral blood flow and metabolism," *Journal of Cerebral Blood Flow & Metabolism*, 2012.

[16] Bouchard, M. B., Chen, B. R., Burgess, S. A., and Hillman, E. M. C., "Ultra-fast multispectral optical imaging of cortical oxygenation, blood flow, and intracellular calcium dynamics," *Opt. Express*, vol. 17, pp. 15670-15678, 2009.

[17] Schulz, K., Sydekum, E., Krueppel, R., Engelbrecht, C. J., Schlegel, F., Schröter, A., Rudin, M., and Helmchen, F., "Simultaneous BOLD fMRI and fiber-optic calcium recording in rat neocortex," *Nature Methods*, vol. 9, pp. 597-602, 2012.

[18] Suadicani, S. O., Cherkas, P. S., Zuckerman, J., Smith, D. N., Spray, D. C., and Hanani, M., "Bidirectional calcium signaling between satellite glial cells and neurons in cultured mouse trigeminal ganglia," *Neuron Glia Biology*, vol. 6, pp. 43-51, 2010.

[19] Kuga, N., Sasaki, T., Takahara, Y., Matsuki, N., and Ikegaya, Y., "Large-scale calcium waves traveling through astrocytic networks *in vivo*," *The Journal of Neuroscience*, vol. 31, pp. 2607-2614, 2010.

[20] Paxinos, G. and Watson, C., *The rat brain in stereotaxic coordinates / George Paxinos, Charles Watson*. Amsterdam:: Elsevier, 2007.

[21] Chapin, J. K. and Lin, C. S., "Mapping the body representation in the SI cortex of anesthetized and awake rats," *J Comp Neurol,* vol. 229, pp. 199-213, 1984.

[22] Sun, R., Bouchard, M. B., and Hillman, E. M. C., "SPLASSH: Open source software for camera-based high-speed, multispectral in-vivo optical image acquisition," *Biomed. Opt. Express,* vol. 1, pp. 385-397, 2010.

[23] Radosevich, A. J., Bouchard, M. B., Burgess, S. A., Chen, B. R., and Hillman, E. M. C., "Hyperspectral in vivo two-photon microscopy of intrinsic contrast," *Opt. Lett.,* vol. 33, pp. 2164-2166, 2008.

[24] Vincelette, R. L., Oliver, J. W., Rockwell, B. A., Thomas, R. J., and Welch, A. J., "Confocal imaging of thermal lensing induced by near-IR laser radiation in an artificial eye," *Selected Topics in Quantum Electronics, IEEE Journal of,* vol. 16, pp. 740-747, 2010.

[25] Oliver, A. E., Baker, G. A., Fugate, R. D., Tablin, F., and Crowe, J. H., "Effects of temperature on calcium-sensitive fluorescent probes," *Biophysical Journal,* vol. 78, pp. 2116-2126, 2000.

[26] Nimmerjahn, A., Kirchhoff, F., Kerr, J. N. D., and Helmchen, F., "Sulforhodamine 101 as a specific marker of astroglia in the neocortex in vivo," *Nat Meth,* vol. 1, pp. 31-37, 2004.

[27] Waters, J., Larkum, M., Sakmann, B., and Helmchen, F., "Supralinear Ca2+ influx into dendritic tufts of layer 2/3 neocortical pyramidal neurons *in vitro* and *in vivo*," *The Journal of Neuroscience,* vol. 23, pp. 8558-8567, 2003.

[28] Takata, N. and Hirase, H., "Cortical layer 1 and layer 2/3 astrocytes exhibit distinct calcium dynamics in vivo," *PLoS One,* vol. 3, p. e2525, 2008.

[29] Schummers, J., Yu, H., and Sur, M., "Tuned responses of astrocytes and their influence on hemodynamic signals in the visual cortex," *Science,* vol. 320, pp. 1638-1643, 2008.

[30] Murayama, M. and Larkum, M. E., "Enhanced dendritic activity in awake rats," *Proceedings of the National Academy of Sciences,* vol. 106, pp. 20482-20486, 2009.

[31] Murayama, M., Perez-Garci, E., Nevian, T., Bock, T., Senn, W., and Larkum, M. E., "Dendritic encoding of sensory stimuli controlled by deep cortical interneurons," *Nature,* vol. 457, pp. 1137-1141, 2009.

[32] Grienberger, C., Adelsberger, H., Stroh, A., Milos, R.-I., Garaschuk, O., Schierloh, A., Nelken, I., and Konnerth, A., "Sound-evoked network calcium transients in mouse auditory cortex in vivo," *The Journal of Physiology,* vol. 590, pp. 899-918, 2012.

[33] Cunha, R. A., "Different cellular sources and different roles of adenosine: A1 receptor-mediated inhibition through astrocytic-driven volume transmission and synapse-restricted A2A receptor-mediated facilitation of plasticity," *Neurochemistry International,* vol. 52, pp. 65-72, 2008.

[34] Agulhon, C., Petravicz, J., McMullen, A. B., Sweger, E. J., Minton, S. K., Taves, S. R., Casper, K. B., Fiacco, T. A., and McCarthy, K. D., "What is the role of astrocyte calcium in neurophysiology?," *Neuron,* vol. 59, pp. 932-946, 2008.

[35] McCaslin, A. F. H., Chen, B. R., Radosevich, A. J., Cauli, B., and Hillman, E. M. C., "In vivo 3D morphology of astrocyte-vasculature interactions in the somatosensory cortex: implications for neurovascular coupling," *J Cereb Blood Flow Metab,* vol. 31, pp. 795-806, 2011.

[36] Fiacco, T. A., Agulhon, C., and McCarthy, K. D., "Sorting out astrocyte physiology from pharmacology," *Annual review of pharmacology and toxicology,* vol. 49, pp. 151-174, 2009.

[37] Zhao, Y., Liu, X., Zhou, W., and Zeng, S., "Astrocyte-to-neuron signaling in response to photostimulation with a femtosecond laser," *Applied Physics Letters,* vol. 97, pp. 063703-3, 2010.

[38] Zhao, Y., Zhang, Y., Liu, X., Lv, X., Zhou, W., Luo, Q., and Zeng, S., "Photostimulation of astrocytes with femtosecond laser pulses," *Opt. Express,* vol. 17, pp. 1291-1298, 2009.

[39] Hale, G. M. and Querry, M. R., "Optical constants of water in the 200-nm to 200-µm wavelength region," *Appl. Opt.,* vol. 12, pp. 555-563, 1973.

[40] Clasadonte, J. and Haydon, P. G., "Astrocytes and epilepsy," *Epilepsia,* vol. 51, pp. 53-53, 2010.

[41] Riera, J., Hatanaka, R., Uchida, T., Ozaki, T., and Kawashima, R., "Quantifying the uncertainty of spontaneous Ca^{2+} oscillations in astrocytes: Particulars of Alzheimer's disease," *Biophysical Journal,* vol. 101, pp. 554-564, 2011.

[42] Kahn, E., D'Haese, P.-F., Dawant, B., Allen, L., Kao, C., Charles, P. D., and Konrad, P., "Deep brain stimulation in early stage Parkinson's disease: operative experience from a prospective randomised clinical trial," *Journal of Neurology, Neurosurgery & Psychiatry*, 2011.

[43] Kitagawa, M., Murata, J., Kikuchi, S., Sawamura, Y., Saito, H., Sasaki, H., and Tashiro, K., "Deep brain stimulation of subthalamic area for severe proximal tremor," *Neurology*, vol. 55, pp. 114-6, 2000.

CHAPTER VI

INFRARED NEURAL STIMULATION OF PRIMARY VISUAL CORTEX IN NON-HUMAN PRIMATES

Jonathan M. Cayce[1], Robert M. Friedman[2], Gang Chen[2,3], E. Duco Jansen[1,3,4], Anita Mahadevan-Jansen[1,3,4], and Anna W. Roe[1,2,3]

[1] Department of Biomedical Engineering, Vanderbilt University

Nashville Tennessee

[2] Department of Psychology, Vanderbilt University

Nashville Tennessee

[3] Institute of Imaging Science, Vanderbilt University

Nashville Tennessee

[4] Department of Neurological Surgery, Vanderbilt University

Nashville Tennessee

Portions of this chapter was submitted to *Neuroimage*

6.1 Abstract

Infrared neural stimulation (INS) is an alternative neurostimulation modality that uses pulsed infrared light to evoke spatially precise neural activity that does not require direct contact with neural tissue. With these advantages INS has the potential to increase our understanding of specific neural pathways and impact current diagnostic and therapeutic clinical applications. In order to develop this technique, we have demonstrated the feasibility of INS (λ=1.875 μm, pulse duration=75-300 μs, radiant exposure=0.5-1.3 J/cm^2, fiber diameter=100-400 μm, repetition rate=100-200 Hz) to activate and modulate neural activity in primary visual (V1) cortex of Macaque monkeys using optical intrinsic signal imaging and electrophysiological methods. Infrared neural stimulation was found to evoke focal optical intrinsic signals (OIS, 0.01 – 0.04%) that are suggestive of direct activation of underlying V1 cortical neurocircuitry. Single unit recordings acquired during INS (0.5 sec stimulus) indicated statistically significant increases in neuron firing rates that demonstrates INS evoked OIS are generated by excitatory neural activity. We also identified the ability of INS to enhance and suppress visually evoked OIS during combined stimulation (simultaneous INS and visual stimulation) of V1 cortex in an eye specific manner. The modulation of OIS by INS was determined to be dependent on the spot size where stimulating fibers with diameters of 100 and 200 μm were determined to be most ideal for modulating V1 neural activity. These findings demonstrate feasibility of INS as a safe and effective neurostimulation modality for use in non-human primates.

6.2 Introduction

In order to increase our understanding of neural circuitry of the brain, scientists continue to improve upon methods for assessing neural function through the development of new neurostimulation and detection techniques [1, 2]. These new techniques with clinical potential are often first vetted in non-human primates before clinical implementation in humans [3]. The primate model permits study of neural circuitry in ways that is not possible to do in humans. Such studies have led to increased understanding of neuronal basis underlying sensation, cognition, and behavior, and have led to development of treatments for neurological disorders [4]. In this study, the non-human primate model is used to evaluate a novel brain stimulation method, termed infrared neural stimulation (INS).

Infrared neural stimulation is a neurostimulation methodology that uses pulsed infrared light to excite neural tissue in a non-contact, artifact-free, and selective manner without the need to genetically modify neural tissue [5, 6]. The biophysical mechanism by which INS evokes neural activity is through absorption of infrared light by water that induces a spatially localized thermal gradient [7]. Several groups have reported findings that indicate multiple cellular mechanisms by which the thermal gradient is transduced into neural activity. Shapiro and colleagues recently have reported on a mechanism where the thermal gradient evokes a reversible change in the electrical capacitance of the cell membrane that leads to depolarization of the cell [8]. A separate study implicates the heat sensitive TRPV4 calcium channel for generation of INS evoked neural activity in retinal ganglion cells [9]; however, the distribution of TRPV4 channels is not uniform throughout the nervous system. The fact that these studies identified a separate

independent cellular mechanism for INS evoked potentials highlights the complexity of the INS mechanism.

Infrared neural stimulation has been shown to effectively evoke neural responses in peripheral nerves [5, 10, 11], in auditory and vestibular systems [12, 13], in dorsal ganglion cells [14], and in cardiac muscle [15, 16]. While clearly applicable for stimulation of peripheral nerves, its use in the central nervous system has not been extensively explored. Initial feasibility and parametric studies were conducted in rat thalamocortical brain slices where INS was found to evoke compound action potentials, and initial laser stimulation parameters were characterized in this preparation [17]. We have also demonstrated that INS can modulate cortical neural activity in rodent somatosensory cortex, as confirmed with optical intrinsic signal imaging and single unit electrophysiology [18].

In this study, we examined the application of INS in nonhuman primate primary visual cortex (V1), an area that is characterized by well-defined functional modules (e.g. ocular dominance columns). We find INS evokes excitatory response in single neurons and induces focal hemodynamic response as revealed by optical imaging. Stimulation of eye specific columns leads to eye specific functional effects. This study represents the first application of INS to cerebral cortex of non-human primates and provides the necessary feasibility data to move forward with studies in awake behaving animals and potential clinical application.

6.3 Methods

Experiments were conducted in two Macaque monkeys implanted with chronic imaging chambers [19-21]. All procedures were performed in accordance with protocols approved by the Vanderbilt University Institute for Animal Care and Use Committee and conformed to the guidelines of the US National Institutes of Health.

6.3.1 Surgical procedures

All surgeries were performed under aseptic conditions. Monkeys were initially anesthetized with ketamine HCL (10 mg/kg, I.M.) and maintained under isoflurane (1.5 – 2% in O_2) anesthesia throughout the duration of the craniotomy, duratomy, and implantation of chronic imaging chamber with artificial dura (Tecoflex or Silicone) [19]. In all anesthetized procedures, vital signs (end-tidal CO_2, oximetry, body temperature, and heart rate) and anesthetic depth (via implanted wire electroencephalographic electrodes) were continuously monitored. The implanted chamber was sealed with a nylon cap and opened under sterile conditions for intrinsic signal optical imaging and electrophysiology.

6.3.2 Animal preparation

For each optical imaging or electrophysiology session, animals were anesthetized and maintained with Brevital (1-2 mg/kg/hr) and paralyzed with Norcuron (100 μg/kg/hr). Eyes were dilated with 1% atropine sulfate eye drops and fitted with contact lenses of appropriate curvature (Danker Laboratories Inc, Sarasota, FL) to focus on a visual stimulus computer monitor placed 57 cm in front of the animal. Foveal positions

on the monitor were determined by plotting the optic disks using a reversible ophthalmoscope [22]. The stimulating fiber optic used to perform INS was placed in direct contact with artificial dura over targeted ocular dominance (OD) columns. Agar (Type I, Sigma-Aldrich, St. Louis MO) and a glass coverslip were carefully applied to stabilize cortex for optical imaging. To permit placement of electrodes and optic fibers during imaging, a plastic brain stabilizer with a 5.5 mm diameter hole was used to stabilize cortex in lieu of agar.

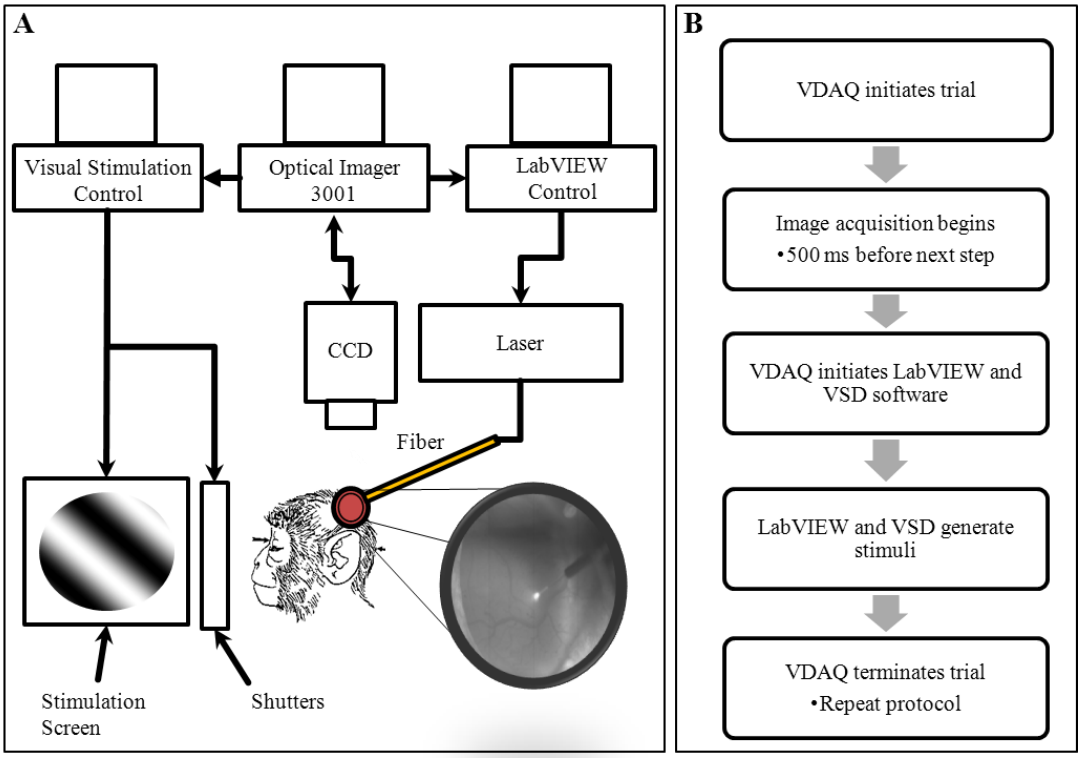

Figure 6.1: Methods for infrared neural stimulation and optical imaging. (A) Schematic diagram of the experimental setup. Experiment is controlled by VDAQ/NT imaging software that acquires images and determines when stimuli are presented through signaling separate computers running VSG software (visual stimulation presentation) and LabVIEW software (INS presentation). VSG software generates the monochromatic drifting square-wave gratings that are presented to the animal through VSG controlled electromagnetics shutters placed over the eyes. The LabVIEW control computer triggers laser stimuli by sending TTL pulses to the laser at the desired repetition rate. The optical fiber used to deliver infrared light is positioned on the artificial Dura covering cortex in the desired stimulation location. Image shows an example of a fiber positioned on cortex through the imaging system. (B) Imaging protocol flow chart of one trial for a given condition.

6.3.3 Optical imaging

Optical imaging of intrinsic signals was collected by an Imager 3001 with VDAQ/NT data acquisition software (Optical Imaging, Germantown, NY). Cortex was illuminated by 632 nm light bandpassed filtered from a halogen light source and focused onto the brain using fiber optics. Light reflected from cortex was collected onto the CCD chip (504 x 504 pixels) using a 85/50 mm lens combination to yield an 8 x 8 mm field of view. Images were acquired at 5 Hz for 6 – 9 seconds (yielding 30 – 45 frames per condition) with an interstimulus interval of 5 seconds. Signal to noise ratios were enhanced by syncing image acquisition to respiration and heart rate to reduce physiological noise and by trial averaging (25 – 40 per stimulus condition). Figure 6.1A displays the experimental set up diagram and figure 6.1B outlines the imaging protocol used to collect images.

6.3.4 Visual stimulation parameters

Full screen high contrast monochromatic drifting square-wave gratings (spatial frequency = 1 cycle/degree, temporal frequency = 3 Hz), were created using custom software writing in Matlab (Mathworks, Natick, MA) controlling a VSG stimulus system (Cambridge Research Systems, Rochester, UK). Gratings were oriented at 0^o or 90^o on a 40 x 30 cm computer monitor and presented to each eye separately using electromechanical shutters in front of each eye. The duration of all visual stimulation was 3.5 seconds. Each block consisted of 6 conditions, presented in a randomly interleaved fashion. The visual stimulus was presented to each eye twice, once for visual stimulation and once for combined stimulation (simultaneous INS and visual stimulation) for a total

of 4 visual stimulation conditions. Two additional conditions were an INS alone condition and a blank condition. During interstimulus intervals, blank condition, and INS condition, the shutters remained closed for both eyes (Figure 6.1B).

6.3.5 Infrared neural stimulation parameters

Wavelength selection for performing infrared neural stimulation was based on the optical penetration depth of light in tissue which was estimated using absorption data for water since biological soft tissue is 70% water [23]. Previous studies using infrared light to stimulate tissue have indicated that an optical penetration depth of 300 – 600 μm was optimal for stimulating neural tissue [6, 17]. A wavelength of 1.875 μm falls within this range of penetration depths. Infrared neural stimulation was performed using a 1.875 μm±0.02 μm diode laser (Capella neural stimulator, Lockheed Martin Aculight, Bothel WA). Light was delivered to the cortex through a 100, 200, or 400 μm diameter fiber optic (Ocean Optics, St. Petersburg, FL) with a numerical aperture (NA) of 0.22. The fiber was placed onto artificial dura using a hydraulic micromanipulator (Narishige, Tokyo, Japan). Laser repetition rate ranged between 100 – 200 Hz, and pulse width ranged between 75 - 300 μs. The average power from the laser was measured at the fiber tip using a Power Max 500D laser power meter with a PM3 detector head (Coherent, Santa Clara, CA). Radiant exposure was calculated assuming the diameter of the fiber optic was equal to the spot size of the incident light onto cortex [6]. The radiant exposure varied between 0.5 – 1.3 J/cm^2 and was dependent on the stimulation parameters used for a given experiment. Pulse train duration for all INS experiments was 500 or 1000 ms. Laser triggering was controlled via a LabVIEW software and National Instruments

hardware interface that was synced with presentation of visual stimulation and/or optical imaging via analog inputs (Figure 6.1 A and B).

6.3.6 Optical imaging data analysis

6.3.6.1 Activation maps

Analysis of optical imaging data was performed with software written in Matlab (Mathworks, Natick, MA). For each condition, to examine change from baseline, the first baseline frame (taken prior to stimulation onset) was subtracted from each subsequent frame. For each condition, the first-frame subtracted values were then summed across trials to maximize signal to noise ratio. Trial by trial assessment of image quality was conducted to remove any bad trials due to lighting abnormalities, large physiological movement, or camera acquisition errors.

Both single-condition maps and difference maps were calculated [24]. Single condition maps were generated by subtracting the blank condition from each experimental condition. Ocular dominance (OD) maps were generated by subtracting right eye stimulation conditions from left eye stimulation conditions, where darker pixels represent preference for left eye stimulation and lighter pixels represent preference for right eye stimulation. In this study, OD maps generated by visual stimulation alone are labeled as *vision* and OD maps generated by simultaneous visual and INS stimulation are labeled as *combined*. All activation maps were clipped based on the maximum observed signal magnitude for across compared activation maps . Large blood vessels were masked to remove from consideration pixels with signals related to surface vasculature (not to neural response). Standard Gaussian low-pass (3-8 pixels squared in size) and median

high-pass filtering (100 – 200 pixels squared in size) were used to remove contamination from uneven illumination and from other physiological noise sources.

6.3.6.2 T-maps

A pixel by pixel student's t-test was used to identify significant pixels activated for INS alone, visual stimulation, and combined stimulation [25]. This analysis was used to identify locations of stimulus-related response, to identify regions of interest for timecourse analysis, and was useful for identifying the borders of OD columns. T-maps were generated in Matlab and were visualized by creating binary maps threshold for a specific P value (i.e. $P < 0.01$ or $P < 0.05$) where p-values falling below the set threshold were assigned a value of 1 and those above threshold assigned a value of zero. Areas containing only a few significant pixels, along blood vessels, or along the edge of the imaging chamber were not included as the significance of these signals were ambiguous.

6.3.6.3 Timecourse analysis

The timecourse of the intrinsic signal was examined at selected sites by averaging the values of pixels within identified regions of interest (ROI). For each condition, the summed pixel value from the first image frame was subtracted from each subsequent frame and then used as a divisor to measure the change in reflectance over background reflectance (dR/R). Two conditions were then subtracted from each other to determine the difference signal timecourse of within the ROI. Laser stimulation alone was blank subtracted to view the direct intrinsic signal evoked by INS. To obtain eye preference within a specified ROI, right eye stimulation was subtracted from left eye stimulation

timecourse; such subtractions were conducted for both visual alone and combined visual+laser stimulation conditions. A paired t-test was performed on averaged data (typically frames 20 - 30 or 15 - 25) to determine statistical significance between INS alone, visual stimulation alone, and combined stimulation conditions.

6.3.7 Electrophysiology recordings

Single unit electrophysiology was used to assess the cortical neuronal responsiveness before, during, and after INS. Glass coated tungsten microelectrodes (1 – 3 MΩ, World Precision Instruments, Sarasota, FL) were inserted into cortex at depths of 50 – 500 μm in targeted OD columns identified with optical imaging. Single units were isolated that responded to brief INS (500 ms in duration). Signals were filtered and digitized using a 16 channel AM-Systems (Sequim, WA) differential amplifier using a 300 – 5 kHz bandpass filter. A LabVIEW interface was used to control presentation of laser stimulation, and Datawave software (Loveland, CO) was used to collect single unit data. Collected single units were spike sorted and peristimulus time histograms (PSTH) were generated using Dataview software. A paired Student's t-test analysis was used to determine the significance of changes observed in the PSTH related to laser stimulation.

6.4 Results

The non-human primate (NHP) model represent the closest animal model to human cortex and is crucial to furthering our understanding of human cortical function and underlying neurological diseases; therefore, demonstrating feasibility of INS as a neurostimulation modality for NHP cortex is important in establishing INS as an effective tool for neuroscientist and future applications of INS in NHP models. In this study, feasibility of INS in NHP was assessed through demonstrating the intensity dependency of the INS-induced optical intrinsic signals, examining the spatially specificity of the INS evoked OISs, whether INS would produce functionally specific effects (i.e. confined to single functional modules such as ocular dominance columns), and by determining the effects of INS on underlying neural activity using both OISI and electrophysiology techniques in primary visual cortex (V1) in two anesthetized Macaque monkeys.

6.4.1 Radiant exposure of INS increases magnitude of OIS

The first crucial step in demonstrating feasibility of INS in NHP is to show that pulsed infrared light evokes OISs in V1 cortex. Previous studies characterizing INS have indicated radiant exposure is a primary parameter for determining strength of activation and represents an initial starting point for determining the effects of pulsed infrared light on OISs in NHP V1 cortex [6, 10, 17, 18, 26, 27]. The direct effects of radiant exposure on the OIS were assessed using OISI under 632 nm illumination using radiant exposures identified as safe in rat somatosensory cortex [18]. The activation maps in Figure 6.2B-D represent the OIS magnitude evoked by INS for 1.3, 0.78, and 0.5 J/cm^2 delivered through a 100 µm fiber. The image maps show that activation was strongest for 1.3 J/cm^2

(Figure 6.2B) and activation decreased for 0.78 J/cm^2 (Figure 6.2 C) and 0.5 J/cm^2 radiant exposures (Figure 6.2D). Significant pixels for the 1.3 J/cm^2 condition were identified with a pixel-by-pixel paired t-test (t-map, $p < 0.001$). The timecourse of response of these pixels to each of the INS stimulation levels (compared to a no stimulation control condition) is shown in figure 6.2E. This demonstrates that the peak intrinsic magnitude increases with radiant exposure, but a similar intrinsic signal timecourse is maintained (Figure 6.2E). Statistical analysis (Welch's t-test) of the peak signal magnitude indicates a statistically significant increase in OIS as radiant exposure increases (Figure 6.2F). These results demonstrate that INS evokes a local OIS and identifies the importance of radiant exposure in determining intrinsic signal magnitude evoked by pulsed infrared light.

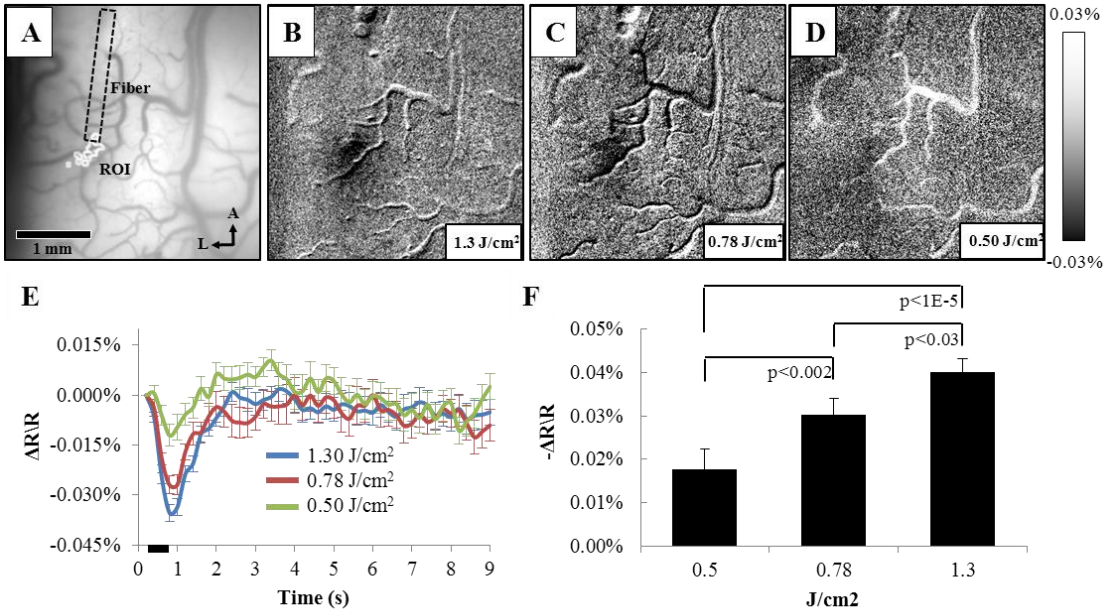

Figure 6.2: Increasing radiant exposure of INS increases intrinsic reflectance signal magnitude. (A) Blood vessel map. Region of interest demarcated by solid white outline were chosen from significant pixels identified in B. (B-D) Activation maps demonstrated increased intrinsic optical signal for greater radiant exposures: (B) 1.3 J/cm^2, (C) 0.78 J/cm^2, and (D) 0.50 J/cm^2. (E) Timecourse of intrinsic signal in response to different radiant exposures. Black bar represents stimulus timing. (F) Peak magnitude of intrinsic reflectance signal increases with statistical significance as radiant exposure increases. P-values obtained from paired Welch's t-test. Laser stimulation parameters: λ = 1.875 µm, pulse width = 250 µs, pulse train length = 500 ms, fiber size = 100 µm. Imaging parameters: 5 fps, ITI = 8 s, Trials = 40 (1.3 J/cm^2), 20 (0.78 J/cm^2), and 22 (0.50 J/cm^2). Image frames 3 through 7 were averaged to generate maps. A = anterior, L = lateral. Error bars represent standard error of the mean. Scale bar = 1 mm.

6.4.2 INS activates focal domains in primary V1 cortex

In order for INS to be a useful neurostimulation modality in NHP experiments, the ability to evoke or modulate functionally relevant responses must be demonstrated. To accomplish this and evaluate possible effects specific to ocular dominance columns, the fiber optic was placed over a right eye ocular dominance column (Figure 6.3A). Infrared neural stimulation was applied through a 100 µm diameter fiber optic, placed in direct contact with the optically clear artificial dura (Tecoflex or Silicone), to confine the stimulation in a single ocular dominance column,. After placement of the fiber, the imaging field of view was stabilized with 3% agarose and a glass coverslip (Figure 6.3A).

Primary visual cortex was stimulated by INS with three sets of laser parameters: 100 Hz for 500 ms (Figure 3B), 200 Hz for 500 ms (Figure 6.3C) and 200 Hz for 1000 ms (Figure 6.3D). Qualitatively, we observed that INS produced a focal region of activation corresponding to the location of the fiber tip in ROI 1 and increasing INS intensity produced increased reflectance changes (Figure 6.3B-D).

To evaluate the effect on three neighboring ocular dominance columns, three regions of interests (ROI) were identified from the single condition maps and timecourses of the INS evoked intrinsic signal was examined (Figure 6.3B-D). Simple ocular dominance imaging revealed ROI 1 was located in a right eye OD column, ROI 2 was located in the neighboring left eye column, and ROI 3 was located in the next right eye column (Figure 6.3A). ROI 1 and ROI 3 correspond to locations which responded with a decrease in reflectance (darkening of pixels), consistent with the optical intrinsic signal associated with neural responses in 632 nm optical imaging. ROI 2 is located in an area of V1 (neighboring left eye OD column) that produced an increase in reflectance (lightening of pixels). The timecourse produced at ROI 1, located at the stimulation site, peaked at 1.8 secs for the 200 Hz, 1000 ms stimulus and had a peak change in reflectance of 0.036±0.002% (Figure 6.3E, green line). As the stimulation strength decreased (100 Hz 500 ms, blue line; 200 Hz 500 ms, red line), the peak signal and time to peak also decreased; however the overall shape and duration of the timecourse remained relatively unchanged. The timecourse of the OIS in ROI 2 produced a positive (lightening of pixels) response for each of the stimulus conditions tested (Figure 6.3F). Local functional activation of OD domains by INS is further supported by the slight activation (peak = 0.014±0.003% for 200 Hz, 1000 ms) observed in ROI 3, corresponding to a right eye OD

column, (Figure 6.3G) in response to laser stimulation. To demonstrate the high spatial precision of INS, ROI 4 was placed at a distant site (1000 μm from ROI 3) to serve as a control ROI. Reflectance changes at ROI 4 were not different from baseline (Figure 6.3H), demonstrating the effect of INS did not spread to distant sites. These results indicate that INS evokes focal OIS in primary visual cortex with a high degree of spatial precision.

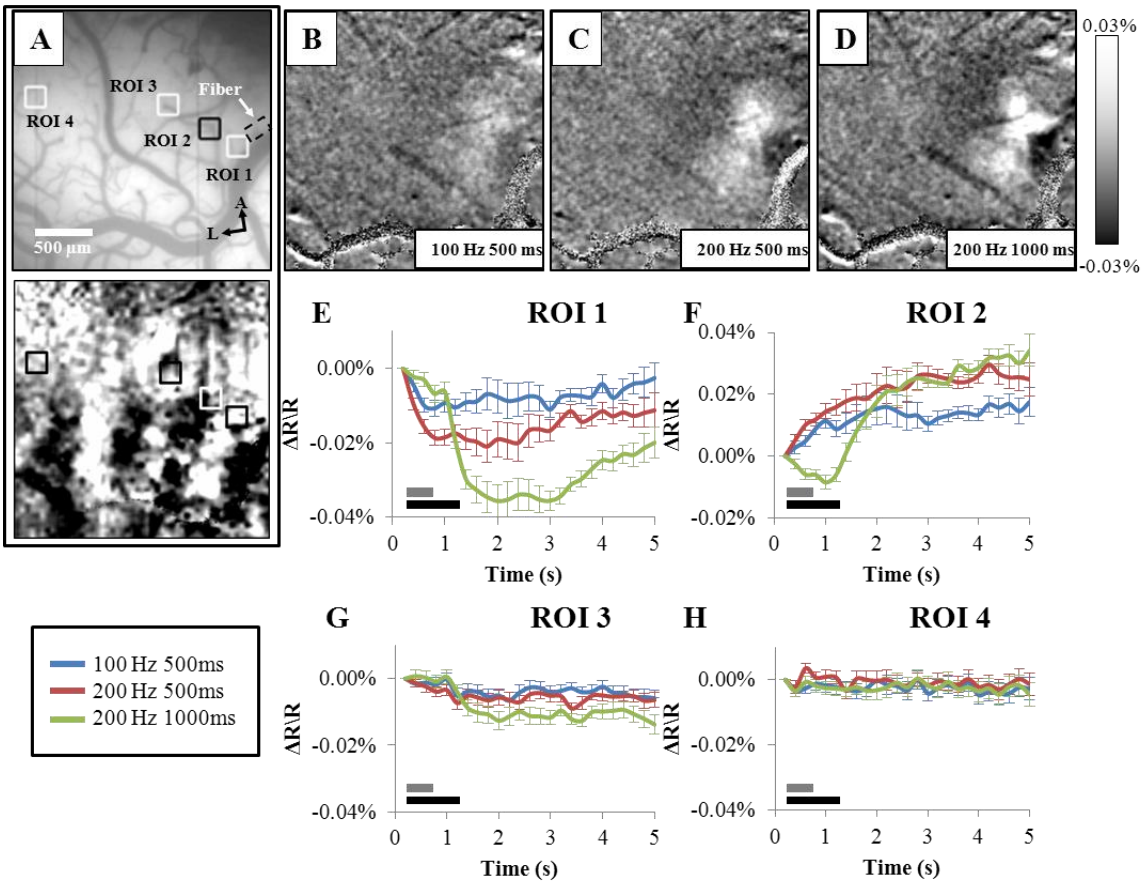

Figure 6.3: Infrared neural stimulation generates focal responses in in primary visual cortex. (A) Blood vessel map. Solid boxes are regions of interest where timecourse data was calculated in response to laser stimulation in V1 cortex. Location of fiber is indicated by dotted rectangle. (B-D) Activation maps in response to laser stimulation demonstrate increased activation in response to increased laser stimulation strength. Parameters for each image are (B) repetition rate (RR): 100 Hz pulse train length (PTL): 500 ms, (C) RR: 200 Hz PTL: 500 ms, and (D) RR: 200 Hz PTL 100 ms. (E-H) Timecourse of intrinsic signals taken from demarcated region of interests in (A-D). Traces in blue, red, and green indicate responses to laser stimulation using following stimulation conditions: RR: 100 Hz PTL: 500 ms, RR: 200 Hz PTL: 500 ms, and RR: 200 Hz PTL 1000. ROI 1: corresponds to region of cortex exhibiting strongest response to laser stimulation near stimulus location. ROI 2 corresponds to a region of cortex exhibiting a positive signal. ROI 3 corresponds to projection area. ROI 4 represents a control region of cortex where no activation was observed. Laser stimulation parameters: λ = 1.875 µm, pulse width = 250 µs, radiant exposure = 0.6 J/cm^2, fiber size = 100 µm. Imaging parameters: 5 fps, ITI = 8 s, trials = 40. Image frames 14 through 25 were averaged to generate maps. A = anterior, L = lateral. Stimulation begins at 0.4 s and ends at 0.94 (gray bar) or 1.4 s (black bar) dependent on indicated pulse train lengths. Error bars represent standard error of the mean. Scale bar = 1 mm (white bar).

6.4.3 Single unit recordings demonstrate neural excitability to INS

In order for INS to be an accepted stimulation modality for cortical stimulation studies, the underlying neural response responsible for generating the observed OIS must be characterized. Figure 6.4A displays an OD column map identified through optical imaging of visual stimulation. The recording electrode, a glass coated tungsten electrode (1.8 MΩ), was located in a left eye column. INS was delivered either to the same left eye column (INS 1) or a neighboring right eye column (INS 2) approximately 1 mm away. Based on our intrinsic imaging results, cortex was stimulated through a 200 μm fiber located in INS 1 or INS 2 using the following INS parameters: a radiant exposure of 0.57 J/cm^2, repetition rate of 200 Hz, pulse width of 250 μs, and stimulation duration of 500 ms.

The isolated single unit shown in Figure 6.4B, recorded at a depth of 340 μm, represents excitatory activity evoked by INS when cortex was stimulated at INS 1. The corresponding post stimulus time histogram (PSTH) indicates increased spike rates during INS and was determined to be statistically significant when compared to the 500 ms prior to stimulation ($p = 3.15E-08$, paired two-tailed t-test) and 500 ms post stimulation ($p = 8.83E-09$, paired two-tailed t-test). A second single unit, isolated at a depth of 650 μm, responded to infrared stimulation at INS 2 located in the adjacent right eye column (Figure 6.4C). Paired t-tests indicated statistical significance when the spike rates acquired during stimulation were compared with spike rates 500 ms before stimulation ($p = 6.01E-06$, paired two-tailed t-test) and spike rates 500 ms after stimulation ($p = 7.35E-06$, paired two-tailed t-test). These single unit recordings demonstrate the capability of INS to evoke excitatory activity in superficial cortical

neurons in V1 cortex and support our optical imaging results that indicate INS evokes optical signals driven by neural activity.

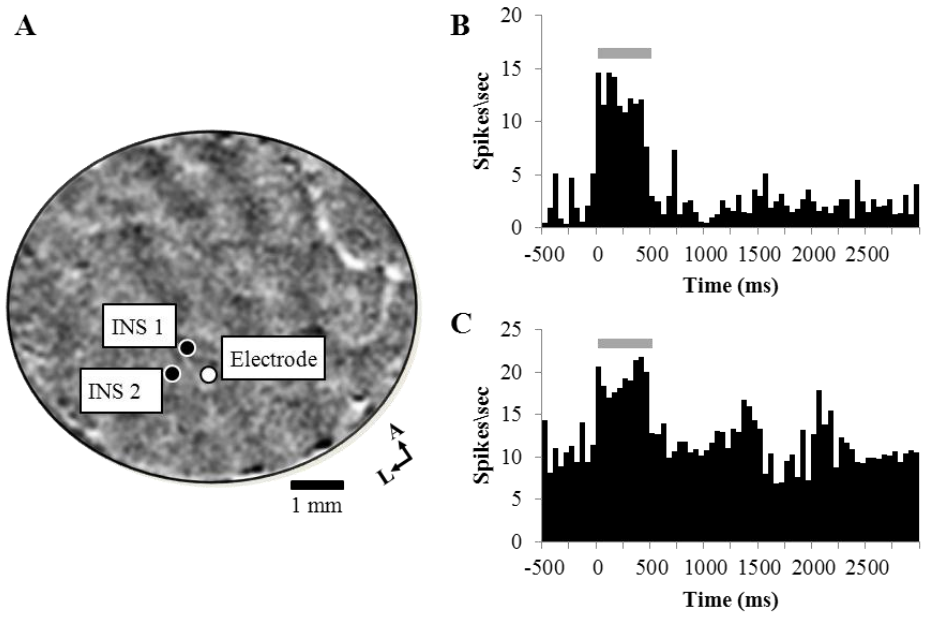

Figure 6.4: Excitatory single unit response evoked by INS of primary visual cortex. **(**A) Ocular dominance map displaying location of left eye OD column (dark pixels) and right eye OD columns (lighter pixels). Electrode is located in left eye column (white circle) and INS sites indicated by black circles. Black scale bar = 1 mm. (B) PSTH of a single unit response to laser stimulation at INS location 1 (INS 1) in (A) located in left eye ocular dominance column. Electrode depth at 340 µm. (C) PSTH of a single unit response to laser stimulation at INS location 2 (INS 2) located in right eye ocular dominance column. Electrode depth at 650 µm. (B&C) Gray bar indicates stimulus timing and corresponds to 500 ms. Laser stimulation parameters: λ = 1.875 µm, pulse width = 250 µs, radiant exposure = 0.57 J/cm^2, fiber diameter = 200 µm, repetition rate = 200 Hz, stimulation duration = 500 ms. A = anterior, L = lateral.

6.4.4 Modulation of visually evoked OIS with INS

Infrared neural stimulation alone has been shown to evoke cortical responses, as assessed with intrinsic signal optical imaging and with electrophysiological recordings. Now this study asks whether INS can be used as a tool for modulating visually evoked activity. Such modulation would make this technique an important and useful tool for furthering our understanding of cortical circuitry and will provide the motivation needed

for future behavioral studies. The ability to change an animal's behavior with INS will provide a new avenue by which neuroscientists can investigate the visual system and its underlying neural circuitry. The capability of INS to modulate visually evoked neural signals was investigated by comparing OIS evoked by visual stimulation to OIS evoked by superimposed INS and visual stimulation where INS is expected to potentiate visually evoked OIS when compared to signals evoked by visual stimulation alone. Here, OD columns were targeted by targeting either a 100, 200, or 400 μm fiber to an individual eye specific column. The small size of these fibers should limit the extent of INS to an individual column as OD columns are typically 400 μm in diameter [24, 28].

Figure 6.5 compares the effects of combined INS and visual stimulation and that of visual stimulation alone. In this experiment, INS parameters were a radiant exposure of 1.3 J/cm^2 at 200 Hz for 500 ms through a 100 μm fiber optic. These parameters were chosen because they had previously been identified to evoke OIS in V1 cortex, Visual stimulation (VS) consisted of full screen square wave gratings (spatial frequency of 1 c/degree and a drift velocity of 3 Hz) for 3.5 seconds, parameters typical of visual cortical stimulation in optical imaging experiments. Combined stimulation refers to synchronization of the start of the 500 ms INS stimulus with the 3.5 seconds of visual stimulation. Optical intrinsic signals evoked by visual stimulation were directly compared to OIS evoked by combined stimulation to assess the effects of pulsed infrared light on OIS magnitudes. The OD map in Figure 6.5B is a subtraction of left eye VS minus right eye VS, and the map in Figure 6.5C is a subtraction of combined left eye VS + INS and right eye VS + INS (LeC-ReC). Left eye and right eye OD columns obtained from combined stimulation are demarcated in red and blue, respectively. Significant pixels

(paired t-test between INS and blank, yellow outline in Figure 6.5A) from laser stimulation alone indicate the 100μm fiber activated pixels on the border of a right and left eye OD column; however the INS evoked cortical response was primarily located in the left eye column. As expected, combined INS+VS was found to enhance intrinsic signal activation in left eye OD columns when compared to visual stimulation alone as indicated by the difference maps calculated between VS alone and combined stimulation (Figure 6.5B and C). This is confirmed by the timecourse analysis of the pixels contained within the demarcated left eye OD columns. Comparison of vision alone (green line) and combined vision and INS (black line) revealed statistically significant enhancement by INS in the left eye OD column (Figure. 6.5D and F, Left Eye OD Columns, $p = 0.031$, paired t-test, two tailed). Interestingly, the magnitude of the intrinsic signal in the right eye OD columns was attenuated by combined stimulation; however this difference was not statistically significant (Figure 6.5D and F, Right Eye OD Columns, $p = 0.26$, paired t-test, two tailed). This attenuation was smaller in magnitude than the enhancement observed in the left eye columns.

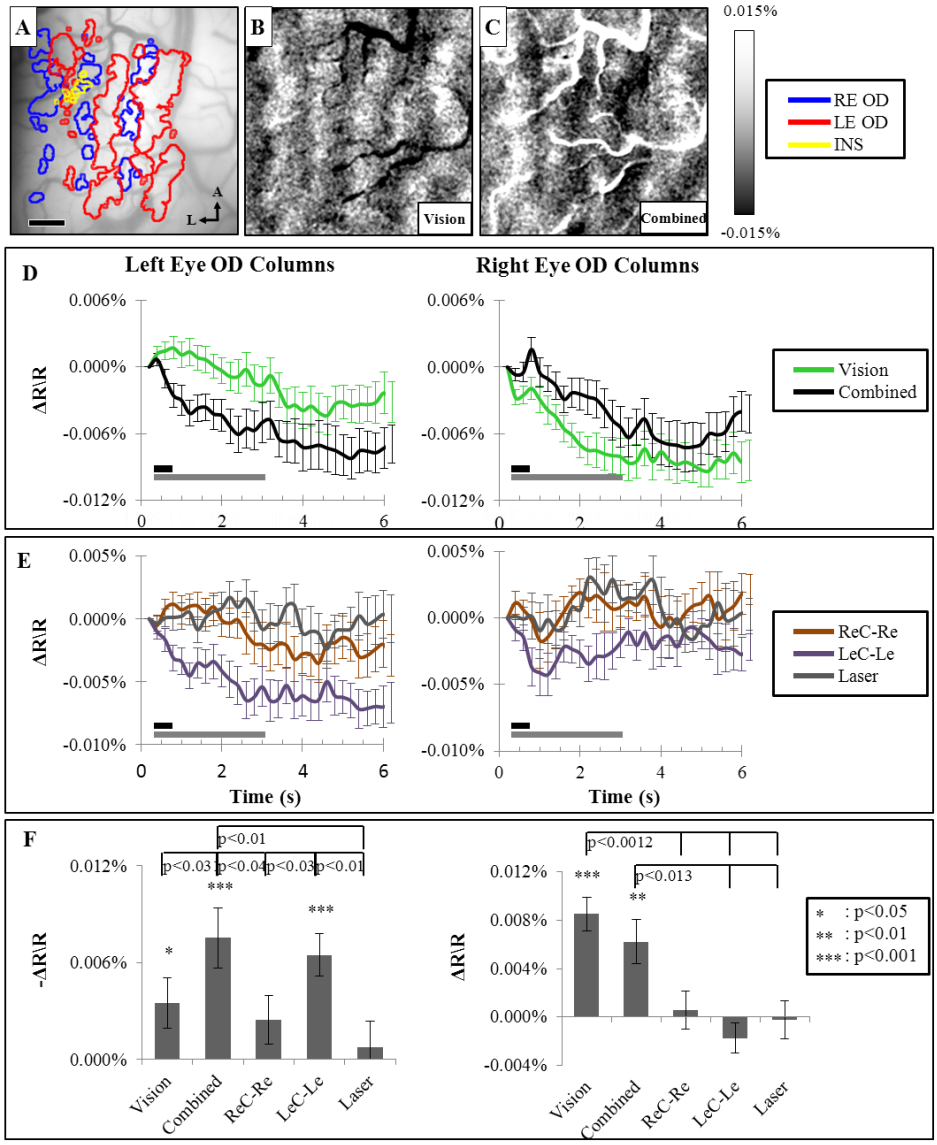

Figure 6.5 Intrinsic optical response to visual stimulation potentiated by INS. (A) Blood vessel map. Left eye OD columns demarcated by red outline and right eye OD Columns demarcated by blue outline. Direct effect of INS demarcated in yellow. Scale bar = 500 µm. (B&C) Ocular dominance columns generated by (B) visual stimulation of both eyes (Vision, Le-Re) and (C) INS during visual stimulation of both eyes (Combined, LeC-ReC). (D) Timecourse of intrinsic signal for visual and combined stimulation for left and right eye OD columns demarcated in A-C. (E) Timecourse difference between combined stimulation and visual stimulation of each eye (ReC-Re, LeC-Le) demonstrates INS stimulation potentiates visually evoked intrinsic signal magnitude for left eye stimulation. Black bar represents stimulus timing for INS and gray bar represents stimulus timing for visual stimulation. (F) Averaged reflectance change corresponding to 4-6 seconds of timecourses in D&E indicates INS potentiates visually evoked intrinsic signals with statistically significance for left eye OD column but not in right eye OD columns. P values comparing visual to combined stimulation and ReC-Re to LeC-Le obtained from paired two-tailed t-test. P values denoted by asterisks obtained from one sample student's t-test comparing averaged signal to zero signal. All error bars represent standard error of the mean. Laser stimulation parameters: λ = 1.875 µm, radiant exposure: 1.3 J/cm^2, repetition rate = 200 Hz, pulse width = 250 µs, pulse train length = 500 ms, fiber size = 100 µm. Visual stimulation parameters: Prestim gray = 1 sec, stimulation duration = 3.5 seconds, Spatial frequency = 1 Hz, Temporal frequency 3 Hz, square wave grating. Imaging parameters: 5 fps, ITI = 8 s, trials = 40. Subtraction maps in B and C correspond to frames 20 to 30 (4 to 6 seconds). (A = anterior, L = medial).

To further understand the modulatory effects of INS on the visual stimulation we examined the difference between combined stimulation and visual stimulation alone was quantified for individual eyes. This was done by calculating the difference timecourses between right eye VS+INS and right eye VS (ReC-Re, brown line) and between left eye VS+INS and left eye VS (LeC-Le, purple) (shown in Figure 6.5E). These comparisons presumably remove the response to visual stimulation alone, leaving only the INS-modulated component of the signal. To establish that the INS-modulated signal was due to simultaneous VS and INS and not simple superposition of OIS from visual and INS alone, the INS-modulated signal components for left eye and right eye stimulation were compared to the INS alone response (blank subtracted laser alone condition, gray line). For both left and right OD columns, the left eye INS modulated signal was greater in magnitude when compared to right eye INS modulated and INS alone signals (Figure 6.5E and F). Specifically, in the left eye column, the average signal magnitude for LeC-Le was shown to be statistically greater than the average signal magnitudes of ReC-Re ($p = 0.030$, paired t-test, two-tailed) and laser stimulation alone ($p = 0.006$, paired t-test, two-tailed); however, in the right eye columns, LeC-Le indicates initial modulation of intrinsic signal during left eye VS+INS compared to right eye VS+INS and INS alone, but these changes in signal magnitude indicated by LeC-Le were not statistically significant when compared against ReC-Re ($p = 0.257$, paired t-test, two-tailed) and laser stimulation alone ($p = 0.468$, paired t-test, two-tailed). These finding confirm that the observed potentiation of OIS evoked during combined stimulation (Figure 6.5C and D) is due to selective stimulation of the left eye OD column. Overall, these results demonstrate

the ability of carefully targeted INS to modulate functional cortical responses to visual stimulation in an eye specific manner.

6.4.5 The effect of INS spot size on OIS

The organization of the brain into distinct modules suggests that the size of the cortical area stimulated by INS will affect the nature of the evoked response. In order to test this hypothesis, intrinsic signal responses induced by three fiber optic sizes (100, 200, and 400 μm fibers) were compared within the same cortical location (fiber placement error within 100 μm). Visual and combined stimulation were performed as previously described, and laser parameters for combined stimulation consisted of a radiant exposure of 0.64 J/cm^2, at a repetition rate of 200 Hz, pulse width of 75 - 300 μs (varied to obtain same radiant exposure out of each fiber), and pulse train length of 500 ms. The blood vessel maps in figure 6.6A display the relative location of each stimulating fiber optic, the location of the targeted left (red) and right (blue) eye OD columns, and the area of effect for each fiber during INS (yellow outline, significant pixels determined by paired t-test between INS and blank, $p < 0.05$).

In figure 6.6B, the subtraction maps demonstrate the effects of combined stimulation relative to visual stimulation for each stimulating fiber optic. The area of effect from the 100 μm fiber suggests that stimulation with this fiber primarily activated OIS in pixels corresponded to the right eye OD column outlined in figure 6.6A (yellow outline, first column). As expected, the subtraction map acquired during combined stimulation shows slight potentiation of OIS in the targeted right eye column and slight

attenuation of OIS in the left eye column. This is confirmed by comparison of response timecourses as shown in figure 6.6C (first column), the 100 μm fiber, which is targeted towards the right eye column, attenuates the response to vision alone in the left eye column (top graph, green line magnitude greater than black line magnitude) and enhances the response to vision alone in the right eye column (bottom graph, black line magnitude greater than green line magnitude). Statistical analysis of the difference between the averaged signal magnitudes corresponding to 3 – 5 seconds for combined and visual stimulation showed near significance for both attenuation of left eye OIS responses ($p = 0.053$, paired t-test, two-tailed) and potentiation of right eye OIS responses ($p = 0.102$, paired t-test, two-tailed) (Figure 6.6D, first column). These findings are consistent with the previous case where combined stimulation with a 100 μm fiber was found to increase intrinsic signal magnitude for the targeted left eye columns and decrease intrinsic signal magnitude in the neighboring right eye columns (Figure 6.5).

Interestingly, combined stimulation with the 200 μm fiber produced noticeably increased intrinsic signal magnitude for both the left and right eye OD columns; however, these findings are supported by significant overlap of the area of effect from the 200 μm fiber with both left and right eye OD columns (Figure 6.6A, yellow outline, second column). Timecourse analysis confirms these trends as combined stimulation produced OIS with greater magnitudes when compared to OIS evoked by visual stimulation alone in both left and right eye OD columns (Figure 6.6B&C, second column, black line magnitude greater than green line magnitude). Statistical analysis of the average signal magnitude differences (t = 3–5 seconds) with a paired t-test show significant differences for the left eye OD column ($p = 0.008$, two-tailed) and near significant differences for

signals in the right eye OD columns (p=0.055, two-tailed) (Figure 6.6 D, second column). This finding indicates that a 200 μm stimulating fiber potentiates IOS in both right and left eye OD columns. No distinguishable trends were identified during combined stimulation with a 400 μm diameter fiber from subtraction map and timecourse analysis even though the area of effect from this fiber indicated overlap with both the right and left eye OD columns (Figure 6.6A-C, third column). A paired t-test between the average signal magnitudes evoked by combined and visual stimulation confirmed no differences could be distinguished between the two stimulation conditions (Figure 6.6D, $p = 0.75$ for left eye OD and $p = 0.84$ for right OD columns, two-tailed). These findings demonstrate the importance of spot size, fiber placement, and fiber choices to modulate visually evoked IOS in primate visual cortex.

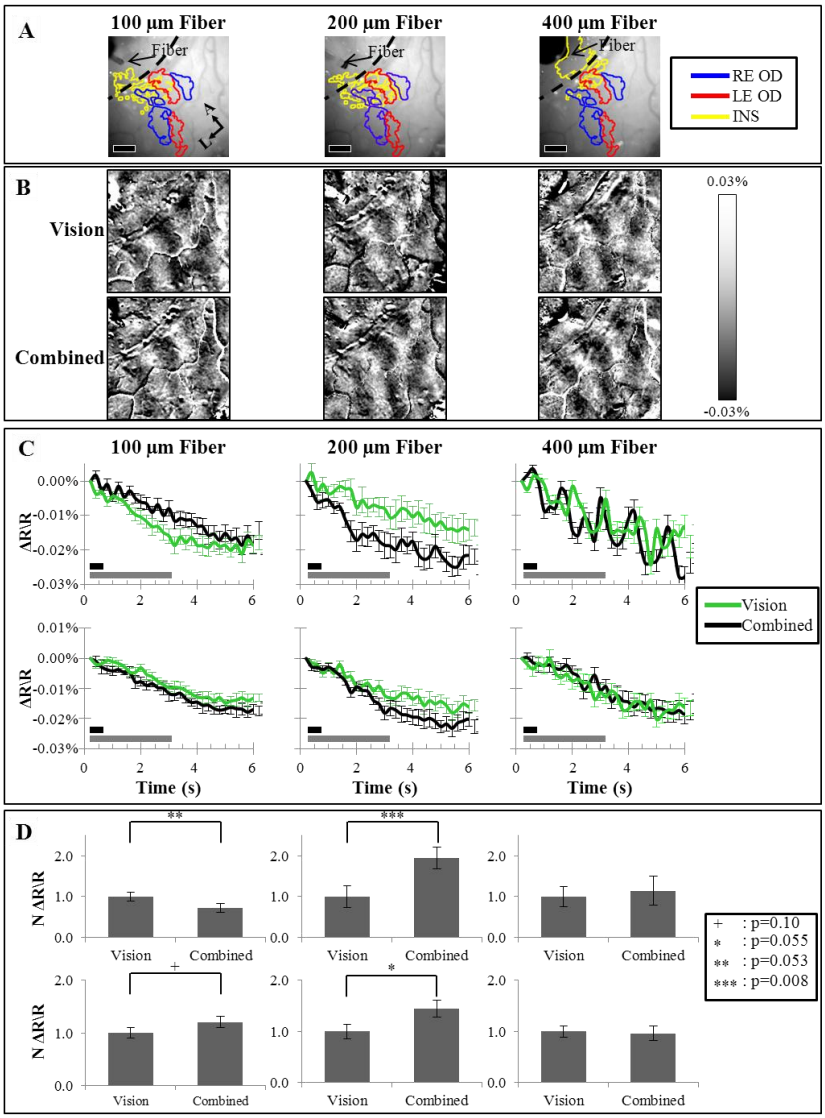

Figure 6.6: Modulation of visual signal by INS dependent on fiber size and placement. (A) Blood vessel maps displaying placement of 100, 200, and 400 µm fibers in relation to outlines demarcating targeted right eye (blue) and left eye (red) OD columns. Error of fiber placement < 100 µm. Black scale bar = 500 µm (B) Ocular dominance columns generated by visual stimulation of both eyes (Vision, Le-Re) and INS during visual stimulation of both eyes (Combined, LeC-ReC). Averaged intrinsic signal contrast noticeably enhanced for 200 um fiber. (C) Timecourse of intrinsic signal from OD outlines in A&B for left eye column (top row) and right eye columns (bottom row). (D) Normalized average intrinsic signal (corresponding to 3 – 5 seconds) for visual and combined stimulation in left eye column (top row) and right eye columns (bottom row). A slight increase in OIS evoked by combined stimulation with a 100 µm in the right eye column was determined to be near significant by a paired t-test (p=0.10, two-tailed), as well as the observed attenuation evoked by combined stimulation of the left eye (p=0.053, two-tailed). Combined stimulation with a 200 µm fiber was shown to potentiate the visually evoked OIS in the left eye OD column with statistical significance (p=0.008) and in the right eye OD columns with near significance (p=0.055). No significant changes were observed during combined stimulation with a 400 µm fiber (left eye columns: p=0.753, right eye columns: p=0.842). All reported p-values obtained from paired two-tailed student's t-tests. Laser stimulation parameters: λ = 1.875 µm, radiant exposure = 0.64 J/cm^2, repetition rate = 200 Hz, pulse width = 75 - 300 µs, pulse train length = 500 ms. Trials = 38 for 100 and 200 µm fiber, Trials = 25 for 400 µm fiber. Subtraction maps in B correspond to frames 15 to 25 (3 to 5 seconds). (A = anterior, L = lateral).

6.5 Discussion

6.5.1 Summary

Our group has established the ability to evoke neural activity in rodent models using pulsed infrared light [17, 18, 26]. In the present study, the ability of INS to evoke meaningful cortical responses in anesthetized non-human primates is demonstrated. Infrared neural stimulation was demonstrated to evoke focal OIS responses in V1 cortex with similarities in spatial and temporal features to previously characterized OIS signals evoked by visual stimulation [20, 29-31]. The organization of activated areas and the timecourses displayed in figure 6.3 suggest functional activation of underlying neural circuitry associated with ocular dominance, orientation domains, and/or color domains, an exciting finding indicating INS could be used to selectively activate neuronal circuitry if targeted properly [24]. This high degree of spatial precision is not surprising as numerous applications of INS have also reported spatially precise evoked neural activity [5, 14, 15, 18, 26, 32-34]. Furthermore, the timecourse of the INS evoked OIS in figure. 6.3 combined with the data characterizing the effects of radiant exposure (Figure 6.2) on OIS display a strength response relationship with stimulation strength (increased repetition rate, increased radiant exposure, and increased stimulation duration) that corresponds to relationships identified in parametric studies of rodent somatosensory cortex that initially characterized OIS responses to INS [18]. In this study, the underlying neural response was confirmed to be excitatory as indicated by the single unit recordings summarized in Figure 6.4. Together the results demonstrate the ability of INS to excite

cortical neurons establishing INS as a viable alternative stimulation modality for study of cortical microcircuitry *in vivo* in non-human primates.

The ability to modulate or perturb underlying cortical microcircuitry is an essential tool in determining exact function of specific cortical structures [35, 36]. Therefore, modulation of functionally relevant responses is an important feature to establish for INS to be accepted as a proven neurostimulation modality for studying cortical microcircuitry, in anesthetized and awake animals. We used brief periods of INS (500 ms) to modulate visually evoked OIS in eye specific OD columns. The results in figure 6.6 show left eye specific enhancement of OIS from combined high intensity (1.3 J/cm^2, fiber size = 100 μm) INS and visual stimulation in a left eye OD column when compared to the OIS evoked by visual stimulation alone. The slight decrease in right eye OD OIS evoked during combined stimulation suggests local inhibition of OIS further supporting the ability of INS to modulate visual responses in an eye specific manner. This trend was confirmed in figure 6.6, where INS with a 100 μm fiber was shown to potentiate responses in targeted right eye columns and attenuate responses in the neighboring left eye columns. The data from INS with a 100 μm optical fiber clearly demonstrates the ability of INS to modulate visually evoked IOS.

It was also determined how stimulating cortex with pulsed infrared light delivered through a 200 and 400 μm fiber modulated visual evoked intrinsic optical signal compared to the modulation observed during INS with a 100 μm fiber. The 200 μm fiber was hypothesized to be the most effective fiber size for modulation of eye specific OIS because the spot size of the laser light could be optimally targeted towards one OD column as the average diameter is 400 μm [24, 28]. The 200 μm was shown to enhance

visually evoked IOS signals in both left and right eye columns. This finding highlights the importance of fiber positioning as the 200 µm fiber was located in the right eye OD column but near a column border. Combined stimulation with the 400 µm fiber demonstrated no modulation of visually evoked IOS signals, which suggests the 400 µm fiber may be ineffective for modulating cortical neural activity and may indicate the 400 µm diameter is too large for effective excitatory activation. These findings support the importance of fiber size selection and positioning when performing INS for evoking excitatory neural activity.

The heat gradient responsible for evoking neural activity has consistently been identified as a concern for its potential in causing damage to neural tissue [11, 18, 32, 37, 38]. While a comprehensive damage study was not possible in these experiments, INS was performed in the same animal over the course of a year with no apparent signs of damage. Visible thermal damage was never observed in cortex following repetitive stimulation in the same location of cortex. The animals never demonstrated loss of visual function in the awake state, and IOS and neural activity was consistent throughout the study. These observations led to the conclusion that the parameters of INS used in this study were safe and did not cause acute or chronic damage to stimulated visual cortex.

6.5.2 INS evoked excitation versus inhibition

In this study, pulsed infrared light was shown to evoke excitatory activity through single unit recordings in V1 cortex; however, it was previously demonstrated that INS inhibited spontaneous neural activity in rat somatosensory cortex [18]. The primarily used stimulating optical fiber diameters of 100 and 200 µm used in this study allowed for

more precise targeting of cortical modules less than the 400 μm in diameter (i.e. size of primate OD columns [28] and rat barrel columns [39]). The smaller diameter of the stimulating fibers allowed for focused INS of specific functional modules in V1 cortex that resulted in the observed INS evoked excitatory neural activity and apparent excitatory OIS activity. In the rodent study, a 400 μm stimulating fiber was exclusively used to activate somatosensory cortex and the spot sizes used during this study ranged between 400 – 800 μm in diameter [18]. This larger spot size used in the rodent study was thought to be the primary reason why inhibition of neural activity was observed as there are many examples across species where large area stimulation have frequently led to inhibition [39-42]. The observations made during the rodent study led to the hypothesis that the large spot size used to stimulate rodent cortex led to INS evoking surround inhibition and that INS with a small spot size would evoke excitatory activity. In support of this hypothesis, we have demonstrated that focused well targeted INS in primates evokes excitatory single unit activity supporting the theory that spot size plays a crucial role in determining INS evoked excitation or inhibition.

While the observed INS evoked inhibition in rodents was most likely due to activation of surround inhibition, the underlying cellular mechanisms for INS may still play a role in determining if INS evokes excitation or inhibition. The TRPV4 mechanisms [9] previously described help explain how INS may excite neural tissue; however, the capacitance mechanism [8] can explain both excitation and inhibition. The INS evoked change in capacitance is not cell specific meaning any cell membrane that absorbs incident light will be depolarized. This indicates that excitatory and inhibitory neurons will be depolarized in the presence of a thermal gradient evoked by INS.

Activation of a higher number of inhibitory neurons could have led to inhibition of spontaneous neural activity as observed in the rodent study [18]. The ability of INS to activate inhibitory neural pathways has also been demonstrated through increasing GABA current in plated cultured neurons [26]. While significant gains have been made over the past year in understanding the cellular mechanisms involved in INS evoked potentials, significant cellular research is needed to fully understand how these mechanisms interact in determining if a neuron will be excited or inhibited.

6.5.3 Implications of INS in non-human primates

This feasibility study in NHPs represents a significant step in the development of INS as a neurostimulation modality for application in the CNS. Pulsed infrared light was shown to evoke and modulate OIS in V1 cortex corresponding to eye specific ocular dominance columns. Additionally, single unit recordings demonstrated that INS evoked excitatory neural responses suggesting OISs evoked by INS were related to excitatory neural activity. Together, these results demonstrate that INS can be used to evoke excitatory neural activity in V1 cortex of NHPs providing a new tool for neuroscientist to study NHP neurocircuitry.

The results from this study directly motivated NHP studies that assessed the compatibility of INS with fMRI in Squirrel monkey somatosensory cortex, and assessed if INS could be used to modulate behavior in a Macaque monkey visual cortex (Appendix B). Functional magnetic resonance imaging of pulsed infrared light stimulation in Squirrel monkey somatosensory cortex showed INS evoked depth specific changes in cerebral blood volume at the stimulation site as well as in projection areas within

somatosensory cortex. These results support the findings of this chapter by providing further evidence that INS evokes signaling in neural networks. The ability to modulate behavior with INS was demonstrated in Macaque monkey visual cortex when short duration pulsed infrared light stimulation caused the monkey to saccade to the area on the visual stimulation screen that corresponded to the retinotopic location stimulated by INS. This indicates that the animal perceived stimulation of visual cortex with pulsed infrared light, a significant demonstration as modulation of behavior is an important tool for understanding how the nervous system functions. Together, the results outlined in this chapter and the results described in Appendix B effectively establish INS as a neurostimulation modality for applications in NHPs, a significant advancement for INS as the NHP model represents the closest animal model to human cortex. Further investigations in NHP models with INS will continue the development of the technique towards eventual clinical applications.

6.6 Acknowledgements

The authors would like to acknowledge Mary R. Feutado, and Yasmina A. Paramastri for animal care and Andrea Brock, Brian Lustig, Jeremy Winberry, and Lisa Chu for their assistance. This work was supported by the National Institutes of Health (NIH R01 NS052407-01 and NS44375), DOD-MFEL Program (DOD/AFOSR F49620-01-1-4029), and the Human Frontiers Science Program.

6.7 References

[1] Han, X., Qian, X., Bernstein, J. G., Zhou, H., Franzesi, G. T., Stern, P., Bronson, R. T., Graybiel, A. M., Desimone, R., and Boyden, E. S., "Millisecond-timescale optical control of neural dynamics in the nonhuman primate brain," *Neuron*, vol. 62, p. 191, 2009.

[2] Heider, B., Nathanson, J. L., Isacoff, E. Y., Callaway, E. M., and Siegel, R. M., "Two-Photon Imaging of Calcium in Virally Transfected Striate Cortical Neurons of Behaving Monkey," *PLoS ONE*, vol. 5, p. e13829, 2010.

[3] Velliste, M., Perel, S., Spalding, M. C., Whitford, A. S., and Schwartz, A. B., "Cortical control of a prosthetic arm for self-feeding," *Nature*, vol. 453, pp. 1098-1101, 2008.

[4] Capitanio, J. P. and Emborg, M. E., "Contributions of non-human primates to neuroscience research," *The Lancet*, vol. 371, pp. 1126-1135, 2008.

[5] Wells, J., Konrad, P., Kao, C., Jansen, E. D., and Mahadevan-Jansen, A., "Pulsed laser versus electrical energy for peripheral nerve stimulation," *J Neurosci Methods*, vol. 163, pp. 326-37, 2007.

[6] Wells, J., Kao, C., Mariappan, K., Albea, J., Jansen, E. D., Konrad, P., and Mahadevan-Jansen, A., "Optical stimulation of neural tissue in vivo," *Opt Lett*, vol. 30, pp. 504-6, 2005.

[7] Wells, J., Kao, C., Konrad, P., Milner, T., Kim, J., Mahadevan-Jansen, A., and Jansen, E. D., "Biophysical mechanisms of transient optical stimulation of peripheral nerve," *Biophys J*, vol. 93, pp. 2567-80, 2007.

[8] Shapiro, M. G., Homma, K., Villarreal, S., Richter, C.-P., and Bezanilla, F., "Infrared light excites cells by changing their electrical capacitance," *Nat Commun*, vol. 3, p. 736, 2012.

[9] Albert, E. S., Bec, J., Desmadryl, G., Chekroud, K., Travo, C., Gaboyard, S., Bardin, F., Marc, I., Dumas, M., and Lenaers, G., "TRPV4 channels mediate the infrared laser-evoked response in sensory neurons," *Journal of Neurophysiology*, vol. 107, pp. 3227-3234, 2012.

[10] Tozburun, S., Lagoda, G. A., Burnett, A. L., and Fried, N. M., "Subsurface near infrared laser stimulation of the periprostatic cavernous nerves," *Journal of biophotonics*, 2012.

[11] Teudt, I. U., Nevel, A. E., Izzo, A. D., Walsh, J. T., Jr., and Richter, C. P., "Optical stimulation of the facial nerve: a new monitoring technique?," *Laryngoscope,* vol. 117, pp. 1641-7, 2007.

[12] Rajguru, S. M., Richter, C.-P., Matic, A. I., Holstein, G. R., Highstein, S. M., Dittami, G. M., and Rabbitt, R. D., "Infrared photostimulation of the crista ampullaris," *The Journal of Physiology,* vol. 589, pp. 1283-1294, 2011.

[13] Izzo, A. D., Richter, C.-P., Jansen, E. D., and Walsh, J. T., Jr., "Laser stimulation of the auditory nerve," *Lasers in Surgery and Medicine,* vol. 38, pp. 745-753, 2006.

[14] Katz, E. J., Ilev, I. K., Krauthamer, V., Kim, D. H., and Weinreich, D., "Excitation of primary afferent neurons by near-infrared light in vitro," *NeuroReport,* vol. 21, pp. 662-666, 2010.

[15] Jenkins, M. W., Duke, A. R., GuS, DoughmanY, Chiel, H. J., FujiokaH, WatanabeM, Jansen, E. D., and Rollins, A. M., "Optical pacing of the embryonic heart," *Nat Photon,* vol. 4, pp. 623-626, 2010.

[16] Dittami, G. M., Rajguru, S. M., Lasher, R. A., Hitchcock, R. W., and Rabbitt, R. D., "Intracellular calcium transients evoked by pulsed infrared radiation in neonatal cardiomyocytes," *The Journal of Physiology,* vol. 589, pp. 1295-1306, 2011.

[17] Cayce, J. M., Kao, C. C., Malphrus, J. D., Konrad, P. E., Mahadevan-Jansen, A., and Jansen, E. D., "Infrared Neural Stimulation of Thalamocortical Brain Slices," *Selected Topics in Quantum Electronics, IEEE Journal of,* vol. 16, pp. 565-572, 2010.

[18] Cayce, J. M., Friedman, R., Jansen, E. D., Mahadevan-Jansen, A., and Roe, A. W., "Pulsed infrared light alters neural activity in rat somatosensory cortex in vivo," *Neuroimage,* vol. 57, pp. 155-166, 2011.

[19] Chen, L. M., Heider, B., Williams, G. V., Healy, F. L., Ramsden, B. M., and Roe, A. W., "A chamber and artificial dura method for long-term optical imaging in the monkey," *Journal of Neuroscience Methods,* vol. 113, pp. 41-49, 2002.

[20] Roe, A. W., "Long-term optical imaging of intrinsic signals in anesthetized and awake monkeys," *Appl. Opt.,* vol. 46, pp. 1872-1880, 2007.

[21] Tanigawa, H., Lu, H. D., and Roe, A. W., "Functional organization for color and orientation in macaque V4," *Nature neuroscience,* vol. 13, pp. 1542-1548, 2010.

[22] Smith, E. L., Chino, Y. M., Ridder, W. H., Kitagawa, K., and Langston, A., "Orientation bias of neurons in the lateral geniculate nucleus of macaque monkeys," *Visual neuroscience,* vol. 5, pp. 525-545, 1990.

[23] Hale, G. M. and Querry, M. R., "Optical constants of water in the 200-nm to 200-µm wavelength region," *Appl. Opt.,* vol. 12, pp. 555-563, 1973.

[24] Lu, H. D. and Roe, A. W., "Functional Organization of Color Domains in V1 and V2 of Macaque Monkey Revealed by Optical Imaging," *Cerebral Cortex,* vol. 18, pp. 516-533, 2008.

[25] Wang, G., Tanaka, K., and Tanifuji, M., "Optical imaging of functional organization in the monkey inferotemporal cortex," *Science (New York, NY),* vol. 272, p. 1665, 1996.

[26] Feng, H.-J., Kao, C., Gallagher, M. J., Jansen, E. D., Mahadevan-Jansen, A., Konrad, P. E., and Macdonald, R. L., "Alteration of GABAergic neurotransmission by pulsed infrared laser stimulation," *Journal of Neuroscience Methods,* vol. 192, pp. 110-114, 2010.

[27] Richter, C. P., Matic, A. I., Wells, J. D., Jansen, E. D., and Walsh, J. T., "Neural stimulation with optical radiation," *Laser & Photonics Reviews,* vol. 5, pp. 68-80, 2010.

[28] Horton, J. C. and Hocking, D. R., "Intrinsic Variability of Ocular Dominance Column Periodicity in Normal Macaque Monkeys," *The Journal of Neuroscience,* vol. 16, pp. 7228-7339, 1996.

[29] Grinvald, A., Lieke, E. E., Frostig, R. D., and Hildesheim, R., "Cortical point-spread function and long-range lateral interactions revealed by real-time optical imaging of macaque monkey primary visual cortex," *J. Neurosci.,* vol. 14, pp. 2545-2568, 1994.

[30] Ts'o, D. Y., Frostig, R. D., Lieke, E. E., and Grinvald, A., "Functional organization of primate visual cortex revealed by high resolution optical imaging," *Science,* vol. 249, pp. 417-420, 1990.

[31] Lu, H. D. and Roe, A. W., "Optical imaging of contrast response in macaque monkey V1 and V2," *Cerebral Cortex,* vol. 17, pp. 2675-2695, 2007.

[32] Duke, A. R., Peterson, E., Mackanos, M. A., Atkinson, J., Tyler, D., and Jansen, E. D., "Hybrid electro-optical stimulation of the rat sciatic nerve induces force

generation in the plantarflexor muscles," *Journal of Neural Engineering,* vol. 9, p. 066006, 2012.

[33] Richter, C. P. and Matic, A. I., "Optical Stimulation of the Auditory Nerve," *Auditory Prostheses,* pp. 135-156, 2012.

[34] Duke, A. R., Lu, H., Jenkins, M. W., Chiel, H. J., and Jansen, E. D., "Spatial and temporal variability in response to hybrid electro-optical stimulation," *Journal of Neural Engineering,* vol. 9, p. 036003, 2012.

[35] Toth, L. J., Rao, S. C., Kim, D. S., Somers, D., and Sur, M., "Subthreshold facilitation and suppression in primary visual cortex revealed by intrinsic signal imaging," *Proceedings of the National Academy of Sciences,* vol. 93, pp. 9869-9874, 1996.

[36] Stepniewska, I., Friedman, R. M., Gharbawie, O. A., Cerkevich, C. M., Roe, A. W., and Kaas, J. H., "Optical imaging in galagos reveals parietal–frontal circuits underlying motor behavior," *Proceedings of the National Academy of Sciences,* vol. 108, pp. E725–E732, 2011.

[37] Wells, J., Thomsen, S., Whitaker, P., Jansen, E. D., Kao, C. C., Konrad, P. E., and Mahadevan-Jansen, A., "Optically mediated nerve stimulation: Identification of injury thresholds," *Lasers Surg Med,* vol. 39, pp. 513-26, 2007.

[38] Goyal, V., Rajguru, S., Matic, A. I., Stock, S. R., and Richter, C. P., "Acute damage threshold for infrared neural stimulation of the cochlea: functional and histological evaluation," *The Anatomical Record: Advances in Integrative Anatomy and Evolutionary Biology,* 2012.

[39] Derdikman, D., Hildesheim, R., Ahissar, E., Arieli, A., and Grinvald, A., "Imaging Spatiotemporal Dynamics of Surround Inhibition in the Barrels Somatosensory Cortex," *The Journal of Neuroscience,* vol. 23, pp. 3100-3105, 2003.

[40] Ghose, G. M., "Attentional Modulation of Visual Responses by Flexible Input Gain," *Journal of Neurophysiology,* vol. 101, pp. 2089-2106, 2009.

[41] Levitt, J. B. and Lund, J. S., "Contrast dependence of contextual effects in primate visual cortex," *Nature,* vol. 387, pp. 73-76, 1997.

[42] Simons, D. J. and Carvell, G. E., "Thalamocortical response transformation in the rat vibrissa/barrel system," *Journal of Neurophysiology,* vol. 61, pp. 311-330, 1989.

CHAPTER VII

CONCLUSIONS AND FUTURE DIRECTIONS

7.1 Summary and Conclusions

7.1.1 Summary

The overall objective of this dissertation was to develop infrared neural stimulation (INS) as a neurostimulation modality for application in the central nervous system. Previously, INS had only been well characterized for evoking action potentials in axons located in peripheral nerves with high spatial precision and a contact free delivery interface [1]. Chapter II of this dissertation overviewed specific previous applications of INS in the peripheral nervous system, discussed the high degree of modular organization of the cerebrum cortex motivating the application of INS for surface cortical stimulation, and reviewed optical detection techniques used to characterize INS evoked cortical signals. The work contained in this dissertation describes feasibility of INS for activating cortical neurons in thalamocortical brain slices (Chapter III); the first *in vivo* application of INS for stimulating the cortex of the brain (Chapter IV); investigated the cortical cellular components activated by INS (Chapter V); and demonstrated feasibility for evoking meaningful neuronal signals in non-human primates (Chapter VI).

Chapter III discusses the initial feasibility studies conducted in rat thalamocortical brain slices demonstrating that INS evokes excitatory neural activity in cortical tissue for the first time. Pulsed infrared light was shown to evoke artifact-free neural signals pulsed locked with the repetition rate of the laser while maintaining a contact free interface

demonstrated for INS in the peripheral nervous system. The laser evoked neural potentials were shown to be dependent on the stimulating light's absorption coefficient decreasing stimulation threshold as absorption increased agreeing with previous studies in the sciatic nerve [2]. Increasing the spot size was also found to decrease stimulation thresholds as high volumes of cortical tissue were activated with larger spot sizes. The data from investigating wavelength and spot size effects on stimulation threshold highlight the importance of stimulated tissue volume in determining cortical activation from infrared light. Increased repetition rate of the laser were shown to decrease the stimulation threshold for evoked potentials in the thalamocortical brain slice identifying an important difference between applications in the peripheral nerve where stimulation was limited to low repetition rates [3]. The final portion of this manuscript characterized intracellular recordings of INS evoked neural activity demonstrating the ability to record artifact free intracellular potentials using traditional electrophysiological techniques for the first time. The primary conclusion drawn from this study was that pulsed infrared light could evoke neural potentials in cortical tissue and motivated the first *in vivo* application of INS in cortical tissue.

Chapter IV describes the first *in vivo* application of pulsed infrared light for modulating neuronal activity in rodent somatosensory cortex. Due to the small potentials and high spatial precision associated with INS demonstrated in the brain slice study, optical intrinsic signal imaging (OISI) methods were employed to visualize INS evoked signals. The OISI signals evoked by INS were shown to be similar to OISI signals evoked by vibrotactile stimulation of forepaw digits and whisker barrels in signal magnitude and both spatial and temporal extent. The INS evoked responses were determined to be

consistent and stable over time and were modulated by varying repetition rate and radiant exposure identifying similar trends that were observed in the brain slice study; however INS was found to inhibit the underlying spontaneous neural activity contradicting the accepted excitatory neural activity typically associated OISI and the excitatory responses seen in the brain slice. This finding suggested that the OISI signal generated during INS was through different mechanisms than those generated by vibrotactile stimulation. Several hypotheses were developed to explain the observed inhibition including the OISI response was generated from direct activation of inhibitory neurons located in layers I and II of cortex; modulation of neural activity in apical dendrites; direct activation of astrocytes modulating blood flow to cortex; and activation of surround inhibition due to large volume of activated cortical tissue. While individually testing all of these proposed hypotheses was beyond the scope of this dissertation, the final two chapters broadly addressed these hypotheses to determine the effects of infrared irradiation on neural and glia activity.

Chapter V characterized the effects of INS on *in vivo* cortical calcium signaling in rat somatosensory cortex in an effort to better understand the cellular dynamics activated during pulsed infrared irradiation of cortex. These results provided a more direct measure of cellular activity compared to OISI as the calcium indicator dye's fluorescence intensity is correlated with intracellular calcium concentrations, a critical ionic current during cortical cellular signaling in both astrocytes and neurons. Optical imaging of calcium signals in somatosensory cortex during INS revealed a two component, fast and slow, calcium response that was evoked by pulsed infrared light. Additionally, calcium signals evoked by INS were shown to exhibit wave-like properties supporting activation of a

cellular network. These characteristics observed in INS evoked calcium signals led to the hypothesis that the slow component corresponded to astrocyte activity and the fast component reflected neuronal calcium signaling. These hypotheses were further investigated through pharmacological studies and two-photon imaging. The glutamate antagonist CNQX decreased the fast component of the signal but had no statistical effect on the slow component indicating that the fast component of INS evoked calcium signals is related to neuronal glutametergic activity. The astrocyte poison fluoroacetate (FAC) was found to significantly decrease INS evoked calcium signal magnitudes overall supporting astrocyte calcium signaling as the primary source of the signal's slow component. Interestingly, the combined effects of both CNQX and FAC further decreased the INS evoked calcium signal suggesting synergistic mechanisms from both astrocytes and neurons in generating INS evoked calcium signals. Two-photon imaging of calcium signaling during INS further supported the pharmacological results where INS evoked calcium signals were observed to propagate through an astrocyte network, and a local calcium signal response was observed in the surrounding neuropil suggesting INS evokes calcium signaling in apical dendrites. The results of this study confirm multiple cortical cell types, astrocytes and neurons, are sensitive to pulsed infrared light. The significant involvement of astrocytes in INS evoked calcium signals suggest that the observed OISI in Chapter IV were likely heavily influenced through astrocyte activity. Furthermore, this study identified the importance of local cellular anatomy exposed to infrared light in determining observed responses as astrocytes are more numerous in the superficial layers of cortex where majority of absorption takes place during INS. These observations identify the importance of future subcortical application of INS in furthering

the development of INS in the CNS as observed signals are likely to change as neuronal activation is more likely in deeper layers of cortex.

Chapter VI demonstrates feasibility of INS to modulate meaningful functional cortical signals in the non-human primate (NHP). The NHP model is the closest animal model for human cortex and feasibility of INS in NHPs is a crucial step in the development of INS for clinical applications. Additionally, increased neural density and neuronal organization present in NHP cortex offered an improved model for assessing the observed excitatory and inhibitory effects of INS characterized in previous chapters of this dissertation. Here, feasibility of INS was assessed in primary visual cortex of Macaque monkeys by targeting stimulation to functionally distinct ocular dominance columns. Infrared neural stimulation was shown to evoke focal OISI responses and these responses were related to excitatory neural activity through single unit recordings. Visually evoked OISs were shown to be modulated by short duration INS in eye specific columns demonstrating the ability to modulate functionally relevant cortical responses with pulsed infrared light. The findings reported in this chapter have motivated further experimentation in NHPs in studies not included in this dissertation (Appendix B). Functional imaging in somatosensory cortex of squirrel monkeys during INS has demonstrated depth specific activation of cerebral blood volume signal corresponding to layers III-V of cortex and has identified areas of activation distal to stimulation site corresponding to other somatosensory cortical areas [4]. Initial behavioral studies in fixating macaque monkeys have shown that stimulation of primary visual cortex with pulsed infrared light causes the animal to saccade towards the retinotopic location stimulated by infrared light suggesting the animal perceived INS [5]. The combination of

the initial feasibility study presented in this dissertation and these additionally studies described in Appendix B effectively establish INS as a neurostimulation modality for application in non-human primates.

7.1.2 Implications

In this dissertation, I found that pulsed infrared light could excite and inhibit neural activity and evoke astrocyte calcium signaling using similar stimulation parameters. Therefore, it is important to establish plausible explanations for these observed responses. As stressed in Chapter II, the anatomy and physiology of cortex is complex and consists of a 3-dimensional network of neurons and supporting glia cells that are organized into distinct functional modules. This complex anatomical organization of cortex can be used to relate the diverse cortical cellular responses characterized here and explain the overall implications of this dissertation.

7.1.2.1 Neural excitation versus inhibition

In Chapter III, pulsed infrared light routinely evoked excitatory neural responses in rat brain slices; however, in Chapter IV, INS was found to inhibit spontaneous neural activity in cortex *in vivo* while evoking OIS typically associated with excitatory neural activity. These differences prompted further studies in visual cortex of non-human primates (Chapter VI) where INS was demonstrated to drive single unit excitation using fiber optics with similar diameters to functional modules located in visual cortex. Additionally, INS was found to modulate visually evoked OIS in eye specific functional modules (ocular dominance column) targeted for stimulation. Further evidence of

excitatory neural activation was identified with calcium signal imaging in rat somatosensory cortex (Chapter V) that indicated the fast component of the INS evoked calcium signal was due to glutametergic activity in the apical dendritic tree. Each of these diverse responses observed in response to INS can be explained by the local cytoarchitecture and the volume of tissue that absorbs incident infrared light.

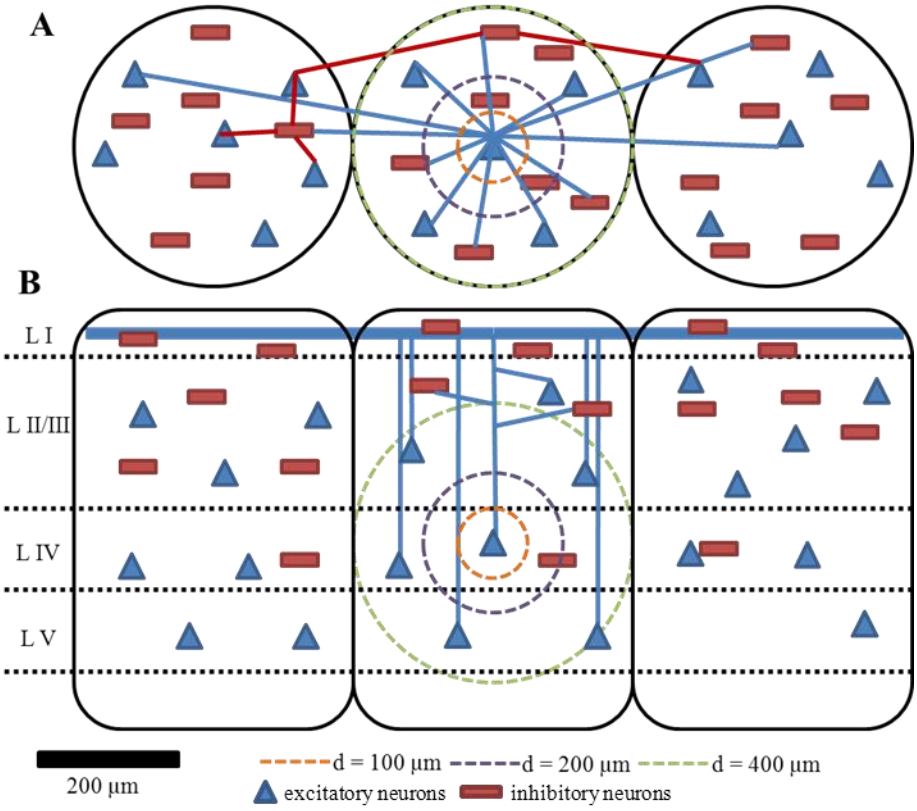

Figure 7.1: Illustration spot size and orientation importance of cortical tissue in determining excitatory or inhibitory neural response. A.) Dorsal view of three functional domains that are 400 µm in diameter displaying simplified location of pyramidal cells (blue triangles), inhibitory neurons (red rectangles), and simplified dendritic projections (blue lines from pyramidal cells, red lines from inhibitory neurons). B.) Sagittal view of functional modules in representing location of pyramidal cells, inhibitory neurons, and dendrites as a function of depth. Circles in A&B represent typical spot size diameters tested in this dissertation (100, 200, and 400 µm).

Figure 7.1 displays an idealized section of cortical tissue showing relative position of excitatory pyramidal cells and inhibitory cells for three functional cortical modules for dorsal (representative of *in vivo* stimulation) and sagittal (representative of brain slice stimulation) orientations. In the central module, the dendritic and axonal projections are illustrated for both pyramidal and inhibitory neurons to demonstrate intra and inter-cortical connections that influence cortical processing. It should be noted that inhibitory neurons are more numerous in superficial layers (I-II) of cortex compared to pyramidal neurons, and pyramidal neurons have a higher density in deeper cortical layers (III-V) but project apical dendrites up to layer I of cortex. Three spot size diameters are displayed on the central module to indicate the area of tissue and relative number of cells that are stimulated in both the dorsal and sagittal views.

In rat cortex (Chapter IV), I identified that large spot size diameters ($d \geq 400$ μm) inhibited spontaneous activity. As can be seen in Figure 7.1A, a 400 μm spot size diameter of well-targeted stimulation will activate an entire functional module. In these experiments, multiple cortical modules were likely stimulated due to the large spot size diameter and spread of the thermal gradient outside the spot size of the laser beam. Stimulation of multiple functional modules may lead to inhibitory neurons being directly stimulated and can evoke surround inhibition as first hypothesized in Chapter IV. To test this hypothesis, I used INS with smaller spot sizes in well-defined non-human primate primary visual cortex (Chapter VI) where I identified that smaller spot size diameters (100 and 200 μm) can be used to evoke excitatory responses. The smaller spot sizes, as illustrated in Figure 7.1A, can be localized to a point where only a few excitatory neurons and their processes are stimulated with limited stimulation of surrounding inhibitory

neurons. This type of activation by INS leads to an excitatory response or increased neural firing, as demonstrated in Chapter VI. However as the spot size increases, more neurons, both excitatory and inhibitory, and dendrites are stimulated evoking an integrated signal that can present as overall excitation or inhibition. In Chapter VI, I demonstrated that a 400 μm spot size diameter was incapable of modulating visually evoked OIS; whereas, INS with 100 and 200 μm spot size diameters enhanced visually evoked OIS suggesting an excitatory response to INS with a smaller fiber. These results support the findings discussed in Chapter IV where a spot size diameter of 400 μm and greater evoked inhibition of neural activity as the 400 μm optical fiber had no effect on visually evoked signals. The results from Chapters IV and VI indicate the importance of spot size in determining excitation or inhibition and provides tantalizing evidence that INS can be used for both excitatory and inhibition applications.

Interestingly, the pharmacological studies described in Chapter V, using similar stimulation parameters to Chapter IV, demonstrated that INS evoked calcium transients related to glutamate release supporting the hypothesis that INS modulates dendritic signaling. Dendrites are the major neural component present in the superficial layers (Figure 7.1B) and represent the first neural process to absorb infrared light. Relating the calcium signal evoked by INS to neural signals was a crucial finding for this dissertation because it demonstrates that pulsed infrared light can evoke local transients at the dendrite. While inhibition was only observed in rat cortex as outlined in Chapter IV, excitation was observed in primate cortex described in Chapter VI. The most likely conduit for the observed excitation and inhibition in Chapter IV and VI was through stimulation of a neuron's apical dendrite tree located in the superficial layers of cortex.

While further research is needed to fully understand interactions of pulsed infrared light with dendrites, somas, and axons of neurons located in the CNS, each *in vivo* study contained in this dissertation effectively demonstrates that INS activates cortical neurons.

While a large spot size diameter was found to inhibit neural activity in *in vivo* preparations, INS stimulation threshold was found to decrease with increasing spot size diameter *in vitro* in thalamocortical brain slices (Chapter III) seemingly contradicting the findings in Chapter IV and VI. However, these findings can also be explained by the geometry of the tissue stimulated and the location of neurons within the brain slice. The brain slice model simplifies the cortex neural network down to a network containing only a few neurons and neurons, typically located deep in cortex, and translate these to the surface allowing for the somas of these neurons to be easily stimulated by pulsed infrared light. Additionally, processes perpendicular to the cut plane are severed decreasing the influence of laterally projecting inhibitory neurons. The sagittal view in Figure 7.1B can be used to model neuron location as a function of depth as seen in the brain slice model. Increasing the spot size diameter of INS targeted at layer IV increases the number of excitatory neurons that are stimulated, and does not activate the superficial layers where inhibitory neurons are more concentrated. As additional excitatory neurons are stimulated by INS, the integrated excitatory neural response strengthens the magnitude of the evoked local field potential allowing for detection at lower radiant exposures. The major overall implication of INS of cortical neurons is that neurons can be excited or inhibited. The ability to excite or inhibit neural activity with INS will provide a powerful tool for basic science and future INS based cortical implants.

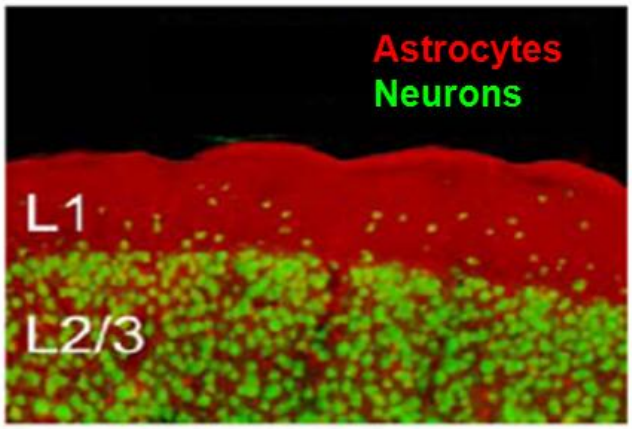

Figure 7.2: Density of astrocytes and neurons in superficial layers of somatosensory cortex. Tissue stained red (anti-S100β) indicates location of astrocytes and tissue stained green (NeuN) identifies location of neurons (modified from [6]).

7.1.2.2 Astrocytes and cortical hemodynamics

In Chapter IV, INS was found to evoke a robust OIS response while inhibiting spontaneous neural activity, an interesting finding considering hemodynamic responses are typically associated with excitatory neural activity. While the OIS could be influenced by direct activation of inhibitory neural pathways, the magnitude of the OIS was unlikely to be fully explained through INS of inhibitory neurons. This disconnect between the evoked OIS and observed inhibition during INS led to the theory that INS modulated astrocyte signaling which in turn drove the hemodynamic changes observed in Chapter IV. This hypothesis is supported by the relatively high concentration of astrocytes in the superficial layers of cortex. Figure 7.2 displays a section of rat somatosensory cortex that emphasizes the high density of astrocytes (red, stained with SB-101) compared to neurons (green, stained with NeuN) in cortical layers I-III [6]. The high densities of astrocytes in these cortical layers indicate that these cells are primary absorbers of infrared light during surface cortical stimulation.

Imaging of calcium dynamics (Chapter V) in rat somatosensory cortex allowed for the effects of INS on astrocyte signaling to be identified. In these studies, INS was found to evoke a slow propagating calcium wave that was heavily influenced by astrocyte calcium signaling. This finding implies that astrocyte activation by INS was a primary component in generating cortical hemodynamic changes responsible for the OISs discussed in Chapter IV. Interestingly, the calcium signals evoked by INS were also related to glutametergic neural activity, and INS was found to evoke and modulate visual OISs within functionally relevant modules in non-human primate cortex (Chapter VI) indicating that neurons also played a role in generating OIS evoked by INS. These observations led to the conclusion that both astrocytes and neurons play an active role in generating INS evoked hemodynamic changes and identify the importance of furthering our understanding of neuron-astrocyte coupling moving forward with future applications of INS in the brain.

7.1.3 Conclusion

Prior to this dissertation and the work contained within, pulsed infrared light had not been demonstrated as a neurostimulation modality in the central nervous system. This dissertation effectively establishes INS as a neurostimulation modality for cortical stimulation in the brain as pulsed infrared light was found to evoke neural potentials both *in vitro* and *in vivo*; however, a number of additional interesting observations were made that highlight the complexity of infrared evoked cortical activity. Infrared neural stimulation was demonstrated to inhibit neural activity for the first time, and astrocyte sensitivity to pulsed infrared light was characterized indicating that INS can be used

modulate cellular signaling in non-excitable cells. These observations motivate the need for further mechanistic studies to untangle how infrared light modulates both neural and glial signaling. Furthermore, INS was demonstrated to excite cortical neurons and modulate functionally relevant signals in non-human primates advancing the technique towards clinical implementation. Overall, this dissertation provides the necessary foundation and motivation needed for future experiments aimed at advancing the development of INS as a neurostimulation modality in central nervous system applications.

7.2 Future Directions

7.2.1 Complete characterization of INS mechanisms and their interactions

In this work, pulsed infrared light was shown to evoke/modulate neural signals and astrocyte signaling, identifying the importance of understanding the underlying cellular mechanisms responsible for INS evoked signals. Infrared neural stimulation was demonstrated to excite (Chapter III and VI) and inhibit (Chapter IV) cortical neurons, and was shown to evoke calcium transients in cortex that was heavily influenced by astrocyte calcium signals (Chapter V). Furthermore, a separate *in vitro* study by colleagues demonstrated that infrared light could be used to modulate GABA currents in plated cortical neurons [7]. These diverse responses observed during the development of INS as a neurostimulation modality for cortical applications indicate multiple cellular mechanisms respond to pulsed infrared light irradiation. Identification and understanding of how these cellular mechanisms interact are of the upmost importance in terms of further development of INS for CNS applications.

To date, three distinct mechanisms have been identified that explain how thermal gradients induced by infrared light effect neural signaling, each acting on a separate component for action potential generation. Shapiro et al. showed pulsed infrared light induced transient changes in membrane capacitance in non-excitable cells and demonstrated this concept through modeling of the Gouy-Chapman-Stern (GCS) theory of double layer capacitance where thermal forces affect the distribution of ions near the cell membrane. Modeling of GCS also predicted action potential generation and was confirmed in transfected oocytes expressing voltage sensitive ion channels [8]. Recent

experiments in vestibular and retinal ganglian cells demonstrated that INS evoked neural signals were generated through activation of heat sensitive TRPV IV channels [9]. This study was the first to directly relate INS evoked neural activity to a specific transmembrane ion channel. A third study indicated that thermal gradients can be used to inhibit neural propagation through modulating the heat sensitive component of the gating mechanisms for sodium and potassium channels in the Hodgkin and Huxley model [10, 11], and was recently confirmed in both the *Aplysia* buccal nerves and the rat sciatic nerve [12]. Each of these mechanisms were discovered independently of the other mechanisms and do not consider the effects of other mechanisms that may be involved. Additionally, only the capacitance gradient mechanism can be universally applied to all tissues stimulated by infrared light. Heat sensitive TRPV channels are not expressed in all tissue, and the heat block mechanisms of neural conduction are based on inhibition in the axonal component of a neuron only and do not consider thermal effects at the soma, dendrites, or synapses. This diverse set of confirmed cellular mechanisms for INS evoked neural activity highlight the complexity by which thermal gradients are transduced into action potentials. Further characterization of INS mechanisms are needed to efficiently design future experiments for perturbing neural signaling in the CNS.

To fully elucidate the mechanisms of INS, experiments must be performed on cultured cells and simplified nervous systems to isolate individual cellular mechanisms of INS evoked activity. Cellular pharmacology and electrophysiology techniques can be used to isolate individual currents or transients in cultured neurons or astrocytes [7, 13]. Additionally, microfluidic devices have been developed to isolate axons or to study neuron astrocyte interactions [14, 15]. These techniques can identify how infrared light

modulates individual cellular currents and can be used to identify possible interactions between neurons and astrocytes during INS. Models that simplify the nervous system should also be incorporated in future studies on understanding the mechanisms of INS. The *Aplysia californica* buccal ganglion represents an example of a complete nervous system that can be maintained in a petri dish. Each individual neuron located in the buccal ganglion is well characterized for function, certain somas are approximately 200 μm in diameter, and the buccal nerves extended from the ganglion offer an ideal location to monitor evoked potentials [16]. Complete understanding of evoked potentials in buccal ganglion will assist in understanding how INS evokes or modulates neural activity and how this INS evoked activity compares to electrical stimulation. The large size of the soma in the ganglion will allow single cell targeting of infrared light to one neuron cell body, allowing for the characterization of effects of infrared irradiation directly at the cell body. Monitoring at the buccal nerves will allow the direct assessment of INS evoked potential as they travel through the buccal ganglion neural network. These highlighted advantages of neurophysiology studies in *Aplysia* buccal ganglion model will allow for assessment of INS mechanisms with single cell resolution while maintaining a neural network. Combining brain slice studies with two-photon imaging will allow cellular resolution of INS evoked activity. The brain slice model translates deep cortical neurons to near surface locations while also maintaining native circuitry with other structures located in the slice [17]. This *in vitro* model will also allow the assessment of astrocyte function during INS and can increase our understanding of neuro-astrocyte coupling. Two-photon imaging of brain slices can resolve cellular processes at the synapse and allow for assessment of effects due to INS on synaptic transmission (i.e. glutamate,

GABA, or calcium signaling) of evoked potentials. The proposed experiments outlined here will identify what cellular signaling components are modulated by the thermal gradients induced by INS; however, understanding the interplay of these mechanisms may prove difficult. Computational modeling may offer a potential solution for incorporating individual mechanisms identified for INS.

Computational modeling has already proved invaluable in identifying the capacitance and "heat block" mechanisms associated with INS [8, 10]. Extensive development of computational modeling of neuronal circuits has been accomplished in NEURON, an open source community driven platform for neural signaling modeling[18]. This platform has been used to model neural signals ranging from single neurons up to complex neural networks [19-21]. These models are open source and modular indicating significant further development is only needed to incorporate the thermal gradients evoked by INS and identified thermal based mechanisms into the NEURON environment. Simple modeling of individual neurons would improve our understanding of how temperature gradients modulate membrane currents at different cellular locations and possibly identify where INS should be targeted in cortical tissue. An example would be modeling of INS targeted at apical dendrites of a neuron in layers I and II versus INS targeted at the soma of the neuron located in layer IV or V. This model based study could identify where INS inhibits or excites neural activity. Further development of finite element models of INS in cortical tissue could provide an overview of expected signals in cortex. Modeling will also help to identify safe and effective laser parameters for stimulating cortical tissue and improve the efficacy of the technique in animal and clinical studies. Cellular and *in vitro* based INS studies combined with modeling of INS

evoked neural activity will ultimately improve our understanding of INS mechanisms and aid in identifying future applications of the technique for stimulating CNS structures.

7.2.2 Subcortical INS in the brain

The *in vivo* studies discussed in this dissertation were limited to stimulating the cortex surface and did not investigate INS of subcortical structures in the brain. The penetration depths of the light used in these studies were limited to 300 – 600 μm in depth biasing stimulation to the most superficial layers of cortex (layers I and II) where astrocytes and apical dendrites are mainly located; therefore, effects of INS on cortical neuron somas is not well characterized. However, evaluation of INS in thalamocortical brain slices demonstrated that pulsed infrared light can be used to evoke neural potentials in cortical neurons (Chapter III) motivating further studies investigating the utility of INS for stimulating subcortical structures in the brain.

Initial subcortical experiments should focus on characterizing INS signal modulation based on placing the fiber tip at specific depths corresponding to the cortical layers outlined in Chapter II. Placing the fiber at depths where cortical neuron somas are located will increase the likelihood of evoking excitatory activity and could identify specific neurons that are sensitive to pulsed infrared light. These experiments should also employ the optical detection techniques used during this dissertation to compare subsurface INS evoked optical signals to those evoked by surface stimulation of cortex with infrared light. This comparison will allow for further characterization of cellular sources of INS evoked signals.

Infrared neural stimulation should also be targeted towards stimulation of specific thalamus nuclei in an effort to assess the feasibility of INS as a neurostimulation modality for deep brain stimulation (DBS) applications. Electrical based DBS has been effective at treating movement disorders, such as Parkinson's disease [22] and essential tremor [23], pain [24], and epilepsy[25]; however, these techniques can induce adverse side effects due to the inherent electrical field spread associated with electrical stimulation [26-28]. Stimulation of these deep brain structures with INS could prove direct clinical utility if appropriate stimulation can be achieved with infrared light to provide therapeutic benefit achieved by traditional electrical DBS without disabling side effects. Several studies using optogenetics have identified critical neurocircuitry for specific DBS based applications such as Parkinson's disease and epilepsy and can be used to design future INS based experiments [29, 30]. Successful demonstration of INS based DBS in animals that improve upon electrical standards would dramatically increase the clinical utility of this technique as INS relies on endogenous mechanisms to activate neural tissue.

7.2.3 Behavioral Studies

Infrared neural stimulation was shown to evoke and modulate functionally relevant responses in the NHP (Chapter VI). The results discussed in Chapter VI and Appendix B suggest that INS may be used to modulate behavior in alert animals performing a specified task. Changing the behavior of an animal indicates perception of INS and will be useful in determining the functional effects of INS in the awake state. Feasibility of INS evoked perception was recently demonstrated in a fixating NHP (discussed in Appendix B) and further support these proposed studies [5]. Understanding

how INS evoked neural activity is perceived will be important for future clinical development of brain machine interfaces (i.e. visual prosthesis) incorporating INS techniques.

7.2.4 Infrared neural stimulation of the spinal cord

Pulsed infrared light has been documented as widely successful for activating bundles of axons throughout the peripheral nervous system; however, INS has not been attempted in the spinal cord where sensory and motor information are transferred to and from the brain in well characterized spinal tracts consisting of bundled axons. The dorsal columns of the spinal cord represent the most accessible target for INS. These columns are located on the dorsal surface of the spinal cord and can be stimulated with INS without the need to penetrate tissue maintaining minimal invasiveness of the technique. The tract organization of the spinal cord also allows for stimulating electrodes to be placed directly in the path of propagating action potentials, a major advantage over the complex neural networks present in the brain. Activation of the dorsal columns by INS would allow for evoked potentials to be tracked up to somatosensory cortex and cerebellum, potentially indicating types of sensory information encoded by INS. Additionally, INS could be used to inhibit propagation of pain in the spinal cord as has been demonstrated using electrical stimulation methods [31]. Once stimulation has been established in the dorsal columns of the spinal cord, the stimulating fiber optic can be placed within the spinal cord to target deep structures to stimulate motor pathways and other sensory tracts to fully characterize INS in the spinal cord. Successful application of

INS in the spinal cord would motivate development of INS based neural implants for spinal cord stimulation.

7.2.5 Application of hybrid techniques for CNS applications

Hybrid stimulation takes advantage of the robustness of electrical stimulation techniques while preserving the high spatial precision of INS, and was recently characterized for stimulating peripheral nerves [12]. These techniques were shown to decrease required radiant exposures of infrared light by up to 60% improving the safety ratio identified for peripheral nerve stimulation from 2:1 to 6:1. This dramatic improvement in safety ratio combined with the preserved spatially precise stimulation would prove beneficial for CNS applications. Implementation of hybrid techniques for surface cortical stimulation would not only reduce required radiant exposures but could also help elucidate the complicated INS evoked signals characterized in this dissertation as targeted hybrid stimulation would be expected to increase excitability of neural processes exposed to the electric field. Application of hybrid techniques toward DBS applications could employ sub-therapeutic electrical currents combined with minimal optical irradiation to better localize therapeutic effects of DBS while also minimizing adverse side effects associated with electrical based DBS. Hybrid stimulation in the central nervous system should be developed in parallel to further studies characterizing INS for CNS applications.

7.3 Protection of Research Subjects

As this research project focused on developing infrared neural stimulation as a neurostimulation modality for cortical stimulation, animal model research was required. Proper ethical use and treatment of animals in this research was ensured for all experiments comprising. All experiments were conducted in accordance to approved protocols by the Institutional Animal Care and Use Committee (IACUC) and conformed to guidelines of the United States National Institutes of Health. Lab personnel involved in this research completed required training through the American Association for Laboratory Animal Science (AALAS) Learning Library

In a parallel project to this dissertation, efficacy and safety of INS in humans was investigated. All protocols and procedures followed during this clinical trial were approved by the Vanderbilt University Institutional Review Board (IRB#: 050822). Personnel involved in this research completed training provided by the Collaborative Institutional Training Initiative and received proper training for working in the operating room environment. For all patients enrolled in the study, informed consent was obtained from the parent or legal guardian of the children that participated in this study.

Appropriate training on general lab safety and standard chemical, biological, and radiation safety was required for all personnel involved in this study in compliance with institutional guidelines.

7.4 Contribution to the Field and Societal Impact

Throughout the course of this dissertation, I have made numerous contributions to my field of research and this project has positively impacted society in a variety of ways. To my knowledge, the research discussed in Chapter III was the first to demonstrate that pulsed infrared light could be used to evoke excitatory neural potentials in cortical neurons. This finding effectively established INS as a neurostimulation modality for applications in the CNS. Infrared neural stimulation in the CNS will improve our overall understanding of neural system functions and signaling by taking advantage of the high spatial precision associated with INS. This study provided the needed feasibility for motivating applicability of INS towards CNS applications and was used to design the *in vivo* studies that comprised this dissertation.

The work presented in Chapter IV demonstrated, for the first time, that INS can inhibit cortical neural activity *in vivo*. Inhibition of neural activity by infrared light could potentially impact both basic science and clinical applications as pulsed infrared light could be used to turn off specific neuro-circuit components. Application towards DBS clinical applications could prove more efficient than traditional electrical methods through inhibition of targeted circuitry.

In addition to identifying the ability of pulsed infrared light to inhibit neural activity, INS was found to evoke IOSs typically associated with cortical hemodynamics; however, the inhibition of neural activity underlying contradicted excitatory neural signals typically associated with hemodynamic signaling. The work discussed in Chapter V discovered that surface cortical stimulation in rodent somatosensory cortex evoked a complex calcium signal that is strongly influenced by astrocyte calcium signals.

Identification of astrocyte sensitivity represents the first report of "non-excitable" cells responding to INS *in vivo* and confirms non-excitable cell sensitivity to infrared light first demonstrated by Shapiro et al. in cultured HEK cells and oocytes [8]. The discovery of astrocyte sensitivity to pulsed infrared light identifies a new methodology for perturbing astrocyte function providing a new tool in furthering our understanding of astrocyte functions in the nervous system potentially impacting our understanding of neural disease processes involving astrocytes such as epilepsy and Alzheimer's disease.

The demonstration that INS can evoke and modulate functionally relevant responses in non-human primates represents a significant step in the development of INS for CNS applications. Chapter VI discusses research that demonstrates INS modulates meaningful OISs that are correlated to eye specific ocular dominance columns located in primary visual cortex. In addition to modulating OISI responses, INS was shown to drive excitatory single units confirming the results first observed in the thalamocortical brain slice. These observations together effectively demonstrate feasibility of INS to modulate neural activity in NHP cortex and have motivated additional NHP studies that further support these observations (Appendix B). This demonstration is significant because the NHP model represents the closest model to human cortex and suggests that INS results reported in this dissertation will translate for human applications establishing significant clinical potential of INS for cortical stimulation in humans.

The ultimate goal of a biomedical engineer is to develop clinically applicable technologies that improve current standard of care in specific applications, and this dissertation represents the first steps towards developing INS for clinical applications in the CNS. This dissertation also includes the first report describing INS of human dorsal

root nerves demonstrating both safety and efficacy of the technique in humans (Appendix B). While this report demonstrated efficacy of INS in human nerve tissue typically considered a part of the PNS, the implications of this study indicates that infrared stimulation of human neural tissue is possible providing feasibility for future diagnostic and therapeutic clinical applications. Clinical neurosurgical applications that may benefit from adapting INS for clinical use include improve spatial precision of cortical mapping for tumor resection or cortical ablation for epilepsy, deep brain stimulation applications for treating chronic pain or movement disorders, and INS technology could potentially be incorporated into future cortical implants designed to encode somatosensory or visual information in disabled individuals. Significant research is still needed to realize these potential applications of INS; however implementation of the future directions outlined in this chapter will ensure further the advancement of INS for clinical applications.

7.5 References

[1] Wells, J., Kao, C., Mariappan, K., Albea, J., Jansen, E. D., Konrad, P., and Mahadevan-Jansen, A., "Optical stimulation of neural tissue in vivo," *Opt Lett,* vol. 30, pp. 504-6, 2005.

[2] Wells, J., Kao, C., Jansen, E. D., Konrad, P., and Mahadevan-Jansen, A., "Application of infrared light for in vivo neural stimulation," *J Biomed Opt,* vol. 10, p. 064003, 2005.

[3] Wells, J., Kao, C., Konrad, P., Milner, T., Kim, J., Mahadevan-Jansen, A., and Jansen, E. D., "Biophysical mechanisms of transient optical stimulation of peripheral nerve," *Biophys J,* vol. 93, pp. 2567-80, 2007.

[4] Chen, G., Cayce, J. M., Friedman, R. M., Wang, F., Tang, T., Jansen, E. D., Mahadevan-Jansen, A., Gore, J. C., and Roe, A. W., "Functional tract tracing in non-human primates using pulsed infrared laser light with optical imaging and fMRI," in *Society for Neuroscience*, New Orleans 2012.

[5] Chen, G., Cayce, J. M., Ye, X., Jansen, E. D., Mahadevan-Jansen, A., and Roe, A. W., "Optical control of the visual perception of awake non-human primate with infrared neural stimulation," in *Photonics West BiOS*, San Francisco, CA 2013.

[6] Takata, N. and Hirase, H., "Cortical layer 1 and layer 2/3 astrocytes exhibit distinct calcium dynamics in vivo," *PLoS One,* vol. 3, p. e2525, 2008.

[7] Feng, H.-J., Kao, C., Gallagher, M. J., Jansen, E. D., Mahadevan-Jansen, A., Konrad, P. E., and Macdonald, R. L., "Alteration of GABAergic neurotransmission by pulsed infrared laser stimulation," *Journal of Neuroscience Methods,* vol. 192, pp. 110-114, 2010.

[8] Shapiro, M. G., Homma, K., Villarreal, S., Richter, C.-P., and Bezanilla, F., "Infrared light excites cells by changing their electrical capacitance," *Nat Commun,* vol. 3, p. 736, 2012.

[9] Albert, E. S., Bec, J., Desmadryl, G., Chekroud, K., Travo, C., Gaboyard, S., Bardin, F., Marc, I., Dumas, M., and Lenaers, G., "TRPV4 channels mediate the infrared laser-evoked response in sensory neurons," *Journal of Neurophysiology,* vol. 107, pp. 3227-3234, 2012.

[10] Zongxia, M., Triantis, I. F., Woods, V. M., Toumazou, C., and Nikolic, K., "A Simulation Study of the Combined Thermoelectric Extracellular Stimulation of the Sciatic Nerve of the Xenopus Laevis: The Localized Transient Heat Block," *Biomedical Engineering, IEEE Transactions on,* vol. 59, pp. 1758-1769, 2012.

[11] Hodgkin, A. L. and Huxley, A. F., "The components of membrane conductance in the giant axon of Loligo," *J Physiol,* vol. 116, pp. 473-496, 1952.

[12] Duke, A. R., "Selective Control of Electrical Neural Activation using Infrared Light," Doctor of Philosophy Dissertation, Biomedical Engineering, Vanderbilt University, 2012.

[13] Suadicani, S. O., Cherkas, P. S., Zuckerman, J., Smith, D. N., Spray, D. C., and Hanani, M., "Bidirectional calcium signaling between satellite glial cells and neurons in cultured mouse trigeminal ganglia," *Neuron Glia Biology,* vol. 6, pp. 43-51, 2010.

[14] Park, J., Koito, H., Li, J., and Han, A., "Microfluidic compartmentalized co-culture platform for CNS axon myelination research," *Biomedical microdevices,* vol. 11, pp. 1145-1153, 2009.

[15] Hosmane, S., Yang, I. H., Ruffin, A., Thakor, N., and Venkatesan, A., "Circular compartmentalized microfluidic platform: Study of axon–glia interactions," *Lab on a Chip,* vol. 10, pp. 741-747, 2010.

[16] Susswein, A. and Byrne, J. H., "Identification and characterization of neurons initiating patterned neural activity in the buccal ganglia of Aplysia," *The Journal of Neuroscience,* vol. 8, pp. 2049-2061, 1988.

[17] Agmon, A. and Connors, B. W., "Thalamocortical responses of mouse somatosensory (barrel) cortex in vitro," *Neuroscience,* vol. 41, pp. 365-79, 1991.

[18] Brette, R., Rudolph, M., Carnevale, T., Hines, M., Beeman, D., Bower, J. M., Diesmann, M., Morrison, A., Goodman, P. H., and Harris, F. C., "Simulation of networks of spiking neurons: a review of tools and strategies," *Journal of computational neuroscience,* vol. 23, pp. 349-398, 2007.

[19] Fellous, J. M., Rudolph, M., Destexhe, A., and Sejnowski, T. J., "Synaptic background noise controls the input/output characteristics of single cells in an in vitro model of in vivo activity," *Neuroscience,* vol. 122, p. 811, 2003.

[20] Anderson, J., Binzegger, T., Kahana, O., Martin, K., and Segev, I., "Dendritic asymmetry cannot account for directional responses of neurons in visual cortex," *Nature neuroscience,* vol. 2, pp. 820-824, 1999.

[21] Chono, K., Takagi, H., Koyma, S., Suzuki, H., and Ito, E., "A cell model study of calcium influx mechanism regulated by calcium-dependent potassium channels in

Purkinje cell dendrites," *Journal of Neuroscience Methods*, vol. 129, pp. 115-127, 2003.

[22] Kahn, E., D'Haese, P.-F., Dawant, B., Allen, L., Kao, C., Charles, P. D., and Konrad, P., "Deep brain stimulation in early stage Parkinson's disease: operative experience from a prospective randomised clinical trial," *Journal of Neurology, Neurosurgery & Psychiatry*, 2011.

[23] Kitagawa, M., Murata, J., Kikuchi, S., Sawamura, Y., Saito, H., Sasaki, H., and Tashiro, K., "Deep brain stimulation of subthalamic area for severe proximal tremor," *Neurology*, vol. 55, pp. 114-6, 2000.

[24] Tasker, R. R. and Vilela Filho, O., "Deep brain stimulation for neuropathic pain," *Stereotact Funct Neurosurg*, vol. 65, pp. 122-4, 1995.

[25] Pollo, C., Villemure, J.-G., Sakas, D. E., and Simpson, B. A., "Rationale, mechanisms of efficacy, anatomical targets and future prospects of electrical deep brain stimulation for epilepsy," in *Operative Neuromodulation*. vol. 97/2, ed: Springer Vienna, 2007, pp. 311-320.

[26] Tommasi, G., Krack, P., Fraix, V., Le Bas, J. F., Chabardes, S., Benabid, A. L., and Pollak, P., "Pyramidal tract side effects induced by deep brain stimulation of the subthalamic nucleus," *Journal of Neurology, Neurosurgery & Psychiatry*, vol. 79, pp. 813-819, 2008.

[27] Nada, Y. and Xuguang, L., "Modeling the current distribution across the depth electrode?brain interface in deep brain stimulation," *Expert Review of Medical Devices*, vol. 4, p. 623, 2007.

[28] Constantoyannis, C., Kumar, A., Stoessl, A. J., and Honey, C. R., "Tremor induced by thalamic deep brain stimulation in patients with complex regional facial pain," *Mov Disord*, vol. 19, pp. 933-6, 2004.

[29] Gradinaru, V., Mogri, M., Thompson, K. R., Henderson, J. M., and Deisseroth, K., "Optical deconstruction of parkinsonian neural circuitry," *Science*, vol. 324, pp. 354-359, 2009.

[30] Kokaia, M. and Ledri, M., "An optogenetic approach in epilepsy," *Neuropharmacology*, 2012.

[31] Martin, R., Sadowsky, C., Obst, K., Meyer, B., and McDonald, J., "Functional Electrical Stimulation in Spinal Cord Injury: From Theory to Practice," *Topics in Spinal Cord Injury Rehabilitation*, vol. 18, pp. 28-33, 2012.

APPENDIX A

CHARACTERIZATION OF SPATIAL EXTENT AND PARAMETRIC SPACE OF INS EVOKED CALCIUM SIGNALS

A.1 Abstract

The following data was included as supplemental information for chapter V that investigated the cellular mechanisms responsible for generating calcium signal in response to pulsed infrared light. This data describes the spatial extent of INS evoked calcium signals, and characterizes the laser parametric space for evoking calcium transients.

A.2 Motivation

One of the major advantages of INS is the high spatial precision of stimulation and has been demonstrated in all applications which have used pulsed infrared light to excite neural tissue [1-6]. Characterization of spatial extent for INS evoked calcium signals is important to continue to highlight this advantage associated with INS. Additionally, demonstrating that calcium signals evoked by INS are similar in spatial extent to INS evoked optical intrinsic signals (OIS) under 632 illumination provides support to compare these signals and help to identify possible cellular mechanisms common between each signal type [3].

Understanding how the laser parametric space effects INS evoked cortical signaling is important in developing this technique for evoking calcium signals *in vivo*. A well characterized set of laser parameters will provide an appropriate starting point for

other researchers who may wish to further investigate cortical calcium signaling modulation using pulsed infrared light in future studies. The results in this appendix that characterize the effects of radiant exposure, repetition rate, pulse width, and pulse train length provide an appropriate range of parameters for evoking calcium transients with INS *in vivo*.

A.3 Methods

All data described here followed the methods outlined in Chapter V of this dissertation with the following modifications. To analyze the spatial extent of the evoked calcium signal, a 3X3 ROI was translated in the anterior/posterior and medial/lateral directions away from the center of activation (identified as region with peak signal) to calculate the timecourse of calcium signals as a function of distance. Peak signal was plotted as a function of distance to understand the spatial extent of INS evoked calciums signals.

Effects of radiant exposure (RE), repetition rate (RR), pulse width (PW), and pulse train length (PTL) were determined on INS evoked calcium signals. For each tested parameter, only the experimental parameter was varied for each animal. All other laser parameters were kept constant using the following parameters: λ=1.875 μm, PW= 250 μs, RR= 200 Hz, and PTL= 500 ms. Radiant exposure varied between animals in a range between 0.42 – 0.65 J/cm^2 due to small changes in fiber throughput from experiment to experiment, but radiant exposure was kept constant for each stimulation condition tested in individual animals. In order to account for variation in radiant exposure and other

experimental variables, peak fluorescence was normalized for each experiment to allow data across animals to be compared.

A.4 Results and Discussion

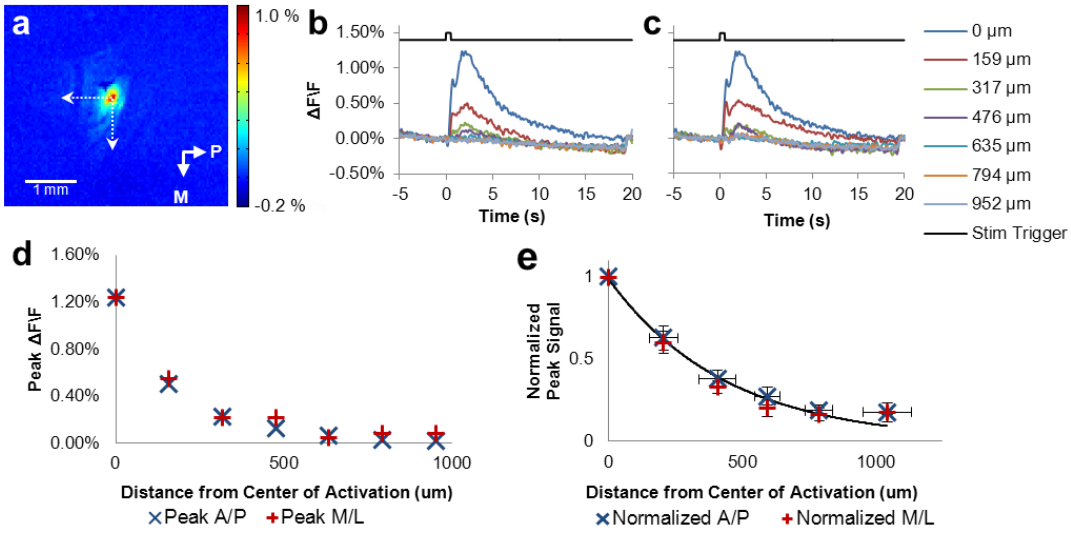

Figure A.1: Calcium signal decays exponentially from center of activation in response to infrared stimulation. (A) Activation map of INS evoked calcium signal. Arrows indicate direction of ROI translation using 3X3 pixel box spaced 2 pixels apart in medial and anterior directions (B&C.) Smoothed timecourse signals for each positional ROI in the medial and anterior directions of calcium signal respectively. (D) Peak change in fluorescence for each ROI as a function of distance from the center of activation for data displayed in B&C. Laser parameters: λ: 1.875 um, RR: 200 Hz, PW: 250 us, PTL: 500 ms, RE: 0.66 J/cm2. (E) Normalized peak signal as a function of distance for all animals (n = 12). Signal decays to 1/e point at 435±67 µm. Error bars are ±s.e.m.

A.4.1 Spatial extent of INS-evoked calcium signals.

The spatial components of the INS-evoked calcium signal were characterized in 12 animals. A 3x3 pixel ROI was translated from the center of response across cortex in the anterior/posterior and medial/lateral directions to determine how INS-evoked calcium response signal strength varied with distance from stimulus location. In each experiment,

the calcium signal decays exponentially as a function of distance from the stimulus location (Figure A.1 A-D). In order to compare data between experiments, fluorescence signal was normalized to the signal at the stimulus location to account for signal variability. ROI distances from the stimulus location were binned to account for spatial variability between experiments (Figure A.1 E). This analysis allowed the spatial extent of the INS induced calcium signal to be estimated by fitting the data to an exponential curve and calculating the radius of effect to be 435±67 μm. This indicates only a 235 μm spread of signal outside the beam radius (200 μm), and an area of activated cortex of 0.594±0.013 mm^2. The small spatial extent of the INS evoked calcium signal is consistent with high spatial precision reported in previous INS studies[1-6], and is similar to the spatial extent of calcium signals evoked by stimulation of the hindpaw (d = 1 mm)[7].

A.4.2 Parametric evaluation for INS-evoked calcium signals

In order to fully characterize the INS-evoked calcium response, the relationship between INS parameters and evoked calcium transients in cortex must be understood. Radiant exposure was characterized for radiant exposures between 0.1-0.88 J/cm^2 (n=9) where the normalized peak calcium signal increases linearly with increasing radiant exposure (Figure A.2A). Repetition rates, between 50 and 200 Hz (n=6), displayed an exponential increase in fluorescence with increasing repetition rate (Figure A.2B). These trends were expected as increasing radiant exposure and repetition rate represent stronger stimulus conditions that elicit a stronger response. Pulse widths between 200 and 450 μs (n=6) showed no significant change in peak fluorescence signal which is consistent with observations made in peripheral nerve stimulation (Figure A.2C) [8]. Peak fluorescence

signal increased linearly for stimulation durations (n=5) between 0.2 – 2.0 seconds; however, no significant change was observed between 2.0 – 3 seconds suggesting the cellular mechanisms responsible for inward calcium transients were maximized(Figure A.2D). Characterization of these parameters demonstrates the dependency of the INS evoked calcium signal on radiant exposure, repetition rate, and stimulation duration. Additionally, the parametric set characterized here provides a reliable set of laser settings for evoking infrared calcium transients in cortex.

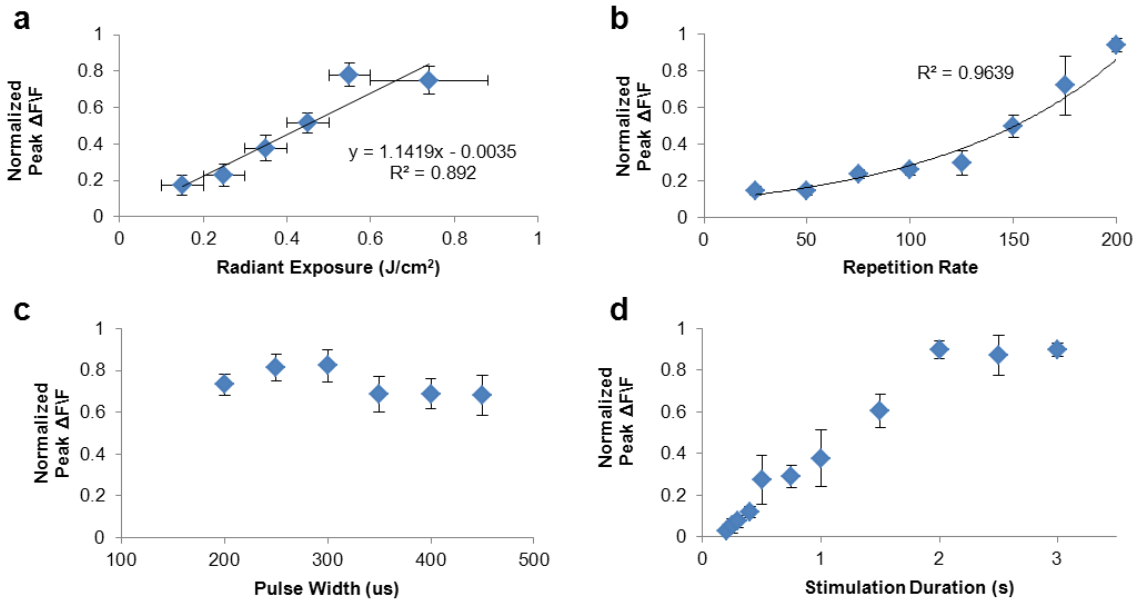

Figure A.2: Effects of laser parametric variation on INS evoked calcium signal. A.) Increasing radiant exposure increases the calcium signal magnitude linearly between 0.1 – 0.88 J/cm^2 (n=9). Data normalized for each animal and binned for radiant exposure. Laser parameters: λ=1.875 µm, pulse width= 250 µm, Repetition Rate = 200 Hz, and Stimulation Duration = 500 ms B.) Calcium signal magnitude increases exponentially with increasing repetition rate from 50 hz to 200 hz (n=6). Radiant exposure held constant for each animal at each repetition rate. Laser parameters: λ=1.875 µm, Radiant exposure=0.5 – 0.65 J/cm^2, pulse width= 250 µm, and Stimulation Duration = 500 ms C.) No statistical significant change was observed for laser pulse width. Radiant exposure was held constant for each pulse width in a given animal (n=6). Data normalized for each animal to account for differences in laser parameters between experiments. Laser parameters: λ=1.875 µm, Radiant exposure=0.42 – 0.63 J/cm^2, repetition rate=100 or 200 Hz, and Stimulation Duration = 500-2000 ms. D.) Calcium signal magnitude increased linearly with increasing stimulation duration from 200 ms to 2000 ms. From 2000 ms to 3000 ms, no change in signal magnitude was observed (n = 5). Data normalized for each animal to account for differences in laser parameters between experiments. Peak signal represents the peak of the signal between 1 and 5 seconds after stimulation ends. Laser parameters: λ=1.875 µm, Radiant exposure=0.5 – 0.65 J/cm^2, pulse width= 250 µm, and repetition rate=200 Hz.

A.5 References

[1] Wells, J., Konrad, P., Kao, C., Jansen, E. D., and Mahadevan-Jansen, A., "Pulsed laser versus electrical energy for peripheral nerve stimulation," *J Neurosci Methods*, vol. 163, pp. 326-37, 2007.

[2] Cayce, J. M., Kao, C. C., Malphrus, J. D., Konrad, P. E., Mahadevan-Jansen, A., and Jansen, E. D., "Infrared Neural Stimulation of Thalamocortical Brain Slices," *Selected Topics in Quantum Electronics, IEEE Journal of*, vol. 16, pp. 565-572, 2010.

[3] Cayce, J. M., Friedman, R., Jansen, E. D., Mahadevan-Jansen, A., and Roe, A. W., "Pulsed infrared light alters neural activity in rat somatosensory cortex in vivo," *Neuroimage*, vol. 57, pp. 155-166, 2011.

[4] Fried, N. M., Lagoda, G. A., Scott, N. J., Su, L.-M., and Burnett, A. L., "Noncontact Stimulation of the Cavernous Nerves in the Rat Prostate Using a Tunable-Wavelength Thulium Fiber Laser," *Journal of Endourology*, vol. 22, pp. 409-414, 2008.

[5] Izzo, A. D., Richter, C.-P., Jansen, E. D., and Walsh, J. T., Jr., "Laser stimulation of the auditory nerve," *Lasers in Surgery and Medicine*, vol. 38, pp. 745-753, 2006.

[6] Jenkins, M. W., Duke, A. R., GuS, DoughmanY, Chiel, H. J., FujiokaH, WatanabeM, Jansen, E. D., and Rollins, A. M., "Optical pacing of the embryonic heart," *Nat Photon*, vol. 4, pp. 623-626, 2010.

[7] Bouchard, M. B., Chen, B. R., Burgess, S. A., and Hillman, E. M. C., "Ultra-fast multispectral optical imaging of cortical oxygenation, blood flow, and intracellular calcium dynamics," *Opt. Express*, vol. 17, pp. 15670-15678, 2009.

[8] Wells, J., Kao, C., Konrad, P., Milner, T., Kim, J., Mahadevan-Jansen, A., and Jansen, E. D., "Biophysical mechanisms of transient optical stimulation of peripheral nerve," *Biophys J*, vol. 93, pp. 2567-80, 2007.

APPENDIX B

PRELIMINARY RESULTS IN NON-HUMAN PRIMATES: FUNCTIONAL MAGNETIC IMAGING AND BEHAVIORAL RESPONSES TO INS

FUNCTIONAL TRACT TRACING IN NON-HUMAN PRIMATES USING PULSED INFRARED LASER LIGHT WITH FMRI

Gang Chen[1], Jonathan M Cayce[2], Robert M Friedman[3], Feng Wang[1], Chaohui Tang[1], E. Duco Jansen[1,2,4], Anita Mahadevan-Jansen[1,2,4], John C. Gore[1,2,4], and Anna W Roe[1,2,3]

OPTICAL CONTROL OF THE VISUAL PERCEPTION OF AWAKE NON-HUMAN PRIMATE WITH INS

Gang Chen[1], Jonathan M Cayce[2], Xiang Ye[3], E. Duco Jansen[1,2,4], Anita Mahadevan-Jansen[1,2,4], and Anna W Roe[1,2,3]

[1] Institute of Imaging Sciences, Vanderbilt University, Nashville, TN

[2] Department of Biomedical Engineering, Vanderbilt University, Nashville, TN

[3] Department of Psychology, Vanderbilt University, Nashville, TN

[4] Department of Neurological Surgery, Vanderbilt University, Nashville, TN

This appendix discusses two separate studies. I am second author on each study and assisted in collecting all data. A manuscript is in preparation for *Nature Neuroscience* to discuss the fMRI studies. The behavioral results will be presented at *Photonics West* 2013.

B.1 Abstract

The study described in Chapter VI demonstrated feasibility of INS in non-human primate (NHP) for evoking functional relevant responses. These results directly motivated new studies in NHPs to further the development of INS as a neurostimulation modality. The first study investigated INS to evoke functionally relevant cerebral blood volume (CBV) signal in functional magnetic resonance imaging (fMRI) by stimulating Squirrel monkey somatosensory cortex. Infrared neural stimulation was found to not only evoke robust CBV signals at the stimulation site but also in projection areas within primary somatosensory cortex. A second study was designed to determine if INS could evoke behavioral responses in awake Macaque monkeys. In this study, INS was applied in V4 cortex in an animal trained to perform a fixation task. When INS was applied after reward for fixation, the animal would saccade to the location on the visual stimulation monitor that corresponded to the retinotopic location stimulated by INS. No saccade movement was made in the absence of INS. These results infer that INS induced visual percepts that affected the animal's behavior. Together, these studies provide additional evidence that infrared neural stimulation is an effective neurostimulation modality for surface cortical stimulation in NHPs.

B.2 Motivation

The final aim of this dissertation was to establish feasibility of INS in non-human primate (NHP) models. Chapter VI demonstrated that INS evoked optical intrinsic signals (OIS) in primary visual cortex that could be related to functional modules responsible for visual processing. Infrared neural stimulation was also shown to evoke excitatory neural

activity through single unit recordings as well as modulate OIS evoked by visual stimulation. These findings effectively demonstrate that INS of NHP visual cortex evokes functionally relevant responses. The results described in Chapter VI motivated additional NHP studies to investigate the utility of INS in functional magnetic resonance imaging (fMRI) and to determine if INS can modulate the behavior in awake animals performing a specific task. The addition of these preliminary results provides further support that INS is an effective neurostimulation modality for use in NHPs.

One of the major potential advantages of INS typically overlooked is the fact that the technique is inherently MR compatible as the fiber optic used to deliver INS is composed of fused silica which is magnetically inert. Additionally, light can be transmitted through a fiber optical over theoretical infinite distances due to internal reflection allowing the laser to be located outside the room containing the magnet. Prior to this study, INS had not been attempted during fMRI procedures providing motivation to attempt these experiments; therefore, the efficacy of INS compatibility with fMRI was assessed in Squirrel monkey primary somatosensory cortex. In these experiments, the primary objectives were to demonstrate that INS evokes functionally relevant changes in CBV signals and to determine if INS was capable of evoking CBV signal in distal somatosensory areas. Achieving these two objectives provides additional evidence that INS evokes meaningful neural signals and that INS can be used for functional tract tracing through cortical stimulation with fMRI.

With the successful demonstration of INS in NHP described in Chapter VI, the next logical experiment was to assess if an awake behaving primate could perceive cortical INS. The objective for this study was to show that the animal perceived INS

through a consistent behavioral response for each episode of INS. These experiments were conducted in a behaving Macaque monkey, trained to fixate on a screen, that had an optical imaging chamber implanted over V2 and V4 cortex. Infrared neural stimulation was applied in the implanted chamber and the eye position of the animal was tracked to detect saccades in response to INS. Demonstrating that the animal perceives stimulation not only further supports the claims made in Chapter VI but also provides feasibility for further more complex behavioral studies aimed at understanding how INS affects animal behavior and will aid in determining the extent and nature of INS evoked neural activity.

B.3 Methods

All procedures were performed in accordance with protocols approved by the Vanderbilt University Institute for Animal Care and Use Committee and conformed to the guidelines of the US National Institutes of Health.

B.3.1 fMRI methods

Two Squirrel monkeys were initially anesthetized and implanted with an optical imaging chamber and Tecoflex artificial dura over somatosensory cortex following methods outlined in Chapter VI to provide access to cortex during fMRI experiments.

For all fMRI experiments, the methods used for animal preparation, tactile stimulation, and imaging protocols are explained in detail by Chen et al and Zhang et al. [1, 2]. Briefly, animals were initially anesthetized with ketamine hydrochloride (10 mg/kg)/atropine (0.05 mg/kg) and maintained with isoflurane anesthesia delivered in 70/30 O_2/NO_2 mixture. Animals were intubated and artificially ventilated and vital signs

(end-tidal CO_2, oximetry, body temperature, and heart rate) were externally monitored for the duration of the experiment. Once the subject was prepared for the procedure, the animal was placed in a custom stereotactic frame designed to fit in the bore of the magnet.

Functional imaging experiments were performed in a 9.4 T 21 cm narrow-bore Varian Inova magnet (Varian Medical System, Palo Alto, CA) with a 3 cm surface coil to collect MR signals. Initial scout images were collected using a fast gradient-echo sequence to define the volume covering somatosensory cortex and to optimize static magnetic field homogeneity. These images were also used to plan the oblique slices for structural and functional imaging. $T2^*$-weighted gradient-echo structural images were acquired to identify blood vessel structures and somatosensory cortex. These images were also used co-register functional data. Prior to functional imaging, the animal received an injection of MION (8-10 mg/kg) to increase contrast for detection of cerebral blood volume changes. Functional images were acquired with a gradient echo-planar image sequence (echo time 10 ms, 128 x 128 image matrix, 273 x 273 x 2000 μm resolution). The repetition time between scans was adjusted to match the respiration rate to minimize physiological noise in functional timecourses.

Functional data processing was performed in custom software designed for Matlab (Mathworks, Natick, MA) that smoothed and interpolated the data onto anatomic images. The timecourses of the signal was drift corrected using a linear model fitted to each timecourse and temporally smoothed with low-pass filtering. The correlation of each functional timecourse was calculated to a reference waveform and functional maps were generated by identifying regions of clustered voxels with statistically significant ($p \leq$

10E-5) correlation to the reference waveform. These activated regions of cortex were overlaid onto corresponding anatomical images.

Initial fMRI experiments were conducted to map the digit locations in somatosensory cortex of each animal to determine where to target INS. Digit mapping was accomplished by stimulating the contralateral digits with three piezoelectric benders (Noliac, Kvistgaard, Denmark) positioned over D2, D3, and D5 at 8 Hz driven by a Grass S48 square wave stimulators (Grass-Telefactor, West Warwick, RI) in a 30 seconds on and 30 seconds off block design that was controlled by the MR scanner.

Once the digit locations were identified in somatosensory areas 3a, 3b, 1, and 2, a custom acrylic chamber insert was designed to target Area 1 in subject 1 and Area 3b in subject 2 with INS through a 400 μm fiber secured within the insert. The insert was placed in the chamber and secured with a plastic ring with silicone oil placed between the artificial dura and the insert. Warm agar was placed on and around the insert to remove air from the chamber reducing susceptibility MR artifacts. Laser stimulation was performed using a 1.875 μm diode laser (Capella neural stimulator, Lockheed Martin Aculight, Bothel, WA) at a repetition rate of 200 Hz, pulse width of 250 μs, pulse train length of 500 ms, and an inter-train interval of 2 seconds. Infrared neural stimulation was performed in the same block format used during vibrotactile stimulation with 30 second of stimulation followed by 30 seconds of no stimulation. In each case, stimulation was initially performed at 0.4 J/cm^2. In the second case, the effects of radiant exposure on functional signal were assessed.

B.3.2 Behavioral methods

Behavioral experiments were conducted in a Macaque monkey implanted with a chronic imaging chamber over V2/V4 and head post following methods outlined in Chapter VI and Chen et al., Roe et al., and Tanigawa et al. [3-5]. The animal was previously trained to sit quietly in an upright primate chair with head secured and fixate on a small central dot (0.15^o X 0.15^o, fixation window radius < 0.75^o) located on a computer screen placed at a distance of 120 cm from the animal [6]. The fixation point was displayed to the animal for a total of 3 seconds. Monkey compliance with correctly performing the task was accomplished through a water regulation regime and water reward system for correctly performed tasks. Eye position was continuously monitored with an infrared eye tracker to assess task performance (500 Hz, Eyelink II, SR Research, Toronto, ON Canada).

The efficacy of INS to effect behavior was tested by stimulating in cortex exposed in the chamber through the overlaid silicon artificial dura. To place the fiber optic, the chronic chamber was opened under sterile conditions and cleaned following previously outlined procedures [3]. A 100 μm fiber was placed onto cortex with a computerized micromanipulator (NAN-S4, Nan Instruments, Israel) mounted on the chamber. As can be seen in figure B.1A, the fiber optical was placed in an area of V4 cortex corresponding to a right eye retinotopic location on the visual stimulation screen. Stimulation was performed at 200 Hz, 250 μs pulse width for 500 ms with a radiant exposure of 0.6 J/cm^2. Once the animal manipulations were completed, an initial 50 trials of visual fixation were presented to the animal to ensure proper behavior. After the initial 50 trials, the animal was presented with interleaved conditions consisting of visual fixation cue only, visual

fixation cue + INS simultaneously and visual fixation cue followed by reward then INS (Figure B.1B). Typically 200-250 trials were successfully collected in one session with the animal. Eye movements detected by the eye tracker were used to determine behavioral responses by measuring the degrees of saccades made by the animal during each trial. Eye movements detected in each stimulation condition were averaged together to determine trends in eye movements throughout the experiment.

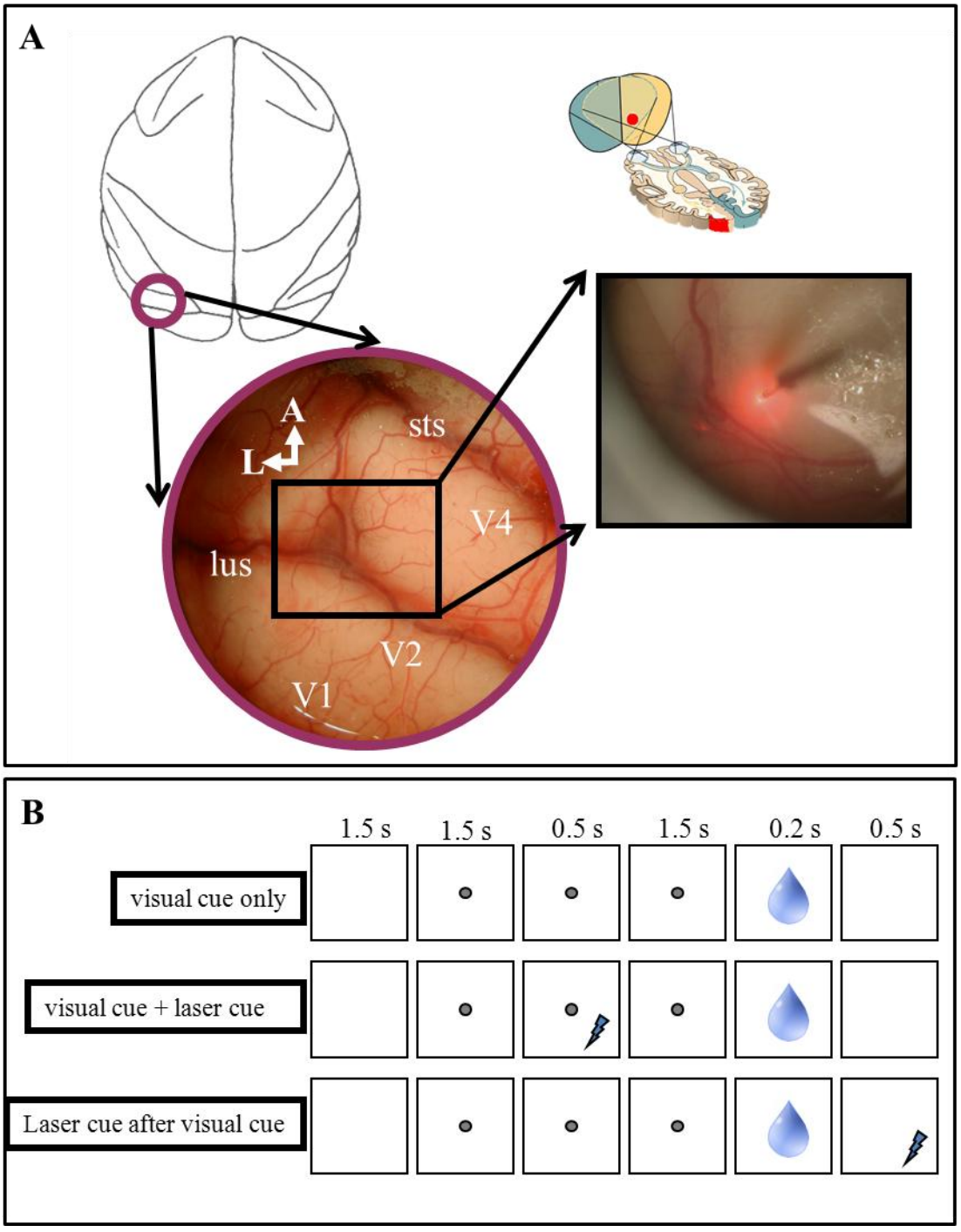

Figure B.1: Methods diagram for behavioral study. (A) Anatomical orientation of cortex exposed by chronic imaging chamber. lus = lunate sulcus, sts = superior temporal sulcus, V1 = primary visual cortex, V2 = area 2 of visual cortex, V4 = area 4 of visual cortex. Black box represents field of view displaying fiber stimulation location in V4 (inset image). Graphic in top right hand corner displays retinotopic location stimulated by INS. (B) Behavioral conditions presented to animal during experiment and timing of fixation dot (dot), INS (bolt), and reward presentation (water drop).

B.4 Results and Discussion

B.4.1 Functional magnetic resonance imaging of INS in NHP somatosensory cortex

Demonstrating compatibility of INS with fMRI methods is an important capability to establish for INS to become an accepted neurostimulation modality. The primary advantages of fMRI methods is the ability to detect functional signal (i.e. CBV or BOLD) over a wide area of cortex with high spatial resolution in a 3-deminsonal volume, and these methods are minimally invasive. Due to these advantages associated with fMRI, this technique is widely applied to study neural activation in the brain ranging from rodents to humans. Additionally, the high spatial resolution and the 3 dimensional volume that is monitored during fMRI allows this imaging method to be used as a functional tract tracing tool and has contributed to our understanding of neural connectivity in the brain [2, 7]. In this study, functional responses evoked by INS were characterized by detecting changes in CBV using fMRI methods in two anesthetized Squirrel monkeys. The purpose of these experiments were to demonstrate that INS evokes functional responses detectable by fMRI and to show that INS evokes cortical signals in distal somatosensory sites from the stimulation location (Figure B.2).

In both cases, INS was applied at 200 Hz (pulse width=250 μs), for 500 ms, with a inter train interval of 2 seconds. A custom acrylic insert was designed to secure the fiber optic in the chamber and allow for targeting stimulation to specific cortical areas with a 400 μm stimulating fiber. Stimulation was performed in a block format where INS was applied for 30 seconds followed by 30 seconds of no stimulation for a minimum of 8 repetitions for a given imaging run.

In subject 1, INS was targeted at Area 1 of somatosensory cortex. Within Area 1, robust widespread CBV signal was detected in response to INS at 0.4 J/cm^2 (Figure B.2A). The CBV signal evoked by INS was detected at depths corresponding to layers 1-5 of cortex, indicating the extent of INS activated signal was at the same level of somas of neuron located in layers 3 – 5 of cortex an approximate depth of 0.5 – 1 mm. This finding is exciting as CBV signal at these depths may indicate direct activation of cortical neurons in response to INS. Additional activation was detected distal to the stimulation site in areas 3b and 2 of somatosensory cortex. This activation corresponded to layers 1 – 3 of cortex and suggests that INS in Area 1 directly activated neural circuits that projected to Area 3b (Figure B.2A, slice 2) and Area 2 (Figure B.2A, slice 2 and 3). These findings support that the CBV signal evoked by INS correspond to intracortical neural activity.

INS was targeted to activate Area 3b of somatosensory cortex with a radiant exposure of 0.4 J/cm^2 in subject 2 (Figure B.2B). Cerebral blood volume changes evoked by INS were more spatially localized in depth in Case 2 (Figure B.2B, slice 1-3)when compared to the results observed in Case 1 (Figure B.2A, slice 1-3); however, the areas distal to the stimulation site that indicated increases in CBV during INS are more distinct when compared to the distal cortical areas activated in Case 1. Here, INS of Area 3b evoked distal CBV changes in Area 3a (slice 1 and 2), and in Area 1 (slice 2). The distance between the distal activation sites and the stimulation site was approximately 2 mm indicating that the observed CBV changes evoked by INS were due to activation of neural signals and not thermally driven changes in blood flow (i.e. vasodilation due to

heat). This is an important finding that supports INS directly evokes neural activity in NHP somatosensory cortex.

Effects of radiant exposure on INS evoked CBV changes were also characterized in subject 2. Functional imaging was performed using five distinct radiant exposures to determine how the CBV magnitude changed with different radiant exposures (Figure B.2C). The percent change in CBV signal was observed to increase with increasing radiant exposure with a linear relationship (Figure B.2D) corresponding with trends identified in previous CNS studies [8, 9].

This study demonstrates that INS is compatible with fMRI methods and can be used to evoke functional magnetic signals related to blood flow in the brain. The depth resolved activation evoked by INS suggests direct focal activation of neuron located in deep cortical layers 3-5. Additionally, INS was observed to evoke functional signals distal from the stimulation site indicating that pulsed infrared light activated intracortical neural networks leading to projection activatoin in other somatosensory cortical areas and identifies the potential of INS as an *in vivo* functional tract tracing tool. Together, these results demonstrate the efficacy of INS to evoke meaningful neural activity in NHP somatosensory cortex, and provide needed feasibility to conduct future awake fMRI studies in behaving animals.

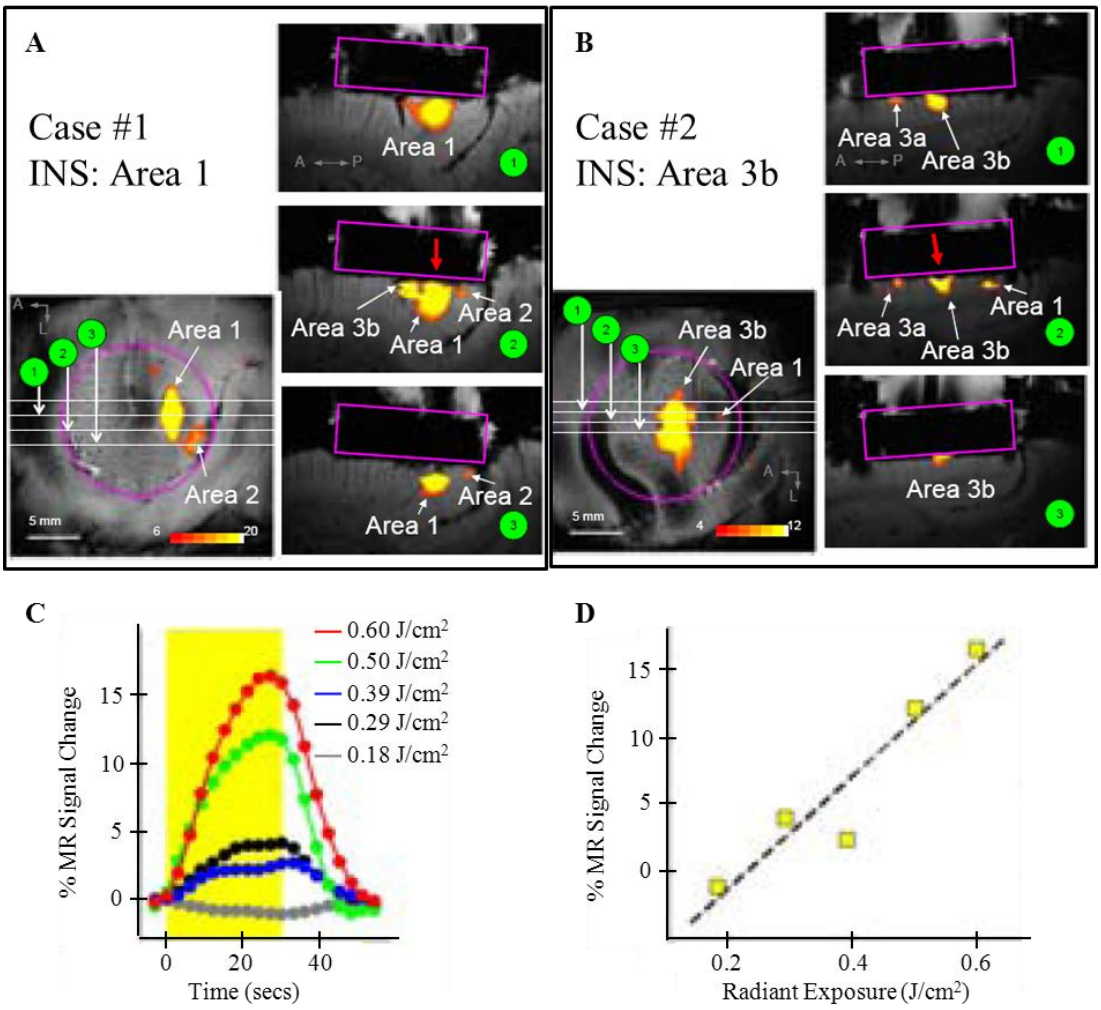

Figure B.2: INS evokes CBV change detected by fMRI in stimulated area of cortex and projected somatosensory areas.(A) INS (0.4 J/cm^2) in Area 1 of somatosensory cortex in subject 1. Robust focal CBV signal evoked by INS directly in area 1 (slice 1,2, and 3). CBV signal detected in layers 1-5 of cortex in response to INS. Projected activation evoked by INS detected in Area 2 (slice 2 and 3) and Area 3B (slice 2). (B) INS (0.4 J/cm^2) in Area 3b of somatosensory cortex in subject 2. Focal activation evoked by INS observed in Area 3b (slice 1, 2, and 3). CBV signal detected in layers 1 – 3 of cortex in response to INS. Projected activation evoked by INS detected in Area 3a (slice 1 and 2) and Area 1 (slice 2). For (A) and (B), projected areas of activation confirmed through functional imaging of vibrotactile stimulation of digits (data not shown). (C) Timecourse of CBV signal for five radiant exposures demonstrates (yellow box indicates stimulus timing). (D) CBV signal magnitude increases linearly with increasing radiant exposure.

B 4.2 Behavioral responses evoked by INS in NHP visual cortex

Evoking behavioral changes in an animal model is a primary objective for establishing INS as a neurostimulation modality for CNS applications as demonstrating animal perception of INS confirms modulation of neural activity. Perception by the animal may be more sensitive than point source electrophysiology techniques and an INS evoked behavioral response would reduce ambiguity in determining physiological source for INS evoked signals providing support for neurological origin of signals. Establishing the ability to affect animal behavior with INS will provide an additional tool for neuroscientist to study behavior in a variety of cortical studies.

The efficacy of INS to evoke behavioral responses was investigated in a Macaque monkey implanted with a chronic imaging chamber placed over V2/V4 cortex. The animal was well trained to fixate on a dot centered on a computer monitor and ignoring other stimuli on the screen until receiving a water reward; therefore, the animal was expected to respond to INS evoked perception only after the fixation point and reward had been received. To test this hypothesis, INS was performed in V4 cortex after visual cue stimulation and reward had been presented to the animal (Figure B.1B). As expected, the animal consistently made saccade movements corresponding to the retinotopic location that was stimulation by INS as displayed Figure B.3. During the visual fixation cue, the animal continually maintained its gaze on the dot (within 1 degree) displayed on the monitor. The timecourse of eye movements during the visual fixation cue and reward presentation showed little deviation of eye movement from zero degrees (Figure B.3A-D, columns 1 and 2). However, when INS was applied after removal of the visual cue and reward presenation, the animal was observed to saccade to the same lower right quadrant

on the monitor (Figure B.3A-D, column 3). Interestingly, the saccade movement was typically observed only after 250 ms of INS had been delivered to the cortex (Figure B.3A-D, column 1). These findings demonstrate that INS activates neural activity that is perceived by the animal.

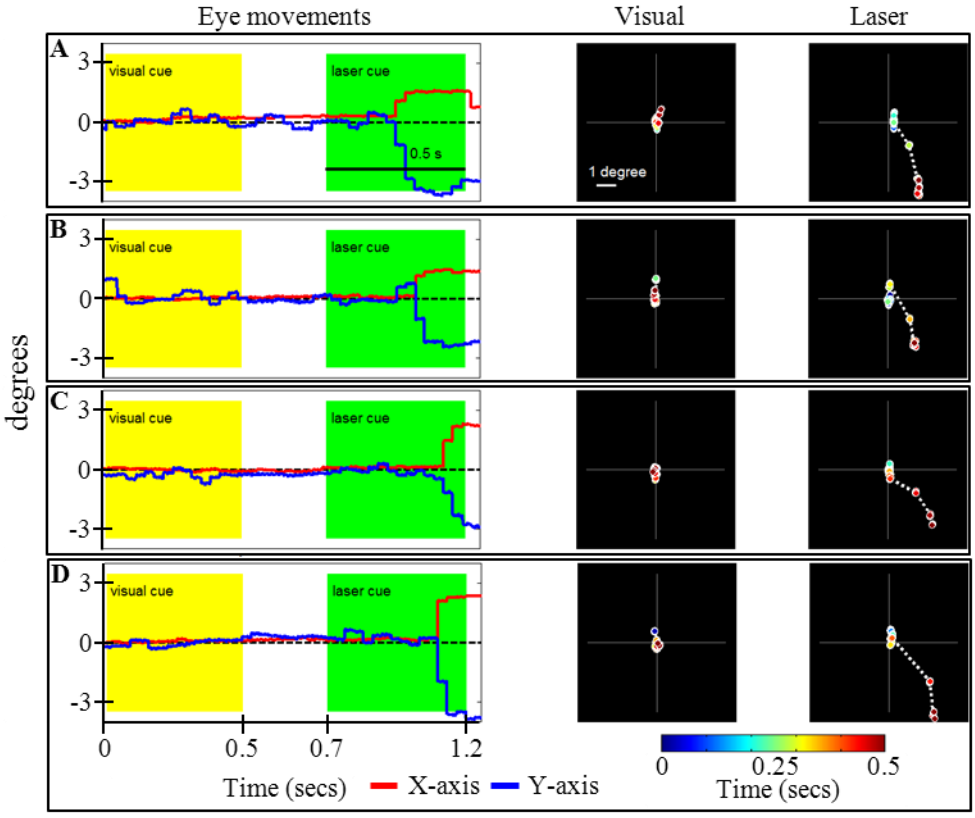

Figure B.3: INS evokes eye saccades in fixating primate. (A-D) Four individual behavioral trials monitoring eye movement during visual fixation cue followed by INS in V4 cortex demonstrates consistent saccade to lower right quadrant of visual field corresponding to stimulated retinotopic cortical location. First column represents eye position in degrees in the x and y directions as a function of time. Yellow box represents visual cue and green box represents INS duration. Second column displays two-dimensional representation of eye position on screen as a function of time in response to fixation cue. Third column represents eye position in two-dimensions in response to INS in V4 cortex. Each trial of INS is shown to evoke saccade to lower right quadrant.

In order to ensure the animal was responding to INS in V4 cortex, we designed two additional stimulation conditions to be presented to the animal during behavioral sessions. In addition to INS following visual fixation cue and reward, two additional stimulation conditions were presented to the animal. The first condition was a simple control condition consisting of a 3 second visual fixation cue followed by a water reward given to the animal. The second condition superimposed a 500 ms INS stimulation during the middle of presentation of the visual fixation cue followed by presentation of reward. As expected, the animal maintained a consistent gaze on the visual cue during the presentation of the visual cue only (Figure B.4A). Additionally, the animal did not respond to INS delivered while a visual cue was displayed to the animal (Figure B.4B). This finding is not surprising because this animal had been trained to fixate on the visual cue and ignore other stimuli present on the screen, and indicates proper behavior by the animal. The only condition that produced behavioral responses occurred when INS was presented after removal of the visual cue to evoke fixation followed by reward for proper behavior by the animal (Figure B.4C). The animal consistently made the same eye movements characterized in figure B.3. The timecourse displayed in figure B.4C, contains over 100 trials and the relatively tight 95% confidence interval (shaded regions) indicate a consistent response; therefore, the conclusion can be made that INS of V4 cortex evoked neural activity that was perceived by the animal evoking a behavioral change.

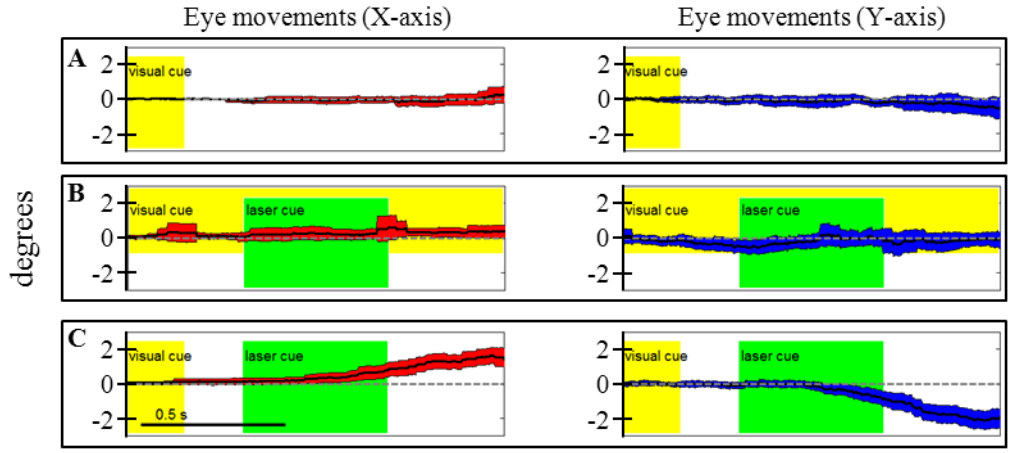

Figure B.4: Behavioral response to INS only observed after reward for fixation. Average eye position timecourse for (A) visual fixation alone, (B) simultaneous visual fixation and INS, and (C) INS following visual fixation and reward. Shaded yellow region corresponds to fixation point displayed to animal, shaded green region corresponds to INS timing. For each timecourse, n>100 trials. Shaded region represents 95% confidence interval. Black bar represents y-axis scale (0.5 seconds)

It should be noted that the behavioral response characterized here represents only a feasibility study and more experiments are needed to understand how INS evokes behavioral responses in awake animals. One interesting finding that cannot be completely explained by this study was the observed delayed response to INS. As can be seen in both figure B.3 and figure B.4, the animal response was delayed by a minimum of 250 ms. This delayed response may have been caused by superposition of thermal energy which has previously been shown to stimulate peripheral neural tissue using continuous infrared neural stimulation [10]. Another hypothesis is that the animal required a threshold duration of INS before stimulation was perceived or the animal was trying to stay on the fixation task and brief periods of INS did not distract the animal to cause a behavioral change. More experiments are needed to identify why perception of INS is delayed. A simple experiment would use the current protocol and adjust the stimulation duration, radiant exposure, repetition rate, and stimulus timing (i.e. further delay between reward

and INS). Changing the stimulation duration would allow for assessment of behavioral change onset. Varying the radiant exposure and repetition rate would assist in identifying stimulation thresholds for evoking a behavioral response; and adjusting stimulus timing would identify effects on behavior changes related to stimulation delay between visual cue/reward and INS. Additional experiments are also needed to demonstrate that INS of any cortical retinotopic location evokes behavioral changes through eye moments corresponding to the stimulated region. These experiments would require a minimum of two chronic imaging chambers to be implanted to allow stimulation to be applied in either chamber in the same behavioral session. Demonstration of eye movements corresponding to multiple retinotopic locations stimulated by INS would confirm the results described in this feasibility study. Results from these experiments would be useful in designing tasks requiring an animal to make a decision based on presented stimuli. Such a task would involve training the animal to choose a specific visual stimulus through a saccade movement corresponding to the location on the screen were the stimulus was presented [11]. This type of task could then be used to determine what sensory information INS is encoding into cortex (i.e. stimulation of orientation domains vs color domains). Demonstrating the ability of INS to encode specific information would lead to significant advances in cortical prosthetics.

B.5 Conclusions

The results from the two studies summarized in this appendix provide further support that INS is a useful neurostimulation technique in NHP. Pulsed infrared light was shown to evoke meaningful functional responses (as detected by fMRI) at the site of stimulation and in projection areas demonstrating the feasibility of INS for functional tract tracing in fMRI experiments. Initial feasibility behavioral studies demonstrated that INS modulates behavior in a fixating monkey indicating that INS is perceived by the animal. Together, these results provide further motivation for the continued development of INS for use in NHP and highlight the clinical potential of INS for both diagnostic and therapeutic purposes.

B.6 References

[1] Zhang, N., Gore, J. C., Chen, L. M., and Avison, M. J., "Dependence of BOLD signal change on tactile stimulus intensity in SI of primates," *Magnetic resonance imaging*, vol. 25, pp. 784-794, 2007.

[2] Chen, L. M., Turner, G. H., Friedman, R. M., Zhang, N., Gore, J. C., Roe, A. W., and Avison, M. J., "High-Resolution Maps of Real and Illusory Tactile Activation in Primary Somatosensory Cortex in Individual Monkeys with Functional Magnetic Resonance Imaging and Optical Imaging," *The Journal of Neuroscience*, vol. 27, pp. 9181-9191, 2007.

[3] Chen, L. M., Heider, B., Williams, G. V., Healy, F. L., Ramsden, B. M., and Roe, A. W., "A chamber and artificial dura method for long-term optical imaging in the monkey," *Journal of Neuroscience Methods*, vol. 113, pp. 41-49, 2002.

[4] Roe, A. W., "Long-term optical imaging of intrinsic signals in anesthetized and awake monkeys," *Appl. Opt.*, vol. 46, pp. 1872-1880, 2007.

[5] Tanigawa, H., Lu, H. D., and Roe, A. W., "Functional organization for color and orientation in macaque V4," *Nature neuroscience*, vol. 13, pp. 1542-1548, 2010.

[6] Wang, Z. and Roe, A. W., "Trial-to-trial noise cancellation of cortical field potentials in awake macaques by autoregression model with exogenous input (ARX)," *Journal of Neuroscience Methods,* vol. 194, pp. 266-273, 2011.

[7] Chen, G., Wang, F., C.D., D., Friedman, R. M., Chen, L. M., Gore, J. C., Avison, M. J., and Roe, A. W., "Magnetic resonance imaging in awake monkeys: methods of improving imaging quality," *Magnetic resonance imaging,* vol. 30, pp. 36-47, 2012.

[8] Cayce, J. M., Kao, C. C., Malphrus, J. D., Konrad, P. E., Mahadevan-Jansen, A., and Jansen, E. D., "Infrared Neural Stimulation of Thalamocortical Brain Slices," *Selected Topics in Quantum Electronics, IEEE Journal of,* vol. 16, pp. 565-572, 2010.

[9] Cayce, J. M., Friedman, R., Jansen, E. D., Mahadevan-Jansen, A., and Roe, A. W., "Pulsed infrared light alters neural activity in rat somatosensory cortex in vivo," *Neuroimage,* vol. 57, pp. 155-166, 2011.

[10] Tozburun, S., Cilip, C. M., Lagoda, G. A., Burnett, A. L., and Fried, N. M., "Continuous-wave infrared optical nerve stimulation for potential diagnostic applications," *Journal of Biomedical Optics,* vol. 15, pp. 055012-055012-4, 2010.

[11] Schiller, P. H., Slocum, W. M., Kwak, M. C., Kendall, G. L., and Tehovnik, E. J., "New methods devised specify the size and color of the spots monkeys see when striate cortex (area V1) is electrically stimulated," *Proceedings of the National Academy of Sciences,* vol. 108, pp. 17809-17814, 2011.

APPENDIX C

INFRARED NEURAL STIMULATION OF HUMAN SPINAL NERVE ROOTS

Jonathan M. Cayce[1], Jonathon D. Wells[2], Jonathan D Malphrus[1], Chris Kao[3],

Sharon Thomsen[4], Noel B Tulipan[3], Peter E. Konrad[1,3],

E. Duco Jansen[1,3], and Anita Mahadevan-Jansen[1,3]

[1] Department of Biomedical Engineering, Vanderbilt University

Nashville Tennessee

[2] Lockheed Martin Aculight

Bothell Washington

[3] Department of Neurological Surgery, Vanderbilt University

Nashville Tennessee

[4] Department of Biomedical Engineering, University of Texas

Austin Texas

This chapter was prepared for submission to *Science Translational Medicine*

C.1 Abstract

Infrared neural stimulation (INS) is a precise neurostimulation modality that uses pulsed infrared light to evoke artifact free neural activity using a non-contact interface; however, safety and efficacy of this technique has not been demonstrated in humans. Feasibility of INS in humans was conducted in patients (n=7) undergoing selective dorsal root rhizotomy where hyperactive dorsal roots are identified for transection with diagnostic neural stimulation and monitoring techniques. Dorsal roots identified for transection were subsequently stimulated with INS on 2-3 sites per nerve. We found INS routinely activated human dorsal roots with an efficacy of 63% for radiant exposures between 0.53-1.23 J/cm2. A 2:1 safety ratio was identified through analysis of section dorsal roots for thermal. These findings demonstrate that INS can be used to safely stimulate human neural tissue and provides the foundation for future clinical studies where spatially precise, artifact free neural stimulation is desired.

C.2 Introduction

Infrared neural stimulation (INS) is a novel stimulation modality that employs low energy, pulsed infrared light to reliably excite nerves [1]. The resulting action potentials in peripheral nerves are produced without direct contact from a probe, as opposed to electrical stimulation (ES) which requires a contact between an electrode and tissue [1-3]. We have demonstrated the specificity of INS to activate individual nerve fascicles, and the use of laser energy for neural stimulation allows artifact-free electrical recordings to be obtained close to the site of stimulation [4, 5]. These features of INS make it an attractive alternative to electrical stimulation, especially in certain clinical applications.

The advantages of INS provide the ability to circumvent limitations of clinical electrical stimulation used for diagnostic and therapeutic applications. High spatially precise electrical stimulation for clinical procedures require an electrode to physically contact the surface or impale neural tissue resulting in local damage to neural tissue. Electrical recording of the neural response becomes more challenging the closer the recording electrodes are to those used for stimulation because the electrical artifact of the stimulation field masks the small neural signals generated by stimulation [6-8]. In neural monitoring applications, inadvertent non-visible current spread from the site of electrode contact can lead to stimulation of distant neural structures and misdiagnosis of whether local connectivity of neural structures is viable. Additionally, current spread with ES can excite multiple neural structures near the electrode leading to unwanted stimulation of adjacent neural structures which also limits the precision in therapeutic applications such as deep brain stimulation of subthalamic nucleus or cochlear implants [9, 10].

The specificity and delivery of laser based stimulation provides an alternative method to overcome many of these problems associated with electrical stimulation as we have demonstrated in past animal experiments [3-5]. The rat sciatic nerve was first used to demonstrate efficacy and safety of INS for stimulation of peripheral nerves where a 2:1 safety ratio exists between damaging radiant exposures and threshold energy levels needed for stimulation [3]. The initial results from our group's efforts have led to the development of INS aimed at clinically relevant diagnostic and therapeutic applications including neural monitoring [5, 11, 12], cochlear and vestibular stimulation [13-15], cardiac pacing [16, 17], and applications in the central nervous system [18-21].

The underlying biophysical mechanism of INS has been known to activate neural tissue through a transient thermal gradient [4]. Shapiro and colleagues provided evidence that the INS evoked thermal gradient depolarizes lipid membrane bilayers through a thermally mediated change in membrane capacitance independent from specific ion channels. This simplified mechanism indicates all neural tissue can be excited using INS. Alternatively, the authors hypothesized that other cellular mechanisms may be involved [22]. Recently, heat sensitive TRPV4 channels were implicated as the primary mechanism behind for INS evoked action potentials in retina ganglion cells suggesting multiple mechanisms are involved in transducing the thermal heat gradient of INS into action potentials [23]. These mechanistic findings indicate INS is a robust stimulation method that can be used as an alternative clinical stimulation method to augment current diagnostic and therapeutic neurostimulation applications.

There is a diagnostic need for precise physiological identification and stimulation of peripheral and cranial nerves. The present use of electrical microstimulation probes are

seen with numerous surgical procedures involved in either safely identifying portions of a peripheral nerve to avoid damage or to select such fibers for therapeutic treatment. Examples of the value of such selective precision include the routine use of facial nerve stimulation during resection of acoustic neuromas where fascicles of the facial nerve may be quite splayed over the back surface of the tumor. Use of small electrical probes in identifying the facial nerve may give a false sense of spacial precision when the stimulation energy is excessive and activates neural fibers that are quite distant from the operative site [24-26]. Another surgical example is the use of electrical microstimulation for identification of viable peripheral nerve fibers during neural reconstructive procedures. In these procedures, peripheral nerve fascicles need to be identified that are electrically viable versus non-viable, and therefore requiring a nerve graft. Grafted sections of the nerve are usually 1-2mm in diameter and represent only a portion of the peripheral nerve needing an anastomotic graft usually harvested from elsewhere in the patient. It is therefore valuable to identify with less than 1mm precision, the appropriate sections requiring resection and anastomosis within a larger peripheral nerve undergoing repair. In both these examples, a light based stimulation probe that confines the region of stimulation to the spot size of the stimulation effect is superior to an “invisible” electric field. While we have shown that INS can achieve this level of precision in animal models, its efficacy and safety in human surgery must be validated.

The goal of this study is to translate this technology to clinical use and demonstrate efficacy and safety of INS in humans when used as a diagnostic tool during neurosurgical procedures that require detailed nerve root mapping. In order to accomplish these goals, we stimulated dorsal spinal roots identified for transection in patients

undergoing selective dorsal rhizotomy for treatment of medically refractory spasticity. Selective dorsal rhizotomies (SDR) were chosen for several reasons: 1) the human dorsal root is of similar size to the rat sciatic nerve, 2) ES and electromyogram (EMG) recordings are routinely used to precisely identify specific dorsal roots, 3) and it is procedure whereby a nerve (dorsal spinal root) is intentionally transected, thereby allowing the option to harvest a small (1cm) section of the nerve without added deficits. These characteristics of the SDR procedure allowed for direct assessment of INS for efficacy and safety in human nerves and validate our results in rat sciatic nerves through EMG recordings and histological analysis [3, 5].

We report that INS effectively stimulates human dorsal roots with the same high spatial precision demonstrated in animal models without generating a stimulation artifact on recording electrodes. Histological analysis of the dorsal roots exposed to infrared irradiation identified a 2:1 safety margin between stimulation threshold and first signs of damage that corresponds to the safety ratio identified for INS of the rat sciatic nerve [3]. This study reports on the first human clinical use of INS and establishes feasibility and safety ranges needed for clinical applications of INS. These results will form the foundation to investigate the utility of the technique for clinical diagnostic and therapeutic applications.

C.3 Methods

C.3.1 Patient recruitment

All protocols and procedures implemented during this preclinical trial were approved by the Vanderbilt University Institutional Review Board (IRB# 050822). Informed consent was obtained in all cases.

Seven patients, ages 3 – 16 (M=5, F=2), undergoing selective dorsal root rhizotomy (SDR) for the treatment of lower extremity spasticity were recruited for this study [27-29]. Inclusion into this study required patients to undergo electrodiagnostic EMG monitoring as a normal part of the procedure, and it allowed for direct comparison of the physiologicl response between INS and electrical stimulation. Patients were excluded if a sufficient segment of nerve (>1 cm) could not be identified for resection at the time of surgery as determined by the pediatric neurosurgeon or if the patient was medically unstable to tolerate an additional 20 minutes of experimental testing during the surgery.

C.3.2 Surgical procedure

Selective dorsal root rhizotomy is a standard surgical procedure used to identify dorsal afferent spinal roots that contribute to excessive muscular tone or spacticity in the lower extremities [30, 31]. Once identified a select number of nerve roots are cut while others spared for each lumbar segment, leading to an overall decrease in the afferent sensory tone of that region of the spinal cord and presumably diminished spasticity. The surgery normally involves performing a laminectomy of the lumbar spine, opening the

dura overlying the lumbar spinal nerve roots, and physiologically identifying the dorsal spinal nerve roots involved in the spastic reflex using standard electrical stimulation techniques. Note that the dorsal roots (sensory inputs) are stimulated and the signal is transmitted through a synapse via the reflex arc to motor fibers which elicits a muscle response, monitored by EMG recordings in all major muscles groups of each leg. Once identified as a contributor to spasticity, a certain percentage of the abnormal nerves are sectioned.

Electrical stimulation parameters to elicit threshold responses are recorded in response to single pulse electrical stimulation (1-10 mA, 100 μsec pulse duration) of individual spinal nerves (L2 – S1). Physiological abnormal spinal roots involved in spastic reflexes are identified by stimulating the rootlet with a train of threshold stimulatory electrical pulses delivered at 20 Hz. Nerve roots exhibiting spastic firing patterns or incorrect wiring to multiple muscles as determined from surgical monitoring of EMG signals are identified for sectioning [32, 33].

C.3.3 Laser setup and INS parameters:

Once a nerve has been designated for sectioning, INS was performed using a clinical Holmium:YAG laser to stimulate 2 – 3 locations on the nerve for 10 seconds at 2 Hz. The clinical laser operates at higher radiant energies and repetition rates than the stimulation parameters required for this study. A light tight optical box was constructed to control the output radiant exposure and to reduce the repetition rate to 2 Hz (Figure B.1). High energy laser light entered the box from a 550μm optical fiber (Low OH multimode fiber [FG550LEC], Thor Labs, NA = 0.22) connected to the clinical system.

A biconvex lens (f=25 cm, Thor Labs), was used to focus the divergent beam from the input fiber through a 20/80% beam splitter and couple the attenuated beam of laser light into the delivery fiber (d=550 μm). A photodiode, placed between the input fiber and lens, detected high frequency input light pulses and triggered an optical shutter to adjust the output frequency to 2 Hz using a pulse generator. Since animal and human nerves have similar optical properties, we expected the radiant exposure required for both stimulation and damage in animal nerves to be comparable in human peripheral nerves; 0.34 - 0.48 J/cm^2 and 0.7-1.0 J/cm^2, respectively. Therefore, light output from the clinical laser (1000 mJ/pulse at 6 Hz) was modified to an adjustable output energy from 0 to 25 mJ (0 – 2.5 J/cm^2) pulsing at 2 Hz. An external micromanipulator attached to the optical fiber mount inside the black box allowed for fine control of the light coupling efficiency and thus the amount of light entering the output 550 μm core optical fiber (NA=0.22). The output end of this fiber was mounted onto a sterilized, handheld optical fiber probe (600 μm, NA = 0.22) for ease of use by the neurosurgeon during stimulation. A red HeNe aiming beam output from the clinical system was maintained though the probe output, providing a known stimulation site. The laser-probe system was footswitch controlled.

The first 5 spinal nerves selected for resection were stimulated using infrared energy before the nerves were resected. The neurosurgeon maintained the distance between the nerve and handheld optical probe tip between 1 – 2 mm during stimulation, yielding a spot size of approximately 1.2 mm^2, estimated using the angle of divergence of light out of the fiber. Stimulated nerves were surrounded by a sterile silastic sheet, to insure no aberrant laser stimulation of adjacent normal tissue and help guarantee that

recorded muscle responses were elicited due to the laser energy incident on the chosen nerve root. Each nerve was irradiated on 2 to 3 adjacent sites before marking, sectioning, and harvesting of the nerve. One or two sites on each nerve was irradiated with 20 laser pulses (2 Hz) with a constant radiant exposure between stimulation and damage threshold as defined in mammalian studies (0.3 – 1.0 J/cm^2). One to two millimeters adjacent to this spot, the nerve was stimulated with 20 pulses (2 Hz) using laser energies greater than damage threshold but less than the ablation threshold identified in mammalian studies (control lesion, 2.0 – 2.2 J/cm^2) [3]. The nerve segment, measuring less than 1 cm, was then harvested and submitted for histological analysis.

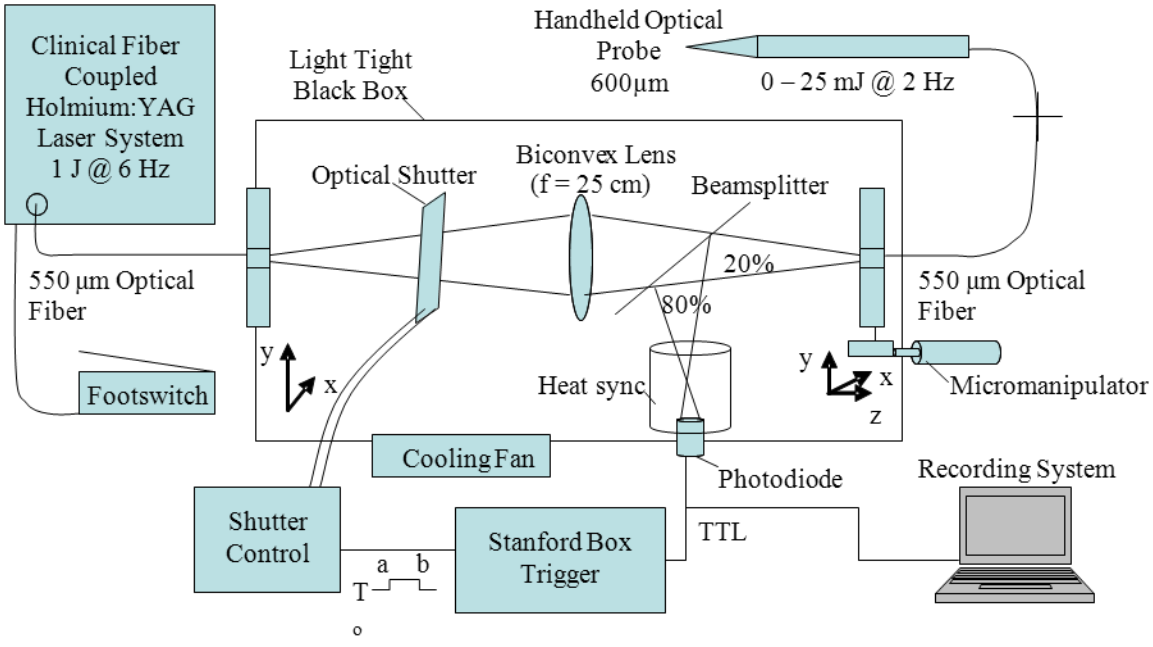

Figure C.1: Schematic diagram of optical box for modifying high power and high frequency clinical system to optimal parameters for INS.

C.3.4 Data recording and analysis

The evoked electromyographic (EMG) data was collected in a standard clinical electrophysiological setting and protocol. EMG responses to optically and electrically stimulated nerves were recorded with the clinical electrophysiological system used routinely in the surgery (Nicolet Endeavor; Version 2.5.80, Nicolet Biomedical Inc. Madison, WI 53744). Muscle-EMG recordings were simultaneously monitored and collected from all major muscles groups of both legs; namely, the adductor longus, vastus lateralis, biceps femoris, medial gastronemeus, peroneus longus, and anterior tibialis muscles in response to ES and INS. Once a rootlet has been identified for sectioning, a 10 second continuous EMG recording was captured during INS beginning 2 ms prior to stimulation of the nerve through screen capture every 2 seconds during INS.. Each response was recorded after the signal was amplified (1000x) and bandpass filtered (50 – 500 Hz).

A comparison was made with electrical and INS performed at the same or adjacent points on the nerve, and the resulting muscle action potentials recorded. Successful stimulation of the rootlet by INS was determined by the presence of EMG signal in muscle groups activated by diagnostic ES stimulation (Figure C.2). Muscle groups exhibiting spastic activity (indicated by high frequency EMG activity) during the entirety of the procedure were excluded from analysis in determining INS activation.

C.3.5 Tissue preparation and analysis

Once a nerve that was identified for sectioning was exposed to INS the nerve stimulation sites were marked with methyl blue ink to aid in histological analysis. The nerve segment containing the 2-3 irradiated zones were excised (1 – 2 cm), immediately

placed in formalin, and prepared into slides of 5 μm thin longitudinal sections cuts perpendicular to the stimulation sites. Sections were sent for an independent blinded review of acute histological changes occurring from laser stimulation, interpreted by an expert in histopathology associated with laser-tissue irradiation [34, 35]. Areas of coagulation, axonal disruption, and perineurium damage were assessed using light microscopy and routine hematoxylin and eosin (H & E) staining. Changes sought in laser irradiated tissue follow the methods outlined for acute studies in previous mammalian studies [3]. These criteria help define the following three point grading scheme assigned to each specimen indicating extent of damage at the site of optical stimulation: 0 - no visible thermal changes, 1 - pathological changes in the section that cannot be confirmed as thermal damage (mechanical or thermal), 2 - presence of a thermal lesion within the tissue section.

C.3.6 Statistical analysis

In order to determine the probability of damage associated with INS radiant exposures, the binary data (damage vs no damage) resulting from histological analysis was calculated by fitting the data to a probit model typically used to determine damage thresholds associated with laser irradiation [3]. The binary data was inputted into Probit v2.1.2 (Litton TASC, San Antonio, TX) to obtain the cumulative distribution function that describes the probability of damage as a function of radiant exposure [36]*:*

C.4 Results

C.4.1 Infrared neural stimulation evokes neural activity in humans

In the seven patients studied, INS successfully activated individual muscle groups first identified with electrical stimulation. Figure C.2 compares the EMG recordings of ES to INS of a dorsal root identified for sectioning. EMG recordings were taken from the following six muscles in both the right and left leg (12 total EMG recordings): adductor longus (R&L ADD), biceps femoris (R&L HAM), vastus lateralis (R&L QUA), medial gastronemeus (R&L GAS), peroneus longus (R&L PLO), and anterior tibialis (R&L ANTI). Note that threshold ES (20Hz, 2mA train lasting 0.5 seconds) of a single dorsal nerve root branch elicited EMG responses in over 10 muscles, both ipsi- and contra-lateral limbs. In this particular patient, this nerve root was considered to be pathologically involved in the spasticity of the patient and was selected for transection. Once identified as a root that was to be transected, INS was performed using a handheld probe positioned by the neurosurgeon approximately 1-2 mm above the surface of the root (no direct contact with the tissue) and within 1 mm of the site of ES stimulation that ilicited the response seen in Figure C.2A. In Figure C.2B, EMG recordings taken during INS demonstrate that only the ipsilateral adductor longus muscle (L ADD) is activated through INS of the sensory root. Even in a state of hyperexcitability seen with ES only one monitored muscle is activated validating the spatial precision of INS (Figure C.2)., High spatial precision of INS was observed in all stimulated dorsal roots in the seven patients enrolled in this study.

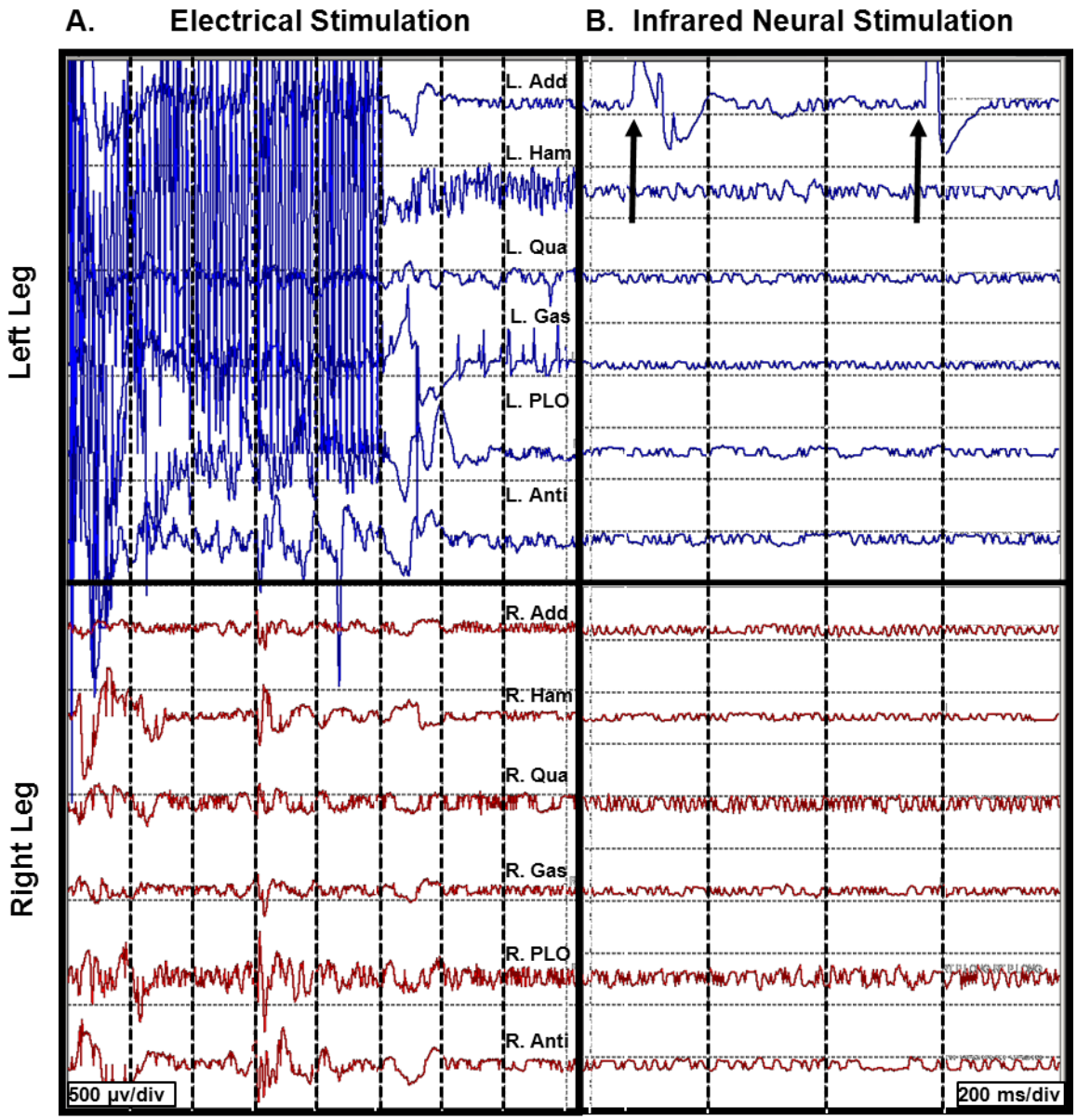

Figure C.2: Pulsed infrared light evokes compound muscle action potentials through stimulation of human dorsal root. EMG recordings from 12 muscles in the lower extremities (top 6 traces = left leg, bottom 6 traces right leg) in response to electrical stimulation (20 Hz, 100 µs, 1 sec) and INS (2 Hz, 350 µs, 10 sec) on a left dorsal root L4. A.) Responses obtained from 20 Hz train of electrical stimulation (~2.0 mA) visualized on a voltage scale of ± 500µV. EMG recordings indicate a response in all left and right side muscles. B.) Reponses obtained from INS (1.03 J/cm^2) of same nerve with a voltage scale of ±500 µV. A single response is observed in the left Adductor muscle (denoted by black arrows).

Another feature that differentiates ES from INS is the stimulation artifact seen in the EMG recordings. The electrical stimulation artifact in Figure C.2A obscures physiologically relevant signal in the EMG trace. The artifact saturates the recording amplifier resulting in loss of physiological relevant information. Infrared neural stimulation evokes potentials on EMG recordings where the distinct potentials are locked to the laser repetition rate (2 Hz) (Note arrows repeat at 500msec in Figure C.2A). No stimulation artifact is visible to obscure the evoked potential. The lack of stimulation artifact associated with INS highlights the clinical potential of the technique for neural monitoring applications where electrical artifacts can obscure subtle evoked neural responses due to the close proximity of neural stimulation and recordings sites.

C.4.2 Infrared neural stimulation can be applied without damaging neural tissue

Patient safety is the most important criteria to establish before INS can be applied to therapeutic and diagnostic clinical procedures. During this feasibility study in humans, we performed extensive histological analysis of specimen exposed to infrared light. For each specimen, 2 to 3 sites were irradiated by the laser with one location serving as a positive control. Excised nerves were sectioned and stained with hematoxylin and eosin (H&E) to visualize thermal damage associated with INS. Figure C.3A presents an example of the normal pathophysiology after laser irradiation (0.91 J/cm^2). The axons in this image have a wavy appearance and no discoloration can be seen throughout the image, and this section indicates that near-threshold radiant exposures needed to stimulate the dorsal root do not cause acute damage. An example of thermal damage from laser irradiation (1.32 J/cm^2) is seen in Figure C.3B and C.3C. This lesion contains

swelling and hyperchromasia of the collagen in the endoneurium, granular degeneration of the myelin, straightening of the axons, vacuolization, and expansion of endoneurial tubes.

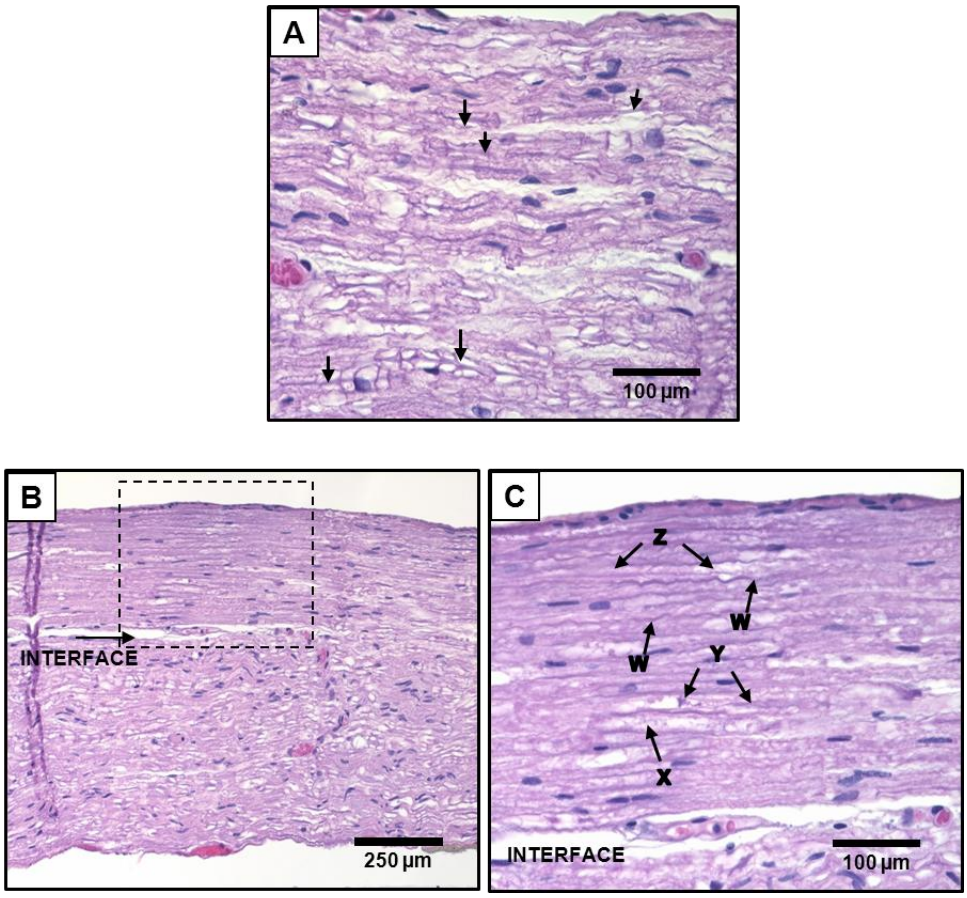

Figure C.3: Histological comparison of safe versus non-safe of optically stimulated experimental sites in dorsal lumbar nerve roots. A. Experimental site (500X magnification) resulting in the stimulated muscle recordings using 0.91 J/cm^2 for a total of 20 laser pulses (damage score = 0). Numerous axons (arrows) can be seen in the nerve fibers in this image. B. An overview of the thermal lesion produced within the dorsal root nerve (200X magnification) using 1.32 J/cm2 (damage score = 3). The lesion is generally hyperchromatic and the endoneurial tubes are straightened out in the center. The arrow represents the interface between the thermally damaged tissue and the underlying normal tissue. C. The demarcated area from B at 500X magnification. This lesion has the following features characteristic of thermal damage: swelling and hyperchromasia of the collagen in the endoneurium (**W**), granular degeneration of myelin (**X**), straightening of the nerve fibers as compared to the intact fibers at the bottom of the image, vacuolization, and expansion of the endoneurial tubes in some areas (**X**). Although some axons show axonal thermal damage (**Y**), others in the lesion (**Z)** do not at this level of magnification.

In order to quantify safety of INS in humans, a three point grading scale, designed by a blinded neuropathologist (author ST), was used to grade damage in each sectioned dorsal root. Irradiated areas that exhibited no signs of thermal damage (Figure B.3A) were given a damage score of 0. Lesions containing any thermal damage features highlighted in Figure C.3B and C.3C were given a damage score of 2. In some cases, ambiguous damage possibly resulting from surgical trauma or laser irradiation was noted. These lesions were assigned a damage score of 1.

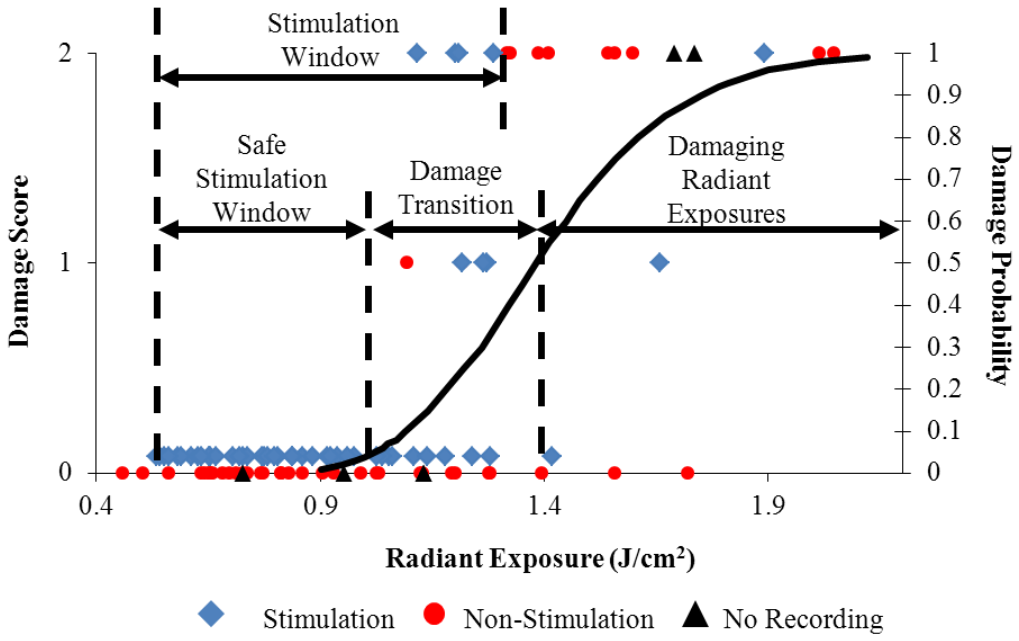

Figure C.4: Identification of safe radiant exposures for stimulation of human dorsal roots. Results from the safety and efficacy study from seven patients (102 stimulation sites) graded on a three point scale. Laser radiant exposure used for each stimulation (20 pulses at 2 Hz recorded for 10 seconds) is graphed as a function of thermal damage score assigned to each site based on histopathology from optical stimulation over a range of laser energies (0.46 – 2.05 J/cm^2). Probability of damage is given by cumulative distribution function from statistical analysis of binary damage data. Successful stimulation indicated by blue diamonds (stimulation events resulting in stimulation slightly offset from zero axis for clarity), no stimulation indicated by red dots, and stimulation sites with no corresponding EMG recordings indicated by black triangles. Compound muscle action potentials first observed at 0.53 J/cm^2. Stimulation range identified as 0.53 – 1.28 J/cm^2. Safe stimulation range identified as 0.53 – 1.00 J/cm^2

A total of 102 stimulation sites from 35 spinal roots were evaluated using the described damage scoring criteria. Figure C.4 displays the results of the histology and the radiant exposures which resulted in measurable EMG signals. Recordings were obtained from 95 stimulation sites, which resulted in 51 (53%) observed stimulation events. Reliable stimulation was observed for radiant exposures ranging from 0.53 – 1.28 J/cm^2 with an efficacy of 63% (Figure C.4). No measurable response was observed for radiant exposures of 0.503 and 0.46 J/cm^2 indicating stimulation threshold of the human dorsal root occurs between 0.50 and 0.53 J/cm^2. Radiant exposures up to 1.14 J/cm^2 resulted in no damage; however ambiguous grade 1 damage was first noted at 1.09 J/cm^2 and grade 2 damage first occurred at 1.12 J/cm^2 identifying a transition zone from non-damaging to damaging irradiation levels between 1.09 and 1.38 J/cm^2 (Figure C.4A). The cumulative distribution function generated by probit analysis of the binary histological data identified the 50% probability of damage to be 1.38 J/cm^2 with 10% probability of damage corresponding to the first observed indication of damage at 1.09 J/cm^2 further supporting the bounds identified for the transitional zone in Figure C.4. Additionally, the transitional zone (1.00 – 1.14 J/cm^2) from non-damaging to damaging radiant exposures using short term stimulation correlates with the results from animal survival studies where 50% probability of damage was 0.91 to 0.97 J/cm^2 [3]. The safety ratio, defined as the ratio of radiant exposures where damage is first observed to that where stimulation is first seen, is 2:1, the same safety ratio reported in animal studies [3]. Slight movement of the surgeon's hand combined with physiological motion of the patient during stimulation led to variations in reported radiant exposures due to the divergent beam from the hand held probe Due to this variance in delivered radiant exposures of the tissue target site, the safe

stimulation radiant exposure range for human dorsal roots was identified as radiant exposures between 0.53 J/cm^2 and 1.00 J/cm^2 because no damage was observed for these reported irradiation levels. The reported efficacy will increase with a collimated beam or fixed probe position above the nerve since variance in spot size would be minimized.

C.5 Discussion

This is the first report that INS can produce discrete, precise stimulation of spinal nerve roots similar to ES in humans. The advantages of INS, non-contact delivery, artifact-free recordings, and high spatial selectivity, were maintained in this study as the neurosurgeon used a hand held probe to stimulate the dorsal root without contacting neural tissue. Single muscle activation was observed during INS within diseased hyperactive dorsal roots demonstrating the high spatial precision of INS. Histology results explicitly show that we can safely stimulate human nerves without causing acute thermal damage when the intensity of INS is held below 1.09 J/cm^2. The results of this study establish the feasibility needed to support further clinical evaluation of INS in humans.

This study documents the use of INS for sensory root stimulation. Encoding somatosensory information through neural stimulation is an important objective for the neuroprosthetic community in the pursuit of close looped neural prosthetics[37-39]. Activation of efferent neurons in peripheral nerves with INS has been well established in peripheral nerves [2, 5, 11, 12]; however, direct evidence of INS evoked action potentials in peripheral sensory afferents has not been confirmed. The results from this study show that pulsed infrared light can be used to evoke action potentials in isolated sensory

nerves. Infrared neural stimulation directly evoked action potential in sensory axons located in dorsal roots that propagated transynaptically in the spinal cord to activate primary motor neurons in the sciatic nerve. These results imply INS may be an appropriate stimulation modality for encoding sensory information in future neural prosthetics with further development.

The high spatial precision associated with INS arises from the wavelength of light and the spot size of the laser beam, and these variables together determines the volume of tissue activated by infrared light [1]. The wavelength of the laser determines the depth the light penetrates the tissue based on the absorption characteristics of the light while spot size is a variable set by the user. Since spot size is easily manipulated and different wavelengths of light can be obtained from an assortment of lasers, it stands to reason that a wide variety of stimulation geometries can be obtained allowing INS techniques to be customized for specific clinical applications

This study demonstrates the applicability of INS for diagnostic use in humans undergoing procedures requiring precise mapping of neural structures. An important diagnostic need in neural monitoring is identification of small groups of neural fibers during surgery, such as surgery involving peripheral nerve reconstruction, the spinal cord, the central pontine angle where cranial nerves need to be identified and preserved, or the cavernous nerve surrounding the prostate gland which may be hidden within the region of resection. All these examples highlight the concern about inadvertent injury to even a millimeter of neural tissue that may result in significant neurological deficits. This diagnostic need is directly addressed by the high spatial precision of INS. Peripheral nerve monitoring with INS has been well characterized in animal models where sciatic

[5], facial [11], and cavernous nerves [12] are mapped. Both the rat sciatic and facial nerve have been mapped with INS to identify regions on the nerve that innervate individual muscles downstream from the stimulation site [5, 11]. Recently, researchers have demonstrated the ability of infrared light to stimulate subsurface through connective tissue overlaying the rat cavernous nerve and evoke a physiological response [12]. These applications of INS towards neural monitoring highlight the advantages of INS in activating nerves with high spatial precision. This is the first report whereby INS was used in human surgery and directly compared with standard ES techniques during spinal root surgery (SDR).

Besides considering INS as diagnostic tool, the technique has potential value as a therapeutic tool. Researchers have demonstrated that INS safely activates the auditory ganglion cells in the cochlea with better spatial precision and improved auditory frequency encoding when compared to current electrical techniques [15, 40-42]. Since INS does not suffer from current spread and has higher spatial selectivity, an INS based cochlear implant would allow for high resolution auditory frequency encoding needed for high fidelity sound perception since more stimulation sites could be incorporated into an INS based implant than a traditional ES implant due to lack of cross talk between electrode leads [10]. INS of the cochlear represents the first therapeutic application of INS.

These example applications of INS given here represent only a small percentage of possible applications where INS may improve the standard clinical care. The high spatial selectivity of INS will allow clinicians to stimulate sub-fascicular for peripheral nerve reconstruction, such as brachial nerve plexus or otolaryngology applications, where

surgeons have a need to identify small groups of fibers to determine function and connectivity [43, 44]. Possible functional applications of INS include incorporation of the stimulation modality in neural prosthesis used to restore function, block pain, or treat movement disorders. Functional electrical stimulation has been used to provide control of the bladder, reanimate paralyzed limbs, control pain, and treat movement disorders [45-48]. In most of these applications, the patient may experience adverse side effects to the functional electrical stimulation attributed to current spread. The lack of current spread associated with INS makes it a viable alternative to electrical stimulation in these applications. Other possible applications of INS include neural grafting, cortical mapping, vestibular system stimulators, or cortical implants related to brain-machine interface applications.

As more researchers enter the INS field and new devices are developed the number of applications for this technique will continue to grow. This study provides the first successful steps needed to translate this new optical technology to the clinic and encourages the scientific community to rethink the accepted paradigm of neural activation to beyond electrical methods.

C.6 Acknowledgements

The authors would like to acknowledge the support of the W. M. Keck Foundation Free Electron Laser Center, MFEL/AFOSR program (FA9550-04-1-0045) and the National Institutes of Health support (R01 NS052407-01). We also thank John Scarafiotti and Sentient Medical Systems (SMS, Cockeysville, MD 21030), a contracted surgical monitoring service that provides routine intraoperative monitoring (IOM) for these rhizotomy cases, for use of existing operating room equipment, and IOM personnel and the surgical nursing staff of Vanderbilt Children's Hospital.

C.7 References

[1] Wells, J., Kao, C., Mariappan, K., Albea, J., Jansen, E. D., Konrad, P., and Mahadevan-Jansen, A., "Optical stimulation of neural tissue in vivo," *Opt Lett,* vol. 30, pp. 504-6, 2005.

[2] Wells, J., Kao, C., Jansen, E. D., Konrad, P., and Mahadevan-Jansen, A., "Application of infrared light for in vivo neural stimulation," *J Biomed Opt,* vol. 10, p. 064003, 2005.

[3] Wells, J., Thomsen, S., Whitaker, P., Jansen, E. D., Kao, C. C., Konrad, P. E., and Mahadevan-Jansen, A., "Optically mediated nerve stimulation: Identification of injury thresholds," *Lasers Surg Med,* vol. 39, pp. 513-26, 2007.

[4] Wells, J., Kao, C., Konrad, P., Milner, T., Kim, J., Mahadevan-Jansen, A., and Jansen, E. D., "Biophysical mechanisms of transient optical stimulation of peripheral nerve," *Biophys J,* vol. 93, pp. 2567-80, 2007.

[5] Wells, J., Konrad, P., Kao, C., Jansen, E. D., and Mahadevan-Jansen, A., "Pulsed laser versus electrical energy for peripheral nerve stimulation," *J Neurosci Methods,* vol. 163, pp. 326-37, 2007.

[6] Donoghue, J. P., Leibovic, S., and Sanes, J. N., "Organization of the forelimb area in squirrel monkey motor cortex: representation of digit, wrist, and elbow muscles," *Exp Brain Res,* vol. 89, pp. 1-19, 1992.

[7] Popovic, D., Gordon, T., Rafuse, V. F., and Prochazka, A., "Properties of implanted electrodes for functional electrical stimulation," *Ann Biomed Eng,* vol. 19, pp. 303-16, 1991.

[8] Strauss, C., "The facial nerve in medial acoustic neuromas," *J Neurosurg,* vol. 97, pp. 1083-90, 2002.

[9] Tommasi, G., Krack, P., Fraix, V., Le Bas, J. F., Chabardes, S., Benabid, A. L., and Pollak, P., "Pyramidal tract side effects induced by deep brain stimulation of the subthalamic nucleus," *Journal of Neurology, Neurosurgery & Psychiatry,* vol. 79, pp. 813-819, 2008.

[10] Landsberger, D. M. and Srinivasan, A. G., "Virtual channel discrimination is improved by current focusing in cochlear implant recipients," *Hearing Research,* vol. 254, pp. 34-41, 2009.

[11] Teudt, I. U., Nevel, A. E., Izzo, A. D., Walsh, J. T., Jr., and Richter, C. P., "Optical stimulation of the facial nerve: a new monitoring technique?," *Laryngoscope,* vol. 117, pp. 1641-7, 2007.

[12] Tozburun, S., Lagoda, G. A., Burnett, A. L., and Fried, N. M., "Subsurface near infrared laser stimulation of the periprostatic cavernous nerves," *Journal of biophotonics,* 2012.

[13] Richter, C. P., Rajguru, S. M., Matic, A. I., Moreno, E. L., Fishman, A. J., Robinson, A. M., Suh, E., and J. T. Walsh, J., "Spread of cochlear excitation during stimulation with pulsed infrared radiation: inferior colliculus measurements," *Journal of Neural Engineering,* vol. 8, p. 056006, 2011.

[14] Rajguru, S. M., Richter, C.-P., Matic, A. I., Holstein, G. R., Highstein, S. M., Dittami, G. M., and Rabbitt, R. D., "Infrared photostimulation of the crista ampullaris," *The Journal of Physiology,* vol. 589, pp. 1283-1294, 2011.

[15] Izzo, A. D., Richter, C.-P., Jansen, E. D., and Walsh, J. T., Jr., "Laser stimulation of the auditory nerve," *Lasers in Surgery and Medicine,* vol. 38, pp. 745-753, 2006.

[16] Jenkins, M. W., Duke, A. R., GuS, DoughmanY, Chiel, H. J., FujiokaH, WatanabeM, Jansen, E. D., and Rollins, A. M., "Optical pacing of the embryonic heart," *Nat Photon,* vol. 4, pp. 623-626, 2010.

[17] Dittami, G. M., Rajguru, S. M., Lasher, R. A., Hitchcock, R. W., and Rabbitt, R. D., "Intracellular calcium transients evoked by pulsed infrared radiation in

neonatal cardiomyocytes," *The Journal of Physiology*, vol. 589, pp. 1295-1306, 2011.

[18] Wu, X. Y., Mou, Z. X., Hou, W. S., Zheng, X. L., Yao, J. P., Shang, G. B., and Yin, Z. Q., "Irradiation of 850-nm laser light changes the neural activities in rat primary visual cortex," *Lasers in Medical Science*, pp. 1-8, 2012.

[19] Cayce, J. M., Friedman, R., Jansen, E. D., Mahadevan-Jansen, A., and Roe, A. W., "Pulsed infrared light alters neural activity in rat somatosensory cortex in vivo," *Neuroimage*, vol. 57, pp. 155-166, 2011.

[20] Feng, H.-J., Kao, C., Gallagher, M. J., Jansen, E. D., Mahadevan-Jansen, A., Konrad, P. E., and Macdonald, R. L., "Alteration of GABAergic neurotransmission by pulsed infrared laser stimulation," *Journal of Neuroscience Methods*, vol. 192, pp. 110-114, 2010.

[21] Cayce, J. M., Kao, C. C., Malphrus, J. D., Konrad, P. E., Mahadevan-Jansen, A., and Jansen, E. D., "Infrared Neural Stimulation of Thalamocortical Brain Slices," *Selected Topics in Quantum Electronics, IEEE Journal of*, vol. 16, pp. 565-572, 2010.

[22] Shapiro, M. G., Homma, K., Villarreal, S., Richter, C.-P., and Bezanilla, F., "Infrared light excites cells by changing their electrical capacitance," *Nat Commun*, vol. 3, p. 736, 2012.

[23] Albert, E. S., Bec, J., Desmadryl, G., Chekroud, K., Travo, C., Gaboyard, S., Bardin, F., Marc, I., Dumas, M., and Lenaers, G., "TRPV4 channels mediate the infrared laser-evoked response in sensory neurons," *Journal of Neurophysiology*, vol. 107, pp. 3227-3234, 2012.

[24] Kircher, M. L. and Kartush, J. M., "Pitfalls in intraoperative nerve monitoring during vestibular schwannoma surgery," *Neurosurgical Focus*, vol. 33, p. 5, 2012.

[25] Minahan, R. E. and Mandir, A. S., "Neurophysiologic intraoperative monitoring of trigeminal and facial nerves," *Journal of Clinical Neurophysiology*, vol. 28, p. 551, 2011.

[26] Wiedemayer, H., Fauser, B., Sandalcioglu, I. E., Schäfer, H., and Stolke, D., "The impact of neurophysiological intraoperative monitoring on surgical decisions: a critical analysis of 423 cases," *Journal of Neurosurgery*, vol. 96, pp. 255-262, 2002.

[27] Salame, K., Ouaknine, G. E., Rochkind, S., Constantini, S., and Razon, N., "Surgical treatment of spasticity by selective posterior rhizotomy: 30 years experience," *Isr Med Assoc J,* vol. 5, pp. 543-6, 2003.

[28] Sindou, M. P. and Mertens, P., "Neurosurgery for spasticity," *Stereotact Funct Neurosurg,* vol. 74, pp. 217-21, 2000.

[29] Albright, A. L., "Neurosurgical treatment of spasticity and other pediatric movement disorders," *J Child Neurol,* vol. 18 Suppl 1, pp. S67-78, 2003.

[30] Park, T., "Selective dorsal rhizotomy for the spasticity of cerebral palsy," in *Neurosurgical Operative Atlas*. vol. 4, S. Rengachary and W. RH, Eds., ed Park Ridge, IL: American Association of Neurological Surgeons, 1994, pp. 183-190.

[31] Engsberg, J. R., Ross, S. A., Collins, D. R., and Park, T. S., "Effect of selective dorsal rhizotomy in the treatment of children with cerebral palsy," *Journal of Neurosurgery,* vol. 105, p. 8, 2006.

[32] Park, T. S., "Selective dorsal rhizotomy: an excellent therapeutic option for spastic cerebral palsy," *Clin Neurosurg,* vol. 47, pp. 422-39, 2000.

[33] Park, T. S. and Johnston, J. M., "Surgical techniques of selective dorsal rhizotomy for spastic cerebral palsy. Technical note," *Neurosurg Focus,* vol. 21, p. e7, 2006.

[34] Thomsen, S., "Identification of lethal injury at the time of photothermal treatment," in *SPIE*, Bellingham, WA, pp. 459-467 1995.

[35] Thomsen, S., "Mapping Thermal Injury in Biologic Tissues Using Quantitative Pathologic Techniques," in *SPIE Proceedings*, pp. 82-95 1999.

[36] Lund, B. J., "The probitfit program to analyze data from laser damage threshold studies," DTIC Document2006.

[37] Scherberger, H., "Neural control of motor prostheses," *Current opinion in neurobiology,* vol. 19, pp. 629-633, 2009.

[38] Marasco, P. D., Schultz, A. E., and Kuiken, T. A., "Sensory capacity of reinnervated skin after redirection of amputated upper limb nerves to the chest," *Brain,* vol. 132, pp. 1441-1448, 2009.

[39] Weber, D. J., London, B. M., Hokanson, J. A., Ayers, C. A., Gaunt, R. A., Torres, R. R., Zaaimi, B., and Miller, L. E., "Limb-state information encoded by peripheral and central somatosensory neurons: implications for an afferent

interface," *Neural Systems and Rehabilitation Engineering, IEEE Transactions on,* vol. 19, pp. 501-513, 2011.

[40] Izzo, A. D., Walsh, J. T., Jr., Jansen, E. D., Bendett, M., Webb, J., Ralph, H., and Richter, C. P., "Optical parameter variability in laser nerve stimulation: a study of pulse duration, repetition rate, and wavelength," *IEEE Trans Biomed Eng,* vol. 54, pp. 1108-14, 2007.

[41] Izzo, A. D., Walsh, J. T., Ralph, H., Webb, J., Bendett, M., Wells, J., and Richter, C.-P., "Laser stimulation of auditory neurons: effect of shorter pulse duration and penetration depth," *Biophys. J.,* p. 107.117150, 2008.

[42] Rajguru, S. M., Matic, A. I., Robinson, A. M., Fishman, A. J., Moreno, L. E., Bradley, A., Vujanovic, I., Breen, J., Wells, J. D., Bendett, M., and Richter, C.-P., "Optical cochlear implants: Evaluation of surgical approach and laser parameters in cats," *Hearing Research,* vol. 269, pp. 102-111, 2010.

[43] Martin, H. C., Sethi, J., Lang, D., Neil-Dwyer, G., Lutman, M. E., and Yardley, L., "Patient-assessed outcomes after excision of acoustic neuroma: postoperative symptoms and quality of life," *J Neurosurg,* vol. 94, pp. 211-6, 2001.

[44] Ueno, H., Kaneko, K., Taguchi, T., Fuchigami, Y., Fujimoto, H., and Kawai, S., "Endoscopic carpal tunnel release and nerve conduction studies," *Int Orthop,* vol. 24, pp. 361-3, 2001.

[45] Changfeng, T., Jicheng, W., Xianchun, W., William, C. d. G., and James, R. R., "Bladder inhibition or voiding induced by pudendal nerve stimulation in chronic spinal cord injured cats," *Neurourology and Urodynamics,* vol. 26, pp. 570-577, 2007.

[46] Gritsenko, V. and Prochazka, A., "A functional electric stimulation--assisted exercise therapy system for hemiplegic hand function," *Archives of Physical Medicine and Rehabilitation,* vol. 85, pp. 881-885, 2004.

[47] Fregni, F., Boggio, P. S., Lima, M. C., Ferreira, M. J. L., Wagner, T., Rigonatti, S. P., Castro, A. W., Souza, D. R., Riberto, M., Freedman, S. D., Nitsche, M. A., and Pascual-Leone, A., "A sham-controlled, phase II trial of transcranial direct current stimulation for the treatment of central pain in traumatic spinal cord injury," *Pain,* vol. 122, pp. 197-209, 2006.

[48] Konrad, P. and Shanks, T., "Implantable brain computer interface: Challenges to neurotechnology translation," *Neurobiology of Disease,* vol. 38, pp. 369-375, 2010.